Chiral Brønsted Acid: Innovations and Application to Regiodivergent Glycosylations

by

Tay Jiahui Rosenthal

A dissertation submitted in partial fulfillment
of the requirements for the degree of
Doctor of Philosophy
(Chemistry)
in the University of Michigan
2018

Doctoral Committee:

Professor Pavel Nagorny, Chair
Professor John Montgomery
Professor Melanie S. Sanford
Professor David H. Sherman

Tay J. Rosenthal

tayro@umich.edu

ORCID iD: 0000-0002-6858-6779

DEDICATION

To my *basherter* Will, who brings me infinite joy and wisdom.

ACKNOWLEDGMENTS

I would like to thank my advisor, Dr. Pavel Nagorny, for keeping it real and pushing me to achieve far more than what I intended or thought possible. His unrelenting passion for science has taught me important lessons about perseverance and being diligent in achieving goals. I am grateful for the ample opportunities that he offered throughout my graduate studies, and I will miss his openness to the exchange of scientific ideas at any time.

I am thankful to have Dr. John Montgomery, Dr. Melanie Sanford, and Dr. David Sherman serving on my doctoral committee. In addition to their unwavering support, they have each modeled high standards, rigor and impeccable respect for scientific ethics, the likes of which I will always endeavor to maintain.

I am indebted to my undergraduate research advisor at University of Virginia, Dr. Lin Pu, and my undergraduate mentor, Wei Chen. Their guidance and training enabled me to become the chemist I am today.

I would also like to thank Dr. Brian Coppola for the opportunity to participate as an organizing committee member for CALC|UM. The experience helped me to develop leadership and communication skills that I know I will utilize throughout my career.

I am grateful for the members of the Nagorny group and the chemistry staff members, whose support was indispensable to the success of my research. I would like to especially thank my collaborators: Bijay Bhattarai, Alonso Argüelles, Dr. Matthew DeMars, Valentine Dorokhov and Miyuki Hotta. Each made invaluable contributions to the projects on which we collaborated.

Specifically, the production of the 6-dEB macrolactone described in Chapter 2 was accomplished in collaboration with Dr. Matthew DeMars of the Sherman group (*U of Michigan*). The computational studies discussed in that same chapter were completed by Alonso Argüelles under the guidance of Dr. Paul Zimmerman (*U of Michigan*). In addition, Valentine Dorokhov, a visiting scholar from *Higher Chemical College of the Russian Academy of Sciences*, made a significant contribution to the optimization of the glycosylation reaction described in Chapter 5.

My graduate school experience would not have been the same without these dear friends: Alan, Alina, Alonso, Bijay, Danielle, Gracie, Kendra, Melissa, Naoko, Nathan, and Will. Thank you for shaping my experience at Michigan in so many positive ways.

I would be remiss were I not to mention that I am grateful for the company of my claw-some cats, Fay and Maude, with whom I have shared many paw-sitive meow-ments. They always remind me that it is OK to pro-cat-stinate sometimes and that I don't have to be purr-fect to be happy.

To my family in Malaysia, thank you for always being there for me, no matter what.

Last, but certainly not least, I would like to offer my heartfelt gratitude to my husband Will, to whom this dissertation is dedicated. Thank you for proofreading my dissertation and showering me with love and joy.

TABLE OF CONTENTS

LIST OF FIGURES

FIGURE

LIST OF SCHEMES

SCHEME

LIST OF TABLES

TABLE

LIST OF ABBREVIATIONS

$(PhO)_2PO_2H$	diphenylphosphoric acid
6-dEB	6-deoxy-erythronolide B
Ac	acyl
AcOH	acetic acid
ACS	American Chemical Society
Ar	aryl
atm	atmosphere (unit)
BINOL	1,1'-bi-2-naphthol
bis-gly.	bis-glycoside
Bn	benzyl
Boc	*tert*-butyloxycarbonyl
brsm	based on recovered starting material
By-prod.	by-product
Bz	benzoyl
C_6D_6	deuterated benzene
calcd.	calculated
C-H	carbon-hydrogen
conc.	concentration
COSY	correlation spectroscopy
CPA	chiral phosphoric acid
Cy	cyclohexyl
DBU	1,8-diazabicyclo[5.4.0]undec-7-ene

DCE	1,2-dichloroethane
DCM	dichloromethane
DMAP	4-dimethylaminopyridine
DMF	dimethylformamide
DMSO	dimethyl sulfoxide
DPPA	diphenylphosphoric acid
ee	enantiomeric excess
equiv.	equivalent
Et	ethyl
EtOAc	ethyl acetate
EtOH	ethanol
g	gram
gly.	glycoside
h	hours
HEPES	4-(2-hydroxyethyl)-1-piperazineethanesulfonic acid
HMBC	heteronuclear multiple bond correlation
HPLC	high-performance liquid chromatography
HRMS	high resolution mass spectra
HSQC	heteronuclear single quantum correlation
Hz	hert
i-Pr	*iso*-propyl
IPTG	isopropyl-beta-D-thiogalactopyranoside
IR	infrared
L	liter
LAH	lithium aluminum hydride
LB	Luria-Bertani broth
LUMO	lowest unoccupied molecular orbital
M	molar (unit)
M.S.	molecular sieve
Me	methyl
MeCN	acetonitrile

MeOH	methanol
Mesityl	1,3,5-trimethylphenyl
mg	milligram
MHz	megahert
min	minutes
mL	milliliter
mol%	mole percentage
Ms	mesyl / methanesulfonyl
MS-ESI	mass spectrometry – electrospray ionization
N	normal
n-BuLi	butyl lithium
neg.	negative
NIS	N-iodosuccinimide
nm	nanometer
NMR	nuclear magnetic resonance
^{o}C	degree Celsius
OD	optical density
PG	protecting group
Ph	phenyl
PhMe	toluene
ppm	parts per million
p-TsOH	*para*-toluenesulfonic acid
R	alkyl group
r.t.	room temperature
R^2	coefficient of determination
rpm	revolutions per minute
SAR	structure-activity relationship
SPINOL	1,1’-spirobiindane-7,7’-diol
T	temperature
t	time
TBS	*tert*-butyldimethylsilyl

t-Bu	*tert*-butyl
TCA	trichloroacetimidate
Tf	trifyl / trifluoromethylsulfonyl
THF	tetrahydrofuran
TMS	trimethylsilyl
TMSCN	trimethylsilyl cyanide
TMSOTf	trimethylsilyl trifluoromethanesulfonate
Ts	tosyl / *para*-toluenesulfonyl
v/v	volume/volume
VAPOL	2,2’-diphenyl-3,3’-biphenanthryl-4,4’-diol
w/w	weight/weight
μg	microgram
μmol	micromole

ABSTRACT

Since the term "organocatalysis" was coined by MacMillan in 2000, it has become a major research topic with growing interest. The introduction of chiral Brønsted acid as an organocatalyst in particular has enabled the development of new asymmetric reactions to access chiral compounds that are difficult to access otherwise. Described herein is the application of chiral Brønsted acids as organocatalysts to selective glycosylation reactions and the development of new methods that improved the synthesis and characterization of chiral Brønsted acids.

Chapter 1 is an introduction to phosphorus-based chiral Brønsted acids and an overview of different reaction mechanisms involving activation by chiral phosphoric acid.

Chapter 2 describes the first example of the application of chiral Brønsted acids to control site-selective glycosylations of complex polyol compounds. Through judicious selection of catalysts and reaction conditions, regioisomeric glycoforms of 6-deoxy-erythronolide B and oleandomycin-derived macrolactones were selectively synthesized. Mechanistic investigation revealed that the mechanism of the reaction proceeded through a covalently linked anomeric phosphate intermediate.

Chapter 3 describes a new method for the conversion of BINOL-derived chiral Brønsted acids to their H8-BINOL-based analogs through a single-step hydrogenation catalyzed by platinum (IV) oxide. Using the method, five new H8-BINOL-based chiral Brønsted acids were synthesized.

Chapter 4 describes a new method to determine the enantiopurity of chiral phosphoric acids based on the use of chiral amines as the discriminating agent and ^{31}P NMR analysis. This method was used to investigate the racemization stability of chiral phosphoric acids under hydrogenation conditions and thermal stress.

Chapter 5 describes the development of an efficient one-pot protocol for selective glycosylation of natural products containing a 1,3-diol moiety. The protocol relies on the use of simple boronic acid as the transient protecting group, which can be easily put on and taken off under mild conditions. The new protocol was used to synthesize various glycosides of antibiotic-derived macrolactones, strophanthidol, and anhydro-ouabagenin.

CHAPTER 1

Introduction

(This chapter was partially published in: Tay, J. H.; Nagorny, P. "Brønsted Acid Catalysts Derived from Phosphorous" Book chapter in *Non-nitrogenous Organocatalysis*, Harned, A. M., Ed., CRC Press, **2017)**

1.1 Selected Milestones in Catalysis

"It is, then proved that several simple or compound bodies, soluble and insoluble, have the property of exercising on other bodies an action very different from chemical affinity. By means of this action they produce, in these bodies, decompositions of these same elements to which they remain indifferent." – J. J. Berzelius

In an annual report published in 1836, titled "Quelques Idées sur une nouvelle Force agissant dans les Combinaisons des Corps Organiques," (*Some ideas about a new force acting in combinations of organic bodies*), Swedish chemist Jöns Jacob Berzelius described what he termed the "catalytic force".[1] The report summarized prior observations in homogeneous and heterogenous systems where chemical bodies were found to have certain effects on the combination or decomposition of other chemical entities, while remaining unchanged themselves. The report marked first conceptualization of catalysis.

Initially, the study and development of catalysis was centered around metallic compounds. A few years before Berzelius's report, Louis Jacques Thénard recorded an early observation regarding the reactivity pattern of transition metals. He observed the decomposition of ammonia into nitrogen and hydrogen when passed over red-hot iron, copper, silver, gold and platinum decreased in the same order.[2] Later, in 1909, Wilhelm Ostwald was awarded the Nobel Prize in Chemistry partly for his work on catalysis. He is most credited for developing the Ostwald process, which converts ammonia to nitric acid through oxidation in the presence of platinum as catalyst.

Subsequently, Karle Ziegler and Giulio Natta were recognized by the Nobel Committee in 1963 for their discoveries in polymer science using transition metal-based catalysts.

In the early 2000's, organocatalyst (catalyst made up of hydrocarbon and other nonmetal elements) received attention from the chemistry community and has subsequently become a major focus in the research area of catalysis.[3] However, at the time the idea of using a small organic molecule to catalyze asymmetric reactions certainly was not new. Notable examples of organocatalysis date as far back as 1912, when German chemists Bredig and Fiske reported the use of cinchona alkaloids to catalyze the addition of hydrogen cyanide to benzaldehyde.[4] Another famous example came from two independent reports in 1971 by Hajos and Parrish[5], *and* Eder, Sauer and Wiechert[6] on the application of proline, a natural amino acid, as chiral catalyst in Aldol reaction. In 2000, MacMillan coined the term "organocatalysis", which marked an important turning point in the development of organocatalyst and helped to more clearly define that area of research.[7] Contemporaneous reports by List,[8] Jacobsen,[9] Corey,[10] Denmark,[11] Jørgensen[12] and others further promoted the growing interest in the field of organocatalysis.

1.2 Phosphorus-based Brønsted acid

Phosphorus-based organic compounds, such as phosphine, phosphine oxide and phosphoric acid, represent one of the many subclasses of organocatalyst. Sir John Cornforth, who received the Nobel Prize in Chemistry in 1975 for his work on the stereochemistry of enzyme-catalyzed reactions, reported the first systematic study and application of phosphorus (V) based acids in organocatalysis. In his 1978 lecture, titled "The imitation of enzymatic catalysis," Cornforth describes on small molecule catalysts that can mimic the functionality of an enzyme to catalyze the hydration of olefins.[13] He designed and synthesized a series of phosphinic acids with different structural backbones, based on several prescriptions that he composed: (1) the catalyst must be acidic; (2) it has a non-rigid cavity where the acidic group must be located and the olefin substrate could fit; (3) the acidic group must have the right acidity (not too strong or too weak); (4) the synthesis must be short, scalable and modular at late stage to provide different cavity shapes. Interestingly, the designs of more recent phosphorus-based Brønsted acid catalysts is essentially guided by the same blueprints laid out by Cornforth decades ago.

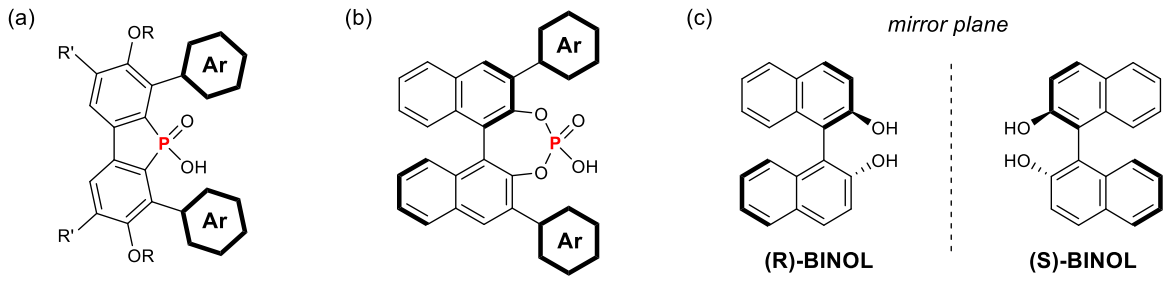

Figure 1.1. General structures of (a) phosphinic acid proposed by Cornforth in 1978 and (b) chiral phosphoric acid reported by Akiyama and Terada in 2004. (c) Enantiomeric pairs of axially chiral and C_2-symmetric 1,1'-bi-2-naphthol (BINOL).

Research on phosphorus-based acid experienced a spike in interest when the seminal and independent reports by Akiyama[14] and Terada[15] came out in 2004. Both groups disclosed their findings on the application of phosphoric acids with a 1,1'-bi-2-naphthol (BINOL) backbone in catalyzing Mannich-type reactions (Scheme 1.1). One of the biggest advancements in catalyst design (compared to Cornforth's), was the incorporation of an axially chiral BINOL backbone because it enabled the development of stereoselective reactions. Akiyama and Terada also noticed in their studies that the substituent groups on the 3,3'-position of the BINOL backbone had a significant impact on the enantioselectivity outcome of the reaction. In Akiyama's example, the enantioselectivity increased as the size of the 3,3'-aromatic substituents increased. Interestingly, Terada was able to achieve the same level of enantioselectivity by using catalyst with electron-withdrawing group. Their observations echoed Cornforth's emphasis on the rigidity and shape of the active site cavity in his catalyst design.

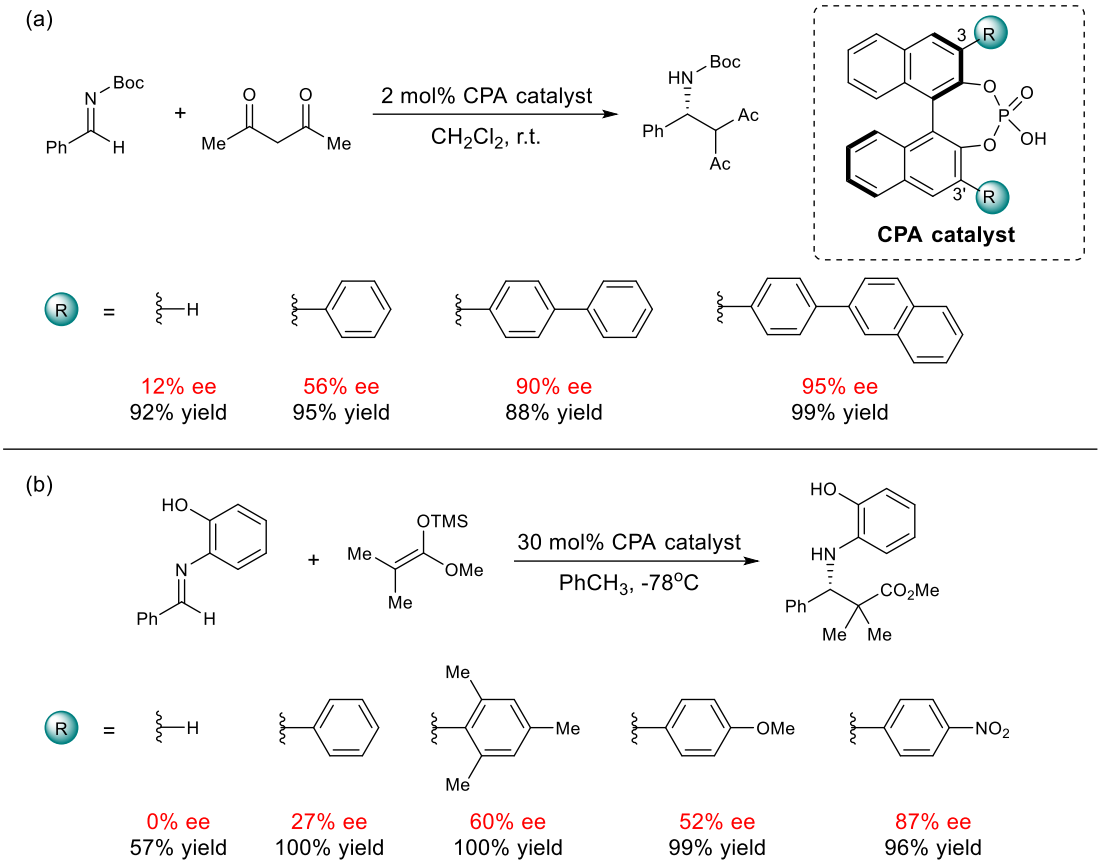

Scheme 1.1. Effect of 3,3'-substituents of chiral phosphoric acid catalysts on the enantioselectivity for Mannich-type reactions reported by (a) Akiyama and (b) Terada in 2004.

Since 2004, as chiral phosphorus-based acid catalysts continue to surge in popularity, the scope of reactions reported to be catalyzed by this class of organocatalyst has also significantly expanded.[16] This growth is fueled in part by creative design of new catalysts with different chiral backbones and Brønsted acidic functionalities that encompass a wide range of acidity. Through computational and spectroscopy experimentation, the acidity of many of these phosphorus-based acids has been quantified.[17] It emerged that the acidity of these acids may be modulated through several means, including changes in the substitution on the phosphorus atom, in the structure of the backbones, and by substitution *on* the backbones.

(a) Effect of substitution on phosphorus atom on acitidy of phosphoric acid.

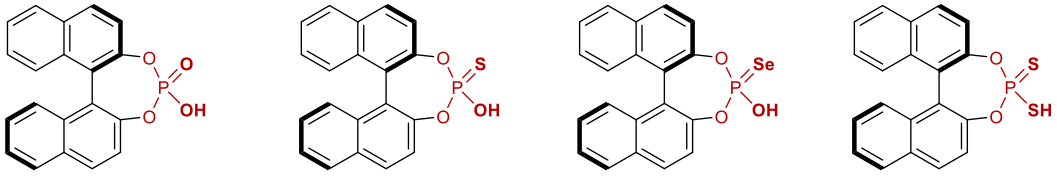

pK_a (DMSO) = 3.4 | pK_a (DMSO) = 1.1 | pK_a (DMSO) = -1.2 | pK_a (DMSO) = -4.2

(b) Effect of chiral backbone on acitidy of phosphoric acid.

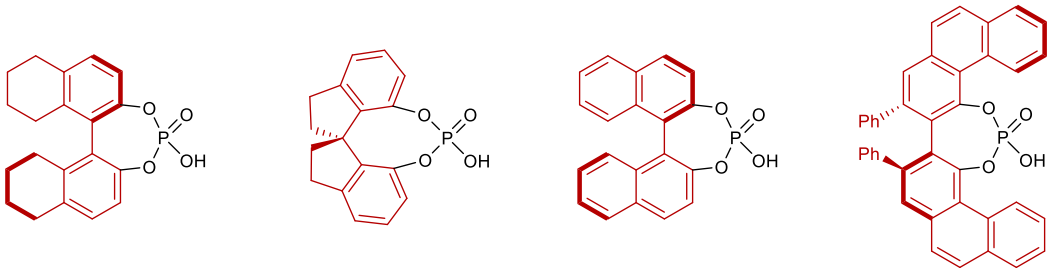

H8-BINOL | **SPINOL** | **BINOL** | **VAPOL**

pK_a (DMSO) = 4.6 | pK_a (DMSO) = 4.2 | pK_a (DMSO) = 3.4 | pK_a (DMSO) = 2.0

(c) Effect of 3.3'-substituents on acitidy of phosphoric acid.

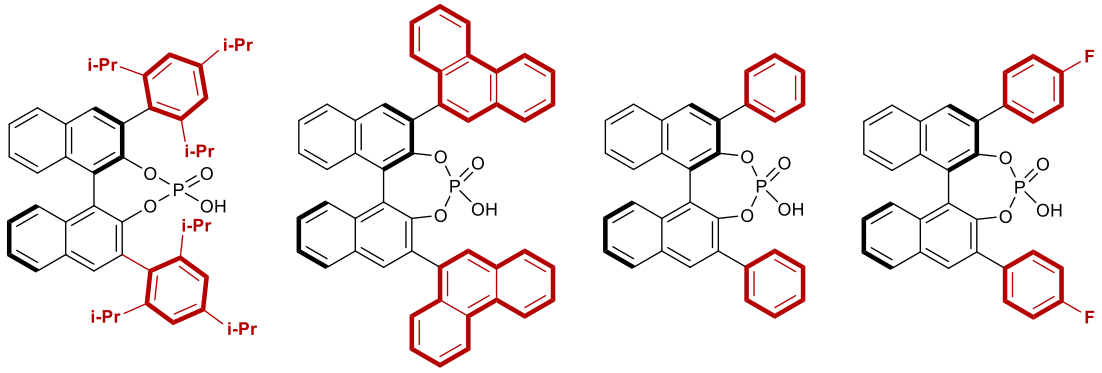

pK_a (MeCN) = 13.6 | pK_a (MeCN) = 13.3 | pK_a (MeCN) = 12.7 | pK_a (MeCN) = 12.5

Figure 1.2. Effects of structural variations on the acidity of chiral phosphoric acids.

1.3 Activation Modes Involving Chiral Phosphorus Acid

Chiral phosphoric acid (CPA) with a pentavalent phosphorus center is a prevalent class of phosphorus-based acids seen in the literature.[18] They are also the most studied for their reaction mechanisms. A typical CPA possesses both a Brønsted acidic proton and a Lewis basic lone pair, which allows them to engage in different modes of reaction. The Lewis basic lone pair can

participate in hydrogen bonding with nucleophiles possessing acidic protons, thereby increasing its nucleophilicity. On the other hand, the acidic proton can activate basic electrophile through either protonation or hydrogen bonding, and essentially enhances the electrophilicity of electrophiles by lowering their LUMO energies. In most cases, CPA engages in a bifunctional activation of substrates through hydrogen bonding and provides great stabilization to the intermediary complex or transition states. The highly directional nature of hydrogen bonding interactions also helps to maximize the asymmetric induction originated from the chiral backbone.

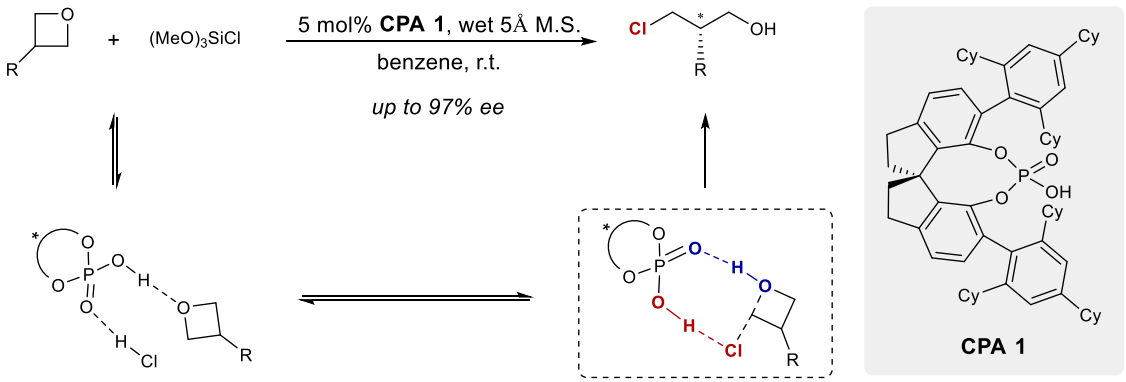

Scheme 1.2. Example of enantioselective reaction catalyzed by CPA involving bifunctional hydrogen bonding activation of nucleophile and electrophile.[19]

Besides acting as a hydrogen bonding catalyst, CPAs are involved in counterion catalysis, relying on electrostatic interactions between ionic species to control the course of a reaction. This is an especially appealing strategy in developing asymmetric reactions since a majority of organic transformations proceed through partially or fully charged transition states. In general, CPA can be introduced as a chiral phosphate counterion in one of several ways: (1) protonation of substrate[20]; (2) dehydration of substrate[21]; or (3) anion exchange with phosphate salt[22] (Scheme 1.3). In addition, counterion catalysis relies on the formation of a tight or contact ion pair to achieve high degrees of asymmetric induction. Indeed, most methods using a CPA as counterion catalyst reported a higher selectivity in nonpolar media.

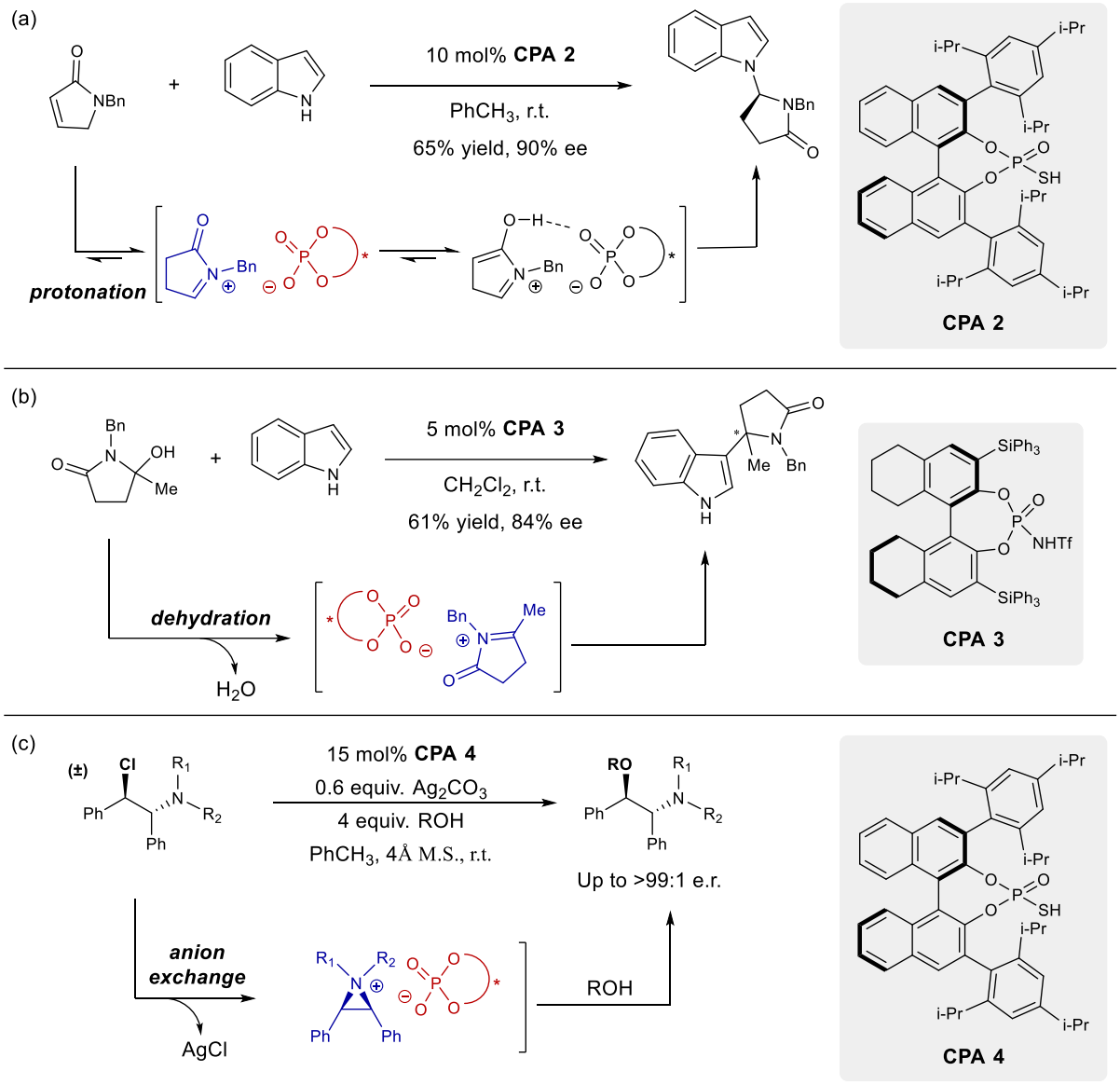

Scheme 1.3. Examples of counterion catalysis involving introduction chiral phosphate ion through (a) protonation[20], (b) dehydration[21], and (c) anion exchange[22].

CPA may also be thought of as a chiral surrogate for proton sources and involved in the formation of a new chiral center through enantioselective protonation. The idea of accessing chiral compounds through stereoselective protonation of π bonds is simple, but implementation as such is challenging. This is because of the fast rate of protonation that makes it hard to exert a high level of stereocontrol and the probability of newly formed stereocenters undergoing undesired racemization. With the recent introduction of CPA catalysts possessing a diverse range of *p*Ka values, researchers such as Yamamoto[23] and Rueping[24] were able to mitigate previous obstacles

to develop several interesting transformations using CPA as a chiral proton source. These reaction mechanisms differ from other modes of activations, where CPA activates basic electrophile through protonation or it forms an ion pairs through the protonation of a substrate. In Rueping's examples, the protonation step in the reaction mechanism is the enantio-determining step. In other words, protonation is the only viable step that leads to the formation of a new stereocenter (Scheme 1.4).

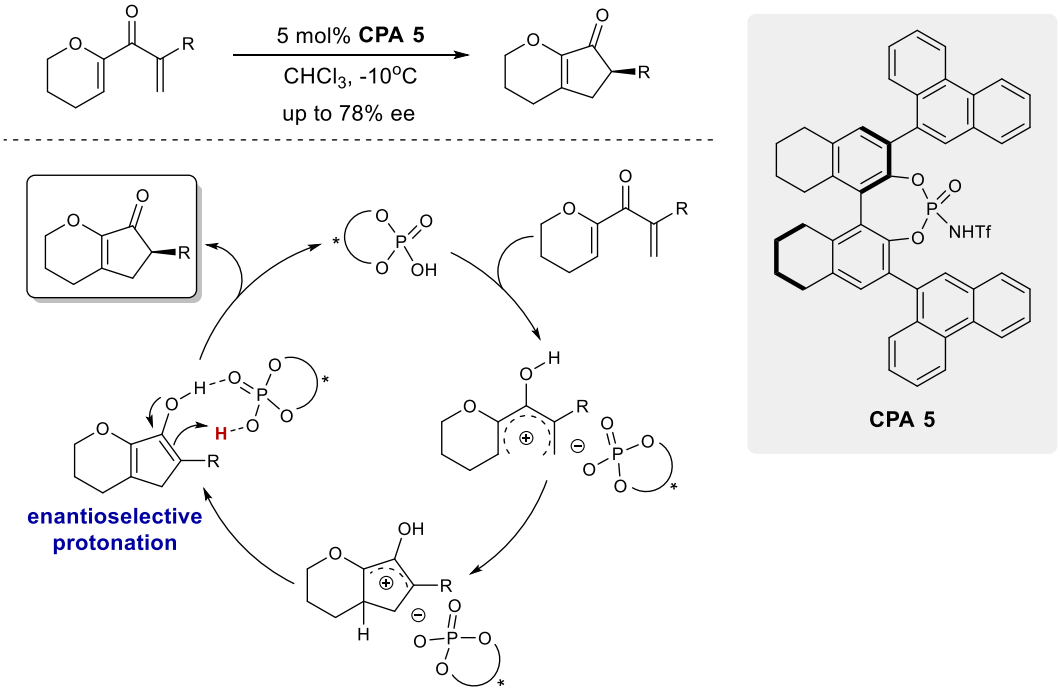

Scheme 1.4. Example of CPA catalyzed Nazarov cyclization involving enantioselective protonation.

In 2011, Toste group reported a new transformation catalyzed by CPA that proceeded through a covalent phosphate intermediate (Scheme 1.5).[25] Based on detailed mechanistic studies, Nagorny group[26] and others[27] also proposed similar covalent intermediates for their transformations, indicating that this is a general mode of reaction involving CPA. The key feature of covalent catalysis is the formation of a transient covalent bond between a substrate and the catalyst, which undergoes further reaction, and subsequent breakage of the bond to regenerate the catalyst. The major advantage of catalysis proceeding through a covalent intermediate is the highly rigid and directional covalent linkage that helps to maximize asymmetric induction from the chiral catalyst. Nonetheless, one of the biggest challenges of developing covalent catalysis is to identify

a catalyst that is both sufficiently nucleophilic and possesses good leaving group ability. One solution presented by Toste is the use of chiral dithiophosphoric acid, a subclass of CPA, where in the phosphorus is substituted with two sulfur atoms, instead of oxygen. He proposes that dithiophosphoric acids are more nucleophilic and serve as a better leaving group than their oxygenated counterparts because of the substitution of more polarizable sulfur atoms.

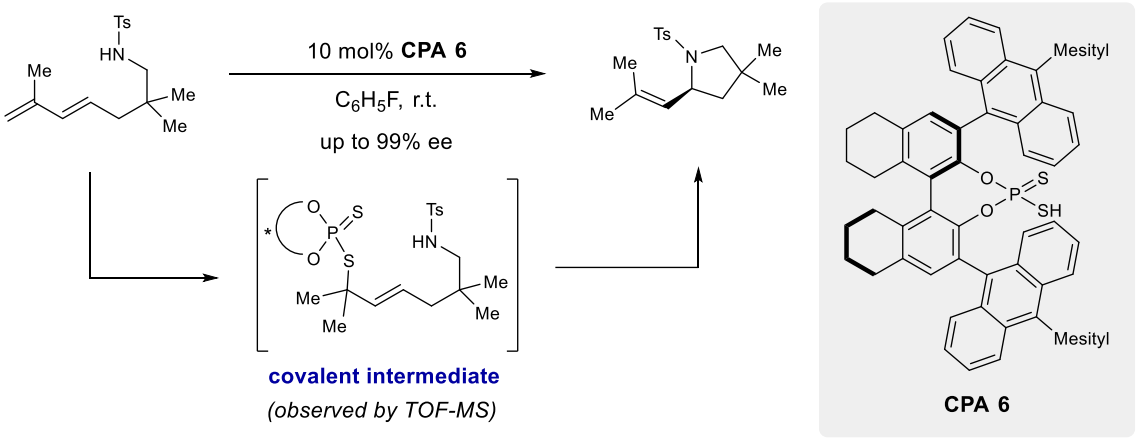

Scheme 1.5. Example of CPA catalyzed reaction proceeding through formation of covalent phosphate intermediate.

Another distinct mode of action for CPA involves the addition of external Lewis acids to modulate the reactivity of CPA itself. The amphoteric nature of CPA allows Lewis acid to either exchange with the acidic proton or complex to the Lewis basic lone pair. Ishihara found that the combination of CPA with n-BuLi generated chiral lithium phosphate, which could catalyze the addition of trimethylsilyl cyanide (TMSCN) to ketone.[28] He postulated that the lithium ion enhanced the Lewis basicity of phosphoryl oxygen, which in turn activated TMSCN more effectively.

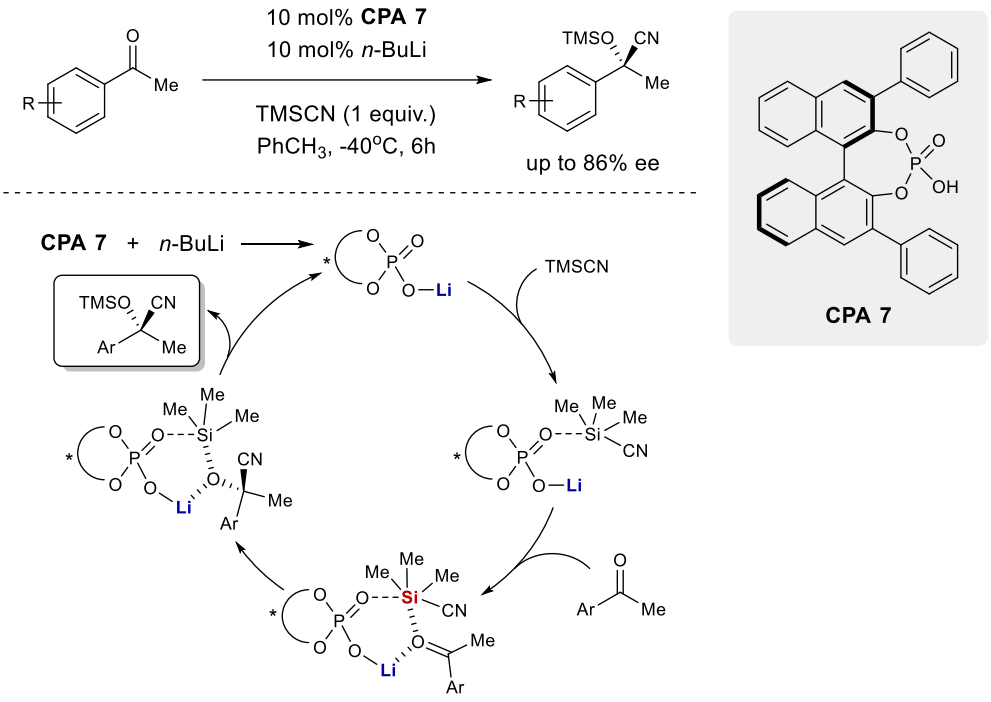

Scheme 1.6. Example of CPA catalysis involving enhancement of phosphate basicity by lithium ion.

In subsequent studies, Ishihara demonstrated the use of CPA in combination with BBr_3 as Lewis acid to catalyze a Diels-Alder reaction.[29] Through computational and NMR experiments, he was able to identify the active catalytic species, which had BBr_3 bound to the phosphoryl oxygen. In additional, their computational analysis also suggested that existence of halogen bonds between bromine and C-H bond of acrolein Presumably, the complexation of BBr_3 enhances the acidity of the CPA and provided addition stabilization through non-covalent bonding interactings, which consequently lead to excellent yield and stereoselectivity.

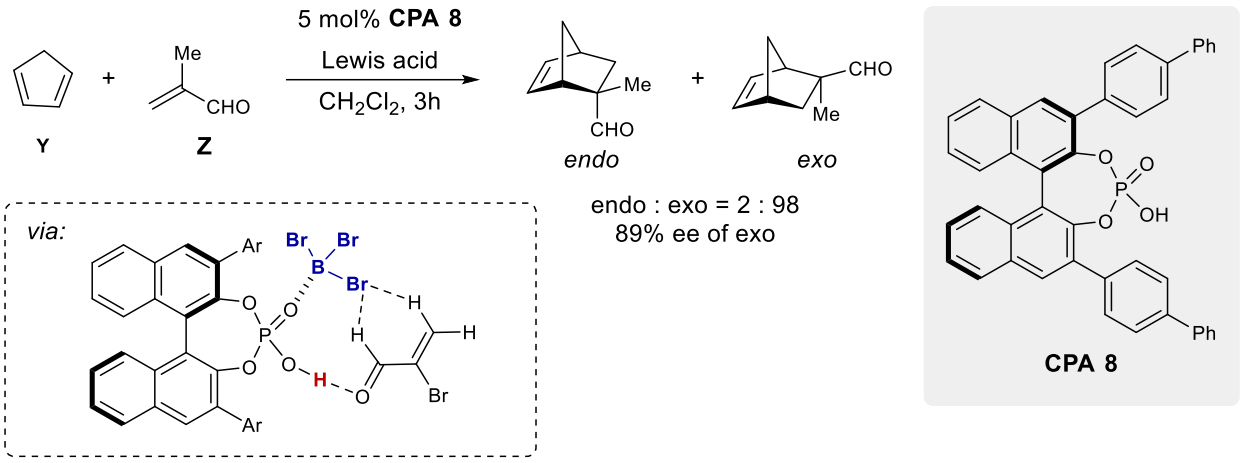

Scheme 1.7. Example of CPA catalysis involving enhancement of Brønsted acidity by additional Lewis acid.

1.4 Summary

As the field of catalysis progresses, so does the pursuit of new catalysts that meet higher standards. While new catalysts with high turnover number and great selectivity are highly sought after, other factors like ease of preparation, recyclability, environmental impact and toxicity are also gaining more considerations. In that regard, organocatalyst has proven its great potential, especially based on the growing studies that have been reported since the early 2000s. Organocatalysis, involving CPA in particular, stand out because of the catalyst's versatility to engage in many distinct modes of activation and a highly tunable structure that is easily amendable to fit the needs of varying reactions. The following chapters of this dissertation discuss a new application of CPA catalysts in glycosylation reaction, and the development of new methods that improve the synthesis and characterization of CPA.

1.5 References

[1] Berzelius, J. J. *Annls. Chim. Phys.* **1836**, *61*, 146.

[2] Thénard, L. J. *Annales de chimie* **1813**, *85*, 61.

[3] Cabrera, S.; Alemán, *J. Chem. Soc. Rev.* **2013**, *42*, 774.

[4] Bredig, G.; Fiske, P. S. *Biochemische Zeitschrift* **1912**, *46*, 7.

[5] Parrish, D. R.; Hajos, Z. G. *J. Org. Chem.* **1974**, *39*, 1615.

[6] Elder, U.; Sauer, G.; Wiechert, R. *Angew. Chem. Internal. Edit.* **1971**, *10*, 496.

[7] Ahrendt, K. A.; Borths, C. J.; MacMillan, D. W. C. *J. Am. Chem. Soc.* **2000**, *122*, 4243.

[8] (a) List, B.; Lerner, R. A.; Barbas, C. F., III *J. Am. Chem. Soc.* **2000**, *122*, 2395. (b) Notz, W.; List, B. *J. Am. Chem. Soc.* **2000**, *122*, 7386. (c) List, B. *J. Am. Chem. Soc.* **2000**, *122*, 9336.

[9] (a) Sigman, M. S.; Vachal, P.; Jacobsen, E. N. *Angew. Chem. Int. Ed.* **2000**, *39*, 1279. (b) Vachal, P.; Jacobsen, E. N. *Org. Lett.* **2000**, *2*, 867.

[10] (a) Zhang, F.-Y.; Corey, E. J. *Org. Lett.* **2000**, *2*, 1097. (b) Corey, E. J.; Choi, S. *Tetrahedron Letters* **2000**, *41*, 2769.

[11] (a) Denmark, S. E.; Wynn, T. *J. Am. Chem. Soc.* **2001**, *123*, 6199. (b) Denmark, S. E.; Ghosh, S. K. *Angew. Chem. Int. Ed.* **2001**, *40*, 4759. (c) Denmark, S. E.; Fu, J. *J. Am. Chem. Soc.* **2001**, *123*, 9488.

[12] (a) Halland, N.; Hazell, R. G.; Jørgensen, K. A. *J. Org. Chem.* **2002**, *67*, 8331. (b) Bøgevig, A.; Juhl, K.; Kumaragurubaran, N.; Zhuang, W.; Jørgensen, K. A. *Angew. Chem. Int. Ed.* **2002**, *41*, 1790.

[13] Conrnforth, J. *Proc. R. Soc. Lond. B.* **1978**, *203*, 101.

[14] Akiyama, T., Itoh, J., Yokota, K., Fuchibe, K. *Angew. Chem. Int. Ed.* **2004**, *43*, 1566.

[15] Uraguchi, D., Terada, M. *J. Am. Chem. Soc.* **2004**, *126*, 5356.

[16] Parma, D.; Sugiono, E.; Raja, S.; Rueping, M. *Chem. Rev.* **2014**, *114*, 9047.

[17] (a) Yang, C., Xue, X.-S., Jin, J.-L., Li, X., Cheng, J.-P. *J. Org. Chem.* **2013**, *78*, 7076. (b) Christ, P., Lindsay, A. G., Vormittag, S. S., Neudor_, J.-M., Berkessel, A., O'Donoghue, A. C. *Chem. Eur. J.* **2011**, *17*, 8524. (c) Kaupmees, K., Tolstoluzhsky, N., Raja, S., Rueping, M., Leito, I. *Angew. Chem. Int. Ed.* **2013**, *52*, 11569.

[18] (a) Akiyama, T.; Itoh, J.; Fuchibe, K. *Adv. Synth. Catal.* **2006**, *348*, 999. (b) Zamfir, A.; Schenker, S.; Freund, M.; Tsogoeva, S. B. *Org. Biomol. Chem.* **2010**, *8*, 5262. (c) Maji, R.; Mallojjala, S. C.; Wheeler, S. E. *Chem. Soc. Rev.* **2018**, *47*, 1142.

[19] (a) Yang, W., Wang, Z., Sun, J. *Angew. Chem. Int. Ed.* **2016**, *55*, 6954. (b) Champagne, P. A., Houk, K. N. *J. Am. Chem. Soc.* **2016**, *138*, 12356.

[20] Xie, Y., Zhao, Y., Qian, B., Yang, L., Xia, C., Huang, H. *Angew. Chem. Int. Ed.* **2011**, *50*, 5682.

[21] Rueping, M., Nachtsheim, B. J. *Synlett* **2010**, *1*, 119.

[22] Hamilton, G. L., Kanai, T., Toste, F. D. *J. Am. Chem. Soc.* **2008**, *130*, 14984.

[23] Cheon, C. H., Yamamoto, H. A. *J. Am. Chem. Soc.* **2008**, *130*, 9246.

[24] Rueping, M., Leawsuwan, W. *Adv. Synth. Catal.* **2009**, *351*, 78.

[25] Shapiro, N. D., Rauniyar, V., Hamilton, G. L., Wu, J., Toste, F. D. *Nature* **2011**, *470*, 245.

[26] Sun, Z., Winschel, G. A., Zimmerman, P., Nagorny, P. *Angew. Chem. Int. Ed.* **2014**, *53*, 11194.

[27] (a) Liu, L., Leutzsch, M., Zheng, Y., Alachraf, M. W., Thiel, W., List, B. *J. Am. Chem. Soc.* **2015**, *137*, 13268. (b) Lv, J., Zhang, Q., Zhang, X., Luo, S. *J. Am. Chem. Soc.* **2015**, *137*, 15576. (c) Kuroda, Y., Harada, S., Oonishi, A., Kiyama, H., Yamaoka, Y., Yamada, K., Takasu, K. *Angew. Chem. Int. Ed.* **2016**, *55*, 13137.

[28] Hatano, M., Ikeno, T., Matsumura, T., Torii, S., Ishihara, K. *Adv. Synth. Catal.* **2008**, *350*, 1776.

[29] Hatano, M., Goto, Y., Izumiseki, A., Akakura, M., Ishihara, K. *J. Am. Chem. Soc*. **2015**, *137*, 13472.

CHAPTER 2

Regiodivergent Glycosylations of 6-deoxy-Erythronolide B and Oleandomycin Derived Macrolactones Catalyzed by Chiral Brønsted Acids

(This chapter was partially published in: Tay, J. H.; Arguelles, J. A.; DeMars, M. D.; Zimmerman, P. M; Sherman, D. H.; Nagorny, P. *J. Am. Chem. Soc.* **2017**, *139*, 8570.)

2.1 Introduction

Across different classes of natural products, many of them were isolated as glycosylated compounds, where the sugar moiety was found to play an essential role in determining their biological activities. According to a survey conducted by Thorson on 15,940 bacterial natural products, 21% of them (3,426 compounds) are found to be glycosides (Figure 2.1).[1] Among the bacterial glycosides, glycosylated macrolactones and macrolactams represent the largest subclass (738 compounds), and over 344 distinct sugar structures were identified. In other words, glycosylated natural products, especially those produced by bacteria, exist in great number and diversity.

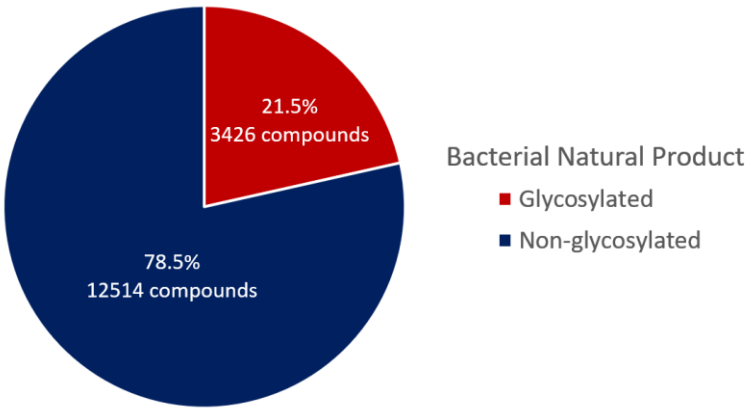

Figure 2.1. Pie chart showing numbers of glycosylated and non-glycosylated natural products produced by bacteria according to survey by Thorson.

Nature relies on enzymes such as glycosyltransferases to catalyze the formation of a glycosidic bond that links the sugar or glycone to the aglycone. Like most enzymatic reactions, enzymatic glycosylation typically proceeds with exclusive regio- and stereocontrol.[2] However, the same transformation is formidably challenging to accomplish with the same level of selectivity in a flask. This is especially true for glycosylation of complex natural products that are highly functionalized and contain multiple reactive sites. In order to prevent the formation of multiple regio- and stereoisomeric glycosides during the reaction, most synthetic strategies rely on multistep protection and deprotection sequences to achieve selective glycosylation of natural products. Nonetheless, these extra steps often also present additional synthetic challenges during the process of development and optimization. Ideally, a convergent approach based on a catalyst-controlled glycosylation reaction to selectively access glycoform of complex natural products would be more effective.

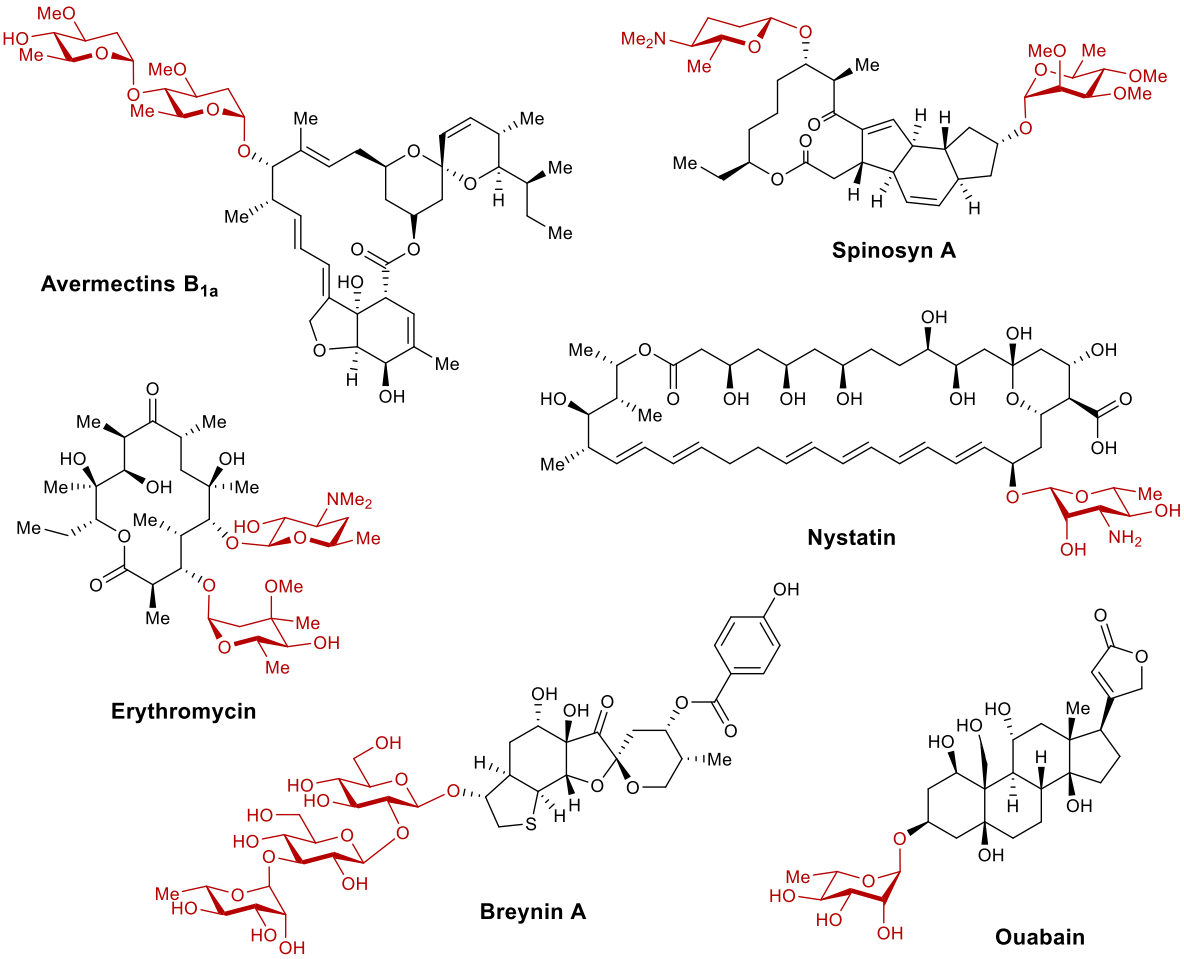

Figure 2.2. Examples of complex natural product possessing sugar side-chain.

2.2 Prior Art Related to Site-Selective Functionalization of Polyol Compounds

Many research groups have reported remarkable examples of selective functionalization of polyol compounds based on catalyst-controlled reactions (Figure 2.3). Being one of the pioneers in the field, Miller focuses on research using small peptide chain as organocatalyst to regioselectively functionalize complex natural products, such as erythromycin[3], vancomycin[4] and apoptolidin A[5]. In 2013, the Tan group reported the design of a pair of pseudo-enantiomeric organocatalysts, which catalyzed the regiodivergent mesylation or acylation of unprotected monosaccharides, and natural products, such as mupirocin and digoxin.[6] Around the same time, the Nagorny group also published their findings on the application of CPA to discriminate monosaccharide substrates with 1,2-diol for regioselective acetalization reactions.[7]

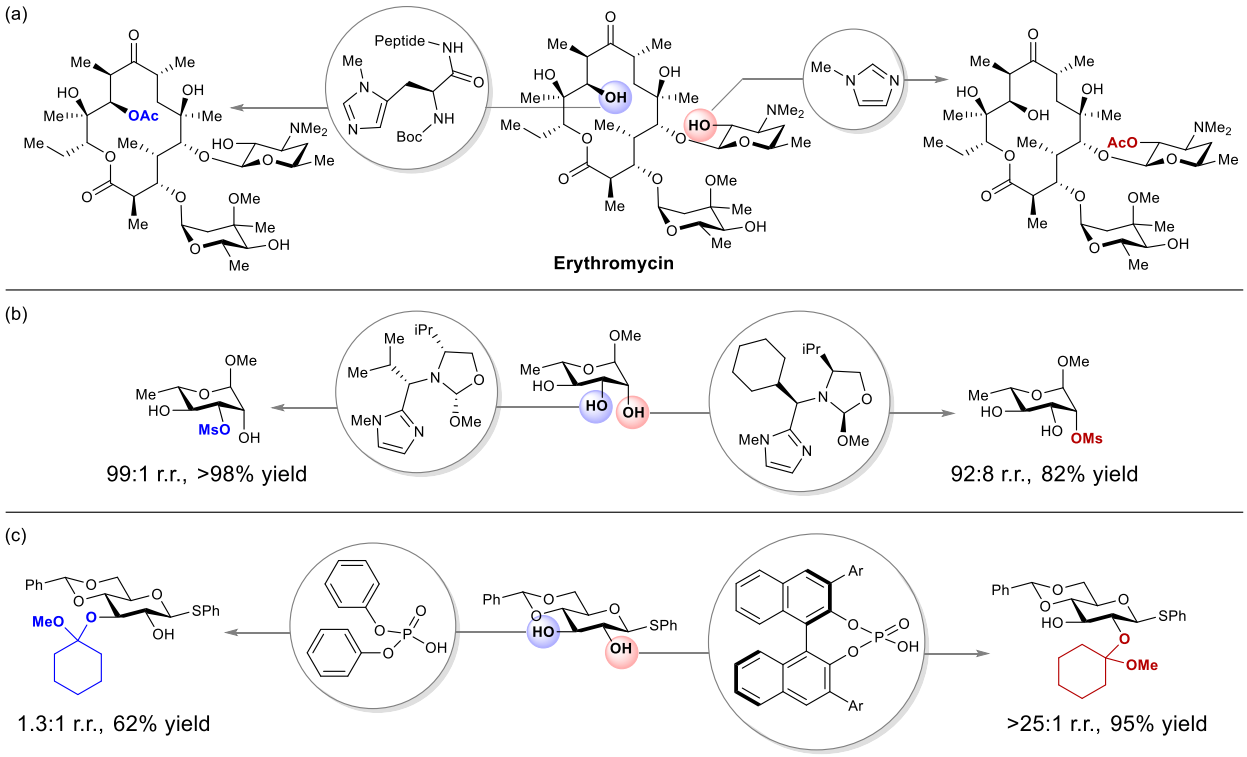

Figure 2.3. Applications of organocatalysis towards regiodivergent functionalization of poly-ol compounds reported by (a) Miller, (b) Tan, and (c) Nagorny.

Aside from the simple functionalization with common protecting groups, there are also many excellent examples of strategies focus on selective glycosylation of unprotected polyol compounds. In 2011, the Taylor group reported a highly regioselective glycosylation method using

borinic acid as the catalyst to generate disaccharides.[8] The catalyst was proposed to form a cyclic complex with monosaccharide substrate, and selectively activate one of the three hydroxy groups for glycosylation. The Montgomery group developed a method based on the formation of a silane intermediate in combination with an intramolecular aglycone delivery to selectively synthesize 1,6-linked disaccharides.[9] More recently, Miller reported their studies on selective glycosylation of polysaccharides in an aqueous solution using calcium salt as the catalyst.[10] Under the reaction conditions, sugar moiety was selectively delivered to oligosaccharide with up to 14 free hydroxy groups.

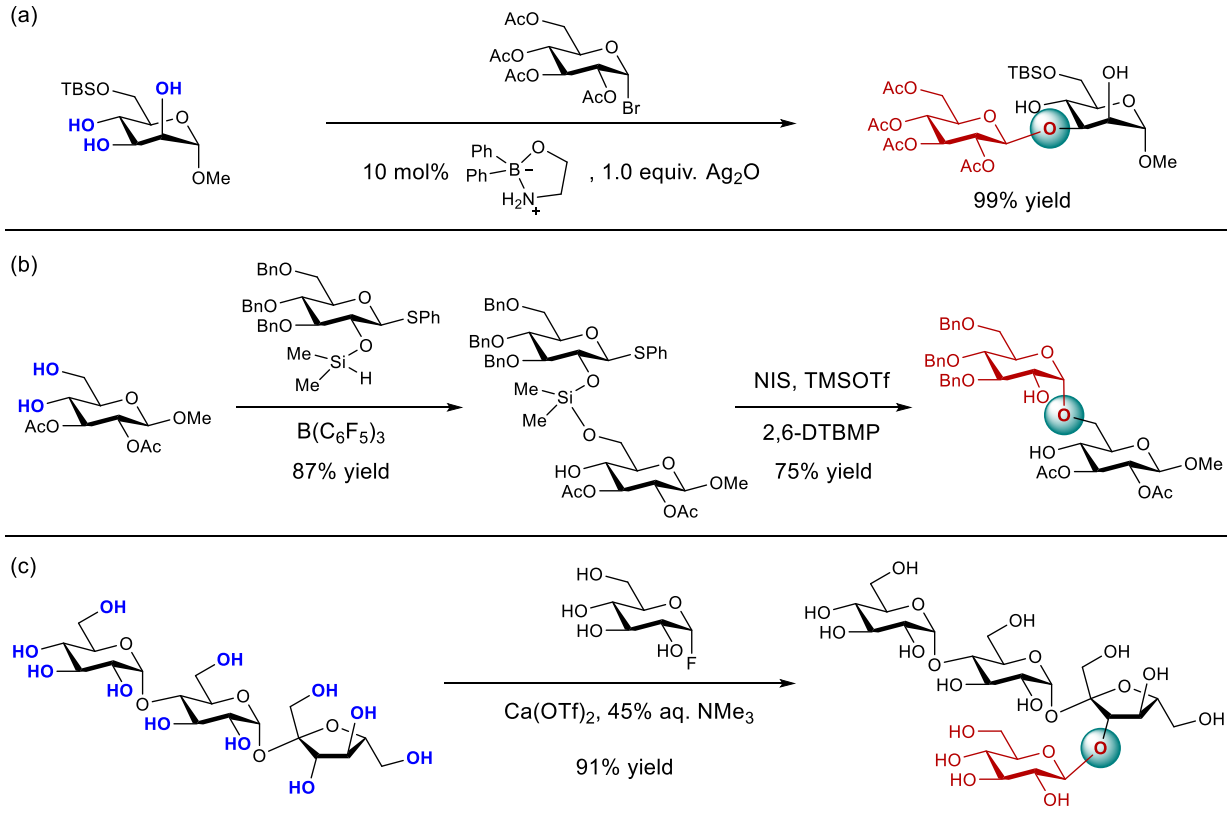

Scheme 2.1. Examples of site-selective glycosylations reported by (a) Taylor, (b) Montgomery, and (c) Miller.

A detailed survey of the literature reveals that most catalyst-controlled regioselective functionalization of polyol compounds focus on selective installation of a common protecting group. On the other hand, almost all methods for regioselective glycosylation of polyol compounds rely on substrate control for the observed selectivity. In other words, the exclusive selectivity is achieved based on enhancement of the substrate innate bias in terms of reactivity. Notably, there

is a lack of research in regioselective glycosylation of polyol compounds based on catalyst-controlled reactions.

2.3 Experimental Designs

The goal of the following studies was to develop a regiodivergent glycosylation method, which would enable access to all regioisomeric glycoforms of the same polyol compounds based on judicious selection of catalyst and reaction condition. We hypothesized that CPA would provide a chiral pocket where the glycosyl donor is activated and glycosylation reaction takes place, and the local chiral environment would lead to discrimination of hydroxy groups with different stereoelectronic properties on the acceptor for selective glycosylation. To test our hypothesis, we selected 6-deoxy-erythronolide B (6-dEB) **1** as our initial substrate. 6-dEB is medicinally important, and it has three secondary hydroxy groups with similar stereoelectronic properties, which is crucial for verifying and testing the limit of our proposed strategy.

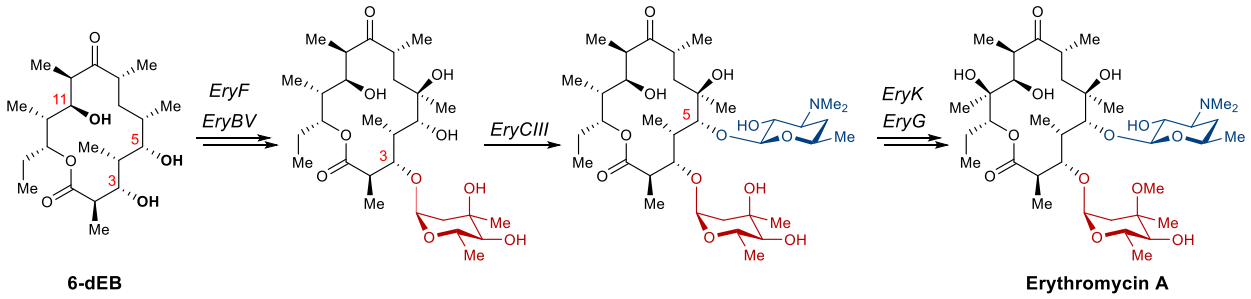

Scheme 2.2. Biosynthetic pathway of erythromycin A from 6-deoxy-erythronolide B.

6-dEB is a precursor in the biosynthesis of the 14-membered macrolide antibiotics erythromycin A and B.[11] Studies on the biogenic pathway reveal that 6-dEB undergoes sequential glycosylations first at the C3 position and then at the C5 position (Scheme 2.2). Previous attempts to replicate the selective installation of sugars on 6-dEB using engineered glycosyltransferase or glycosylation of similar macrolactones using various chemical methods were unsuccessful. In 2008, Liu reported a study on the substrate specificity of macrolide glycosyltransferase Des VII/DesVIII.[12] While the enzyme showed excellent regiospecificity in catalyzing the attachment of desosamine to various macrolactones and linear substrates, the in-vitro glycosylation of 6-dEB

catalyzed by the same enzyme led to formation of a mixtures of isomers with low conversion. (Scheme 2.3) In Woodward's total synthesis of erythromycin, the desosamine moiety was introduced to a 14-membered macrolactone intermediate through a silver triflate mediated glycosylation with a desosamine-derived thioglycoside donor.[13a] (Scheme 2.4) While the reaction produced the desired C5-glycoside as the major product, three other unidentified glycosides were also isolated. These circumstances provided additional motivation for us to develop a new method to allow the selective formation of regioisomeric glycosides from unprotected 6-dEB and to demonstrate the potential of CPA organocatalyst as a powerful tool in the selective synthesis of glycosylated natural products.

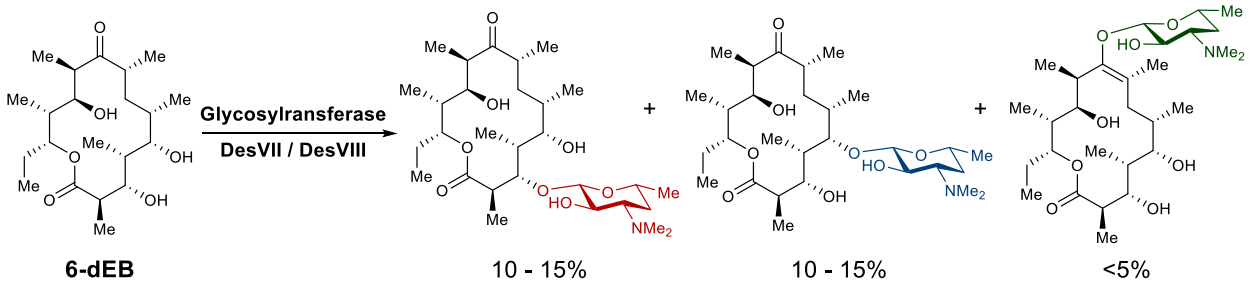

Scheme 2.3. In-vitro glycosylation of 6-dEB catalyzed by Glycosyltransferase DesVII/DesVIII.

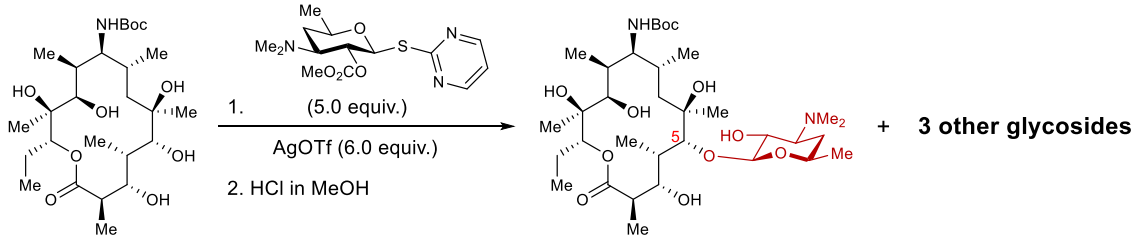

Scheme 2.4. Silver triflate mediated glycosylation of macrolactone with desosamine-derived thioglycoside donor reported by Woodward.

2.4 Glycosylation of 6-dEB Catalyzed by Achiral Lewis and Brønsted Acids

The 6-dEB used in the following studies was harvested from a culture of an *Escherichia Coli* strain that had previously been engineered and optimized for production of the macrolactone.[14] First, control experiments were carried out to establish the inherent reactivity pattern of the three hydroxy groups on 6-dEB. 6-dEB (**1**) was subjected to glycosylation reactions

with a trichloroacetimidate glycosyl donor derived from D-6-deoxyglucose **2**, and typical activators for trichloroacetimidate donor were used (Table 2.1). The reaction catalyzed by TMSOTf resulted in formation of the α-C5 glycoside **4** as the major product, along with the bis-glycosylated product **5** at the C3 and C11 positions (entry 1). BF_3•OEt_2, another common Lewis acid catalyst for trichloroacetimidate donor activation, lead to formation of the C5-glycoside as the major regioisomer, while a mixture of diastereomers with α and β glycosidic linkages were formed (entry 2). In addition, Brønsted acids such as diphenylphosphoric acid and anhydrous tosylic acid were tested; both tests still lead to the glycosylation at the C5 position preferably (entry 3 and 4). In short, the results from the glycosylation of 6-dEB with achiral Lewis and Brønsted acids as activators indicate that the C5-hydroxy group is the most reactive towards the glycosylation reactions, followed by the C3-hydroxy group. The C11-hydroxy group is the least reactive.

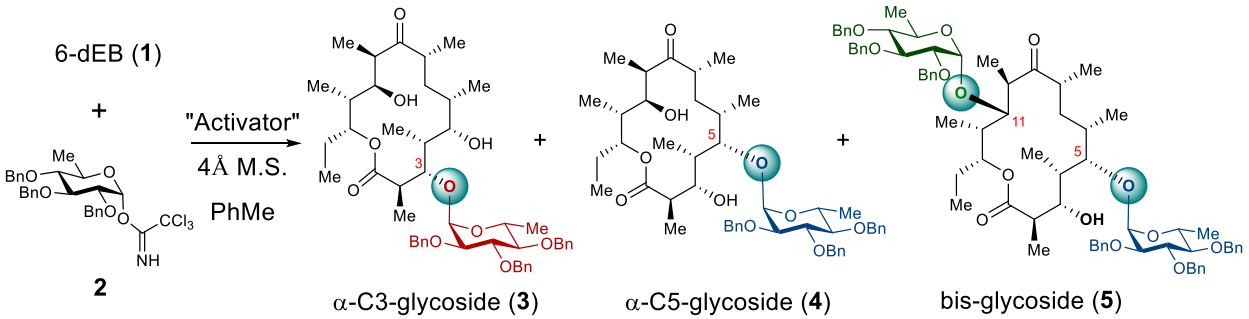

entry	Activator (mol%)	T (°C)	t (h)	Yield	3	:	4	:	5
1	TMS-OTf (20)	-20	17	57%	0	:	88	:	12
2	BF_3•OEt_2 (20)	-20	24	59%	34	:	(66)[a]	:	0
3	$(PhO)_2PO_2H$ (50)	r.t.	26	35%	15	:	85	:	0
4	*p*-TsOH (20)	r.t.	26	<10%	17	:	83	:	0

[a] Mixture of glycosides with α:β linkdge = 2.9:1

Table 2.1. Glycosylation of 6-dEB with donor **2** catalyzed by achiral Lewis and Brønsted acids.

2.5 Glycosylation of 6-dEB Catalyzed by Chiral Brønsted Acids

With the baseline reactivity established, subsequent experiments focused on evaluating various chiral Brønsted acids with the goal of enhancing the selectivity for glycosylation at the

C5-hydroxy group of 6-dEB (Table 2.2). Reactions with catalysts **6** – **17** (entries 1 – 16) in nonpolar solvents identified catalyst **(S)-17** (entry 16) as the optimum catalyst for promoting the formation of α-C5 glycoside **4** of 6-dEB with an excellent yield and selectivity. When the catalyst **(R)-17** (with the same substituent but opposite chirality) was used, the reaction lead to the formation of 1:1 mixtures of C3 and C5-glycosides, but the formation of the α-glycosidic linkage was retained (entry 15). These combined results supported our initial hypothesis that the chirality of the CPA catalyst (or the chiral pocket it possesses) had a significant impact on the regioselectivity outcome of the glycosylation of polyol compounds such as 6-dEB. During the screening process, a commercially available chiral bis-sulfonimide acid, **(R)-18** developed by List,[15] was also found to promote exclusive glycosylation at the C5-hydroxy group, albeit in lower yield (entry 17).

In the biosynthesis of erythromycin A, 6-dEB first undergoes glycosylation at the C3 position. However, the results from our control experiments indicate that such a transformation would be difficult to accomplish in a flask since the C5-hydroxy group of 6-dEB is inherently more reactive. Therefore, the goal for the subsequent set of experiments was to identify th catalysts that could mimic the functionality of glycosyltransferase and catalyze the glycosylation of the less reactive C3-hydroxy group. Previous experiments have shown that CPA with (R) chirality could override the inherent reactivity bias of C5-hydroxy group, to a certain extend. Therefore, CPAs with (R) chirality but different substituents at the 3,3'-position were tested next (Table 2.2). As the meta-substituents of the 3,3'-phenyl ring changes from $-SF_5$ > $-CF_3$ > -Cl > -F groups, we observed a gradual increase in regioselectivity favoring glycosides at the C3-position (entries 12, 15, 19 and 20). Furthermore, we observed even higher regioselectivity for C3-glycosylation when the backbone of the meta-fluoro substituted CPA was switched from a BINOL to a SPINOL backbone (entries 21 – 24). Previous computational studies suggested that SPINOL-based CPA, which has a rigid spirobiindane backbone, is better at differentiating the diastereomeric transition states, and consequently leads to higher selectivity.[16]

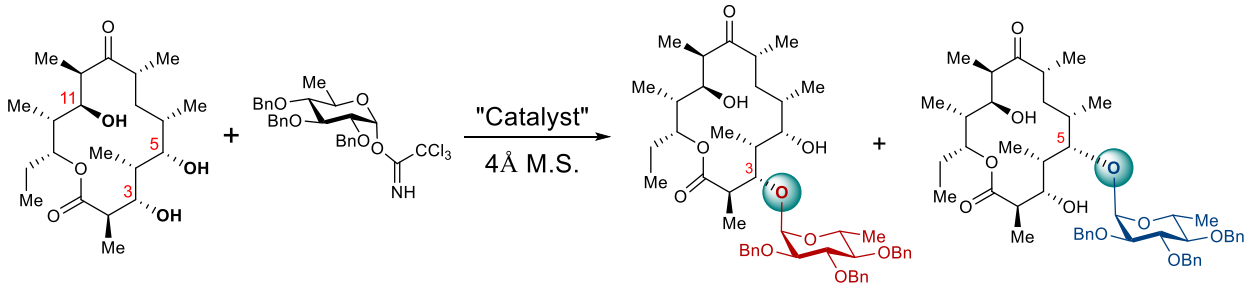

6-dEB (**1**) **2** α-C3-glycoside (**3**) α-C5-glycoside (**4**)

entry	Catalyst (mol%)	Solvent (conc.)	T (°C)	t (h)	Yield	3 : 4
1	**(R)-6** (20)	CH_2Cl_2 (0.05 M)	r.t.	30	13%	13 : 87
2	**(R)-7** (20)	CH_2Cl_2 (0.05 M)	r.t.	30	13%	17 : 83
3	**(R)-8** (20)	PhMe (0.10 M)	r.t.	24	57%	25 : 75
4	**(R)-9** (20)	PhMe (0.10 M)	r.t.	24	57%	40 : 60
5	**(R)-10** (20)	PhMe (0.10 M)	r.t.	24	48%	21 : 79
6	**(R)-11** (20)	CH_2Cl_2 (0.05 M)	r.t.	30	<5%	40 : 60
7	**(R)-12** (20)	PhMe (0.10 M)	r.t.	24	57%	36 : 64
8	**(R)-13** (20)	PhMe (0.10 M)	r.t.	24	34%	37 : 63
9	**(R)-14** (20)	PhMe (0.10 M)	r.t.	24	50%	23 : 77
10	**(R)-15** (20)	CH_2Cl_2 (0.05 M)	r.t.	24	95%	13 : 87
11	**(S)-15** (20)	CH_2Cl_2 (0.05 M)	r.t.	24	51%	4 : 96
12	**(R)-16** (20)	PhMe (0.10 M)	r.t.	24	46%	6 : 94
13	**(S)-16** (20)	PhMe (0.10 M)	r.t.	24	69%	3 : 97
14	**(R)-17** (20)	PhMe (0.20 M)	r.t.	30	82%	35 : 65
15	**(R)-17** (20)	CH_2Cl_2 (0.05 M)	r.t.	26	50%	50 : 50
16	**(S)-17** (20)	PhMe (0.20 M)	r.t.	30	98%	1 : 99
17	**(R)-18** (20)	PhMe (0.10M)	r.t.	24	71%	1 : 99
18	**(R)-19** (20)	PhMe (0.10 M)	r.t.	24	80%	52 : 48
19	**(R)-20** (20)	CH_2Cl_2 (0.05 M)	r.t.	48	51%	69 : 31
20	**(R)-21** (20)	PhMe (0.10 M)	r.t.	48	75%	7 : 93
21	**(S)-21** (20)	PhMe (0.10 M)	r.t.	48	54%	60 : 40
22	**(S)-21** (20)	$PhCF_3$ (0.10 M)	r.t.	64	83%	63 : 37
23	**(S)-21** (20)	CH_2Cl_2 (0.10 M)	r.t.	64	57%	71 : 29
24	**(S)-21** (30)	CH_2Cl_2 (0.10 M)	r.t.	72	82%	73 : 27

Table 2.2. Glycosylation of 6-dEB (**1**) with glycosyl donor **2** catalyzed by chiral Brønsted acids.

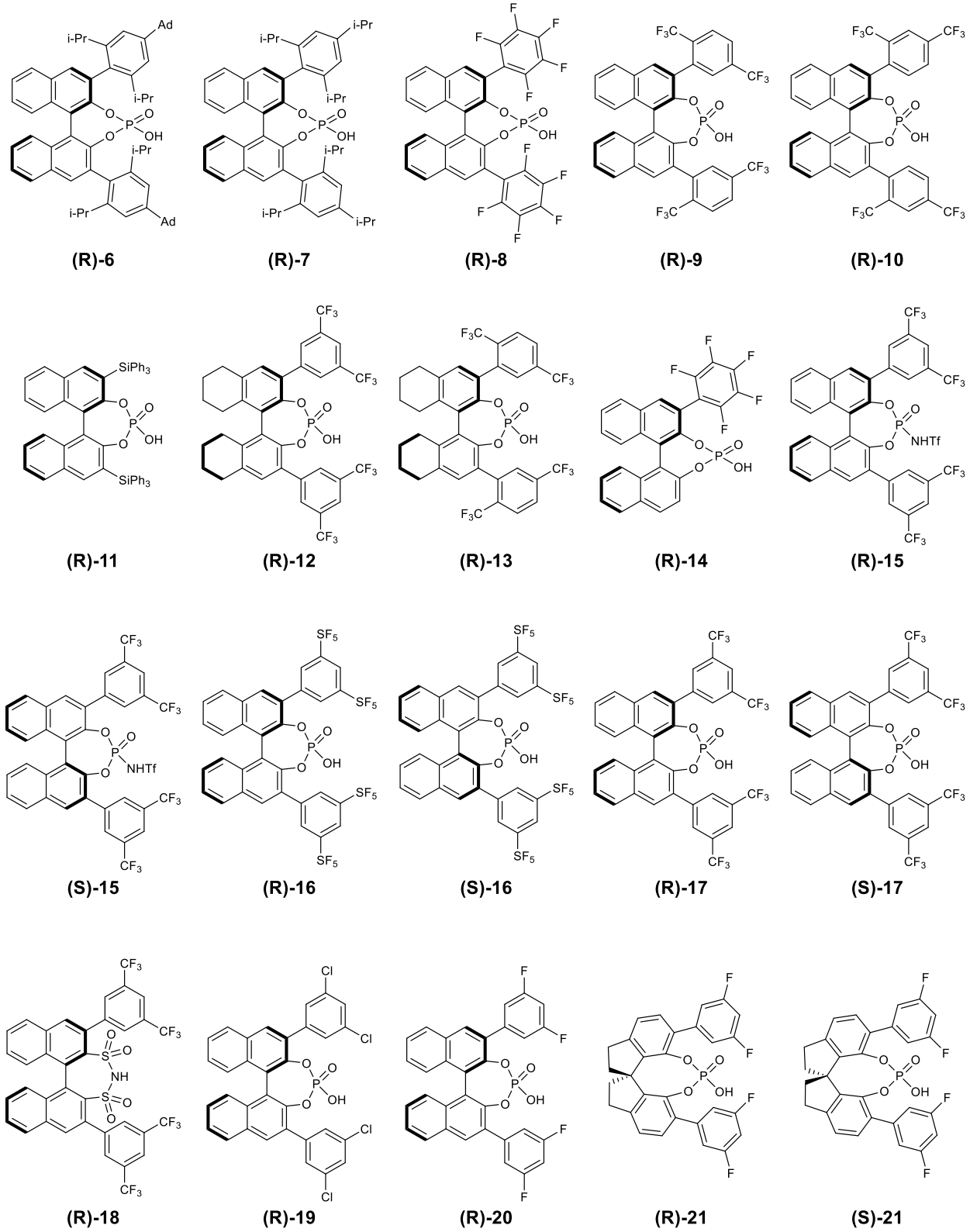

Figure 2.4. Chiral Brønsted acids screened for regioselective glycosylations of macrolactones.

After the optimum catalysts for selective glycosylation at the C3 and C5-position were identified, we proceeded to investigate the scope and limitations of the method (Table 2.3). When 6-dEB (**1**) was subjected to TMSOTf catalyzed glycosylation with the D-Fucose derived glycosyl donor **22**, it resulted, as expected, in a selective formation of the C5-glycoside **24** and a complex mixture of bis-glycosylated products (entry 1). In contrast, the use of catalyst **(S)-21** lead to the formation of the C3-glycoside **23** that was not observed in the control experiment (entry 2). Just like the glycosylation with D-6-deoxyglucose donor **2**, catalyst **(S)-17** lead to exclusive formation of C5-glycoside **24** with no traces of a bis-glycosylated product (entry 3). However, we did observe erosion in diastereoselectivity for the reaction.

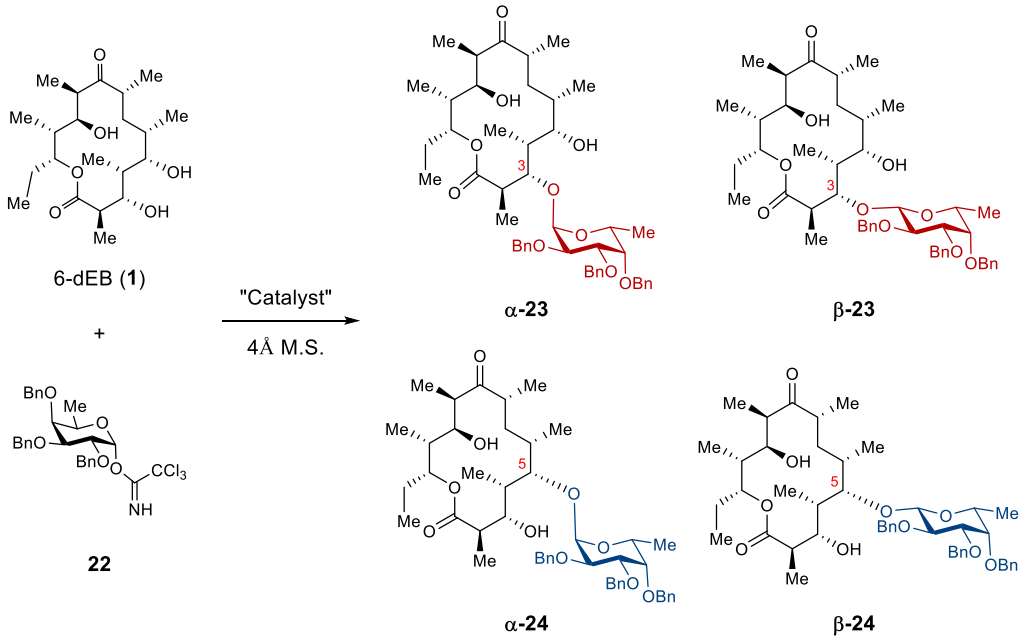

entry	Catalyst (mol%)	Solvent (conc.)	T (°C)	t (h)	Yield	23 (α:β)	:	24 (α:β)	:	bis-gly.
1	TMS-OTf (20)	PhMe (0.05 M)	-20	17	92%	0	:	69 (1.8:1)	:	31
2	**(S)-17** (20)	PhMe (0.20 M)	r.t.	48	82%	1	:	99 (1.7:1)	:	0
3	**(S)-21** (30)	CH_2Cl_2 (0.10 M)	r.t.	72	87%	56 (α-only)	:	44 (1:1.2)	:	0

Table 2.3. Glycosylation of 6-dEB with D-Fucose derived glycosyl donor **22**.

In addition, the benzylated glycoside can be easily converted to the fully deprotected macrolactone glycoside through hydrogenolysis over Pd/C. (Scheme 2.5)

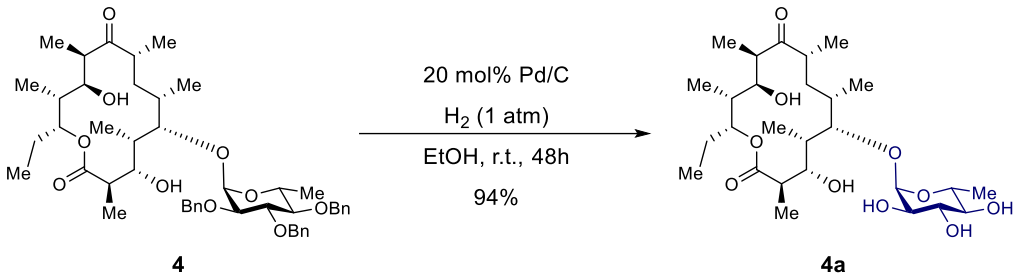

Scheme 2.5. Debenzylation of 6-dEB glycoside under hydrogenolysis condition.

2.6 Glycosylation of Oleandomycin-derived Macrolactone Catalyzed by Chiral Brønsted Acids

To further demonstrate the applicability of the strategy, we targeted selective glycosylation of other macrolatone as our next substrate. We identified a 14-membered macrolactone **25**, derived from oleandomycin, that is structurally similar to 6-dEB. Interestingly, macrolactone **25** exhibited a different reactivity profile compared to the reactions with 6-dEB (Table 2.4). When it was subjected to the glycosylation with the D-6-deoxyglucose donor **2** and TMSOTf, macrolactone **25** was converted to the C5-glycoside **28** and the hemiacetalized C3-glycoside **29** (entry 1). The results indicated that the C3 and C5-hydroxy groups of **25** were almost equally reactive. However, the resulting C3-glycoside **27** was unstable and subsequently underwent intramolecular acetalization to form the by-product **29**. When the reaction was promoted by catalyst **(S)-21** or **(R)-21**, the C3-glycoside **27** was formed as the major product for both cases, but **(R)-21** led to higher regioselectivity (entry 2 and 3). Through further screening and optimization, catalyst **(R)-18** was found to be the optimum promoter for the selective glycosylation of macrolactone **25** at the C5-position (entry 4).

Even though switching the substrate to macrolactone **25** required re-screening of the catalyst, the regioselecitivity profile exhibited by the identified catalysts was conserved when **25** was subjected to glycosylation with different sugar donor (Table 2.4). When **25** was coupled with the D-fucose derived trichloroacetimidate donor **22**, catalyst **(R)-21** promoted the formation of β-C3-glycoside **30** with excellent regio- and diastereoselectivity (entry 6). Similarly, catalyst **(R)-18** led to selective glycosylation at the C5-hydroxy group (entry 7). Similar trends were observed for glycosylation of macrolactone **25** with the L-fucose derived trichloroacetimidate donor **26** (entry 8 and 9).

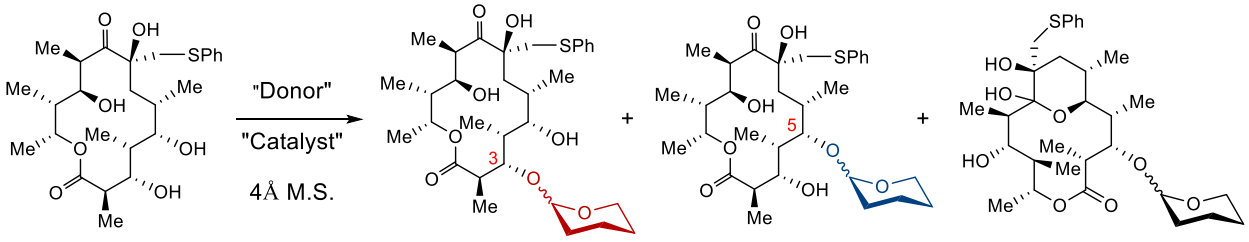

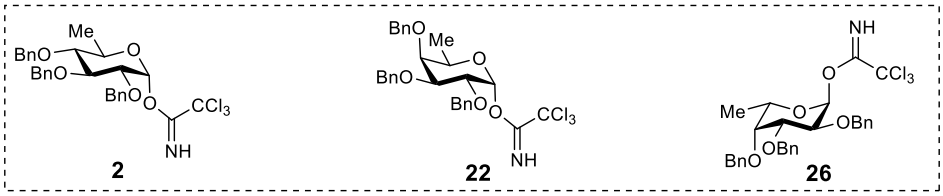

entry	Donor	Catalyst (mol%)	Solvent (conc.)	T (°C)	t (h)	Yield	C3-gly. (α:β)	:	C5-gly. (α:β)	:	By-prod. (α:β)
							27		**28**		**29**
1	**2**	TMS-OTf (20)	PhMe (0.05 M)	-20	18	61%	0	:	51 (1.6:1)	:	49 (1:1)
2	**2**	**(S)-21** (30)	PhMe (0.30 M)	r.t.	48	60%	65 (3.4:1)	:	35 (1:1)	:	0
3	**2**	**(R)-21** (20)	PhMe (0.30 M)	r.t.	48	80%	71 (1:1)	:	29 (1.9:1)	:	0
4	**2**	**(R)-18** (20)	PhMe (0.20 M)	r.t.	24	79%	30 (4:1)	:	70 (3.4:1)	:	0
							30		**31**		**32**
5	**22**	TMS-OTf (20)	PhMe (0.05 M)	-20	18	52%	0	:	54 (2.6:1)	:	46 (1.2:1)
6	**22**	**(R)-21** (20)	PhMe (0.30 M)	r.t.	48	93%	91 (β-only)	:	9 (n.d.)	:	0
7	**22**	**(R)-18** (20)	PhMe (0.20 M)	r.t.	24	82%	29 (1.2:1)	:	71 (1:1.8)	:	0
							33		**34**		**35**
8	**26**	TMS-OTf (20)	PhMe (0.05 M)	-20	18	82%	0	:	53 (1.8:1)	:	47 (α-only)
9	**26**	**(R)-21** (20)	PhMe (0.30 M)	r.t.	48	76%	88 (1:2)	:	12 (α-only)	:	0

Table 2.4. Glycosylation of Oleandomycin-derived macrolactone.

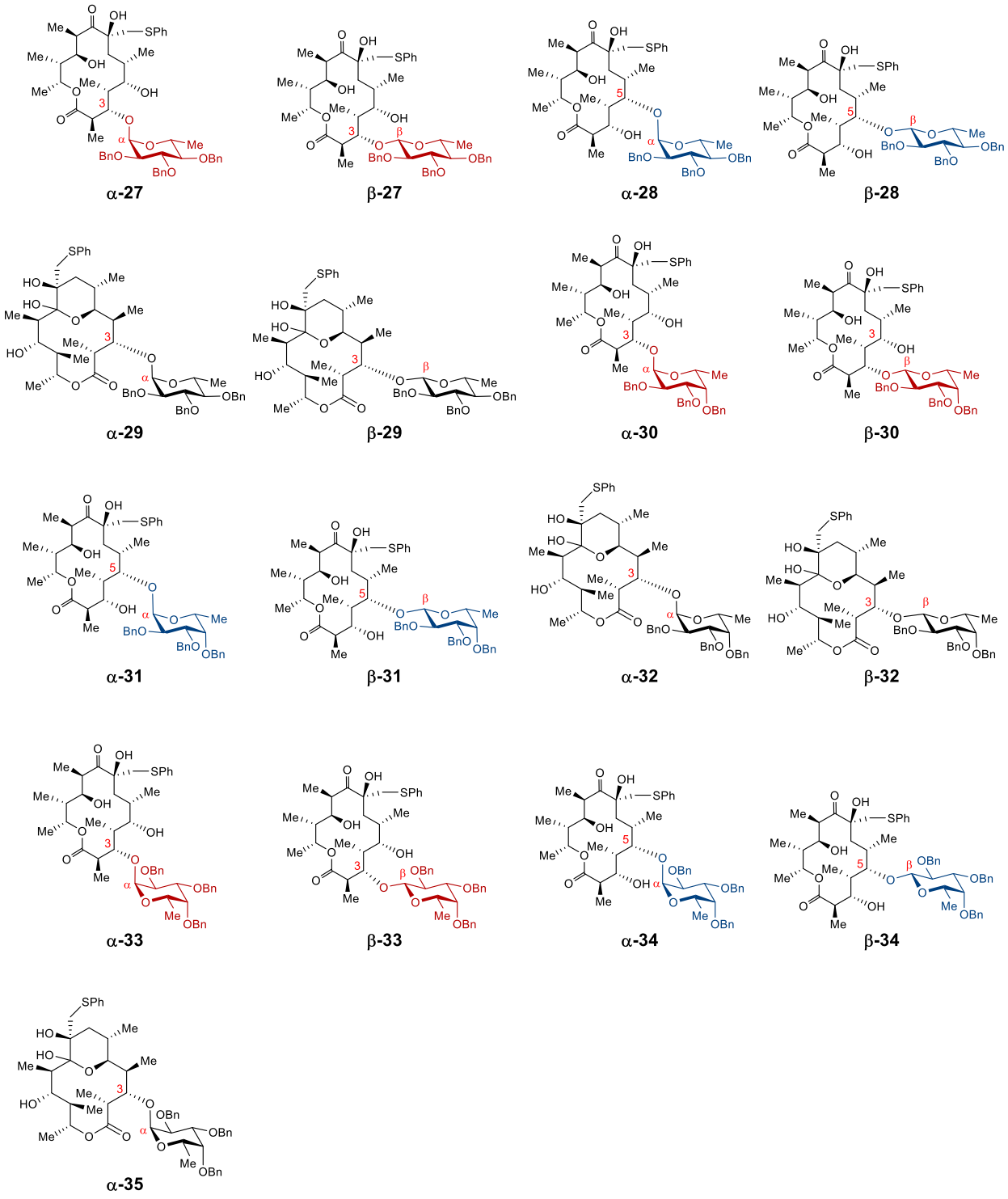

Figure 2.5. Structures of glycosides generated from glycosylation of macrolactone **25**.

2.7 Glycosylation of 6-dEB with Desosamine-derived Trichloroacetimidate Donor

Next, we studied the glycosylation of 6-dEB with a trichloroacetimidate donor derived from desosamine, which is the native sugar moiety on erythromycin. When 6-dEB was subjected to glycosylation with desosamine donor **36** and BF_3•OEt_2 as activator, we observed formation of a mixture of C3- and C5-glycosides (**37a** and **37b**) in 43:57 regioisomeric ratio. (Table 2.5, entry 1) Similar regioisomeric ratio (**37a:37b** = 31:69 r.r.) was observed when diphenylphosphoric acid was used as the activator (entry 2).

When catalyst **(S)-17** was used to catalyze the glycosylation of 6-dEB with desosamine donor **36**, we observed a significant improvement in the regioisomeric ratio, up to **37a:37b** = 16:84 r.r. (entry 3) However, same regioisomeric ratio was obtained when catalyst **(R)-17** was used in the reaction. (entry 4) In addition, the reactions also resulted in formation of bis-glycosylated product (~10%) and orthoester (~15%) by-product.

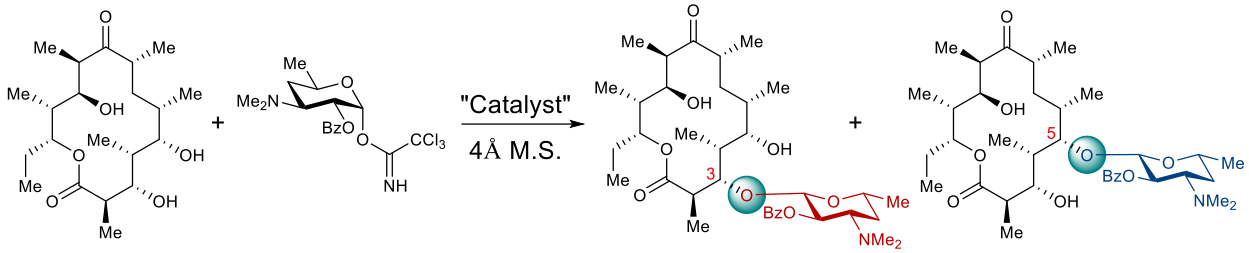

6-dEB **36** **37a** **37b**

Entry	Activator (mol%)	Solvent (conc.)	T (°C)	t (h)	Yield	37a	:	37b
1	BF_3•OEt_2 (130)	CH_2Cl_2 (0.02M)	-30	17	60%	43	:	57
2	PhO_2PO_2H (50)	PhMe (0.1M)	r.t.	48	46%	31	:	69
3	**(S)-17** (20)	PhMe (0.1M)	r.t.	48	53%	16	:	84
4	**(R)-17** (20)	PhMe (0.1M)	r.t.	48	55%	16	:	84

Table 2.5. Glycosylation of 6-dEB with desosamine-derived trichloroacetimidate donor.

2.8 Mechanistic Studies on Glycosylation Catalyzed by Chiral Brønsted Acids

The results from the glycosylation of 6-dEB (**1**) and macrolactone **25**, catalyzed by chiral Brønsted acid, suggests that the catalyst has a significant control over the regioselectivity outcome of the reaction. To better understand the reaction mechanism, we monitored the reaction of macrolactone **25** with donor **22** under a CPA catalyzed condition by NMR (Figure 2.6). We observed the selective formation of the C3-glycoside **β-30** as expected at various time intervals, and there were no changes in the product's regioisomeric composition throughout the experiments. The results indicated that we did not observe high regioselectivity because the minor regioisomer underwent decomposition under the reaction conditions.

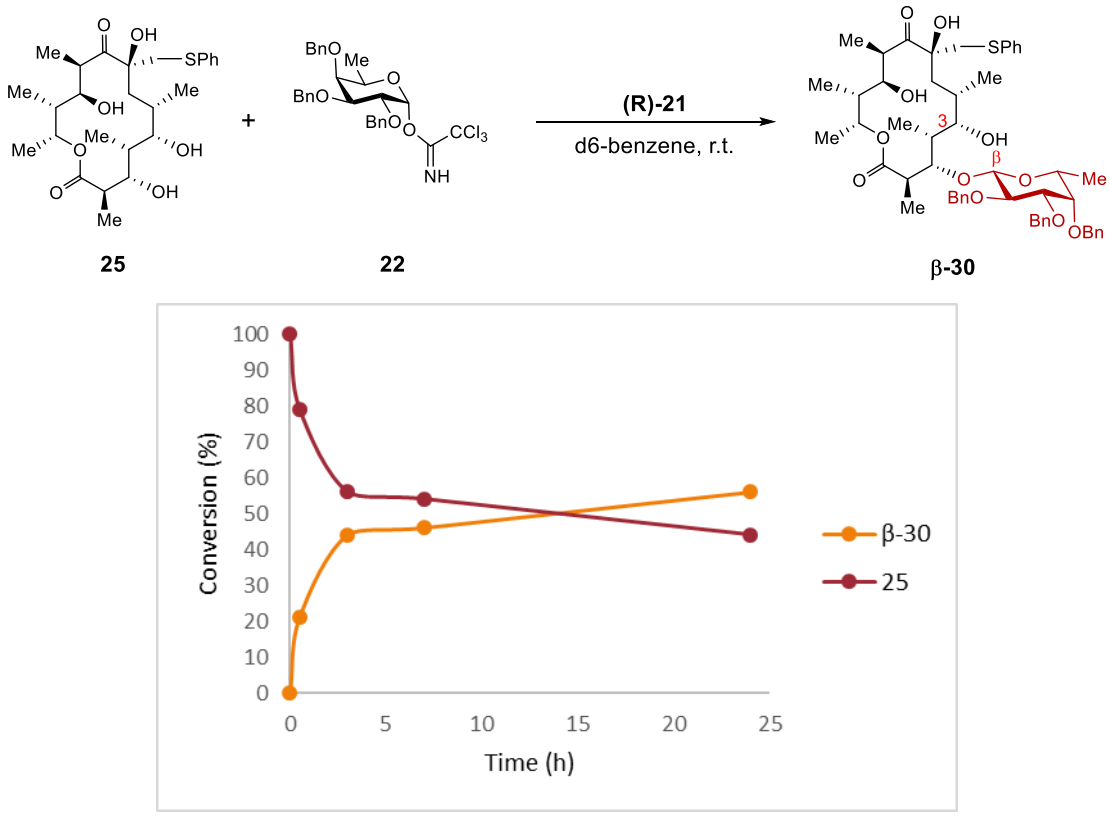

Figure 2.6. Conversion of **25** to glycoside **β-30** monitored by NMR.

Furthermore, the isolated C3-glycoside **β-30** was re-subjected to reaction condition with catalyst **(R)-18**, which favors formation of the C5-glycoside **31**, and we did not observe any formation of the C5-glycoside **31** at the end of the reaction. The experiment ruled out the

possibility that the regioisomeric glycosides undergo isomerization in the presence of chiral Brønsted acid.

To further elucidate the mechanism of the reaction, we turned to computational analysis, which was done in cooperation with the Zimmerman group. Modern reaction path-searching algorithms[17] were used to study a simplified model system of the glycosylation reaction (Figure 2.7). The result of that analysis suggested that most likely the α-trichloroacemtimidate donor (**38**) first underwent a facile S_N2-like displacement by the phosphoric acid to generate a covalent β-phosphate intermediate (**38a**). The glycosyl phosphate then underwent another S_N2-like substitution by the alcohol nucleophile to generate the α-glycoside product (**38b**). The computed mechanism explained the experimental results, where α-glycoside **3** and **4** were formed in the reaction of 6-dEB with the α-trichloroacetimidate donor **2** under CPA catalyzed reaction conditions. The formation of the retentive product was most likely due to a double inversion mechanism.

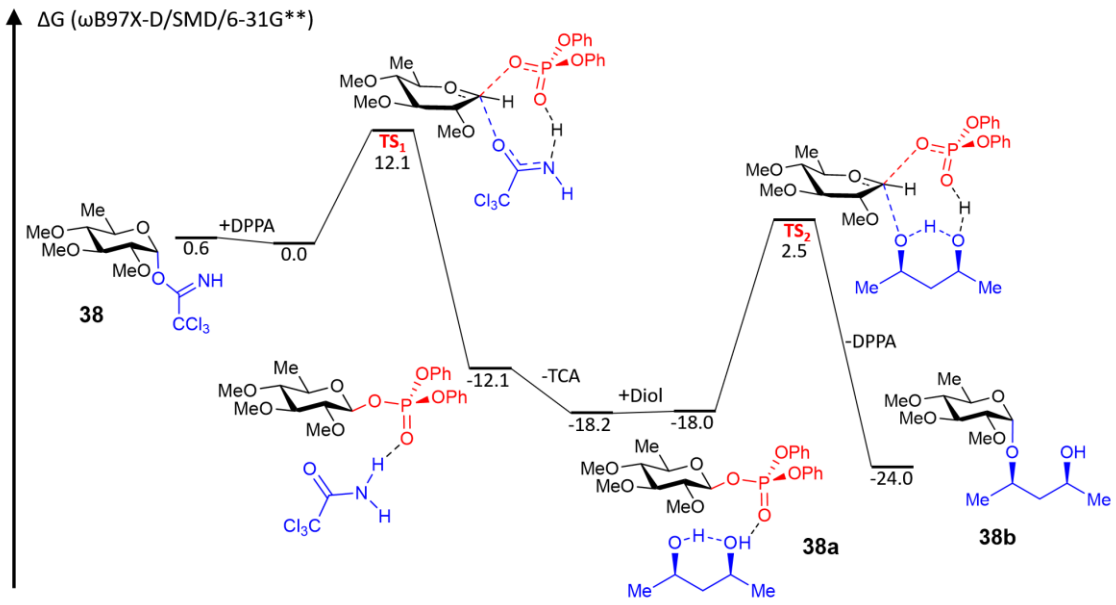

Figure 2.7. Computed reaction mechanism for glycosylation of trichloroacetimidate donor catalyzed by phosphoric acid.

Since the computational analysis predicted that the glycosyl phosphate was relatively stable, we decided to verity the formation of the intermediate in the actual reaction. When trichloroacetimidate donor **2** was mixed with CPA **(R)-21** in deuterated toluene, we observed the

formation of a new species by NMR that was consistent with a covalent phosphate intermediate (Figure 2.8). The 6 Hz coupling constant of the anomeric carbon signal in ^{13}C NMR was consistent with the two-bond carbon-phosphorus coupling reported for similar compounds. The one-bond coupling between anomeric carbon and its hydrogen (166 Hz) suggested the β-linkage configuration.[18] When excess deuterated methanol was added to the solution containing the β-glycosyl phosphate **39**, α-glycoside **40** was formed as the major product. In summation, the experimental results supported the computed mechanism in which the glycosylation reaction proceeded through the formation of a phosphate intermediate and the double inversion substitutions.

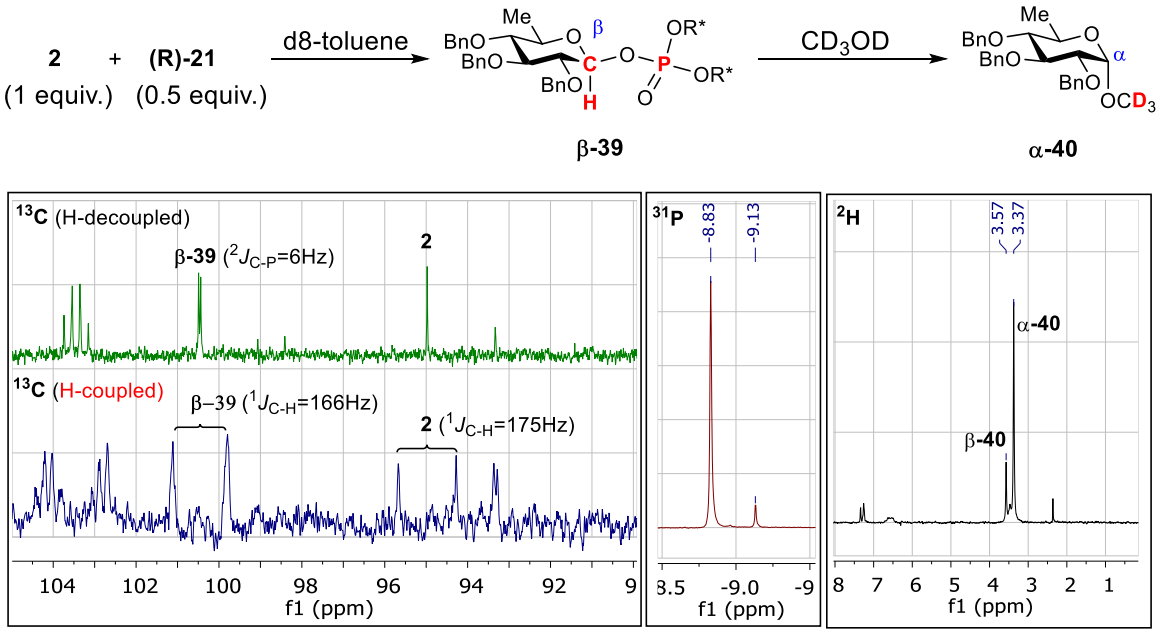

Figure 2.8. Formation of glycosyl phosphate from reaction of glycosyl donor **2** and CPA **(R)-21**.

While the investigation so far explained the results we observed for glycosylation of 6-dEB (**1**) with the D-6-deoxyglucose donor **2**, the low diastereoselectivity that we observed when the fucose derived donor **22** was used instead encouraged us to probe the mechanism further. In this case, the L-fucose derived tricholoacetimidate donor **26** was mixed with CPA **(R)-21**, and the reaction generated a glycosyl phosphate intermediate **41** with the α-configuration (Figure 2.9). The α-glycosyl phosphate **41** then underwent substitution with deuterated methanol to produce β-glycosides **42**. Since the α-trichloroacetimidate donor derived from 6-deoxyglucose and fucose led to formation of the glycosyl phosphate with opposite anomeric configuration, these results

suggested that the mechanism for the formation of anomeric phosphate from trichloroacetimidates may not always be S_N2-like.

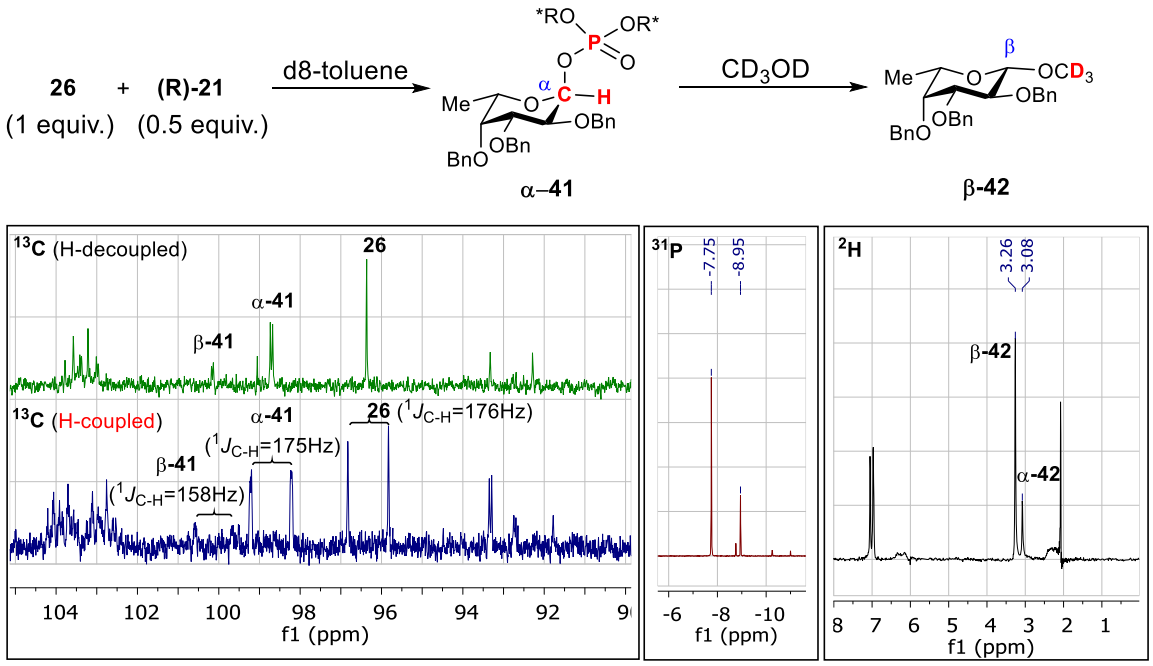

Figure 2.9. Formation of glycosyl phosphate from reaction of donor **26** and CPA **(R)-21**.

To probe the effect of the anomeric configuration of the trichloroacetimidate donor on the diastereoselectivity outcome, macrolactone **25** was subjected to CPA catalyzed glycosylation with α-trichloroacetimidate (**α-22**) and β-trichloroacetimidate (**β-22**) derived from D-fucose (Scheme 2.6). The same regio- and diastereoselectivity was observed for both reactions, which suggested both reactions proceeded through the formation of the same intermediate. Altogether, the results indicated that the mechanism for the formation of anomeric phosphate was driven by the configuration of the sugar. Furthermore, the results also implied that the diastereoselectivity outcome of the glycosylation reaction was partly determined by the stereoselectivity of the phosphate intermediate formation step.

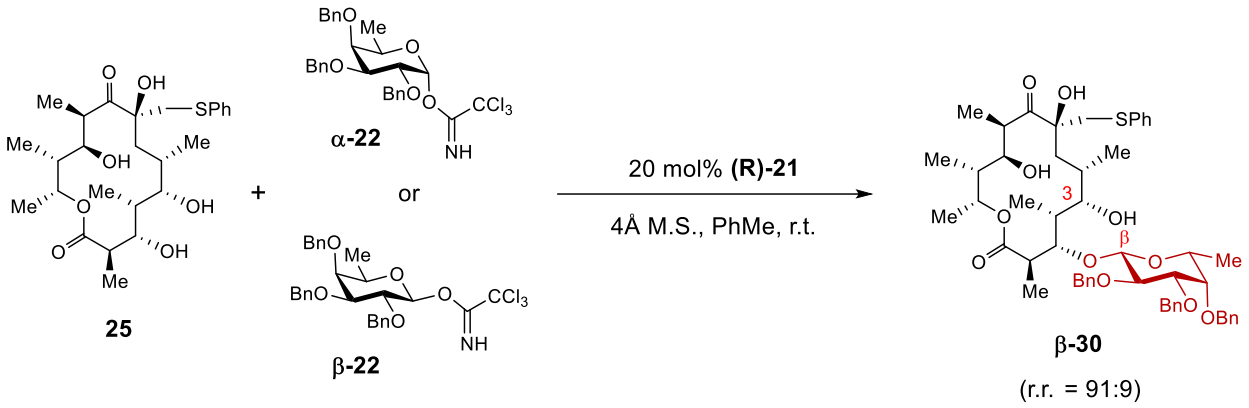

Scheme 2.6. Glycosylation of **25** with D-fucose derived α- or β-trichloroacetimidate donor under the same CPA catalyzed condition.

2.9 Conclusion

In summary, the work described in this chapter represents the first example of a chiral catalyst controlled regiodivergent glycosylation of polyol compounds. The method is especially useful for the synthesis of regioisomeric glycosides of 6-dEB and other macrolactone. More importantly, all the results we gathered supported our initial hypothesis that chiral Brønsted acid can be used to control the regioselectivity of the glycosylation reaction with trichloroacetimidate donors. While the change in macrolactone substrate required reevaluation of the catalysts, the catalysts identified for selective glycosylation for specific macrolactone exhibited a consistent trend in the regioselectivity profile that tolerates changes in the structure of the sugar donor. Finally, mechanistic studies and computational analysis helped us to elucidate the mechanism of the reaction, which involved formation of an anomeric phosphate intermediate. We believe that all the important insights generated in this study will greatly facilitate future development of similar methods.

2.10 Experimental Information

General Methods

All reagents and solvents were purchased from Sigma-Aldrich, Fisher Scientific, and were used as received without further purification unless specified. 4Å molecular sieve was activated prior to use by heating under reduced pressure. Heating was achieved by use of a silicone bath with heating controlled by electronic contact thermometer. Cooling was achieved by use of cryocool machine. Deionized water was used in the preparation of all aqueous solutions and for all aqueous extractions. Solvents used for extraction and chromatography were ACS or HPLC grade. Purification of reactions mixtures was performed by flash chromatography using SiliCycle SiliaFlash P60 (230-400 mesh).

^{1}H NMR spectra were recorded on Varian vnmrs 700 (700 MHz), Varian vnmrs 500 (500 MHz), Varian INOVA 500 (500 MHz) or Varian MR400 (400 MHz) spectrometers and chemical shifts (δ) are reported in parts per million (ppm) with solvent resonance as the internal standard ($CDCl_3$ at δ 7.26, C_6D_6 at δ 7.16). Data are reported as (br = broad, s = singlet, d = doublet, t = triplet, q = quartet, m = multiplet; coupling constant(s) in Hz; integration). Proton-decoupled ^{13}C NMR spectra were recorded on Varian vnmrs 700 (700 MHz), Varian vnmrs 500 (500 MHz), Varian INOVA 500 (500 MHz) or Varian MR400 (400 MHz) spectrometers and chemical shifts (δ) are reported in ppm with solvent resonance as the internal standard ($CDCl_3$ at δ 77.16, C_6D_6 at 128.06). High resolution mass spectra (HRMS) were recorded on Micromass AutoSpec Ultima or VG (Micromass) 70-250-S Magnetic sector mass spectrometers in the University of Michigan mass spectrometry laboratory. Infrared (IR) spectra were recorded as thin film on a Perkin Elmer Spectrum BX FT-IR spectrometer. Absorption peaks were reported in wavenumbers (cm^{-1}). Optical rotations were measured in a solvent of choice on a JASCO P-2000 or Autopol III digital polarimeter at 589 nm (D-line).

Production of 6-deoxy-Erythronolide B (6-dEB)

The *E. coli* strain TB3 (pBP130/pBP144)[14b] was generously provided as a gift from Dr. Blaine Pfeifer (SUNY Buffalo) and was used to access the macrolactone 6-deoxyerythronolide B (6-dEB) via fermentation. Individual colonies plated on LB-agar containing kanamycin (50 μg/mL) and

ampicillin (100 μg/mL) were selected for overnight growth at 37 °C in 10 mL of LB supplemented with the same antibiotics. 6 x 1 L of 6-dEB production medium (2.8 L baffled Fernbach flasks) were inoculated with the 10 mL overnight seed cultures and incubated at 37 °C (180 rpm). When OD_{600} = 0.6-1.0, the cultures were allowed to cool at room temperature (~30 min) before IPTG (0.1 mL of 1 M stock solution), sodium propionate (20 mL of 1 M stock solution at pH 7.6), and Antifoam B (3 mL of 50% (v/v) stock solution) were added to initiate 6-dEB production. The cultures were subsequently incubated at 22 °C (180 rpm) for 5-7 days prior to centrifugation at 7550 x g for 15 min to remove cells. The resulting supernatant was extracted by incubating with Amberlite XAD16 resin (30 g of washed wet resin per 1 L of culture supernatant) overnight with shaking. The resin was collected, rinsed with water, and extracted with 3 x 100 mL of ethyl acetate (per 30 g of resin). The combined organic extracts were washed with brine and dried over anhydrous Na_2SO_4. Solvent was removed under reduced pressure to yield crude 6-dEB (**1**), which was purified by flash column chromatography on silica gel (EtOAc:Hexanes, 30:70 v/v; followed by MeOH:CH_2Cl_2, 2:98 v/v).

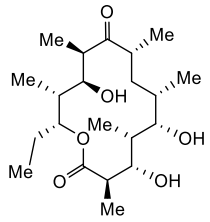

6-dEB (**1**)

^{1}H NMR (700 MHz, $CDCl_3$) δ 5.15 (dd, *J* = 9.6, 2.7 Hz, 1H), 4.05 – 3.96 (m, 1H), 3.92 (d, *J* = 10.4 Hz, 1H), 3.87 (s, 1H), 3.68 (d, *J* = 10.0 Hz, 1H), 2.86 (s, 1H), 2.82 – 2.72 (m, 2H), 2.62 (ddd, *J* = 12.9, 6.4, 3.5 Hz, 1H), 2.03 (dd, *J* = 11.9, 6.8 Hz, 2H), 1.87 (q, *J* = 6.4 Hz, 1H), 1.82 (ddd, *J* = 14.2, 9.6, 7.2 Hz, 1H), 1.77 – 1.71 (m, 1H), 1.67 (ddd, *J* = 14.3, 11.2, 3.5 Hz, 1H), 1.52 (dtd, *J* = 14.7, 7.4, 4.0 Hz, 1H), 1.30 (d, *J* = 6.7 Hz, 3H), 1.26 (td, *J* = 13.6, 4.2 Hz, 1H), 1.07 (d, *J* = 7.0 Hz, 3H), 1.06 (d, *J* = 4.1 Hz, 3H), 1.05 (d, *J* = 4.9 Hz, 3H), 1.02 (d, *J* = 6.8 Hz, 3H), 0.93 (t, *J* = 7.4 Hz, 3H), 0.89 (d, *J* = 7.0 Hz, 3H).

^{13}C NMR (176 MHz, $CDCl_3$) δ 213.7, 178.5, 79.7, 76.6, 76.4, 71.1, 44.1, 43.6, 40.7, 39.4, 37.8, 37.6, 35.7, 25.5, 16.7, 14.9, 13.4, 10.8, 9.3, 7.0, 6.4.

6-dEB Production Medium Recipe:

This medium is the same as the "Enhanced Medium" previously described.[19] To 830 mL of Milli-Q water in a 2.8 L baffled Fernbach flask is added the following: 40 g tryptone, 14 g glycerol, 10 g NaCl, 1 g yeast extract. The pH of the medium is adjusted to 7.6 (NaOH) prior to autoclaving. After the medium has cooled, the following components are added: 100 mL of 1 M HEPES buffer (pH = 7.6, filter sterilized), 5.625 mL of trace metal solution, 1.875 mL of vitamin solution, 1.0 mL of kanamycin (50 mg/mL stock), and 1.0 mL of ampicillin (100 mg/mL stock). Trace metal solution contains the following components dissolved in water at a final volume of 1 L: 27.0 g $FeCl_3$•$6H_2O$, 2.0 g Na_2MoO_4•$2H_2O$, 1.9 g $CuSO_4$•$5H_2O$, 1.3 g $ZnCl_2$, 1.0 g $CaCl_2$, 0.5 g H_3BO_3, 100 mL 12.1 M HCl. The solution is stored at room temperature and filter sterilized prior to addition to cultures. Vitamin solution contains the following components dissolved in water at a final volume of 1 L: 6.0 g nicotinic acid, 5.9 g pantothenic acid (hemicalcium salt), 1.7 g pyridoxine (HCl salt), 0.42 g riboflavin, 0.06 g biotin, 0.04 g folic acid. The pH of the solution is adjusted to 7.6 prior to filter sterilization and addition to cultures.

Synthesis of Trichloroacetimidate donor 2, 22 and 26

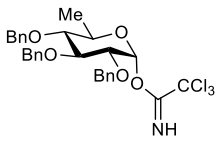

2

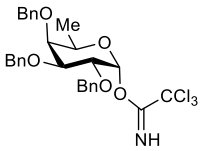

22

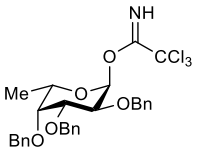

26

Sugar donor **2**, **22** and **26** were synthesized based on previously reported procedures.[20]

Synthesis of Desosamine-derived Trichloroacetimidate Donor 36

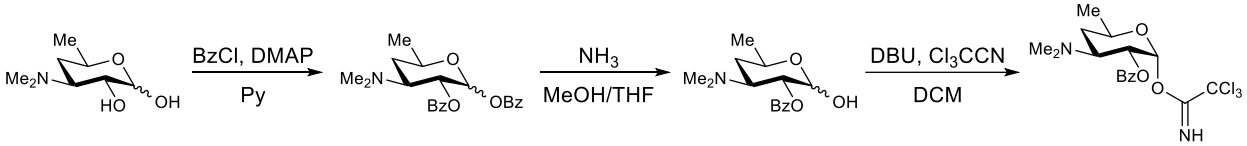

D-desosamine **36a** **36b** **α-36**

Scheme 2.7. Synthesis of desosamine-derived trichloroacetimidate donor **36**.

Erythromycin hydrate (7.0 gr) was dissolved in 50mL ethanol, and 130mL of 6N HCl was added to the solution. The mixture was heated to reflux for 3h. After cooled down to room temperature, the reaction mixture was washed with 50mL of chloroform for three times. The aqueous layer was concentrated under reduced pressure to obtain a deep orange oil containing desosamine. The crude mixture was dissolved in MeOH and passed slowly through Amberlite resin (hydroxide form), and then concentrated under pressure.

The crude mixture containing desosamine was azeotroped with toluene for three times and dissolved in 10mL of dry pyridine under nitrogen. DMAP (67mg) and BzCl (6.4mL) were added to the reaction. After stirring at room temperature for overnight, the reaction was concentrated under reduced pressure. The crude was purified by flash column chromatography on silica gel (EtOAc:MeCN, 70:30 v/v, followed by EtOAc:MeCN:MeOH, 70:20:10 v/v) to obtain 1.35 gr of **36a**.

36a (mixture of α and β anomers) ^{1}H NMR (500 MHz, $CDCl_3$) δ 8.08 (dd, *J* = 8.1, 1.5 Hz, 2H), 8.03 – 7.95 (m, 3H), 7.92 (dd, *J* = 8.1, 1.5 Hz, 2H), 7.62 (td, *J* = 7.3, 1.4 Hz, 1H), 7.54 – 7.46 (m, 6H), 7.40 – 7.31 (m, 6H), 6.59 (d, *J* = 3.6 Hz, 1H), 5.96 (d, *J* = 7.9 Hz, 1H), 5.47 – 5.39 (m, 2H), 4.23 (dqd, *J* = 12.4, 6.2, 2.1 Hz, 1H), 3.89 (dtd, *J* = 10.4, 6.8, 6.2, 4.8 Hz, 1H), 3.44 (ddd, *J* = 12.2, 10.9, 4.0 Hz, 1H), 3.07 (ddd, *J* = 12.2, 10.5, 4.3 Hz, 1H), 2.37 (s, 6H), 2.35 (s, 6H), 1.98 (ddd, *J* = 13.3, 4.1, 2.3 Hz, 1H), 1.91 (ddd, *J* = 13.4, 4.4, 2.0 Hz, 1H), 1.67 – 1.53 (m, 2H), 1.35 (d, *J* = 6.1 Hz, 3H), 1.27 (d, *J* = 6.2 Hz, 3H).

36a was dissolved in THF (0.1M) and subjected to deprotection with 7N NH_3 in MeOH (excess) at 0^{o}C, and the reaction was slowly warmed up to room temperature. After the reaction was done as judged by TLC, the mixture was concentrated under reduced pressure. The crude was purified by flash column chromatography on silica gel (CH_2Cl_2:MeOH, 97:3 v/v) to obtain **36b**.

36b (mixture of α and β anomers) ^{1}H NMR (400 MHz, $CDCl_3$) δ 8.08 (td, *J* = 7.1, 1.5 Hz, 4H), 7.57 (td, *J* = 7.3, 1.5 Hz, 2H), 7.45 (t, *J* = 7.8 Hz, 4H), 5.44 (d, *J* = 3.7 Hz, 1H), 5.17 (dd, *J* = 11.0, 3.7 Hz, 1H), 4.99 (dd, *J* = 10.4, 7.6 Hz, 1H), 4.69 (d, *J* = 7.6 Hz, 1H), 4.31 – 4.20 (m, 1H), 3.74 – 3.64 (m, 1H), 3.37 (td, *J* = 11.6, 4.2 Hz, 1H), 3.00 (ddd, *J* = 12.4, 10.4, 4.4 Hz, 1H), 2.34 (s, 6H), 2.33 (s, 6H), 1.91 – 1.80 (m, 2H), 1.48 (qd, *J* = 12.2, 8.4 Hz, 2H), 1.32 (d, *J* = 6.2 Hz, 3H), 1.23 (d, *J* = 6.3 Hz, 3H).

36b (160mg, 0.57mmol) was dissolved in dry DCM (5.7mL, 0.1M) under nitrogen and cooled in ice-bath. Cl_3CCN (0.86mL, 15 equiv.) was added to the reaction, followed by DBU (26μL, 0.3 equiv.). The reaction was warmed up slowly to room temperature. After stirring for 2h, the reaction was concentrated under reduced pressure. The crude was purified by flash column chromatography on silica gel deactivated with 0.5% Et_3N in hexanes (EtOAc:hexanes, 50:50 v/v) to obtain **α-36** and **β-36** (186mg, 77% combined yield)

α-36 ^{1}H NMR (500 MHz, C_6D_6) δ 8.32 (s, 1H), 8.27 – 8.22 (m, 2H), 7.07 – 6.97 (m, 4H), 5.52 (dd, *J* = 11.0, 3.5 Hz, 1H), 4.15 (dqd, *J* = 12.2, 6.2, 2.2 Hz, 1H), 3.43 (ddd, *J* = 12.3, 10.9, 3.9 Hz, 1H), 2.15 (s, 6H), 1.53 (ddd, *J* = 13.2, 4.0, 2.3 Hz, 1H), 1.28 – 1.15 (m, 1H), 1.05 (d, *J* = 6.2 Hz, 3H).

α-36 ^{13}C NMR (176 MHz, C_6D_6) δ 165.6, 161.0, 133.1, 130.7, 130.2, 128.5, 128.4, 95.9, 70.3, 68.0, 58.7, 40.7, 32.6, 21.1.

β-36 ^{1}H NMR (500 MHz, C_6D_6) δ 8.54 (s, 1H), 8.23 – 8.15 (m, 2H), 7.08 – 6.96 (m, 3H), 6.22 (d, *J* = 7.9 Hz, 1H), 5.63 (dd, *J* = 10.6, 8.0 Hz, 1H), 3.39 (dqd, *J* = 12.3, 6.1, 2.1 Hz, 1H), 2.72 (ddd, *J* = 12.2, 10.5, 4.3 Hz, 1H), 2.10 (s, 6H), 1.26 (ddd, *J* = 13.1, 4.3, 2.1 Hz, 1H), 1.18 – 1.09 (m, 1H), 1.07 (d, *J* = 6.2 Hz, 3H).

β-36 ^{13}C NMR (176 MHz, C_6D_6) δ 165.5, 162.0, 132.8, 131.1, 130.0, 128.5, 128.4, 98.4, 70.8, 70.7, 63.8, 40.7, 30.7, 21.1.

Synthesis of Chiral Phosphoric Acid 21

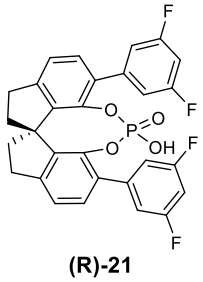

(R)-21

(R)-21 was prepared based on previously reported methods.[21]

^{1}H NMR (500 MHz, $CDCl_3$): δ 7.24 (m, 4H), 6.85 (d, J = 6.4 Hz, 4H), 6.19 (t, J = 8.1 Hz, 2H), 3.16 (ddd, J = 17.1, 11.4, 6.5 Hz, 2H), 2.98 (dd, J = 16.2, 7.8 Hz, 2H), 2.38 (dd, J = 12.1, 6.4 Hz, 2H), 2.21 (q, J = 11.4 Hz, 2H).

^{13}C NMR (126 MHz, $CDCl_3$): δ 162.9 (dd, J = 246.7, 13.3 Hz), 146.4 (d, J = 2.3 Hz), 141.9, 140.8 (d, J = 3.1 Hz), 140.6, 133.3, 130.4 (d, J = 1.8 Hz), 123.1, 112.4 (dd, J = 19.8, 6.2 Hz), 102.3 (t, J = 25.5 Hz), 60.1, 38.8, 30.6.

^{19}F NMR (471 MHz, $CDCl_3$): δ -111.03.

^{31}P NMR (202 MHz, $CDCl_3$): δ -7.55.

HRMS (m/z): $[M-H]^-$ calcd. for $C_{29}H_{19}F_4O_4P$, 537.0879; found, 537.0935

IR (thin film, cm^{-1}): 2953, 1622, 1593, 1455, 1415, 1115, 985

[α]$_D$: +166.9 (c = 1.01 in $CHCl_3$)

Synthesis of Macrolactone 25

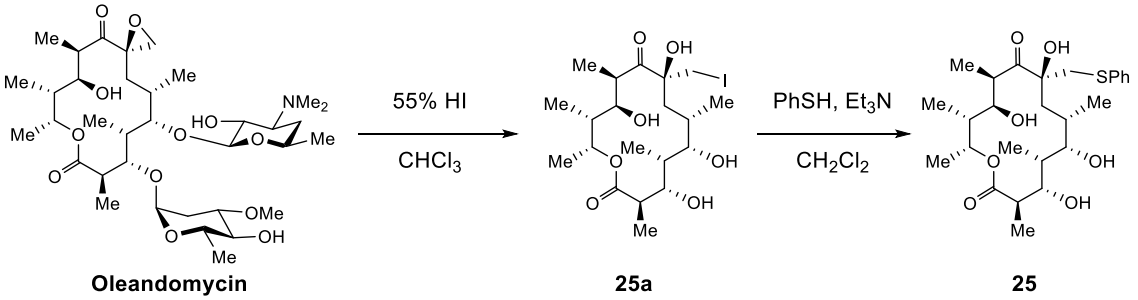

Scheme 2.8. Synthesis of macrolactone **25** from oleandomycin.

25a was prepared from oleandomycin based on previously reported procedures.[22] **25a** (300mg, 0.57mmol) was stirred in CH_2Cl_2 (0.1 M) with PhSH (0.24mL, 4 equiv.) and Et_3N (0.32mL, 4 equiv.) at room temperature. After 48h, reaction mixture was concentrated under reduced pressure. Crude was purified by flash column chromatography on silica gel (EtOAc:Hexanes, 30:70 to 50:50 v/v) to obtain 177 mg of **25** as yellow foamy solid (63% yield).

^{1}H NMR (700 MHz, $CDCl_3$): δ 7.37 (d, J = 7.7 Hz, 2H), 7.33 – 7.25 (m, 2H), 7.19 (t, J = 7.3 Hz, 1H), 5.63 (q, J = 6.4 Hz, 1H), 4.07 (s, 1H), 3.66 – 3.53 (m, 3H), 3.39 (d, J = 13.1 Hz, 1H), 3.32 (d, J = 12.6 Hz, 2H), 3.10 (q, J = 6.6 Hz, 1H), 2.61 (dt, J = 14.1, 6.8 Hz, 1H), 2.37 (s, 1H), 2.02 (s,

1H), 2.01 – 1.89 (m, 3H), 1.72 – 1.62 (m, 2H), 1.52 (s, 1H), 1.26 (d, J = 6.6 Hz, 3H), 1.22 (d, J = 6.7 Hz, 3H), 1.12 (t, J = 6.6 Hz, 6H), 1.03 (d, J = 6.9 Hz, 3H), 0.92 (d, J = 7.0 Hz, 3H).

^{13}C NMR (176 MHz, $CDCl_3$): δ 215.8, 176.0, 136.6, 129.9, 129.1, 126.6, 83.0, 79.4, 77.8, 70.0, 69.9, 44.3, 44.1, 41.8, 40.9, 40.3, 37.9, 36.2, 19.9, 18.7, 14.5, 9.2, 8.9, 7.9.

HRMS (m/z): $[M+Na]^+$ calcd. for $C_{26}H_{40}O_7$, 519.2392; found, 519.2379

TLC (EtOAc:Hexanes, 40:60 v/v): R_f = 0.2

IR (thin film, cm^{-1}): 3449, 2975, 2931, 2863, 1710, 1456, 1381, 1114

[α]$_D$: -20.1 (c = 1.01 in $CHCl_3$)

General Procedures for Glycosylation Reactions

Glycosylation of Macrolide Catalyzed by TMS-OTf or BF_3•OEt_2:

Macrolide (0.020mmol, 1.0 equiv.), sugar donor (0.024mmol, 1.2 equiv.) and 20mg of powdered 4Å molecular sieve were stirred in 400μL of dry toluene (0.05 M) at room temperature under N_2 for 10 min. Reaction mixture was then cooled to -20°C. After stirring for another 10 min., TMS-OTf or BF_3•OEt_2 (0.004mmol, 0.2 equiv.) in 20μL of dry toluene was added to the reaction. After 17 to 24h, reaction was quenched with Et_3N, filtered through a short pad of Celite with CH_2Cl_2 washing and concentrated under reduced pressure. The crude mixture was purified by flash column chromatography (pipette column) on silica gel (EtOAc:Hexanes, gradient) to obtain a mixture of glycosides. Each individual glycoside was isolated by separation on semi-prep HPLC (EtOAc:Hexanes) and characterized.

Glycosylation of Macrolide Catalyzed by Chiral Brønsted Acids:

Macrolide (0.020mmol, 1.0 equiv.), sugar donor (0.024mmol, 1.2 equiv.), chiral Brønsted acid (0.004mmol, 0.2 equiv.) and 10mg of powdered 4Å molecular sieve were stirred in dry toluene (0.1 to 0.3 M) at room temperature. After 24 – 72h, reaction was quenched with Et_3N, filtered through a short pad of Celite with CH_2Cl_2 washing and concentrated under reduced pressure. The crude mixture was purified by flash column chromatography (pipette column) on silica gel (EtOAc:Hexanes, gradient) to obtain a mixture of glycosides. Each individual glycoside was isolated by separation on semi-prep HPLC (EtOAc:Hexanes) and characterized.

Procedure for Deprotection of Macrolide Glycoside

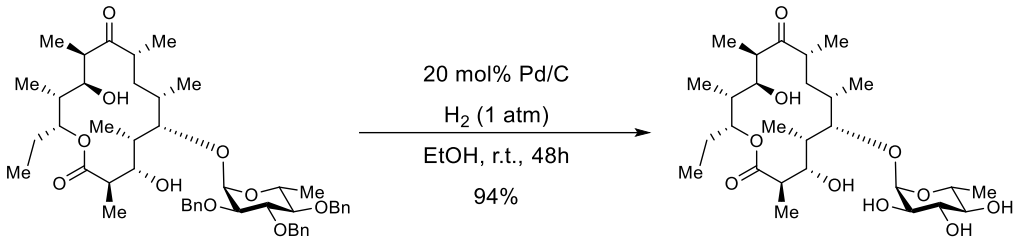

4 **4a**

In a one dram vial, **4** (3.4mg, 4.2μmol) and Pd/C (0.9mg, 0.84μmol) were added, and the vial was sealed with rubber septum. The vial was evacuated and backfilled with N_2 three times, followed by H_2 for another three times. 200μL of EtOH was added to the vial, and the suspension was stirred with H_2 balloon on top for 48h at room temperature. At the end of the reaction, the suspension was filtered through a thin pad of Cealite with EtOAc washing. Combined organic layer was concentrated under reduced pressure, and the crude mixture was purified by flash column chromatography (pipette column) on silica gel (CH_2Cl_2:MeOH, 15:1 v/v) to obtain the debenzylated glycoside **4a** (2.1mg, 94% yield) as colorless oil.

^{1}H NMR (500 MHz, $CDCl_3$): δ 5.13 (dd, *J* = 9.5, 3.0 Hz, 1H), 5.02 (d, *J* = 3.1 Hz, 1H), 3.92 (s, 2H), 3.87 (d, *J* = 10.2 Hz, 1H), 3.83 – 3.74 (m, 1H), 3.69 – 3.51 (m, 3H), 3.08 (q, *J* = 7.3 Hz, 2H), 2.84 – 2.67 (m, 2H), 2.67 – 2.56 (m, 1H), 2.42 – 2.23 (m, 1H), 1.93 (d, *J* = 5.8 Hz, 1H), 1.85 – 1.58 (m, 3H), 1.51 (ddd, *J* = 13.9, 7.2, 4.0 Hz, 1H), 1.32 (d, *J* = 5.4 Hz, 3H), 1.29 (d, *J* = 7.2 Hz, 3H), 1.11 (d, *J* = 6.9 Hz, 3H), 1.02 (m, 9H), 0.93 (t, *J* = 7.3 Hz, 3H), 0.86 (d, *J* = 6.8 Hz, 3H).
^{13}C NMR (126 MHz, $CDCl_3$): δ 213.3, 178.5, 93.8, 79.0, 76.4, 76.1, 74.1, 72.4, 71.1, 68.8, 46.0, 44.9, 43.7, 40.6, 37.5, 32.1, 29.5, 25.6, 18.2, 16.3, 15.4, 13.0, 10.8, 9.3, 8.9, 8.0, 6.4.
HRMS (m/z): $[M+Na]^+$ calcd. for $C_{27}H_{48}O_{10}$, 555.3145; found, 555.3141.
TLC (CH_2Cl_2:MeOH, 10:1 v/v): R_f = 0.4

Characterization of Glycoside Products

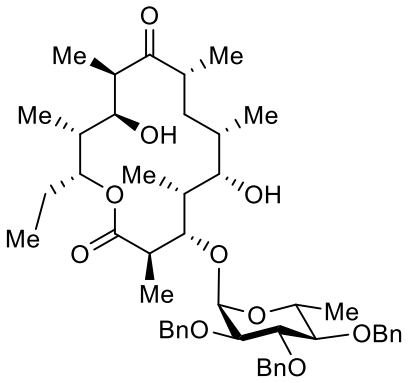

3

^{1}H NMR (700 MHz, C_6D_6): δ 7.29 (d, J = 7.4 Hz, 2H), 7.26 (t, J = 7.2 Hz, 3H), 7.18 – 7.03 (m, 10H), 5.68 (dd, J = 9.8, 3.9 Hz, 1H), 4.89 – 4.79 (m, 3H), 4.75 (d, J = 3.1 Hz, 1H), 4.59 (d, J = 11.9 Hz, 1H), 4.55 (d, J = 11.9 Hz, 1H), 4.50 (d, J = 11.2 Hz, 1H), 4.13 (s, 1H), 4.10 (t, J = 9.4 Hz, 1H), 4.02 (dq, J = 12.3, 6.2 Hz, 1H), 3.92 (d, J = 4.0 Hz, 1H), 3.78 (d, J = 10.1 Hz, 1H), 3.68 (m, 2H), 3.48 (dd, J = 9.9, 3.2 Hz, 1H), 3.06 (t, J = 9.2 Hz, 1H), 2.83 (q, J = 6.7 Hz, 1H), 2.77 (dt, J = 13.5, 6.8 Hz, 1H), 2.71 – 2.63 (m, 1H), 1.81 – 1.74 (m, 2H), 1.65 (dt, J = 16.3, 7.3 Hz, 1H), 1.61 – 1.52 (m, 2H), 1.43 (d, J = 6.8 Hz, 3H), 1.43 – 1.35 (m, 1H), 1.34 (d, J = 6.9 Hz, 3H), 1.24 (d, J = 6.2 Hz, 3H), 1.19 (ddt, J = 14.7, 11.8, 7.3 Hz, 1H), 1.10 (d, J = 6.7 Hz, 3H), 1.08 (d, J = 6.9 Hz, 3H), 0.95 (d, J = 6.7 Hz, 3H), 0.79 (t, J = 7.3 Hz, 3H), 0.74 (d, J = 7.1 Hz, 3H).

^{13}C NMR (176 MHz, C_6D_6): δ 217.8, 176.7, 139.3, 139.1, 137.5, 129.0, 128.9, 128.6, 128.6, 128.4, 128.3, 128.0, 127.8, 127.7, 100.6, 91.7, 84.6, 82.1, 80.6, 77.2, 75.6, 75.4, 75.4, 74.4, 71.1, 68.1, 45.4, 45.0, 42.4, 41.1, 39.8, 38.8, 35.0, 26.2, 18.1, 18.0, 16.0, 16.0, 10.7, 9.4, 9.2, 8.8.

HRMS (m/z): $[M+NH_4]^+$ calcd. for $C_{48}H_{66}O_{10}$, 820.5000; found, 820.4987

TLC (EtOAc:Hexanes, 30:70 v/v): R_f = 0.5

IR (thin film, cm^{-1}): 3500, 2971, 2927, 2971, 1725, 1701, 1454, 1069

[α]$_D$: -10.0 (c = 0.24 in $CHCl_3$)

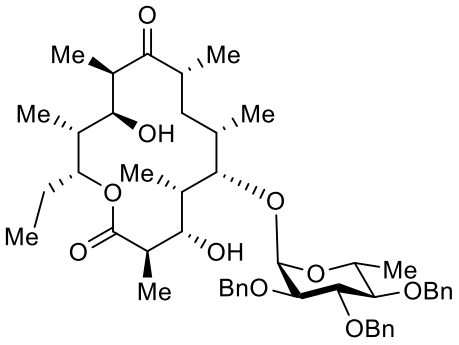

4

^{1}H NMR (700 MHz, C_6D_6): δ 7.31 (d, J = 7.4 Hz, 2H), 7.29 (d, J = 7.4 Hz, 2H), 7.25 (d, J = 7.3 Hz, 2H), 7.17 (d, J = 7.3 Hz), 7.15 – 7.12 (m), 7.11 – 7.04 (m, 3H), 5.19 – 5.13 (m, 1H), 4.93 (d, J = 11.3 Hz, 1H), 4.89 (d, J = 3.7 Hz, 1H), 4.84 (d, J = 11.3 Hz, 1H), 4.78 (d, J = 11.2 Hz, 1H), 4.56 (d, J = 11.7 Hz, 1H), 4.52 (d, J = 2.9 Hz, 1H), 4.51 (d, J = 3.4 Hz, 1H), 4.31 (d, J = 3.4 Hz, 1H), 4.17 (d, J = 10.3 Hz, 1H), 4.10 (dq, J = 12.4, 6.2 Hz, 1H), 4.05 (t, J = 9.3 Hz, 1H), 3.93 (s, 1H), 3.79 (d, J = 9.5 Hz, 1H), 3.65 (s, 1H), 3.50 (dd, J = 9.7, 3.7 Hz, 1H), 3.10 (t, J = 9.2 Hz, 1H), 2.90 – 2.74 (m, 2H), 2.60 (d, J = 6.4 Hz, 1H), 2.24 (s, 1H), 2.03 (q, J = 6.3 Hz, 1H), 1.60 (td, J = 12.8, 11.1, 4.3 Hz, 1H), 1.55 (dt, J = 14.1, 7.1 Hz, 1H), 1.50 – 1.47 (m, 1H), 1.46 (d, J = 6.8 Hz, 3H), 1.26 (d, J = 7.1 Hz, 3H), 1.25 (d, J = 6.3 Hz, 3H), 1.21 (d, J = 6.9 Hz, 3H), 1.16 (d, J = 6.3 Hz, 3H), 1.13 (m, 1H), 1.03 (ddt, J = 13.9, 7.3, 3.9 Hz, 1H), 0.98 (d, J = 7.1 Hz, 3H), 0.66 (t, J = 7.3 Hz, 3H), 0.61 (d, J = 6.9 Hz, 3H).

^{13}C NMR (126 MHz, C_6D_6): δ 212.4, 178.6, 139.5, 139.0, 138.6, 128.7, 128.6, 128.5, 128.4, 128.2, 128.0, 127.9, 127.7, 95.9, 83.8, 82.4, 80.5, 79.2, 76.0, 75.6, 75.3, 73.6, 71.2, 69.1, 44.9, 43.4, 40.9, 39.9, 38.6, 37.6, 25.6, 18.3, 17.2, 15.5, 13.9, 10.6, 9.1, 8.3, 7.1.

HRMS (m/z): $[M+NH_4]^+$ calcd. for $C_{48}H_{66}O_{10}$, 820.5000; found, 820.4985

TLC (EtOAc:Hexanes, 30:70 v/v): R_f = 0.5

IR (thin film, cm^{-1}): 3468, 2971, 2925, 1704, 1453, 1070

[α]$_D$: +31.7 (c = 0.49 in $CHCl_3$)

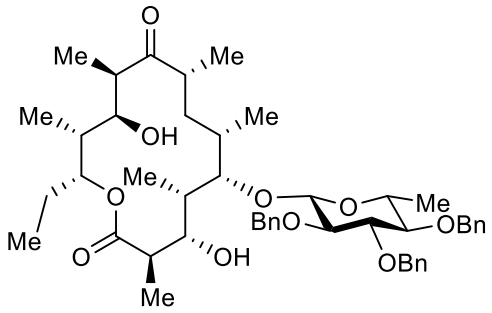

β-4

^{1}H NMR (700 MHz, $CDCl_3$): δ 7.38 – 7.33 (m, 2H), 7.33 – 7.29 (m, 5H), 7.28 (m, 8H), 5.11 (dd, J = 9.6, 2.9 Hz, 1H), 4.91 (d, J = 11.3 Hz, 1H), 4.89 – 4.80 (m, 5H), 4.63 (d, J = 10.9 Hz, 1H), 4.50 (d, J = 7.8 Hz, 1H), 3.96 (d, J = 4.4 Hz, 1H), 3.89 (d, J = 10.3 Hz, 1H), 3.83 (dd, J = 4.8, 1.6 Hz, 1H), 3.69 – 3.64 (m, 2H), 3.44 – 3.38 (m, 2H), 3.26 (s, 1H), 3.20 (t, J = 9.2 Hz, 1H), 2.78 – 2.69 (m, 2H), 2.66 – 2.59 (m, 1H), 2.33 – 2.25 (m, 1H), 1.86 – 1.77 (m, 2H), 1.75 – 1.69 (m, 1H), 1.62 – 1.56 (m, 1H), 1.52 – 1.47 (m, 1H), 1.28 (d, J = 6.8 Hz, 3H), 1.27 (d, J = 6.2 Hz, 3H), 1.22 – 1.15 (m, 1H), 1.05 (d, J = 6.9 Hz, 3H), 1.03 (d, J = 6.5 Hz, 3H), 1.02 (d, J = 6.8 Hz, 3H), 1.00 (d, J = 7.2 Hz, 3H), 0.93 (t, J = 7.4 Hz, 3H), 0.87 (d, J = 6.9 Hz, 3H).

^{13}C NMR (126 MHz, $CDCl_3$): δ 213.6, 179.2, 138.6, 138.1, 137.4, 129.7, 128.9, 128.6, 128.5, 128.4, 128.2, 128.0, 128.0, 127.7, 103.5, 84.8, 83.9, 81.0, 78.2, 76.3, 75.5, 75.4, 75.3, 71.7, 71.1, 44.7, 43.8, 40.7, 39.1, 38.2, 38.0, 35.5, 25.6, 18.0, 17.5, 15.5, 13.1, 10.8, 9.3, 8.3, 6.3.

HRMS (m/z): $[M+NH_4]^+$ calcd. for $C_{48}H_{66}O_{10}$, 820.5000; found, 820.4992

TLC (EtOAc:Hexanes, 30:70 v/v): R_f = 0.55

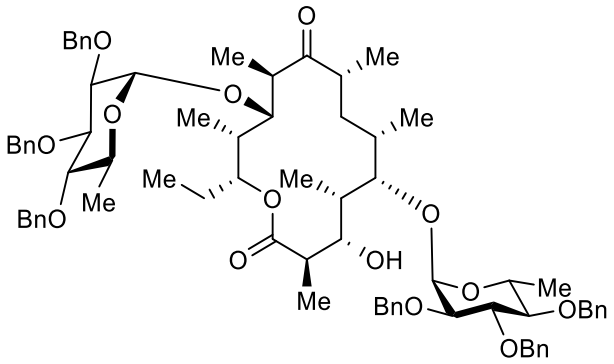

5

^{1}H NMR (700 MHz, C_6D_6): δ 7.35 (d, J = 7.2 Hz, 2H), 7.31 (t, J = 6.4 Hz, 8H), 7.25 (dt, J = 12.5, 6.8 Hz, 6H), 7.14 – 7.03 (m, 20H), 5.81 (t, J = 7.5 Hz, 1H), 5.72 (d, J = 3.6 Hz, 1H), 5.02 (d, J = 11.4 Hz, 1H), 4.99 (d, J = 3.8 Hz, 1H), 4.93 (d, J = 11.2 Hz, 1H), 4.89 – 4.84 (m, 2H), 4.83 (d, J = 11.4 Hz, 1H), 4.77 (dd, J = 11.4, 1.9 Hz, 3H), 4.72 (d, J = 10.6 Hz, 1H), 4.57 (s, 2H), 4.51 (dd, J = 11.1, 9.2 Hz, 2H), 4.36 (d, J = 10.5 Hz, 1H), 4.31 (d, J = 9.4 Hz, 1H), 4.18 (dd, J = 4.9, 2.8 Hz, 1H), 4.17 – 4.14 (m, 1H), 4.08 (m, 3H), 3.82 (s, 1H), 3.56 (dd, J = 9.6, 3.8 Hz, 1H), 3.46 (dd, J = 10.1, 3.6 Hz, 1H), 3.25 (ddt, J = 13.1, 6.2, 3.4 Hz, 1H), 3.09 (m, 2H), 2.85 (dq, J = 10.2, 6.7 Hz, 1H), 2.68 (q, J = 6.3 Hz, 1H), 2.51 – 2.43 (m, 1H), 2.01 (qd, J = 6.6, 6.1, 1.6 Hz, 1H), 1.88 – 1.80 (m, 1H), 1.59 (d, J = 6.7 Hz, 3H), 1.57 (m, 1H), 1.55 (d, J = 6.0 Hz, 3H), 1.46 (d, J = 6.2 Hz, 3H), 1.27 (d, J = 6.7 Hz, 3H), 1.26 – 1.23 (m, 1H), 1.22 (d, J = 7.0 Hz, 3H), 1.19 (d, J = 6.2 Hz, 3H), 1.18 – 1.15 (m, 1H), 1.15 – 1.08 (m, 1H), 0.95 (d, J = 7.1 Hz, 3H), 0.64 (d, J = 7.2 Hz, 3H), 0.47 (t, J = 7.4 Hz, 3H).

^{13}C NMR (126 MHz, C_6D_6): δ 211.0, 177.0, 139.9, 139.5, 139.4, 139.2, 139.1, 138.6, 128.7, 128.7, 128.5, 128.5, 128.5, 128.4, 128.3, 128.0, 127.8, 127.7, 127.7, 127.6, 127.6, 127.5, 100.8, 93.7, 85.0, 83.7, 83.6, 82.5, 82.1, 81.8, 80.3, 80.2, 78.8, 75.6, 75.6, 75.4, 75.1, 74.9, 73.4, 69.1, 69.1, 44.9, 44.6, 41.4, 38.9, 38.1, 28.5, 26.0, 24.6, 18.3, 18.2, 17.0, 15.9, 15.6, 13.7, 13.6, 11.9, 10.1, 10.0, 9.8, 8.9, 8.8, 7.8, 7.4, 6.9.

HRMS (m/z): $[M+NH_4]^+$ calcd. for $C_{75}H_{94}O_{14}$, 1236.6987; found, 1239.6962

TLC (EtOAc:Hexanes, 30:70 v/v): R_f = 0.6

IR (thin film, cm^{-1}): 2921, 2854, 1713, 1454, 1070

[α]$_D$: +40.5 (c = 0.07 in $CHCl_3$)

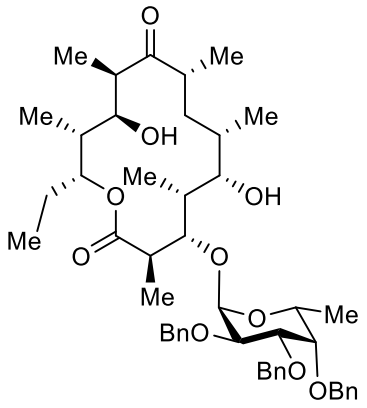

α-23

^{1}H NMR (500 MHz, C_6D_6): δ 7.39 (d, J = 7.3 Hz, 3H), 7.34 – 7.18 (m, 8H), 7.14 – 6.96 (m, 4H), 5.65 (dd, J = 9.9, 3.8 Hz, 1H), 4.96 (d, J = 11.3 Hz, 1H), 4.85 (d, J = 3.5 Hz, 1H), 4.64 (dd, J = 11.8, 4.3 Hz, 2H), 4.57 (d, J = 11.9 Hz, 1H), 4.49 (t, J = 11.6 Hz, 2H), 4.20 (dd, J = 10.4, 3.4 Hz, 1H), 4.14 (d, J = 2.4 Hz, 1H), 4.03 – 3.91 (m, 2H), 3.86 – 3.79 (m, 2H), 3.70 (d, J = 9.8 Hz, 1H), 3.66 (s, 1H), 3.34 (s, 1H), 2.91 – 2.75 (m, 2H), 2.70 – 2.60 (m, 1H), 1.83 – 1.72 (m, 1H), 1.68 – 1.62 (m, 1H), 1.62 – 1.57 (m, 1H), 1.55 (td, J = 7.3, 2.5 Hz, 1H), 1.47 (d, J = 6.8 Hz, 3H), 1.34 (d, J = 6.9 Hz, 3H), 1.25 – 1.18 (m, 1H), 1.15 (d, J = 6.5 Hz, 3H), 1.10 (d, J = 6.8 Hz, 3H), 1.07 (d, J = 6.7 Hz, 3H), 0.97 (d, J = 6.7 Hz, 3H), 0.94 – 0.89 (m, 1H), 0.79 (t, J = 7.4 Hz, 3H), 0.74 (d, J = 7.1 Hz, 3H).

^{13}C NMR (176 MHz, C_6D_6): δ 217.3, 176.8, 139.4, 139.1, 137.7, 130.3, 130.2, 129.1, 128.7, 128.5, 128.4, 128.4, 128.3, 128.1, 128.0, 101.3, 90.6, 79.1, 78.6, 77.3, 76.7, 75.5, 75.3, 74.8, 73.0, 71.0, 67.7, 45.2, 45.0, 42.3, 41.1, 40.1, 38.6, 35.2, 26.2, 18.0, 16.8, 16.0, 15.9, 14.4, 10.7, 9.4, 9.2, 8.6.

HRMS (m/z): $[M+Na]^+$ calcd. for $C_{48}H_{66}O_{10}$, 825.4554; found, 825.4535

TLC (EtOAc:Hexanes, 30:70 v/v): R_f = 0.5

IR (thin film, cm^{-1}): 3494, 2961, 2919, 2873, 2849, 1725, 1705, 1453

[α]$_D$: +8.8 (c = 0.07 in $CHCl_3$)

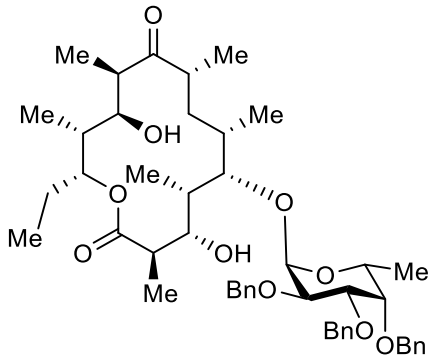

α-24

^{1}H NMR (700 MHz, $CDCl_3$): δ 7.38 – 7.27 (m, 21H), 5.13 (d, J = 3.8 Hz, 2H), 4.97 (d, J = 11.5 Hz, 1H), 4.82 (d, J = 11.7 Hz, 1H), 4.77 – 4.68 (m, 3H), 4.65 (d, J = 11.5 Hz, 1H), 4.10 (dd, J = 9.9, 3.7 Hz, 1H), 3.89 (m, 2H), 3.85 – 3.84 (m, 1H), 3.83 – 3.81 (m, 1H), 3.79 (d, J = 10.4 Hz, 1H), 3.69 (s, 1H), 3.65 (d, J = 9.7 Hz, 1H), 3.41 (s, 1H), 2.82 – 2.69 (m, 2H), 2.64 – 2.53 (m, 1H), 2.32 (m, 1H), 1.90 (q, J = 6.3 Hz, 1H), 1.82 (tt, J = 14.8, 7.3 Hz, 1H), 1.73 (dt, J = 15.7, 6.9 Hz, 1H), 1.67 – 1.61 (m, 1H), 1.52 (ddt, J = 14.6, 11.8, 7.5 Hz, 1H), 1.31 (d, J = 6.7 Hz, 3H), 1.24 (m, 1H), 1.18 (d, J = 6.4 Hz, 3H), 1.11 (d, J = 6.9 Hz, 3H), 1.02 (d, J = 6.7 Hz, 3H), 1.00 – 0.97 (m, 6H), 0.93 (t, J = 7.3 Hz, 3H), 0.88 (d, J = 6.8 Hz, 3H).

^{13}C NMR (176 MHz, $CDCl_3$): δ 213.5, 178.7, 138.7, 138.6, 128.5, 128.5, 128.4, 128.4, 127.8, 127.8, 127.8, 127.7, 127.7, 94.2, 79.5, 79.0, 76.3, 75.9, 74.8, 73.5, 73.5, 71.1, 68.2, 44.4, 43.6, 40.7, 39.2, 37.8, 37.5, 29.9, 25.6, 22.8, 16.9, 16.7, 15.2, 14.3, 13.0, 10.8, 9.3, 8.0, 6.4.

HRMS (m/z): $[M+Na]^+$ calcd. for $C_{48}H_{66}O_{10}$, 825.4554; found, 825.4534

TLC (EtOAc:Hexanes, 30:70 v/v): R_f = 0.5

IR (thin film, cm^{-1}): 3508, 2924, 2851, 1704, 1454, 1095, 1044

[α]$_D$: +19.0 (c = 0.05 in $CHCl_3$)

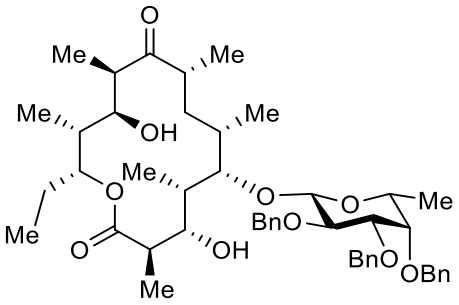

β-24

^{1}H NMR (500 MHz, C_6D_6): δ 7.48 (d, J = 7.3 Hz, 2H), 7.31 (d, J = 7.0 Hz, 3H), 7.27 (d, J = 7.2 Hz, 2H), 7.23 – 7.17 (m, 5H), 7.15 – 6.97 (m, 7H), 5.09 (dd, J = 9.6, 3.1 Hz, 1H), 4.94 (d, J = 11.3 Hz, 1H), 4.85 (d, J = 12.0 Hz, 2H), 4.48 (d, J = 11.5 Hz, 1H), 4.42 (s, 2H), 4.39 (d, J = 4.4 Hz, 1H), 4.32 (d, J = 7.7 Hz, 1H), 4.27 (d, J = 4.6 Hz, 2H), 4.01 (dd, J = 9.7, 7.8 Hz, 1H), 3.95 (d, J = 3.7 Hz, 1H), 3.91 – 3.80 (m, 2H), 3.25 (dd, J = 9.8, 2.8 Hz, 1H), 3.13 (d, J = 2.4 Hz, 1H), 3.03 – 2.90 (m, 1H), 2.91 – 2.78 (m, 2H), 2.68 – 2.53 (m, 2H), 2.00 (q, J = 6.8 Hz, 1H), 1.63 – 1.52 (m, 2H), 1.49 (d, J = 6.7 Hz, 3H), 1.47 – 1.42 (m, 1H), 1.37 (d, J = 6.3 Hz, 3H), 1.31 (d, J = 6.7 Hz, 3H), 1.21 (d, J = 6.9 Hz, 3H), 1.13 (dd, J = 13.7, 3.7 Hz, 1H), 1.10 (d, J = 6.4 Hz, 3H), 1.06 (d, J = 7.2 Hz, 3H), 0.99 (ddt, J = 15.0, 7.6, 3.1 Hz, 1H), 0.66 (t, J = 7.3 Hz, 3H), 0.59 (d, J = 6.9 Hz, 3H).

^{13}C NMR (176 MHz, C_6D_6): δ 211.8, 179.4, 139.2, 138.8, 138.3, 129.1, 128.8, 128.5, 128.4, 128.4, 128.3, 128.1, 128.00, 127.9, 127.8, 104.9, 85.8, 83.8, 78.5, 78.5, 77.0, 76.3, 75.7, 75.2, 72.8, 71.3, 70.9, 45.2, 44.1, 41.0, 39.2, 38.5, 38.5, 35.8, 25.5, 17.8, 17.0, 15.7, 13.6, 10.7, 9.1, 8.6, 6.7.

HRMS (m/z): $[M+NH_4]^+$ calcd. for $C_{48}H_{66}O_{10}$, 820.5000; found, 820.4984

TLC (EtOAc:Hexanes, 30:70 v/v): R_f = 0.5

IR (thin film, cm^{-1}): 3464, 2971, 2927, 2877, 1701, 1598, 1454, 1064

[α]$_D$: -13.1 (c = 0.31 in $CHCl_3$)

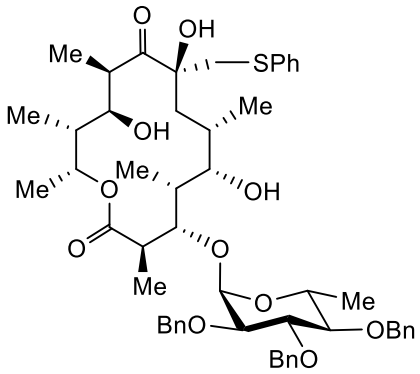

α-27

^{1}H NMR (500 MHz, C_6D_6): δ 7.42 – 7.24 (m, 5H), 7.19 - 7.04 (m, 6H), 6.95 (m, 4H), 5.99 (q, J = 6.6 Hz, 1H), 4.89 – 4.75 (m, 3H), 4.68 (d, J = 3.3 Hz, 1H), 4.62 (d, J = 12.1 Hz, 1H), 4.55 (d, J = 12.1 Hz, 1H), 4.48 (d, J = 11.2 Hz, 1H), 4.20 (s, 1H), 4.06 (t, J = 9.4 Hz, 1H), 3.98 (dq, J = 10.3, 6.3 Hz, 1H), 3.80 (d, J = 4.3 Hz, 1H), 3.67 (d, J = 9.7 Hz, 1H), 3.63 (d, J = 10.1 Hz, 1H), 3.52 – 3.44 (m, 3H), 3.27 (d, J = 13.5 Hz, 1H), 3.12 (d, J = 13.5 Hz, 1H), 3.06 – 2.97 (m, 2H), 2.67 (dq, J = 9.8, 6.5 Hz, 1H), 2.15 (dd, J = 14.5, 10.6 Hz, 1H), 2.06 (d, J = 13.8 Hz, 1H), 1.48 (m, 1H), 1.40 (d, J = 6.7 Hz, 3H), 1.38 – 1.28 (m, 7H), 1.21 (dd, J = 6.4, 4.3 Hz, 6H), 1.00 (d, J = 6.7 Hz, 3H), 0.67 (d, J = 7.1 Hz, 3H).

^{13}C NMR (176 MHz, C_6D_6): δ 217.4, 175.5, 139.2, 139.0, 137.7, 137.4, 129.9, 129.2, 129.2, 129.1, 128.9, 128.8, 128.6, 128.4, 128.4, 127.7, 127.7, 126.3, 100.9, 92.3, 84.6, 84.4, 82.0, 80.5, 80.0, 75.6, 75.4, 74.2, 70.4, 69.4, 67.9, 44.7, 44.5, 43.1, 42.3, 40.1, 39.2, 36.9, 21.0, 18.8, 18.0, 15.4, 9.9, 9.7, 8.7.

HRMS (m/z): $[M+Na]^+$ calcd. for $C_{53}H_{68}O_{11}S$, 935.4380; found, 935.4362

TLC (EtOAc:Hexanes, 30:70 v/v): R_f = 0.4

IR (thin film, cm^{-1}): 3439, 2926, 1720, 1454, 1328, 1069

$[\alpha]_D$: +9.1 (c = 0.07 in $CHCl_3$)

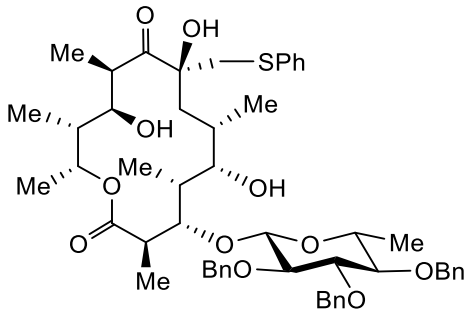

β-27

^{1}H NMR (500 MHz, C_6D_6): δ 7.39 – 7.28 (m, 7H), 7.23 (d, J = 7.1 Hz, 2H), 7.09 (q, J = 7.1 Hz, 3H), 7.01 (t, J = 7.6 Hz, 2H), 6.92 (t, J = 7.4 Hz, 1H), 5.96 (q, J = 6.7 Hz, 1H), 4.92 (t, J = 11.4 Hz, 2H), 4.82 – 4.58 (m, 3H), 4.40 (d, J = 11.3 Hz, 1H), 4.30 (d, J = 7.9 Hz, 1H), 4.16 (s, 1H), 3.72 (d, J = 9.5 Hz, 1H), 3.67 (m, 1H), 3.64 (d, J = 10.1 Hz, 1H), 3.48 (t, J = 9.1 Hz, 1H), 3.36 – 3.24 (m, 3H), 3.17 (d, J = 13.5 Hz, 1H), 3.10 – 2.97 (m, 2H), 2.86 (t, J = 9.2 Hz, 1H), 2.84 – 2.74 (m, 2H), 2.25 – 2.03 (m, 2H), 1.77 (t, J = 6.9 Hz, 1H), 1.53 – 1.42 (m, 5H), 1.39 (d, J = 6.7 Hz, 3H), 1.35 (d, J = 6.9 Hz, 3H), 1.20 (d, J = 6.8 Hz, 3H), 1.12 (d, J = 6.1 Hz, 3H), 1.03 (d, J = 6.6 Hz, 3H), 0.69 (d, J = 7.1 Hz, 3H).

^{13}C NMR (176 MHz, C_6D_6): δ 217.4, 174.7, 139.5, 139.0, 138.9, 137.6, 129.8, 129.2, 128.6, 128.6, 128.6, 128.4, 128.3, 127.9, 127.7, 127.7, 126.4, 104.5, 88.3, 84.7, 84.5, 83.4, 82.6, 80.7, 75.5, 75.2, 75.1, 71.6, 70.5, 69.7, 45.4, 44.3, 42.1, 41.6, 40.4, 38.3, 37.6, 20.8, 18.8, 17.7, 14.4, 9.6, 9.6, 8.8.

HRMS (m/z): $[M+Na]^+$ calcd. for $C_{53}H_{68}O_{11}S$, 935.4380; found, 935.4368

TLC (EtOAc:Hexanes, 30:70 v/v): R_f = 0.45

IR (thin film, cm^{-1}): 3485, 2973, 2925, 2855, 1725, 1454, 1380, 1117, 1067

[α]$_D$: +2.5 (c = 0.29 in $CHCl_3$)

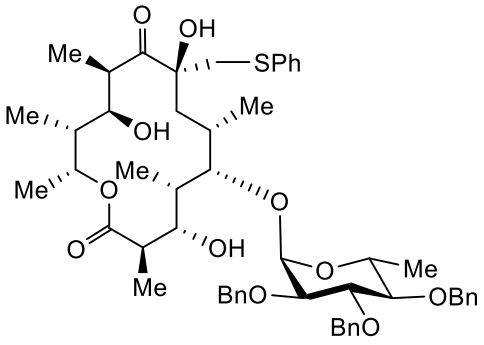

α-28

^{1}H NMR (700 MHz, C_6D_6): δ 7.40 – 7.36 (m, 2H), 7.35 – 7.31 (m, 2H), 7.29 – 7.24 (m, 4H), 7.23 – 7.17 (m, 4H), 7.14 – 7.03 (m, 5H), 6.99 (dd, J = 8.4, 7.1 Hz, 2H), 6.96 – 6.87 (m, 1H), 5.86 (q, J = 6.4 Hz, 1H), 4.98 (d, J = 11.4 Hz, 1H), 4.95 (d, J = 3.7 Hz, 1H), 4.89 (d, J = 11.2 Hz, 1H), 4.82 (d, J = 11.3 Hz, 1H), 4.60 (d, J = 11.3 Hz, 1H), 4.57 – 4.49 (m, 2H), 4.21 (dq, J = 9.5, 6.1 Hz, 1H), 4.12 (dd, J = 9.9, 8.9 Hz, 1H), 4.09 (s, 1H), 3.79 (dd, J = 9.9, 3.6 Hz, 1H), 3.68 (d, J = 9.3 Hz, 1H), 3.51 (s, 1H), 3.46 (dd, J = 9.9, 3.7 Hz, 1H), 3.40 (d, J = 2.6 Hz, 1H), 3.28 (d, J = 13.3 Hz, 1H), 3.12 (t, J = 9.3 Hz, 1H), 3.08 (d, J = 13.3 Hz, 1H), 2.98 (q, J = 7.0 Hz, 1H), 2.71 (d, J = 3.8 Hz, 1H), 2.65 (dq, J = 9.8, 6.7 Hz, 1H), 2.14 (m, 1H), 2.00 (dd, J = 14.8, 2.8 Hz, 1H), 1.84 (dd, J = 8.3, 6.0 Hz, 1H), 1.62 – 1.55 (m, 1H), 1.46 – 1.40 (m, 3H), 1.39 (d, J = 6.7 Hz, 3H), 1.36 (d, J = 6.2 Hz, 3H), 1.30 (d, J = 6.8 Hz, 3H), 1.20 (d, J = 7.1 Hz, 3H), 1.17 (d, J = 6.8 Hz, 3H), 0.97 (d, J = 6.6 Hz, 3H), 0.63 (d, J = 7.1 Hz, 3H).

^{13}C NMR (176 MHz, C_6D_6): δ 216.0, 175.5, 139.6, 139.0, 138.6, 137.6, 130.0, 129.2, 128.8, 128.6, 128.5, 128.4, 128.4, 128.3, 127.7, 127.7, 127.7, 127.6, 126.4, 99.9, 90.1, 84.1, 83.7, 82.0, 81.1, 78.3, 75.5, 75.4, 74.3, 70.4, 69.6, 68.9, 44.8, 44.0, 42.1, 41.8, 40.7, 37.5, 21.2, 18.7, 18.3, 14.5, 9.3, 8.8, 8.8.

HRMS (m/z): $[M+NH_4]^+$ calcd. for $C_{53}H_{68}O_{11}S$, 930.4826; found, 930.4796

TLC (EtOAc:Hexanes, 30:70 v/v): R_f = 0.2

IR (thin film, cm^{-1}): 3406, 2918, 2853, 1718, 1597, 1454, 1369, 1069

[α]$_D$: +15.0 (c = 0.24 in $CHCl_3$)

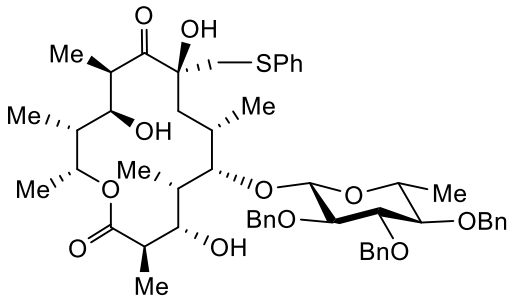

β-28

^{1}H NMR (700 MHz, C_6D_6): δ 7.45 (d, J = 7.5 Hz, 2H), 7.38 (d, J = 7.5 Hz, 2H), 7.31 – 7.23 (m, 3H), 7.19 – 7.12 (m, 4H), 7.09 (d, J = 6.5 Hz, 5H), 7.05 (s, 1H), 6.99 (t, J = 7.4 Hz, 2H), 6.90 (t, J = 7.2 Hz, 1H), 5.80 (q, J = 6.5 Hz, 1H), 5.08 (d, J = 11.7 Hz, 1H), 4.91 (d, J = 11.2 Hz, 1H), 4.86 (d, J = 11.5 Hz, 1H), 4.81 (d, J = 11.7 Hz, 2H), 4.68 (d, J = 7.6 Hz, 1H), 4.49 (d, J = 11.4 Hz, 1H), 4.02 (s, 1H), 3.89 (s, 1H), 3.79 (d, J = 9.6 Hz, 1H), 3.66 (t, J = 9.0 Hz, 1H), 3.59 – 3.52 (m, 3H), 3.40 (d, J = 13.3 Hz, 1H), 3.37 – 3.32 (m, 1H), 3.26 (d, J = 13.2 Hz, 1H), 3.21 – 3.13 (m, 2H), 2.99 – 2.94 (m, 1H), 2.55 (p, J = 6.4 Hz, 1H), 2.16 – 2.03 (m, 2H), 1.94 – 1.89 (m, 1H), 1.73 – 1.68 (m, 1H), 1.50 – 1.45 (m, 1H), 1.44 (d, J = 6.6 Hz, 3H), 1.27 (d, J = 6.0 Hz, 3H), 1.19 (t, J = 7.8 Hz, 6H), 0.95 (d, J = 6.3 Hz, 3H), 0.61 (d, J = 7.0 Hz, 3H).

^{13}C NMR (176 MHz, C_6D_6): δ 214.7, 175.7, 139.5, 139.2, 139.1, 137.8, 130.2, 130.2, 129.2, 128.6, 128.5, 128.5, 128.4, 128.2, 128.1, 128.1, 128.0, 127.9, 127.8, 127.6, 126.5, 102.3, 86.2, 85.5, 84.2, 83.5, 82.8, 77.3, 75.5, 75.1, 71.4, 70.3, 69.5, 44.4, 44.0, 42.1, 41.2, 37.8, 32.4, 29.6, 20.6, 18.6, 18.3, 14.8, 14.4, 9.1, 8.8, 8.7.

HRMS (m/z): $[M+NH_4]^+$ calcd. for $C_{53}H_{68}O_{11}S$, 930.4826; found, 930.4757

TLC (EtOAc:Hexanes, 30:70 v/v): R_f = 0.3

IR (thin film, cm^{-1}): 3382, 3240, 2957, 2912, 2851, 1694, 1617, 1453, 1069

[α]$_D$: -2.5 (c = 0.25 in $CHCl_3$)

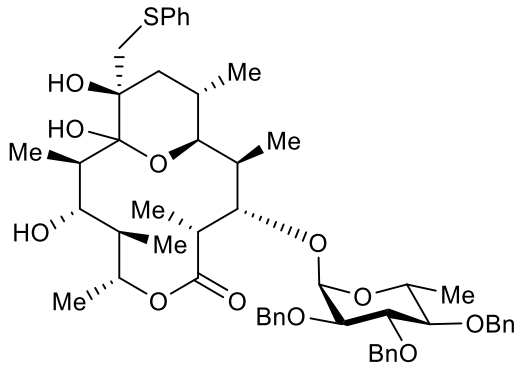

α-29

^{1}H NMR (700 MHz, C_6D_6): δ 7.52 (dd, J = 8.3, 1.0 Hz, 3H), 7.40 – 7.28 (m, 6H), 7.13 (t, J = 7.5 Hz, 3H), 7.11 – 7.03 (m, 7H), 6.95 (t, J = 7.4 Hz, 1H), 5.27 (d, J = 3.4 Hz, 1H), 5.26 – 5.22 (m, 1H), 5.04 (d, J = 11.3 Hz, 1H), 4.93 (dd, J = 20.5, 11.3 Hz, 2H), 4.68 (d, J = 11.6 Hz, 1H), 4.64 (d, J = 11.4 Hz, 2H), 4.54 (dq, J = 12.0, 5.9 Hz, 1H), 4.40 (d, J = 9.2 Hz, 1H), 4.35 – 4.27 (m, 1H), 3.90 (m, 2H), 3.60 (dd, J = 10.0, 3.4 Hz, 1H), 3.49 – 3.36 (m, 2H), 3.27 – 3.14 (m, 2H), 2.59 (q, J = 7.5, 6.9 Hz, 1H), 2.54 – 2.46 (m, 1H), 2.01 (s, 1H), 1.96 (dd, J = 13.7, 3.7 Hz, 1H), 1.83 – 1.68 (m, 2H), 1.50 (d, J = 6.1 Hz, 3H), 1.43 (d, J = 7.2 Hz, 3H), 1.25 (d, J = 7.1 Hz, 3H), 1.17 (d, J = 6.8 Hz, 3H), 1.05 (d, J = 7.2 Hz, 3H), 0.48 (d, J = 7.0 Hz, 3H), 0.39 (d, J = 6.6 Hz, 3H).

^{13}C NMR (176 MHz, C_6D_6): δ 175.1, 139.8, 139.4, 138.9, 138.6, 129.9, 129.3, 128.6, 128.5, 128.5, 128.4, 128.3, 128.0, 127.8, 127.7, 127.6, 127.5, 126.3, 107.4, 98.2, 84.9, 82.3, 81.8, 76.6, 75.6, 75.3, 74.3, 73.0, 72.9, 68.4, 44.1, 43.1, 42.2, 39.6, 37.9, 34.9, 32.4, 27.7, 23.2, 18.8, 16.0, 14.5, 14.4, 13.6, 9.9, 9.4, 7.6.

HRMS (m/z): $[M+Na-H_2O]^+$ calcd. for $C_{53}H_{68}O_{11}S$, 912.4720; found, 912.4690

TLC (EtOAc:Hexanes, 20:80 v/v): R_f = 0.3

IR (thin film, cm^{-1}): 3463, 2923, 2851, 1734, 1454, 1377, 1071

[α]$_D$: +4.0 (c = 0.12 in $CHCl_3$)

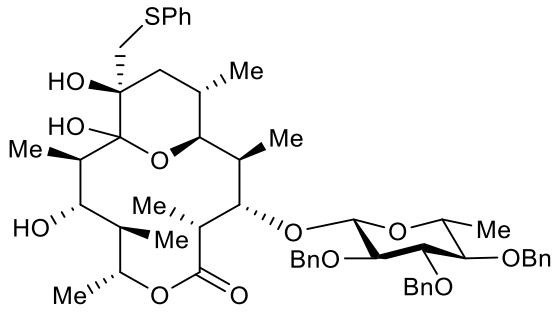

β-29

^{1}H NMR (700 MHz, C_6D_6): δ 7.54 (d, J = 7.3 Hz, 2H), 7.43 (d, J = 7.4 Hz, 2H), 7.30 (d, J = 7.4 Hz, 2H), 7.24 (d, J = 7.3 Hz, 2H), 7.20 – 7.13 (m, 4H), 7.12 – 7.02 (m, 7H), 6.96 (t, J = 7.4 Hz, 1H), 5.31 (d, J = 7.9 Hz, 1H), 5.17 (m, 2H), 4.95 (d, J = 11.4 Hz, 1H), 4.82 (dd, J = 27.1, 11.5 Hz, 2H), 4.71 (d, J = 11.4 Hz, 1H), 4.57 (dd, J = 10.7, 1.8 Hz, 1H), 4.48 (d, J = 11.6 Hz, 1H), 3.98 – 3.83 (m, 2H), 3.70 (t, J = 9.0 Hz, 1H), 3.65 – 3.54 (m, 2H), 3.51 – 3.38 (m, 2H), 3.26 – 3.13 (m, 2H), 2.80 – 2.71 (m, 1H), 2.51 – 2.40 (m, 1H), 2.05 – 1.94 (m, 2H), 1.85 – 1.75 (m, 1H), 1.77 – 1.69 (m, 1H), 1.54 – 1.45 (m, 1H), 1.43 (d, J = 7.3 Hz, 3H), 1.31 (d, J = 6.2 Hz, 3H), 1.22 (d, J = 6.8 Hz, 3H), 1.16 (d, J = 6.8 Hz, 3H), 1.11 (d, J = 7.2 Hz, 3H), 0.46 (d, J = 2.7 Hz, 3H), 0.45 (d, J = 3.1 Hz, 3H).

^{13}C NMR (176 MHz, C_6D_6): δ 177., 139.9, 139.5, 139.4, 138.7, 129.9, 129.3, 128.5, 128.5, 128.5, 128.4, 128.3, 128.1, 128.0, 127.7, 127.6, 127.6, 127.5, 126.3, 107.2, 101.1, 85.3, 84.1, 83.6, 80.8, 75.7, 74.9, 74.8, 73.9, 73.4, 73.4, 73.0, 71.6, 43.3, 43.0, 40.0, 39.5, 37.6, 34.9, 27.7, 18.2, 16.2, 14.4, 13.3, 10.8, 10.0, 7.6.

HRMS (m/z): $[M+Na-H_2O]^+$ calcd. for $C_{53}H_{68}O_{11}S$, 912.4720; found, 912.4703

TLC (EtOAc:Hexanes, 20:80 v/v): R_f = 0.4

IR (thin film, cm^{-1}): 2919, 2851, 1720, 1379, 1068

[α]$_D$: -+15.4 (c = 0.07 in $CHCl_3$)

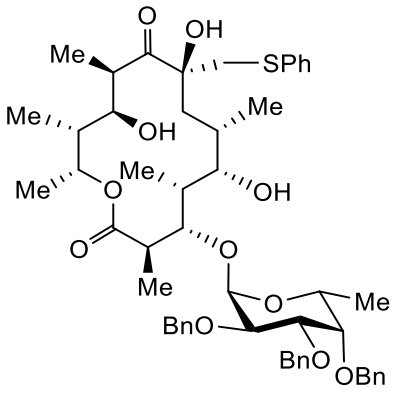

α-30

^{1}H NMR (500 MHz, C_6D_6): δ 7.36 (t, J = 7.7 Hz, 5H), 7.34 – 7.27 (m, 4H), 7.26 – 7.17 (m, 4H), 7.14 – 7.05 (m, 3H), 7.03 – 6.86 (m, 4H), 6.01 (q, J = 6.5 Hz, 1H), 4.93 (d, J = 11.3 Hz, 1H), 4.76 (d, J = 3.4 Hz, 1H), 4.67 – 4.51 (m, 5H), 4.48 (d, J = 11.3 Hz, 1H), 4.24 – 4.16 (m, 4H), 3.91 (dd, J = 10.4, 2.8 Hz, 1H), 3.84 (d, J = 4.4 Hz, 1H), 3.78 (q, J = 6.6 Hz, 1H), 3.68 (d, J = 9.7 Hz, 1H), 3.64 (d, J = 10.1 Hz, 1H), 3.44 (t, J = 2.9 Hz, 2H), 3.33 (d, J = 2.4 Hz, 1H), 3.27 (d, J = 13.5 Hz, 1H), 3.13 (d, J = 13.5 Hz, 1H), 3.03 (q, J = 6.8 Hz, 1H), 2.73 (dq, J = 10.3, 6.9 Hz, 1H), 2.14 (dd, J = 14.8, 10.6 Hz, 1H), 2.05 (d, J = 14.6 Hz, 1H), 1.75 (q, J = 7.8 Hz, 1H), 1.53 – 1.43 (m, 1H), 1.43 (d, J = 6.8 Hz, 3H), 1.36 (d, J = 7.0 Hz, 5H), 1.30 (d, J = 5.7 Hz, 3H), 1.21 (d, J = 6.7 Hz, 3H), 1.14 (d, J = 6.5 Hz, 3H), 1.00 (d, J = 6.7 Hz, 3H), 0.68 (d, J = 7.1 Hz, 3H).

^{13}C NMR (176 MHz, C_6D_6): δ 217.4, 175.4, 139.4, 139.1, 137.7, 137.7, 129.8, 129.2, 129.2, 128.8, 128.7, 128.5, 128.5, 128.4, 128.4, 128.3, 127.9, 127.8, 127.8, 127.7, 126.3, 101.8, 91.3, 84.4, 80.2, 79.1, 78.5, 76.6, 75.2, 74.6, 72.8, 70.4, 69.3, 67.5, 44.8, 44.5, 43.1, 42.3, 40.1, 39.1, 37.0, 21.0, 18.9, 16.8, 15.4, 9.9, 9.7, 8.8.

HRMS (m/z): $[M+Na]^+$ calcd. for $C_{53}H_{68}O_{11}S$, 935.4380; found, 935.4353

TLC (EtOAc:Hexanes, 30:70 v/v): R_f = 0.4

IR (thin film, cm^{-1}): 3399, 2920, 2851, 1723, 1453, 1380, 1099

$[\alpha]_D$: +12.8 (c = 0.09 in $CHCl_3$)

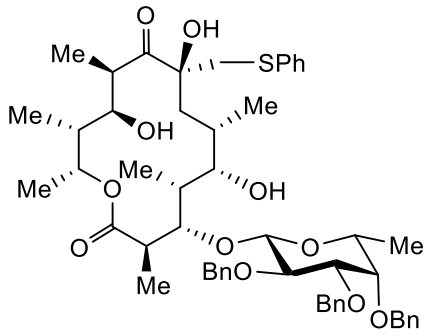

β-30

^{1}H NMR (700 MHz, C_6D_6): δ 7.36 (d, J = 7.5 Hz, 2H), 7.34 – 7.24 (m, 6H), 7.21 – 7.17 (m, 4H), 7.12 (dt, J = 15.3, 7.4 Hz, 4H), 7.08 – 6.89 (m, 4H), 5.96 (q, J = 6.5 Hz, 1H), 4.89 (d, J = 11.4 Hz, 1H), 4.86 (d, J = 11.7 Hz, 1H), 4.73 (d, J = 11.3 Hz, 1H), 4.61 (d, J = 12.0 Hz, 1H), 4.52 (d, J = 12.4 Hz, 2H), 4.30 (d, J = 7.7 Hz, 1H), 4.16 (s, 1H), 3.98 – 3.89 (m, 1H), 3.75 (s, 1H), 3.72 (d, J = 9.9 Hz, 2H), 3.32 (s, 1H), 3.27 (d, J = 13.6 Hz, 1H), 3.23 (dd, J = 9.8, 2.6 Hz, 1H), 3.13 (d, J = 13.5 Hz, 1H), 3.10 (d, J = 2.1 Hz, 1H), 3.03 (m, 2H), 2.84 (q, J = 6.3 Hz, 1H), 2.78 (dt, J = 13.5, 6.8 Hz, 1H), 2.17 – 2.10 (m, 1H), 2.07 (d, J = 14.8 Hz, 1H), 1.76 (q, J = 6.7 Hz, 1H), 1.48 (s, 3H), 1.46 (m, 2H), 1.43 (d, J = 6.7 Hz, 3H), 1.32 (d, J = 6.8 Hz, 3H), 1.20 (d, J = 6.8 Hz, 3H), 1.06 (d, J = 6.3 Hz, 3H), 1.02 (d, J = 6.6 Hz, 3H), 0.66 (d, J = 7.1 Hz, 3H).

^{13}C NMR (176 MHz, C_6D_6): δ 217.6, 175.0, 139.3, 139.2, 139.1, 137.7, 129.8, 129.2, 128.7, 128.5, 128.5, 128.3, 127.8, 127.8, 127.7, 126.3, 104.7, 87.8, 84.5, 82.7, 80.6, 80.2, 76.7, 75.5, 75.0, 73.2, 70.8, 70.5, 69.6, 45.4, 44.3, 42.1, 41.9, 40.3, 38.4, 37.6, 20.9, 18.8, 16.6, 14.5, 9.7, 9.6, 8.8.

HRMS (m/z): $[M+NH_4]^+$ calcd. for $C_{53}H_{68}O_{11}S$, 930.4826; found, 930.4801

TLC (EtOAc:Hexanes, 30:70 v/v): R_f = 0.25

IR (thin film, cm^{-1}): 3447, 2919, 2855, 1720, 1454, 1378, 1064

[α]$_D$: -2.3 (c = 0.69 in $CHCl_3$)

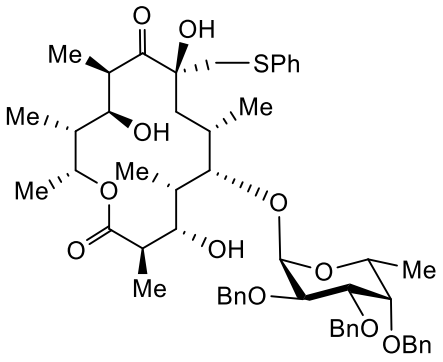

α-31

^{1}H NMR (500 MHz, C_6D_6): δ 7.39 (dd, J = 7.5, 5.9 Hz, 4H), 7.36 – 7.29 (m, 3H), 7.26 – 7.18 (m, 6H), 7.14 – 7.07 (m, 2H), 7.02 – 6.88 (m, 5H), 5.88 (q, J = 6.6 Hz, 1H), 5.05 (d, J = 3.8 Hz, 1H), 4.96 (d, J = 11.4 Hz, 1H), 4.75 – 4.43 (m, 5H), 4.18 (dd, J = 10.2, 3.8 Hz, 1H), 4.13 – 4.05 (m, 1H), 4.00 (s, 1H), 3.96 (dd, J = 10.2, 2.8 Hz, 1H), 3.83 – 3.76 (m, 1H), 3.72 (d, J = 9.8 Hz, 1H), 3.54 (s, 1H), 3.40 (s, 1H), 3.38 (d, J = 2.6 Hz, 1H), 3.25 (d, J = 13.2 Hz, 1H), 3.07 (d, J = 13.1 Hz, 1H), 2.99 – 2.89 (m, 2H), 2.74 (dq, J = 10.6, 6.6 Hz, 1H), 2.14 (dd, J = 14.7, 10.4 Hz, 1H), 1.98 (dd, J = 14.8, 3.1 Hz, 1H), 1.93 – 1.83 (m, 1H), 1.64 – 1.55 (m, 1H), 1.45 (d, J = 6.7 Hz, 3H), 1.43 (m, 1H), 1.30 (d, J = 6.4 Hz, 3H), 1.27 (d, J = 7.1 Hz, 3H), 1.25 (d, J = 6.8 Hz, 3H), 1.18 (d, J = 6.7 Hz, 3H), 0.98 (d, J = 6.7 Hz, 3H), 0.66 (d, J = 7.1 Hz, 3H).

^{13}C NMR (176 MHz, C_6D_6): δ 216.3, 175.4, 139.4, 139.3, 139.0, 129.9, 129.2, 128.8, 128.7, 128.5, 128.4, 128.3, 127.4, 127.4, 127.1, 126.4, 100.6, 89.0, 83.7, 79.7, 78.7, 78.2, 77.0, 75.2, 74.5, 72.9, 70.4, 69.6, 68.6, 44.6, 44.0, 42.1, 41.5, 40.7, 37.5, 20.7, 18.7, 17.0, 14.8, 9.3, 8.7.

HRMS (m/z): $[M+Na]^+$ calcd. for $C_{53}H_{68}O_{11}S$, 935.4380; found, 935.4337

TLC (EtOAc:Hexanes, 30:70 v/v): R_f = 0.2

IR (thin film, cm^{-1}): 3472, 2920, 2880, 2852, 1707, 1455, 1106

[α]$_D$: +38.0 (c = 0.07 in $CHCl_3$)

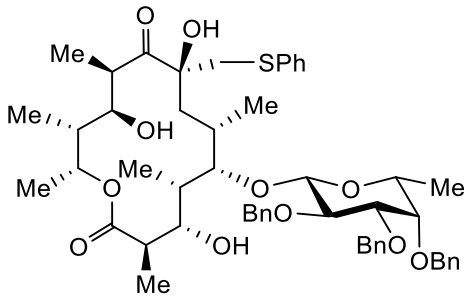

β-31

^{1}H NMR (700 MHz, C_6D_6): δ 7.46 (d, J = 7.5 Hz, 2H), 7.38 (t, J = 7.4 Hz, 4H), 7.30 (d, J = 7.5 Hz, 2H), 7.21 – 7.18 (m, 5H), 7.10 (m, 4H), 7.01 (t, J = 7.7 Hz, 2H), 6.91 (t, J = 7.4 Hz, 1H), 5.74 (q, J = 6.2 Hz, 1H), 4.98 (d, J = 11.3 Hz, 1H), 4.91 (t, J = 12.7 Hz, 2H), 4.57 – 4.47 (m, 4H), 4.26 (s, 1H), 4.05 (dd. J = 9.6, 7.9 Hz, 1H), 3.99 (s, 1H), 3.96 (s, 1H), 3.90 (d, J = 9.8 Hz, 1H), 3.80 (dd, J = 9.6, 4.1 Hz, 1H), 3.63 (s, 1H), 3.39 (d, J = 13.2 Hz, 1H), 3.34 (dd, J = 9.6, 2.6 Hz, 1H), 3.24 (d, J = 13.2 Hz, 1H), 3.20 – 3.15 (m, 1H), 3.07 (q, J = 6.1 Hz, 1H), 2.91 (q, J = 6.9 Hz, 1H), 2.60 (dt, J = 13.2, 6.7 Hz, 1H), 2.49 (s, 1H), 2.05 – 1.90 (m, 4H), 1.47 – 1.41 (m, 1H), 1.33 (d, J = 6.5 Hz, 3H), 1.30 (d, J = 6.7 Hz, 3H), 1.20 (d, J = 7.1 Hz, 3H), 1.18 (d, J = 6.8 Hz, 3H), 1.17 (d, J = 6.3 Hz, 3H), 0.94 (d, J = 6.6 Hz, 3H), 0.61 (d, J = 7.1 Hz, 3H).

^{13}C NMR (176 MHz, C_6D_6): δ 213.8, 176.1, 139.4, 139.2, 139.1, 137.9, 130.1, 129.2, 128.7, 128.5, 128.4, 128.4, 128.3, 128.1, 128.0, 127.8, 127.8, 127.7, 126.4, 103.7, 87.7, 83.8, 83.4, 79.6, 77.7, 77.2, 75.5, 75.2, 72.9, 70.6, 70.4, 69.7, 44.7, 43.2, 42.1, 41.8, 40.4, 38.3, 37.0, 20.1, 18.6, 17.2, 14.8, 8.8, 8.6.

HRMS (m/z): $[M+NH_4]^+$ calcd. for $C_{53}H_{68}O_{11}S$, 930.4826; found, 930.4716

TLC (EtOAc:Hexanes, 30:70 v/v): R_f = 0.2

IR (thin film, cm^{-1}): 3525, 2925, 1705, 1453, 1362, 1067

[α]$_D$: -15.4 (c = 0.08 in $CHCl_3$)

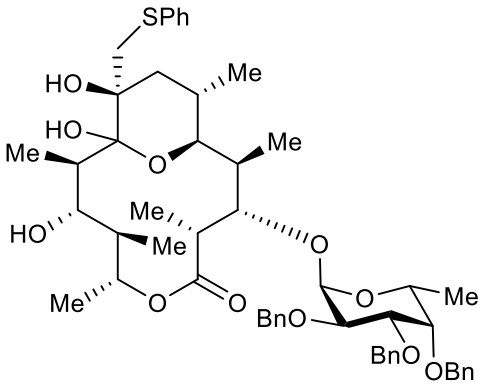

α-32

^{1}H NMR (700 MHz, C_6D_6): δ 7.52 (d, J = 7.3 Hz, 2H), 7.41 (dd, J = 16.9, 7.4 Hz, 4H), 7.32 (d, J = 7.4 Hz, 2H), 7.21 (t, J = 7.6 Hz, 2H), 7.15 – 7.02 (m, 9H), 6.95 (t, J = 7.4 Hz, 1H), 5.34 – 5.26 (m, 1H), 5.24 (d, J = 3.5 Hz, 1H), 5.04 (d, J = 11.2 Hz, 1H), 4.71 (t, J = 11.2 Hz, 2H), 4.63 (d, J = 11.8 Hz, 1H), 4.53 (dd, J = 20.0, 11.3 Hz, 2H), 4.47 – 4.41 (m, 2H), 4.30 (dd, J = 10.4, 3.5 Hz, 1H), 4.17 (dd, J = 10.4, 2.7 Hz, 1H), 3.92 (dd, J = 10.6, 8.3 Hz, 1H), 3.87 (d, J = 10.5 Hz, 1H), 3.52 (s, 1H), 3.48 (d, J = 13.3 Hz, 1H), 3.42 (d, J = 13.3 Hz, 1H), 3.22 (p, J = 7.2 Hz, 1H), 2.61 – 2.51 (m, 2H), 2.01 (s, 1H), 1.98 (dd, J = 13.7, 3.7 Hz, 1H), 1.82 – 1.68 (m, 2H), 1.46 (d, J = 6.3 Hz, 3H), 1.43 (m, 1H), 1.38 (d, J = 7.1 Hz, 3H), 1.19 (d, J = 6.8 Hz, 6H), 1.10 (d, J = 7.2 Hz, 3H), 0.50 (d, J = 7.0 Hz, 3H), 0.38 (d, J = 6.6 Hz, 3H).

^{13}C NMR (176 MHz, C_6D_6): δ 175.0, 139.8, 139.6, 139.4, 138.7, 129.9, 129.3, 128.6, 128.5, 128.4, 128.4, 128.4, 128.3, 128.1, 128.0, 127.8, 127.7, 127.6, 127.6, 126.3, 107.5, 98.8, 81.1, 79.7, 79.2, 77.7, 75.5, 74.6, 74.4, 73.1, 73.1, 73.1, 72.8, 68.0, 44.2, 43.0, 42.4, 39.8, 38.0, 35.0, 27.7, 17.4, 15.9, 14.5, 13.7, 9.4, 9.0, 7.6.

HRMS (m/z): $[M+Na-H_2O]^+$ calcd. for $C_{53}H_{68}O_{11}S$, 912.4720; found, 912.4676

TLC (EtOAc:Hexanes, 20:80 v/v): R_f = 0.3

IR (thin film, cm^{-1}): 2923, 2853, 1726, 1455, 1377, 1100

[α]$_D$: +9.0 (c = 0.08 in $CHCl_3$)

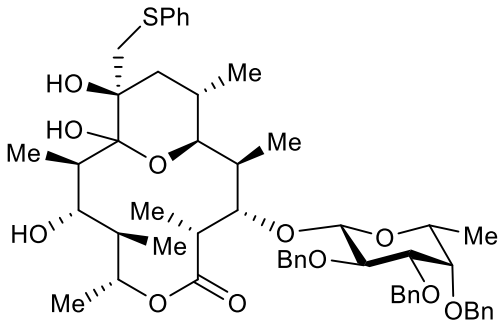

β-32

^{1}H NMR (500 MHz, C_6D_6): δ 7.54 (dd, J = 8.3, 1.1 Hz, 2H), 7.46 (d, J = 7.1 Hz, 2H), 7.35 (t, J = 7.5 Hz, 4H), 7.22 – 7.17 (m, 4H), 7.16 – 7.08 (m, 4H), 7.10 – 7.01 (m, 3H), 7.00 – 6.90 (m, 1H), 5.23 – 5.11 (m, 3H), 4.99 (d, J = 11.7 Hz, 1H), 4.80 (d, J = 11.4 Hz, 1H), 4.71 (d, J = 11.9 Hz, 1H), 4.59 – 4.47 (m, 3H), 4.27 (s, 1H), 4.08 (dd, J = 9.7, 7.8 Hz, 1H), 3.94 – 3.84 (m, 2H), 3.53 – 3.40 (m, 3H), 3.27 (q, J = 6.2 Hz, 1H), 3.25 – 3.18 (m, 1H), 3.19 (d, J = 2.6 Hz, 1H), 2.76 (qd, J = 7.2, 1.7 Hz, 1H), 2.47 (dtd, J = 14.0, 7.0, 1.8 Hz, 1H), 2.04 – 1.91 (m, 2H), 1.78 – 1.64 (m, 2H), 1.46 (d, J = 7.3 Hz, 3H), 1.23 (d, J = 6.4 Hz, 3H), 1.20 – 1.15 (m, 6H), 1.13 (d, J = 7.2 Hz, 3H), 0.48 (d, J = 7.0 Hz, 3H), 0.41 (d, J = 6.4 Hz, 3H).

^{13}C NMR (176 MHz, C_6D_6): δ 177.2, 140.0, 139.7, 139.7, 138.8, 129.9, 129.2, 128.6, 128.4, 128.4, 128.4, 128.4, 128.3, 128.1, 128.0, 127.8, 127.7, 127.6, 127.4, 126.2, 107.2, 101.7, 83.3, 80.8, 80.7, 78.0, 75.3, 75.2, 73.8, 73.7, 73.4, 73.4, 73.0, 70.7, 43.5, 42.9, 40.2, 39.3, 37.5, 34.9, 34.3, 32.4, 27.7, 27.3, 23.2, 17.2, 16.2, 14.6, 14.4, 13.3, 11.0, 10.1, 7.7.

HRMS (m/z): $[M+Na-H_2O]^+$ calcd. for $C_{53}H_{68}O_{11}S$, 912.4720; found, 912.4699

TLC (EtOAc:Hexanes, 20:80 v/v): R_f = 0.3

IR (thin film, cm^{-1}): 2920, 2851, 1718, 1461, 1378, 1086

[α]$_D$: -4.4 (c = 0.28 in $CHCl_3$)

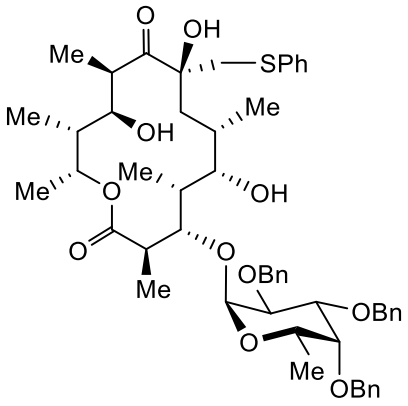

α-33

^{1}H NMR (500 MHz, C_6D_6): δ 7.43 – 7.26 (m, 8H), 7.24 – 7.18 (m, 5H), 7.14 – 6.86 (m, 7H), 5.92 (q, J = 6.7 Hz, 1H), 4.98 (d, J = 11.3 Hz, 1H), 4.84 (d, J = 3.5 Hz, 1H), 4.73 (d, J = 12.0 Hz, 1H), 4.59 (d, J = 12.1 Hz, 1H), 4.49 (dd, J = 19.3, 11.3 Hz, 2H), 4.34 (d, J = 11.5 Hz, 1H), 4.21 (s, 1H), 4.08 (dd, J = 10.2, 3.6 Hz, 1H), 3.96 (q, J = 7.2 Hz, 1H), 3.83 (dd, J = 10.3, 2.6 Hz, 1H), 3.73 (d, J = 10.0 Hz, 1H), 3.67 – 3.54 (m, 3H), 3.44 (s, 1H), 3.37 – 3.28 (m, 2H), 3.19 (d, J = 13.6 Hz, 1H), 3.06 (q, J = 6.5 Hz, 1H), 2.86 – 2.71 (m, 1H), 2.24 (dd, J = 14.7, 10.6 Hz, 1H), 2.00 (d, J = 14.6 Hz, 1H), 1.88 – 1.74 (m, 1H), 1.51 (d, J = 6.8 Hz, 3H), 1.46 (s, 3H), 1.44 (m, 1H), 1.22 (d, J = 6.8 Hz, 3H), 1.19 (d, J = 6.4 Hz, 6H), 0.96 (d, J = 6.6 Hz, 3H), 0.64 (d, J = 7.1 Hz, 3H).

^{13}C NMR (126 MHz, C_6D_6): δ 216.2, 175.2, 139.1, 139.0, 138.9, 138.5, 129.5, 129.1, 128.8, 128.8, 128.3, 128.3, 128.2, 128.2, 128.1, 128.1, 127.9, 127.7, 127.6, 127.3, 127.1, 126.0, 125.6, 100.8, 89.5, 83.9, 80.6, 78.1, 77.9, 77.4, 74.9, 74.1, 73.7, 72.7, 72.3, 71.5, 69.9, 68.9, 68.5, 67.2, 45.1, 44.4, 42.6, 41.7, 40.0, 38.9, 20.5, 18.3, 16.9, 16.2, 15.2, 12.6, 9.1, 9.1, 8.5.

HRMS (m/z): $[M+NH_4]^+$ calcd. for $C_{53}H_{68}O_{11}S$, 930.4826; found, 930.4797

TLC (EtOAc:Hexanes, 40:60 v/v): R_f = 0.36

IR (thin film, cm^{-1}): 3351, 2924, 2850, 1723, 1454, 1377, 1097

[α]$_D$: -27.8 (c = 0.11 in $CHCl_3$)

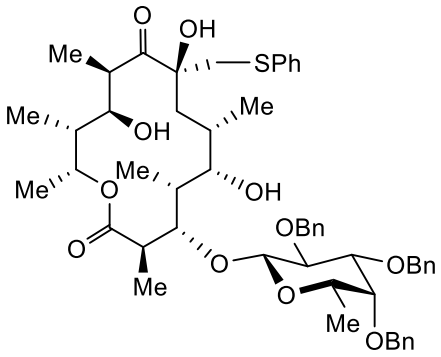

β-33

^{1}H NMR (500 MHz, C_6D_6): δ 7.39 (d, J = 7.3 Hz, 2H), 7.35 (d, J = 7.1 Hz, 2H), 7.31 (d, J = 8.5 Hz, 2H), 7.24 (d, J = 7.2 Hz, 2H), 7.19 - 7.13 (m, 6H), 7.09 (t, J = 7.4 Hz, 3H), 7.00 (t, J = 7.6 Hz, 2H), 6.92 (t, J = 7.4 Hz, 1H), 5.94 (q, J = 6.6 Hz, 1H), 4.94 – 4.78 (m, 3H), 4.49 (d, J = 11.5 Hz, 1H), 4.41 (d, J = 7.7 Hz, 1H), 4.41 – 4.29 (m, 2H), 4.16 (s, 1H), 4.03 – 3.93 (m, 2H), 3.71 (d, J = 11.3 Hz, 2H), 3.31 (s, 1H), 3.23 – 2.95 (m, 7H), 2.79 (dq, J = 9.9, 6.5 Hz, 1H), 2.12 – 1.91 (m, 2H), 1.83 (q, J = 7.2 Hz, 1H), 1.58 (d, J = 6.8 Hz, 3H), 1.49 – 1.39 (m, 2H), 1.35 (d, J = 6.4 Hz, 3H), 1.26 (d, J = 6.9 Hz, 3H), 1.20 (d, J = 2.5 Hz, 3H), 1.18 (d, J = 3.0 Hz, 3H), 0.98 (d, J = 6.6 Hz, 3H), 0.67 (d, J = 7.1 Hz, 3H).

^{13}C NMR (126 MHz, C_6D_6): δ 217.2, 175.6, 139.3, 138.9, 138.5, 137.7, 129.9, 129.2, 128.7, 128.6, 128.5, 128.5, 128.4, 128.2, 128.0, 127.8, 126.4, 103.9, 86.5, 84.2, 84.0, 80.0, 79.8, 77.0, 76.1, 75.3, 73.0, 70.8, 70.4, 69.6, 44.5, 44.3, 42.7, 42.2, 40.3, 38.5, 37.3, 20.8, 18.7, 17.0, 16.0, 9.6, 9.1, 8.8.

HRMS (m/z): $[M+NH_4]^+$ calcd. for $C_{53}H_{68}O_{11}S$, 930.4826; found, 930.4806

TLC (EtOAc:Hexanes, 30:70 v/v): R_f = 0.3

IR (thin film, cm^{-1}): 3479, 2972, 2921, 2854, 1727, 1453, 1378, 1069

[α]$_D$: -6.2 (c = 0.13 in $CHCl_3$)

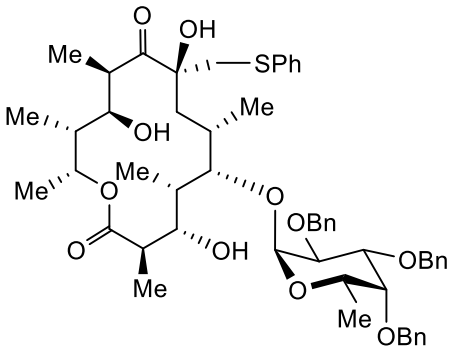

α-34

^{1}H NMR (700 MHz, C_6D_6): δ 7.43 – 7.32 (m, 6H), 7.21 (dt, J = 19.7, 7.7 Hz, 5H), 7.14 – 7.10 (m, 4H), 7.10 – 7.03 (m, 2H), 7.00 (t, J = 7.8 Hz, 2H), 6.89 (t, J = 7.4 Hz, 1H), 5.64 (q, J = 6.5 Hz, 1H), 4.99 (d, J = 11.4 Hz, 1H), 4.97 (d, J = 3.6 Hz, 1H), 4.75 – 4.64 (m, 2H), 4.62 – 4.47 (m, 3H), 4.20 (dd, J = 10.2, 3.7 Hz, 1H), 4.05 (d, J = 9.0 Hz, 1H), 4.00 (d, J = 3.6 Hz, 1H), 3.97 – 3.89 (m, 3H), 3.86 (d, J = 10.4 Hz, 1H), 3.69 – 3.61 (m, 2H), 3.45 (d, J = 13.2 Hz, 1H), 3.40 – 3.34 (m, 1H), 3.22 (d, J = 13.3 Hz, 1H), 2.92 (q, J = 5.9 Hz, 1H), 2.75 (dq, J = 10.2, 6.8 Hz, 1H), 2.24 – 2.16 (m, 1H), 2.03 – 1.94 (m, 2H), 1.78 (dd, J = 14.5, 6.5 Hz, 1H), 1.50 – 1.41 (m, 1H), 1.38 (d, J = 6.7 Hz, 3H), 1.26 (d, J = 7.0 Hz, 3H), 1.21 (d, J = 6.7 Hz, 3H), 1.17 (d, J = 6.5 Hz, 3H), 1.12 (d, J = 7.0 Hz, 3H), 0.95 (d, J = 6.6 Hz, 3H), 0.68 (d, J = 7.0 Hz, 3H).

^{13}C NMR (176 MHz, C_6D_6): δ 211.0, 177.1, 139.4, 139.3, 138.3, 137.8, 130.2, 129.4, 129.0, 128.7, 128.7, 128.6, 128.4, 128.4, 127.8, 126.5, 100.4, 89.7, 82.5, 79.7, 78.4, 78.3, 77.4, 75.2, 74.8, 73.2, 70.5, 69.7, 68.0, 44.9, 43.2, 42.3, 38.9, 35.9, 18.8, 18.6, 17.1, 15.3, 8.9, 8.6, 8.0.

HRMS (m/z): $[M+Na]^+$ calcd. for $C_{53}H_{68}O_{11}S$, 935.4380; found, 935.4365

TLC (EtOAc:Hexanes, 30:70 v/v): R_f = 0.36

IR (thin film, cm^{-1}): 3334, 2923, 2852, 1716, 453, 1178, 1047

[α]$_D$: -34.4 (c = 0.19 in $CHCl_3$)

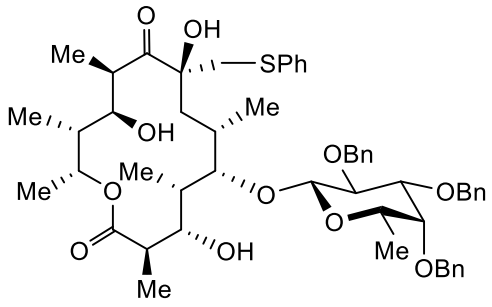

β-34

^{1}H NMR (700 MHz, C_6D_6): δ 7.58 (d, J = 7.6 Hz, 2H), 7.35 (d, J = 7.5 Hz, 2H), 7.31 (d, J = 7.4 Hz, 4H), 7.28 – 7.18 (m, 4H), 7.13 (t, J = 7.4 Hz, 4H), 7.06 (dd, J = 16.3, 8.9 Hz, 2H), 7.00 (t, J = 7.6 Hz, 2H), 6.92 (t, J = 7.4 Hz, 1H), 5.92 (q, J = 6.6 Hz, 1H), 5.09 (d, J = 10.5 Hz, 1H), 4.90 (d, J = 12.0 Hz, 1H), 4.81 (d, J = 10.5 Hz, 1H), 4.64 (d, J = 11.9 Hz, 1H), 4.53 (dd, J = 15.1, 12.1 Hz, 2H), 4.36 (d, J = 7.7 Hz, 1H), 4.28 (s, 1H), 4.15 (s, 1H), 4.05 – 4.02 (m, 1H), 3.99 (d, J = 10.2 Hz, 1H), 3.64 (d, J = 9.5 Hz, 1H), 3.54 (s, 1H), 3.48 (s, 1H), 3.20 (dd, J = 10.0, 2.3 Hz, 1H), 3.15 (d, J = 13.5 Hz, 1H), 3.10 – 3.02 (m, 2H), 2.98 (q, J = 7.2, 6.8 Hz, 1H), 2.87 (q, J = 6.2 Hz, 1H), 2.84 – 2.76 (m, 1H), 2.17 – 2.07 (m, 1H), 2.00 (d, J = 14.5 Hz, 1H), 1.78 (d, J = 7.0 Hz, 1H), 1.60 (d, J = 6.7 Hz, 3H), 1.51 – 1.40 (m, 2H), 1.34 (d, J = 6.5 Hz, 3H), 1.30 (d, J = 7.1 Hz, 3H), 1.19 (d, J = 6.7 Hz, 3H), 1.13 (d, J = 6.2 Hz, 3H), 0.96 (d, J = 6.4 Hz, 3H), 0.62 (d, J = 7.1 Hz, 3H).

^{13}C NMR (176 MHz, C_6D_6): δ 216.3, 175.9, 139.2, 139.1, 137.5, 130.1, 129.2, 128.8, 128.7, 128.6, 128.5, 128.4, 128.3, 127.8, 127.8, 126.5, 106.5, 89.7, 84.1, 82.6, 80.0, 79.7, 76.6, 76.0, 75.0, 73.4, 71.2, 70.3, 69.0, 45.0, 44.6, 42.2, 41.9, 40.3, 40.0, 36.7, 20.4, 18.8, 16.6, 15.1, 9.6, 8.9.

HRMS (m/z): $[M+NH_4]^+$ calcd. for $C_{53}H_{68}O_{11}S$, 930.4826; found, 930.4774

TLC (EtOAc:Hexanes, 30:70 v/v): R_f = 0.2

IR (thin film, cm^{-1}): 3441, 2920, 2825, 1723, 1454, 1378, 1084

[α]$_D$: -7.0 (c = 0.11 in $CHCl_3$)

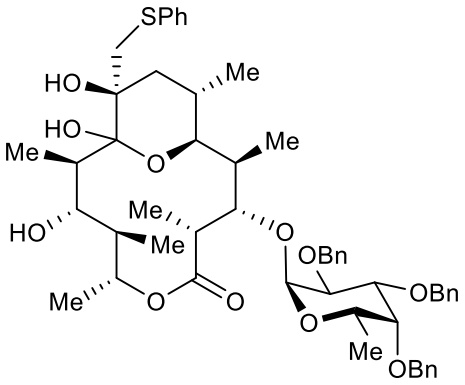

α-35

^{1}H NMR (700 MHz, C_6D_6): δ 7.52 (d, J = 8.2 Hz, 2H), 7.43 (d, J = 7.7 Hz, 2H), 7.37 (dd, J = 15.7, 7.7 Hz, 4H), 7.23 – 7.18 (m, 5H), 7.15 – 7.03 (m, 6H), 6.95 (t, J = 7.0 Hz, 1H), 5.90 (d, J = 3.5 Hz, 1H), 5.26 (q, J = 6.6 Hz, 1H), 5.09 (d, J = 11.3 Hz, 1H), 4.76 (d, J = 11.9 Hz, 1H), 4.66 (d, J = 11.2 Hz, 1H), 4.63 – 4.51 (m, 3H), 4.46 (d, J = 10.5 Hz, 1H), 4.32 (dd, J = 10.4, 3.4 Hz, 1H), 4.13 – 4.05 (m, 2H), 3.97 (d, J = 10.4 Hz, 1H), 3.90 – 3.84 (m, 1H), 3.53 – 3.39 (m, 2H), 3.18 (p, J = 7.4 Hz, 1H), 2.76 (q, J = 7.2 Hz, 1H), 2.45 (p, J = 8.1, 7.5 Hz, 1H), 2.02 – 1.94 (m, 2H), 1.86 – 1.74 (m, 2H), 1.51 – 1.40 (m, 4H), 1.33 (d, J = 6.4 Hz, 3H), 1.20 – 1.14 (m, 6H), 1.12 (d, J = 7.1 Hz, 3H), 0.44 (d, J = 6.8 Hz, 3H), 0.38 (d, J = 6.9 Hz, 3H).

^{13}C NMR (176 MHz, C_6D_6): δ 176.7, 139.7, 139.7, 139.5, 138.6, 129.9, 129.3, 128.6, 128.5, 128.4, 128.4, 128.3, 127.7, 127.7, 127.5, 126.3, 107.3, 96.6, 81.0, 79.6, 79.1, 77.4, 75.2, 74.4, 73.3, 73.3, 73.2, 73.0, 67.5, 43.6, 43.1, 40.5, 39.6, 38.0, 34.9, 27.7, 17.1, 16.1, 14.4, 13.5, 10.4, 10.2, 7.7.

HRMS (m/z): $[M+Na-H_2O]^+$ calcd. for $C_{53}H_{68}O_{11}S$, 912.4720; found, 912.4700

TLC (EtOAc:Hexanes, 20:80 v/v): R_f = 0.36

IR (thin film, cm^{-1}): 3477, 2959, 2923, 2852, 1725, 1454, 1374, 1098

$[\alpha]_D$: -36.7 (c = 0.17 in $CHCl_3$)

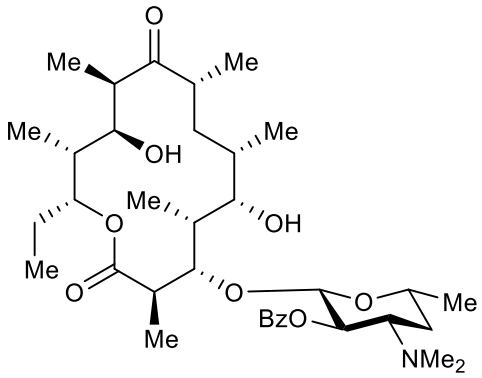

37a

^{1}H NMR (700 MHz, $CDCl_3$) δ 8.05 (d, J = 6.9 Hz, 2H), 7.56 (t, J = 7.4 Hz, 1H), 7.44 (t, J = 7.7 Hz, 2H), 5.15 (m, 2H), 4.70 (d, J = 7.6 Hz, 1H), 3.90 (s, 1H), 3.86 – 3.81 (m, 2H), 3.76 – 3.66 (m, 2H), 3.47 (d, J = 10.1 Hz, 1H), 2.87 (m, 1H), 2.81 (q, J = 6.9 Hz, 1H), 2.76 – 2.69 (m, 1H), 2.57 (dt, J = 10.0, 6.4 Hz, 1H), 2.27 (s, 6H), 1.88 – 1.76 (m, 1H), 1.75 – 1.39 (m, 4H), 1.34 (d, J = 6.1 Hz, 3H), 1.09 (t, J = 6.1 Hz, 6H), 1.06 (m, 2H), 1.03 (dd, J = 6.9, 1.5 Hz, 6H), 0.99 (d, J = 6.8 Hz, 3H), 0.96 – 0.85 (m, 2H), 0.84 (t, J = 7.2 Hz, 6H).

^{13}C NMR (176 MHz, C_6D_6) δ 210.6, 176.1, 129.9, 132.5, 128.3, 75.5, 71.6, 103.5, 76.3, 86.4, 70.7, 69.7, 40.8, 45.1, 63.7, 40.4, 40.4, 37.2, 40.6, 35.6, 40.5, 29.9, 15.0, 8.7, 30.0, 17.8, 7.7, 14.7, 20.5, 10.4, 8.8

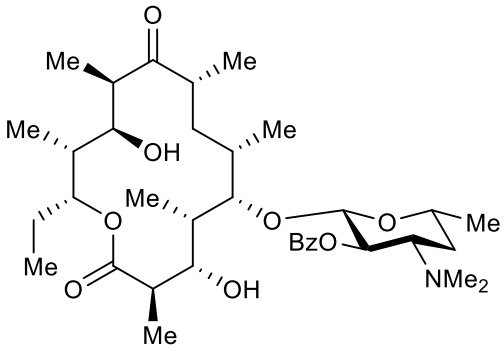

37b

^{1}H NMR (700 MHz, $CDCl_3$) δ 8.08 (d, *J* = 6.9 Hz, 2H), 7.55 (t, *J* = 7.4 Hz, 1H), 7.44 (t, *J* = 7.7 Hz, 2H), 5.12 – 5.02 (m, 2H), 4.65 (d, *J* = 7.6 Hz, 1H), 3.88 (d, *J* = 4.5 Hz, 1H), 3.80 (d, *J* = 4.8 Hz, 1H), 3.64 (dd, *J* = 15.1, 8.6 Hz, 2H), 3.58 (d, *J* = 10.5 Hz, 1H), 2.86 (m, 1H), 2.71 (q, *J* = 6.9 Hz, 1H), 2.61 (dt, *J* = 11.1, 6.0 Hz, 1H), 2.53 (dq, *J* = 10.3, 6.7 Hz, 1H), 2.32 (d, *J* = 25.9 Hz, 1H), 2.26 (s, 6H), 1.81 (d, *J* = 13.1 Hz, 1H), 1.80 – 1.70 (m, 1H), 1.71 – 1.64 (m, 1H), 1.65 – 1.52 (m, 2H), 1.52 – 1.41 (m, 2H), 1.33 (dd, *J* = 15.3, 6.5 Hz, 1H), 1.29 (d, *J* = 6.1 Hz, 3H), 1.27 – 1.19 (m, 2H), 1.08 (d, *J* = 6.4 Hz, 3H), 1.04 (d, *J* = 7.0 Hz, 3H), 1.00 (d, *J* = 6.8 Hz, 3H), 0.91 (d, *J* = 3.4 Hz, 3H), 0.90 (d, *J* = 3.0 Hz, 2H), 0.87 (t, *J* = 7.4 Hz, 3H), 0.80 (d, *J* = 6.9 Hz, 3H).

^{13}C NMR (126 MHz, $CDCl_3$) δ 212.5, 165.9, 133.0, 130.1, 128.4, 103.5, 86.3, 78.1, 76.1, 72.0, 71.0, 69.9, 64.0, 44.3, 43.4, 40.9, 40.7, 38.2, 37.5, 34.7, 30.9, 29.9, 25.5, 21.3, 17.4, 14.7, 13.6, 10.8, 9.3, 8.1, 6.5.

Structural Elucidation of Glycoside Products

The structure of each isolated glycoside was characterized and assigned based on 1D and 2D NMR experiments. Each proton signal on ^{1}H NMR was assigned by analyzing cross-peaks on COSY, HSQC, and HMBC spectra. Figure 2.10 shows **(a)** easily identifiable starting points for NMR assignments, and **(b)** propagation of frequently observed COSY or HMBC correlations for each isolated spin systems.

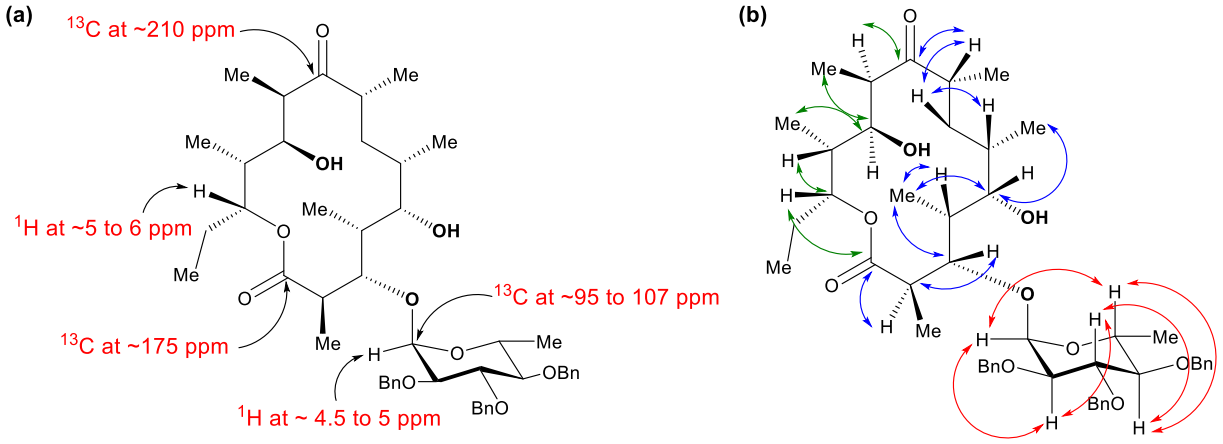

Figure 2.10. General guidelines for NMR signal assignments for glycoside products.

The stereochemical configuration of glycosidic linkage (α or β) was assigned based on the ^{3}J coupling constant between anomeric proton **H1'** and its vicinal proton **H2'**. For α-anomer, **H1'** and **H2'** are in *gauche* conformation; for β-anomer, **H1'** and **H2'** are in *anti* conformation. According to Karplus equation, the ^{3}J coupling constant between **H1'** and **H2'** in α-anomer should be smaller (~ 3 to 4 Hz) compared to the ^{3}J coupling constant between **H1'** and **H2'** in β-anomer (~7.5 to 8.0 Hz).

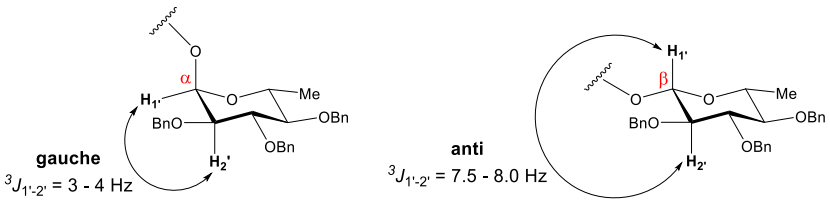

Figure 2.11. Assignments for anomeric configuration of glycosidic linkage.

The site of glycosylation on macrolide was assigned based on the observation of HMBC cross-peak between anomeric carbon and proton geminal to hydroxyl group or cross-peak between anomeric proton and carbon with hydroxyl group.

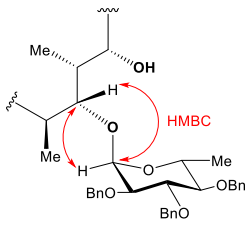

Figure 2.12. Determining site of glycosylation based on HMBC correlations.

Table 2.6 summarizes ^{3}J coupling constants and key HMBC correlations used to assign the stereochemical configuration of glycosidic linkages and sites of glycosylation for each glycoside:

Compound	**^{3}J ($H_{1'}$-$H_{2'}$)**	**HMBC Correlations**
3	3.1 Hz	$H_{1'}$ (δ 4.74) - C_3 (δ 91.8) H_3 (δ 3.77) - $C_{1'}$ (δ 100.6)
4	3.7 Hz	$H_{1'}$ (δ 4.92) - C_5 (δ 82.5) H_5 (δ 3.94) - $C_{1'}$ (δ 95.9)
5	3.8 Hz 3.6 Hz	$H_{1'}$ (δ 4.99) - C_5 (δ 80.3) $H_{1'}$ (δ 5.71) - C_{11} (δ 83.7) H_{11} (δ 4.30) - $C_{1'}$ (δ 100.9)
α-23	3.5 Hz	$H_{1'}$ (δ 4.86) - C_3 (δ 89.8) H_3 (δ 3.80) - $C_{1'}$ (δ 100.8)
α-24	3.8 Hz	H_5 (δ 3.85) - $C_{1'}$ (δ 94.2)
β-24	7.7 Hz	$H_{1'}$ (δ 4.32) - C_5 (δ 85.8) H_5 (δ 3.95) - $C_{1'}$ (δ 104.9)
α-27	3.3 Hz	$H_{1'}$ (δ 4.67) - C_3 (δ 92.4) H_3 (δ 3.62) - $C_{1'}$ (δ 101.0)
β-27	7.9 Hz	$H_{1'}$ (δ 4.31) - C_3 (δ 88.3) H_3 (δ 3.64) - $C_{1'}$ (δ 104.4)
α-28	3.6 Hz	$H_{1'}$ (δ 4.95) - C_5 (δ 90.1) H_5 (δ 3.52) - $C_{1'}$ (δ 99.9)
β-28	7.8 Hz	$H_{1'}$ (δ 4.68) - C_5 (δ 86.2)
α-29	3.4 Hz	H_3 (δ 4.39) - $C_{1'}$ (δ 98.2) H_5 (δ 3.92) - C_9 (δ 107.5) H_{11} (δ 3.36) - C_9 (δ 107.5)
β-29	7.9 Hz	H_3 (δ 4.55) - $C_{1'}$ (δ 101.1) H_5 (δ 3.88) - C_9 (δ 107.3)
α-30	3.4 Hz	$H_{1'}$ (δ 4.76) - C_3 (δ 91.3) H_3 (δ 3.63) - $C_{1'}$ (δ 101.7)

Compound	^3J ($H_{1'}$-$H_{2'}$)	HMBC Correlations
β-30	7.7 Hz	$H_{1'}$ (δ 4.29) - C_3 (δ 87.5) H_3 (δ 3.71) - $C_{1'}$ (δ 104.4)
α-31	3.8 Hz	$H_{1'}$ (δ 5.05) - C_5 (δ 89.1) H_5 (δ 3.53) - $C_{1'}$ (δ 100.4)
β-31	7.9 Hz	$H_{1'}$ (δ 4.51) - C_5 (δ 87.7)
α-32	3.5 Hz	$H_{1'}$ (δ 5.24) - C_3 (δ 74.5) H_3 (δ 4.43) - $C_{1'}$ (δ 98.8) H_5 (δ 3.90) - C_9 (δ 107.5) H_{11} (δ 3.93) - C_9 (δ 107.5)
β-32	7.8 Hz	$H_{1'}$ (δ 5.17) - C_3 (δ 73.9) H_3 (δ 4.56) - $C_{1'}$ (δ 101.7) H_5 (δ 3.91) - C_9 (δ 107.3) H_{11} (δ 3.88) - C_9 (δ 107.3)
α-33	3.5 Hz	$H_{1'}$ (δ 4.84) - C_3 (δ 89.6) H_3 (δ 3.73) - $C_{1'}$ (δ 100.8)
β-33	7.7 Hz	$H_{1'}$ (δ 4.41) - C_3 (δ 86.5) H_3 (δ 3.99) - $C_{1'}$ (δ 103.8)
α-34	3.7 Hz	$H_{1'}$ (δ 4.97) - C_5 (δ 89.6) H_5 (δ 4.01) - $C_{1'}$ (δ 100.5)
β-34	7.7 Hz	$H_{1'}$ (δ 4.35) - C_5 (δ 89.7) H_5 (δ 3.54) - $C_{1'}$ (δ 107.4)
α-35	3.5 Hz	H_3 (δ 4.45) - $C_{1'}$ (δ 96.9) H_5 (δ 3.96) - C_9 (δ 107.2) H_{11} (δ 3.87) - C_9 (δ 107.2)

Table 2.6. Summary of coupling constant and key HMBC correlations used to assign the anomeric configuration and site of glycosylation.

2.11 References

[1] Elshahawi, S.; Shaaban, K. A.; Kharel, M. K.; Thorson, J. S. *Chem. Sov. Rev.* **2015**, *44*, 7591.

[2] Liang, D.-M.; Liu, J.-H.; Wu, H.; Wang, B.-B.; Zhu, H.-J.; Qiao, J.-J *Chem. Soc. Rev.* **2015**, *44*. 8350.

[3] Lewis, C. A.; Miller, S. *J. Angew. Chem. Int. Ed.* **2006**, *45*, 5616.

[4] (a) Pathak, T. P.; Miller, S. J. *J. Am. Chem. Soc.* **2012**, *134*, 6120. (b) Fowler, B. S.; Laemmerhold, K. M.; Miller, S. J. *J. Am. Chem. Soc.* **2012**, *134*, 9755. (c) Yoganathan, S.; Miller, S. J. *J. Med. Chem.* **2015**, *58*, 2367. (d) Wadzinski, T. J.; Gea, K. D.; Miller, S. J. *Bioorganic Med. Chem. Lett.* **2016**, *26*, 1025.

[5] Lewis, C. A.; Longcore, K. E.; Miller, S. J.; Wender, P. A. *J. Nat. Prod.* **2009**, *72*, 1864.

[6] Sun, X.; Lee, H.; Lee, S.; Tan, K. L. *Nat. Chem.* **2013**, *5*, 790

[7] Mensah, E.; Camasso, N.; Kaplan, N.; Nagorny, P. *Angew. Chem.,Int. Ed.* **2013**, *52*, 12932.

[8] Gouliaras, C.; Lee, D.; Chan, L.; Taylor, M. S. *J. Am. Chem. Soc.* **2011**, *133*, 13926.

[9] Walk, J. T.; Buchan, Z. A.; Montogmery, J. *Chem. Sci.* **2015**, *6*, 3448.

[10] Pelletier, G; Zwicker, A.; Allen, C. L.; Schepartz, A.; Miller, S. J. *J. Am. Chem. Soc.* **2016**, *138*, 3175.

[11] (a) Cortes, J.; Haydock, S. F.; Roberts, G. A.; Bevitt, D. J.; Leadlay, P. F. *Nature* **1990**, *348*, 176. (b) Donadio, S.; Staver, M. J.; McAlpine, J. B.; Swanson, S. J.; Katz, L. *Science* **1991**, *252*, 675.

[12] (a) Borisova, S.; Kim, H. J.; Pu, X.; Liu, H. *ChemBioChem* **2008**, *9*, 1554. (b) Tang, L.; McDaniel, R. *Chem. Biol.* **2001**, *8*, 547.

[13] (a) Woodward, R. B.; Logusch, E.; Nambiar, K. P.; Sakan, K.; Ward, D. E.; Au-Yeung, B.-W.; Balaram, P.; Browne, L. J.; Card, P. J.; Chen, C. H.; Chênevert, R. B.; Fliri, A.; Frobel, K.; Gais, H.-J.; Garatt, D. G.; Hayakawa, K.; Heggie, W.; Hesson, D. P.; Hoppe, D.; Hyatt, J. A.; Ikeda, D.; Jacobi, P. A.; Kim, K. S.; Kobuke, Y.; Kojima, K.; Krowicki, K.; Lee, V. J.; Leutert, T.; Malchenko, S.; Martens, J.; Matthews, R. S.; Ong, B. S.; Press, J. B.; Rajan Babu, T. V.; Rousseau, G.; Sauter, H. M.; Suzuki, M.; Tatsuka, K.; Tolbert, L. M.; Truesdale, E. A.; Uchida, I.; Ueda, Y.; Uyehara, T.; Vasella, A. T.; Vladuchick, W. C.; Wade, Pa. A.; Willaims, R. M.; Wong, H. N.-C. *J. Am. Chem. Soc.* **1981**, *103*, 3215. (b) Toshima, K.; Nozaki, Y.; Mukaiyama, S.; Tamai, T.; Nakata, M.; Tatsuka, K.; Kinoshita, M. *J. Am. Chem. Soc.* **1995**, *117*, 3717. (b)

[14] (a) Pfeifer, B. A.; Admiraal, S. J.; Gramajo, H.; Cane, D. E.; Khosla, C. *Science* **2001**, *291*, 1790. (b) Zhang, H.; Boghigian, B. A.; Pfeifer, B. A. *Biotechnol. Bioeng.* **2010**, *105*, 567.

[15] García-García, P.; Lay, F.; García-García, P.; Rabalakos, C.; List, B. *Angew. Chem. Int. Ed.* **2009**, *48*, 4363.

[16] Champagne, P. A., Houk, K. N. *J. Am. Chem. Soc.* **2016**, *138*, 12356.

[17] (a) Zimmerman, P. M. *J. Comput. Chem.* **2013**, *34*, 1385. (b) Zimmerman, P. M. *J. Chem. Phys.* **2013**, *138*, 184102. (c) Zimmerman, P. M. *J. Chem. Theory Comput.* **2013**, *9*, 3043. (d) Zimmerman, P. M. *J. Comput. Chem.* **2015**, *36*, 601. (e) Zimmerman, P. M. *Mol. Simul.* **2015**, *41*, 43.

[18] Roy, R.; Tropper, F. D.; Grand-Maître, C. *Can. J. Chem.* **1991**, *69*, 1462.

[19] M. Pistorino, B. A. Pfeifer, *Biotechnol. Prog.* **2009**, 25, 1364.

[20] J. M. H. Cheng, E. M. Dangerfield, M. S. M. Timmer, B. L. Stocker, *Org. Biomol. Chem.* **2014**, 12, 2729.

[21] F. Xu, D. Huang, C. Han, W. Shen, X. Lin, Y. Wang, *J. Org. Chem.* **2010**, 75, 8677.

[22] K. A. Parker, P. Wang, *Org. Lett.* **2007**, 9, 4793.

CHAPTER 3

Direct Conversion of BINOL-Based to H8-BINOL-Based Chiral Brønsted Acids Through Single-Step Hydrogenation

(This chapter was partially published in: Tay, J. H.; Arguelles, J. A.; Nagorny, P. *Org. Lett.* **2015**, *17*, 3774.)

3.1 Introduction

The design of new catalyst scaffolds and shortened synthetic routes are undeniably the major forces that drive the growing applications of chiral Brønsted acids as organocatalysts in various asymmetric transformations. In 2004, Akiyama[1] and Terada[2] independently published seminal works hightlighting the utility of BINOL-based CPA catalysts in catalyzing asymmetric Mannich-type reactions. Since then, the 1,1'-bi-2-naphthol or BINOL scaffold **43** has become a ubiquitous element in the design of phosphoric acid catalysts and has served as an inspiration for the new design of catalyst scaffolds. Its axial chirality is perhaps the most important feature that enables the development of asymmetric reactions using the BINOL-based catalyst. In addition, BINOL scaffold is highly tunable, conformationally rigid and C_2 symmetric, making it a versatile building block for catalysts even beyond chiral Brønsted acid.

One of the most commonly used alternatives to the BINOL-scaffold in chiral Brønsted acid catalysis is the H8-BINOL scaffold **44**. H8-BINOL retains the same C_2 symmetry as BINOL but it has a partially saturated naphthol-derived backbone. This distinction leads to differences in solubility, acidity, geometry and the bite angle between chiral acids built on BINOL and H8-BINOL scaffolds. Although both scaffolds are structurally similar, the preparation of their corresponding CPA requires two distinct synthetic sequences, each necessitating 5 to 7 steps (Scheme 3.1). To synthesize the H8-BINOL equivalent of a BINOL-based CPA, BINOL **43** is hydrogenated to H8-BINOL **44** in the first step. In other words, starting from BINOL **43** and H8-

BINOL **44**, 10 more synthetic steps are needed to prepare two structurally similar CPAs. We envision that the step-count can be greatly reduced if there is a way to convert BINOL-based CPA to H8-BINOL based CPA in a single step.

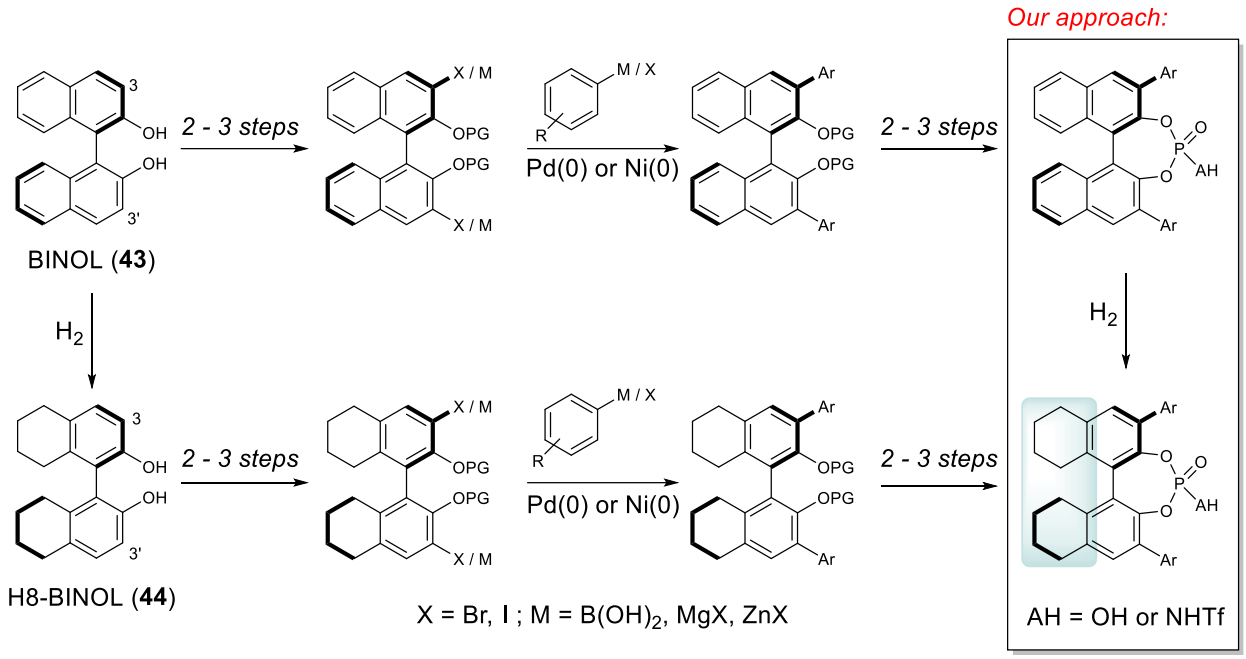

Scheme 3.1. Overview of synthetic route for BINOL-based and H8-BINOL-based Chiral Brønsted acids.

3.2 Results and Discussion

BINOL **43** is normally reduced to H8-BINOL **44** through a hydrogenation reaction in the presence of palladium on carbon[3] (Pd/C) or a platinum oxide[4] (Pt_2O) catalyst. There was no reaction when BINOL-based CPA **(S)-9** was subjected to the hydrogenation reaction with 1 atm hydrogen gas and Pd/C in EtOAc (Table 3.1, entry 1). However, when we switched the hydrogenation catalyst to Pt_2O, we observed a 26% conversion to the desired H8-BINOL-based CPA **(S)-13** based on ^{1}H NMR analysis (entry 2). No hydrogenation was observed when solvents such as acetone, dichloromethane, benzene or dimethylformamide were used (entries 3 – 6). However, the hydrogenation reaction proceeded with quantitative yield in protic solvents such as acetic acid and a mixture of methanol with dichloromethane (entries 7 and 8). More importantly,

we did not observe any reduction of the phosphate functionality or racemization of the CPA catalyst under this reaction condition.

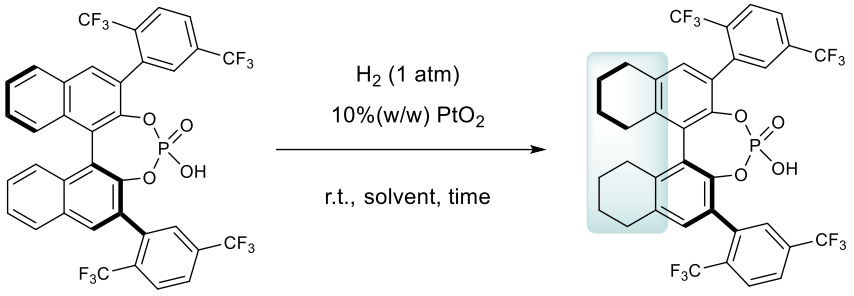

(S)-9 **(S)-13**

entry	Solvent	t (h)	Yield
1 [a]	EtOAc	24	-
2	EtOAc	72	26% [b]
3	acetone	24	<5% [b]
4	CH_2Cl_2	24	<5% [b]
5	benzene	24	<5% [b]
6	DMF	24	<5% [b]
7	AcOH	24	98% [c]
8	MeOH/CH_2Cl_2	16	98% [c]

[a] 10%(w/w) was used instead. [b] Determined by ^{1}H NMR.
[c] Isolated yield.

Table 3.1. Solvent screen for selective hydrogenation of BINOL-based CPA.

To probe the scope of the method, we investigated BINOL-derived CPA substrates with different substituent groups at the 3,3'-position (Table 3.2). BINOL-derived CPA without 3,3'-substitution was converted to the corresponding H8-BINOL-base CPA under the optimization condition with >98% yield. The hydrogenation of CPAs with electron-withdrawing groups, such as 3,5-bis-trifluoromethylphenyl-substituted acid, 3,5-bis-pentafluorosulfanylphenyl substituted acid and 3,5-bis-fluorophenyl-substituted acid, also proceeded smoothly with a quantitative yield. However, when 3,5-bis-chlorophenyl-substituted acid was subjected to the hydrogenation condition, we observed a mixture of products corresponding to dichlorination followed by reductions of the resulting phenyl rings.

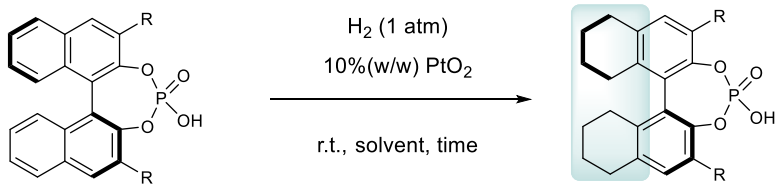

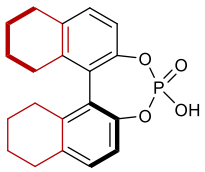	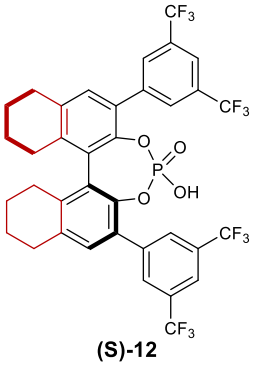	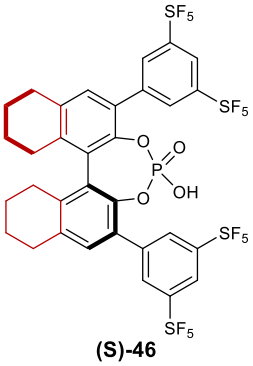	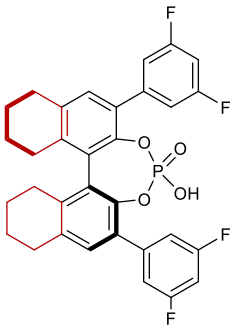
(S)-45	**(S)-12**	**(S)-46**	**(S)-47**
$MeOH/CH_2Cl_2$ (2:3), 16h	$MeOH/CH_2Cl_2$ (1:1), 17h	$MeOH/CH_2Cl_2$ (1:1), 17h	$MeOH/CH_2Cl_2$ (2:3), 17h
>98% yield	>98% yield	>98% yield	>98% yield
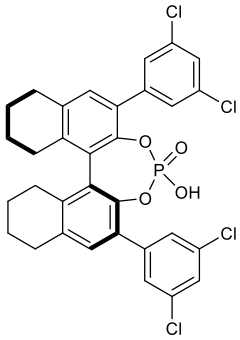	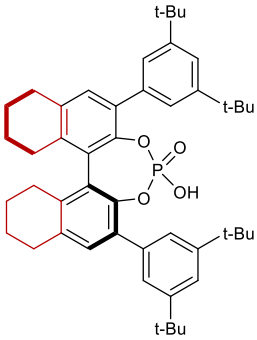	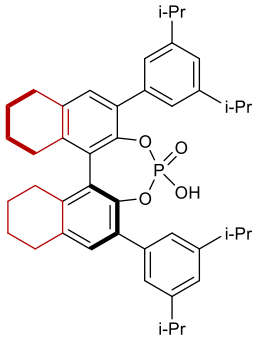	
(S)-48	**(S)-49**	**(S)-50**	
$MeOH/CH_2Cl_2$ (2:3), 17h	$MeOH/CH_2Cl_2$ (2:3), 17h	$MeOH/CH_2Cl_2$ (2:3), 16h	
- [a]	96% yield	>98% yield	
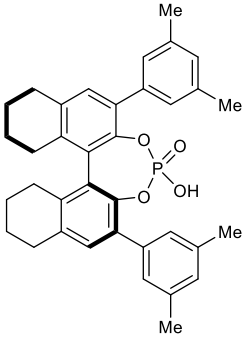	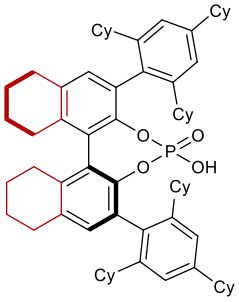	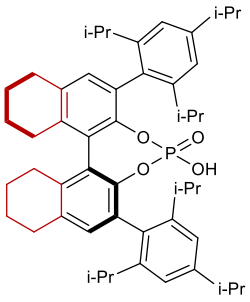	
(S)-51	**(S)-52**	**(S)-53**	
$MeOH/CH_2Cl_2$ (1:1), 17h	$MeOH/CH_2Cl_2$ (2:3), 17h	$MeOH/CH_2Cl_2$ (2:3), 17h	
- [b]	91% yield	>98% yield	

[a] Complex mixture of declorinated and over-reduced products.

[b] Complex mixture of products due to over-reduction of 3,3'-aryl rings.

Table 3.2. Substrate scope of selective hydrogenation of BINOL-based CPAs catalyzed by Pt_2O.

Next, the study continued with the hydrogenation of CPAs with alkyl-substitued-phenyl rings. CPAs with 3,3'-phenyl substituted with bulky tert-butyl and iso-propyl groups at the *meta*-positions were selectively hydrogenated to the corresponding H8-BINOL-based CPAs (**49** and **50**) in excellent yields. Similar CPAs with 2,4,6-tricyclohexyl-substituted phenyl and 2,4,6-triisopropy-substitued phenyl also underwent the selective reduction without any problems. However, overreduction of the 3,3'-phenyl was observed when it was substituted with a less bulky methyl group at the *meta*-position. To test the scalability of the method, hydrogenation of CPA **(S)-9** was repeated on a 1.0-gram scale. The reaction proceeded selectively to produce **(S)-13** with quantitative yield.

BINOL **43** or H8-BINOL **44** can also be appended with acidic functionalities other than phosphoric acid, such as N-trifyl phosphoramide or the disulfonimide group. We were curious how our method would perform in the presence of those functional groups. When compounds **(R)-15** and **(R)-18** were subjected to hydrogenation with Pt_2O, we observed the same chemoselectivity and conversion to **(R)-54** and **(R)-55** with excellent yield (Scheme 3.2). Nonetheless, no conversion was observed when the same condition was applied to the hydrogenation of N-triflyl thiophosphoramide **(R)-56**. Presumably the reaction did not proceed because of catalyst poisoning by the phosphorus sulfur.

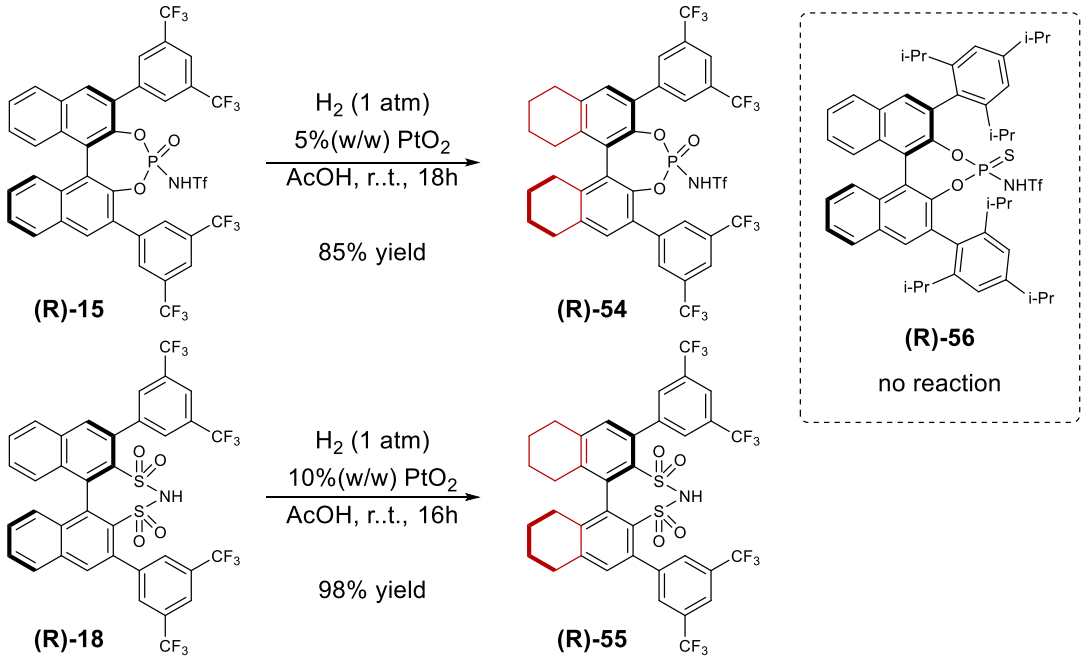

Scheme 3.2. Hydrogenation of BINOL-derived compounds with functionalities other than phosphoric acid.

3.3 Conclusion

In summary, this new method provids a new efficient strategy to synthesize H8-BINOL-based chiral Brønsted acids through a direct reduction of their corresponding BINOL-derived analogs. The condition was general for the selective hydrogenation of BINOL-based chiral acids substituted with an electron-withdrawing group and bulky aliphatic substituents. In addition, the scope of the reaction also extended to the reduction of BINOL-derived compounds with functional groups such as N-trifyl-phosphoramide and disulfonimide. Using our method, five new H8-BINOL based chiral Brønsted acids (**13**, **46**, **49**,**50** and **55**) were synthesized. We believe that the outlined strategy can facilitate the rapid construction of a catalyst library of chiral Brønsted acids and improve the accessibility of H8-BINOL-based Brønsted acids for asymmetric reactions.

3.4 Experimental Information

General Methods

All reagents and solvents were purchased from Sigma-Aldrich, Fisher Scientific, Corvinus Chemicals and were used as received without further purification unless specified. Platinum (IV) oxide was purchased from Sigma-Aldrich with surface area >75m^2/g or similar catalysts from Strem. Chiral acids used in these studies were purchased from Sigma Aldrich or synthesized according to known literature procedures. Heating was achieved by use of a silicone bath with heating controlled by electronic contact thermometer. Deionized water was used in the preparation of all aqueous solutions and for all aqueous extractions. Solvents used for extraction and chromatography were ACS or HPLC grade. Purification of reactions mixtures was performed by flash chromatography using SiliCycle SiliaFlash P60 (230-400 mesh).

^{1}H NMR spectra were recorded on Varian vnmrs 700 (700 MHz), Varian vnmrs 500 (500 MHz), Varian INOVA 500 (500 MHz) or Varian MR400 (400 MHz) spectrometers and chemical shifts (δ) are reported in parts per million (ppm) with solvent resonance as the internal standard ($CDCl_3$ at δ 7.26). Data are reported as (br = broad, s = singlet, d = doublet, t = triplet, q = quartet, m = multiplet; coupling constant(s) in Hz; integration). Proton-decoupled ^{13}C NMR spectra were recorded on Varian vnmrs 700 (700 MHz), Varian vnmrs 500 (500 MHz), Varian INOVA 500 (500 MHz) or Varian MR400 (400 MHz) spectrometers and chemical shifts (δ) are reported in ppm with solvent resonance as the internal standard ($CDCl_3$ at δ 77.16). High resolution mass spectra (HRMS) were recorded on Micromass AutoSpec Ultima or VG (Micromass) 70-250-S Magnetic sector mass spectrometers in the University of Michigan mass spectrometry laboratory. Infrared (IR) spectra were recorded as thin film on a Perkin Elmer Spectrum BX FT-IR spectrometer. Absorption peaks were reported in wavenumbers (cm^{-1}). Optical rotations were measured in a solvent of choice on a JASCO P-2000 or Autopol III digital polarimeter at 589 nm (D-line) and reported as follows $[\alpha]_D^{24}$ (*c* g/100 mL, solvent).

General Procedures for Selective Hydrogenation of BINOL-based Chiral Brønsted Acids

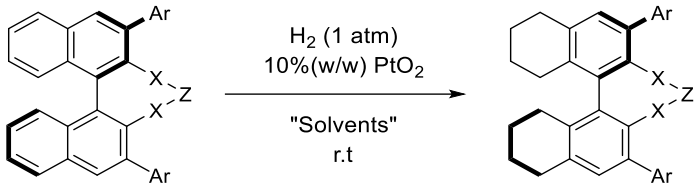

In a two drams vial, Brønsted acid and 10%(w/w) of PtO_2 (>75m^2/g) were added with the corresponding solvent mixture, and the vial was sealed with rubber septum. The vial was evacuated and backfilled with N_2 three times, followed by H_2 for another three times. The suspension was stirred with H_2 balloon on top overnight (16 – 18 h) at room temperature. At the end of the reaction, the suspension was filtered through a thin pad of Cealite on top of silica gel with dichloromethane washing. Combined organic layer was concentrated *in vacuo* to yield the corresponding H8-Brønsted acid with >98% purity.

For large scale reaction carried out in acetic acid, the filtrate was washed with 6N HCl (aq) and the aqueous layer was extracted three times with dichloromethane. Combined organic layer was dried over Na_2SO_4 and concentrated *in vacuo* to yield the corresponding H8-Brønsted acid.

1) H_2 balloon used for the reaction was "double-bagged". Concentration of the reaction was maintained accordingly so that no precipitate crashed out of the solution throughout the reaction to ensure the reaction would go to completion. Stirring should not be too vigorous, otherwise, catalyst or substrate would stick to the wall of the vial above the solvent level. For large scale reaction, a thicker needle should be used to ensure better delivery of H_2 gas and round bottom flask is preferred. In general, the change of the reaction mixture from dark grey suspension to clear suspension is a good indication of reaction completion. Otherwise, reaction could be easily monitored by MS-ESI with negative ion detection.

2) The prior exposure of BINOL-based CPAs to silica gel seems to introduce impurities that deactivate the catalyst. Most likely, such catalyst deactivation is due to the presence of Na^+ and Ca^{2+} phosphates. Therefore, washing the inactive batches of acids with 6 M HCl is recommended for such cases.

3) Some variation in the catalytic activity of platinum (IV) oxide was noticed, and in such instances longer reaction times were required to achieve complete reductions. In addition,

the catalyst slowly deactivates upon prolonged exposure to the acids. For the cases when incomplete conversion is observed, we recommend working up the reaction, washing the mixture of partially hydrogenated CPAs with 6M HCl and subjecting it to another cycle of hydrogenation with a new portion of catalyst.

Determination of the Enantiopurity of Chiral Brønsted Acids after Hydrogenation

To demonstrate that hydrogenation does not result in racemization, enantiopurity of acids **(S)-45** and **(S)-13** obtained from hydrogenation catalyzed by Pt_2O was determined. The optical rotation of CPAs may strongly depend on the protonation state of the acid (due to the presence of metal phosphate impurities). Therefore, the determination of ee's of **(S)-45** and **(S)-13** was accomplished by reduction of acids to the corresponding H8-BINOL derivatives with LAH and measuring their enantiopurity by chiral HPLC as described below:

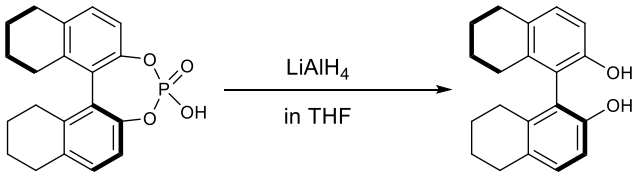

(S)-45 **(S)-44** (>99% ee)

Scheme 3.3. Reduction of the phosphate functionality of **(S)-45** using LAH.

(S)-45 (20.0 mg, 0.056 mmol) was dissolved in anhydrous THF (0.04M) and cooled in ice bath. 10.6 mg of $LiAlH_4$ (5 equiv.) was added to the reaction and the mixture was stirred and warmed up to rt overnight. The reaction was quenched by slowing adding 6N HCl in ice bath (exotherm!!) and extracted with diethyl ether. Combined organic layers was washed with brine, dried over Na_2SO_4, filtered through glass wool plug and concentrated *in vacuo* to afford diol **(S)-44** in quantitative yield. The enantiopurity of **(S)-44** was determined by HPLC analysis to be >99% ee: Chiralcel OD-H column (4.6 mm ϕ x 250 mm L), 95:5 hexanes:isopropanol, 1.0 ml/min flow rate, λ = 218 nm, tR(R) = 7.12 min, tR(S) = 8.52 min.

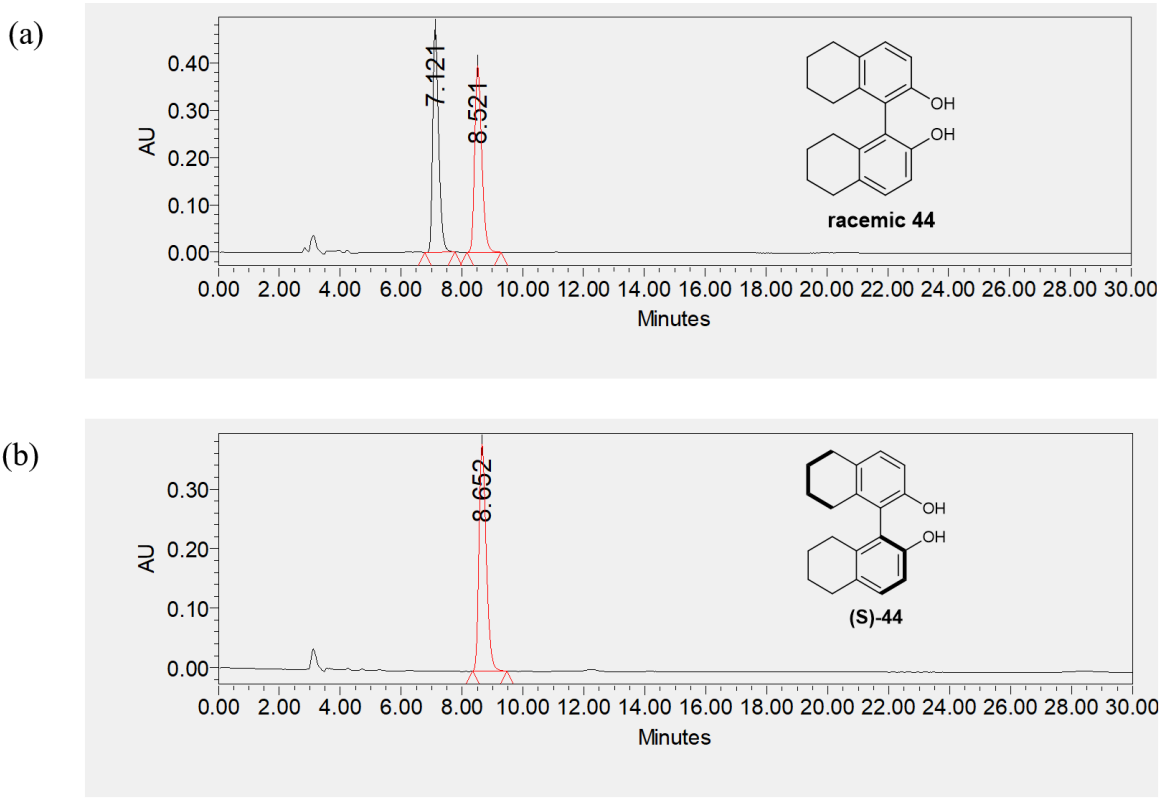

Figure 3.1. HPLC traces of (a) racemic **44** and (b) **44** obtained from reduction of **(S)-45**.

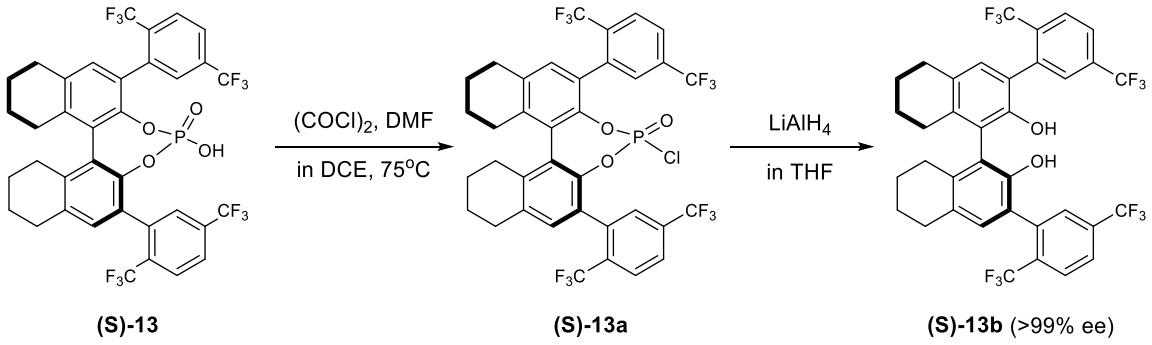

Scheme 3.4. Two-steps reduction of the phosphate functionality of **(S)-13**.

(S)-13 (10.0 mg, 0.013 mmol) was dissolved in DCE (0.06 M) and treated with oxalyl chloride (5 equiv.) and catalytic amount of DMF. The reaction was heated at 75°C and stirred overnight. After the reaction was done, the mixture was concentrated *in vacuo* and the crude was purified by flash chromatography on SiO_2 (30% EtOAc in hexanes) to afford phosphoryl chloride **(S)-13a**. **(S)-13a** was then subjected to reduction by $LiAlH_4$ according to above mentioned procedures. The

corresponding diol **(S)-13b** was obtained after purification by prep TLC (R_f = 0.51, 10% EtOAc in hexanes). The enantiopurity of **(S)-13b** was determined by HPLC analysis to be >99% ee: Chiralcel OD-H column (4.6 mm ϕ x 250 mm L), 100% hexanes, 1.0 ml/min flow rate, λ = 218 nm, tR(R) = 4.99 min, tR(S) = 5.98 min.

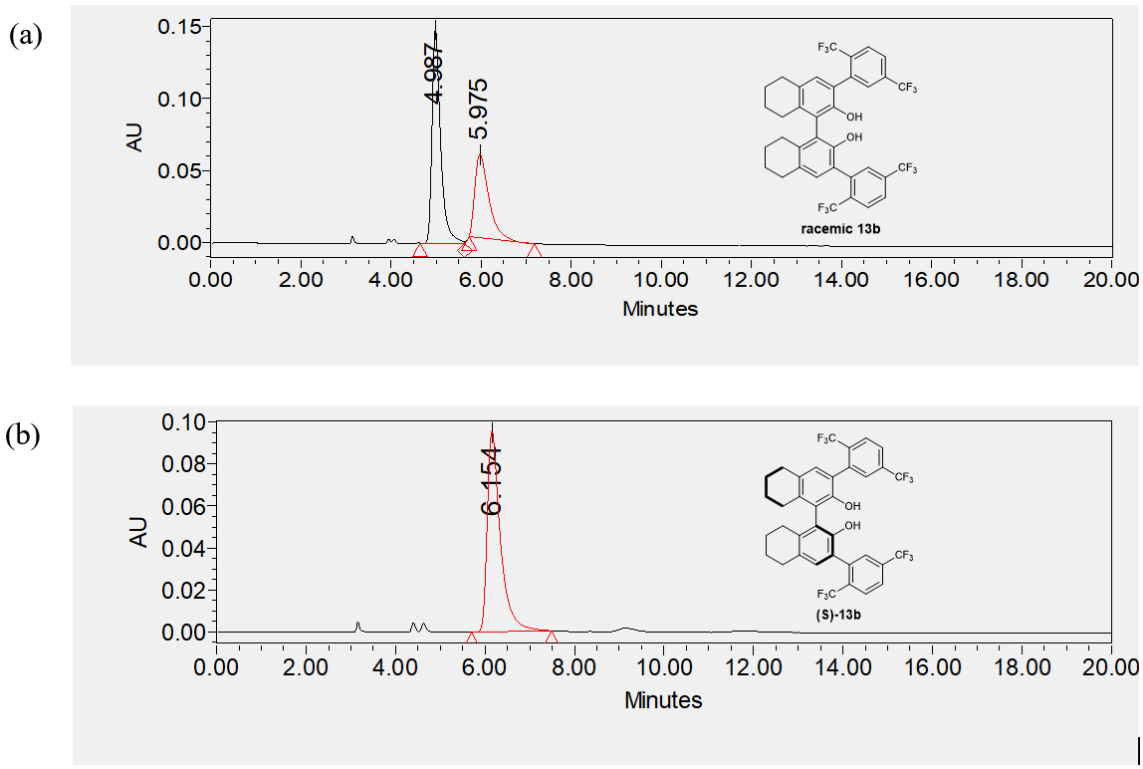

Figure 3.2. HPLC traces of (a) racemic **13b** and (b) **13b** obtained from reduction of **(S)-13**.

Characterization of H8-BINOL-based Brønsted Acids

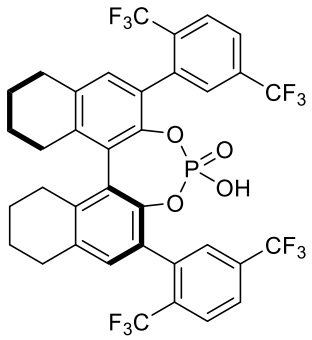

(S)-13

^{1}H NMR (500 MHz, $CDCl_3$) δ 7.97 (s, 4H), 7.91 (s, 2H), 7.16 (s, 2H), 2.94 (m, 4H), 2.75 (ddd, *J* = 16.1, 8.7, 4.4 Hz, 2H), 2.48 – 2.36 (m, 2H), 1.90 (m, 6H), 1.76 – 1.63 (m, 2H)

^{13}C NMR (126 MHz, $CDCl_3$) δ 153.39, 153.24, 153.09, 144.28, 144.21, 140.36, 139.89, 135.63, 130.55, 130.23, 128.18, 128.01, 122.22, 29.27, 28.13, 22.60, 22.46

^{19}F NMR (377 MHz, $CDCl_3$) δ 81.70 (t, *J* = 151.3 Hz, 1F), δ 62.61 (d, *J* = 150.3 Hz, 4F)

^{31}P NMR (162 MHz, $CDCl_3$) δ 2.71

HRMS (ESI neg.) *m/z* calcd for $C_{32}H_{25}F_{20}O_4PS_4$ $[M-H]^-$ 1010.9981, found 1010.9976

IR (thin film, cm^{-1}) 2940, 1445, 1258, 1100, 840.

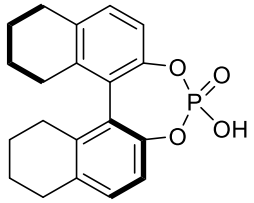

(S)-45

Characterizations of product match with previously reported data.[5]

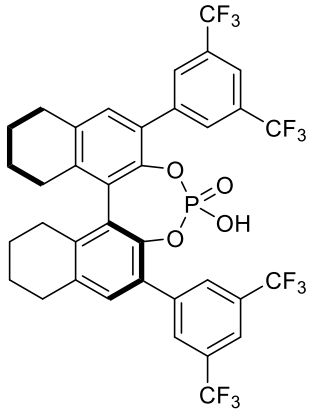

(S)-12

Characterizations of product match with previously reported data.[6]

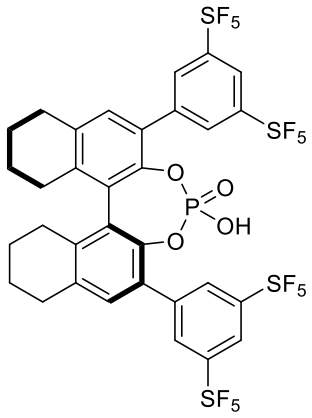

(S)-46

^{1}H NMR (500 MHz, $CDCl_3$) δ 7.97 (s, 4H), 7.91 (s, 2H), 7.16 (s, 2H), 2.94 (m, 4H), 2.75 (ddd, *J* = 16.1, 8.7, 4.4 Hz, 2H), 2.48 – 2.36 (m, 2H), 1.90 (m, 6H), 1.76 – 1.63 (m, 2H)

^{13}C NMR (126 MHz, $CDCl_3$) δ 153.39, 153.24, 153.09, 144.28, 144.21, 140.36, 139.89, 135.63, 130.55, 130.23, 128.18, 128.01, 122.22, 29.27, 28.13, 22.60, 22.46

^{19}F NMR (377 MHz, $CDCl_3$) δ 81.70 (t, *J* = 151.3 Hz, 1F), δ 62.61 (d, *J* = 150.3 Hz, 4F)

^{31}P NMR (162 MHz, $CDCl_3$) δ 2.71

HRMS (ESI neg.) *m/z* calcd for $C_{32}H_{25}F_{20}O_4PS_4$ $[M-H]^-$ 1010.9981, found 1010.9976

IR (thin film, cm^{-1}) 2940, 1445, 1258, 1100, 840.

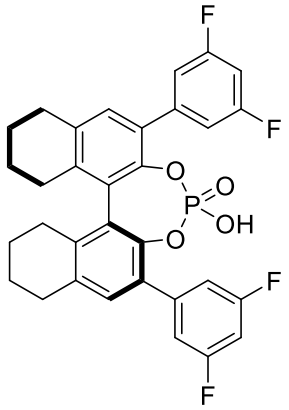

(S)-47

Characterizations of product match with previously reported data.[6]

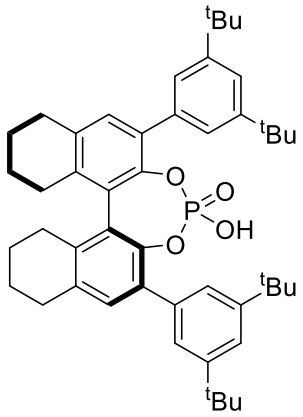

(S)-49

^{1}H NMR (500 MHz, CD_2Cl_2) δ 7.31 (m, 6H), 7.14 (s, 2H), 2.91 (m, 4H), 2.75 (ddd, *J* = 12.6, 8.5, 4.6 Hz, 2H), 2.40 (dt, *J* = 16.8, 5.4 Hz, 2H), 1.89 (m, 6H), 1.78 – 1.63 (m, 2H), 1.23 (s, 36H)

^{13}C NMR (176 MHz, CD_2Cl_2) δ 150.88, 143.82, 137.53, 137.10, 135.47, 133.28, 131.90, 127.74, 124.42, 121.55, 35.25, 31.79, 29.75, 28.33, 23.33, 23.27

^{31}P NMR (162 MHz, CD_2Cl_2) δ 0.27

HRMS (ESI neg.) *m/z* calcd for $C_{48}H_{61}O_4P$ $[M-H]^-$ 731.4235, found 731.4221

IR (thin film, cm^{-1}) 2952, 1595, 1408, 1362, 1248, 1018, 918, 873.

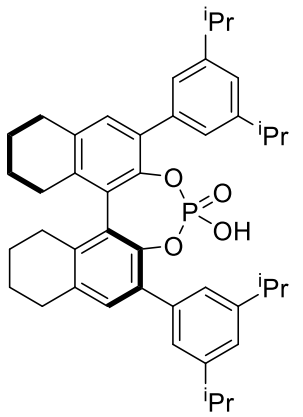

(S)-50

^{1}H NMR (500 MHz, $CDCl_3$) δ 7.18 (s, 4H), 7.13 (s, 2H), 6.94 (s, 2H), 2.92 – 2.75 (m, 4H), 2.70 (ddd, *J* = 12.4, 8.5, 4.4 Hz, 2H), 2.41 – 2.33 (m, 2H), 1.84 (s, 6H), 1.69 – 1.56 (m, 2H), 1.26 (s, 4H), 1.13 (dd, *J* = 6.3, 4.6 Hz, 24H)

^{13}C NMR (126 MHz, $CDCl_3$) δ 148.57, 143.30, 137.29, 137.10, 134.88, 132.39, 131.21, 129.17, 128.36, 127.38, 125.48, 123.30, 34.16, 29.37, 27.97, 24.27, 23.92, 22.89, 22.79

^{31}P NMR (202 MHz, $CDCl_3$) δ -0.96

HRMS (ESI neg.) *m/z* calcd for $C_{44}H_{53}O_4P$ $[M-H]^-$ 675.3609, found 675.3606

IR (thin film, cm^{-1}) 2957, 1597, 1448, 1276, 1220, 1020, 966, 922, 871.

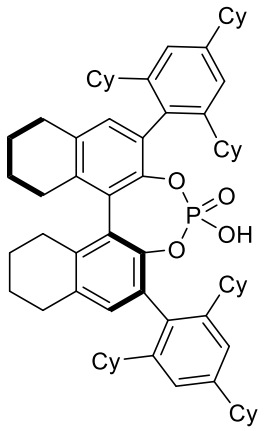

(S)-52

Characterizations of product match with previously reported data.[7]

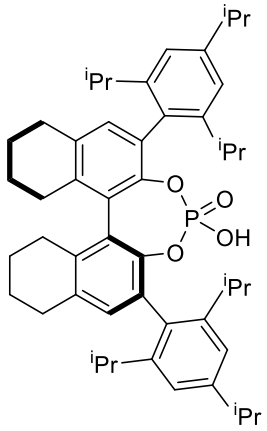

(S)-53

Characterizations of product match with previously reported data.[8]

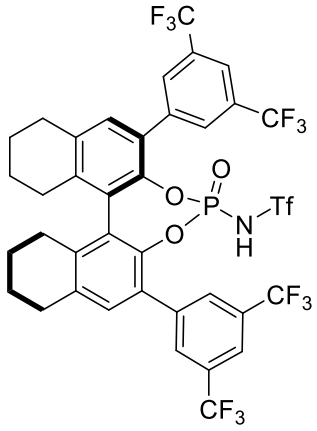

(R)-54

Characterizations of product match with previously reported data.[9]

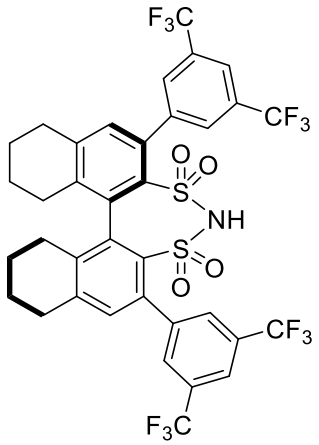

(R)-55

^{1}H NMR (700 MHz, $CDCl_3$) δ 7.87 (s, 2H), 7.80 (s, 2H), 7.74 (s, 2H), 7.14 (s, 2H), 2.99 – 2.88 (m, 4H), 2.45 – 2.27 (m, 4H), 1.89 (m, 2H), 1.87 – 1.76 (m, 6H)

^{13}C NMR (176 MHz, $CDCl_3$) δ 144.94, 141.11, 138.82, 138.79, 135.89, 133.89, 130.70, 128.48, 124.15, 122.60, 121.78, 30.32, 28.02, 22.64, 22.03

^{19}F NMR (377 MHz, $CDCl_3$) δ -62.70 (d, J = 11.7 Hz)

HRMS (ESI neg.) *m/z* calcd for $C_{36}H_{25}F_{12}NO_4S_2$ $[M-H]^-$ 826.0961, found 826.0956

IR (thin film, cm^{-1}) 2936, 1553, 1368, 1276, 1178, 1127, 896, 846.

3.5 References

[1] Akiyama, T., Itoh, J., Yokota, K., Fuchibe, K. *Angew. Chem. Int. Ed.* **2004**, *43*, 1566.

[2] Uraguchi, D., Terada, M. *J. Am. Chem. Soc.* **2004**, *126*, 5356.

[3] Korostylev, A.; Tararov, V. I.; Fischer, C.; Monsees, A.; Börner, A. *J. Org. Chem. 2004*, *69*, 3220.

[4] Reetz, M. T.; Merk, C.; Naberfeld, G.; Rudolph, J.; Griebenow, N.; Goddard, R. *Tetrahedron Lett.* **1997**, *38*, 5273.

[5] Furuno, H.; Hayano, T.; Kambara, T.; Sugimoto, Y.; Hanamoto, T.; Tanaka, Y.; Jin, Y. Z.; Kawaga, T.; Inanaga, J. *Tetrahedron* **2003,** *59*, 10509.

[6] Bartoszek, M.; Beller, M.; Deutsch, J.; Klawonn, M.; Köckritz, A.; Nemati, N.; Pews-Davtyan, A. *Tetrahedron* **2008**, *64*, 1316.

[7] Yang, X.; Toste, D. *J. Am. Chem. Soc*., **2015**, *137*, 3205.

[8] Xie,W.; Jiang, G.; Liu, H.; Hu, J.; Pan, X.; Zhang, H.; Wan, X.; Lai, Y.; Ma, D. *Angew. Chem. Int. Ed.* **2013**, *52*, 12924.

[9] Rueping, M.; Natchtsheim, B. J.; Koenigs, R. M.; Ieawsuwan, W. *Chem. Eur. J.*, **2010**, *16*, 13116.

CHAPTER 4

Method for Determining Enantiopurity of Chiral Phosphoric Acids Based on ^{31}P NMR and the Use of Chiral Amines as Discriminating Agents

(This chapter was partially published in: Tay, J. H.; Nagorny, P. *Synlett* **2016**, *27*, 551.)

4.1 Introduction

Motivated by the goal of improving the preparation of chiral Brønsted acids, we developed a new method to synthesize H8-BINOL-based chiral acids derived from a single step hydrogenation of BINOL-derived chiral acids.[1] The hydrogenation was performed in the presence of platinum (IV) oxide, which prompted us to examine if the chiral Brønsted acids underwent racemization under such reaction conditions. As we searched for a method to determine the enantiomeric excess of the CPA generated in the study, we learned that there is no straightforward method for accessing the enantiopurity of CPAs, and that there is very limited information about the racemization barrier for BINOL- and H8-BINOL-based CPAs.

Generally, HPLC analysis is one of the most reliable techniques for determining the enantiopurity of chiral compounds. Nonetheless, HPLC analysis requires the use of a specialized equipment that is expensive and often not readily available in every lab. Furthermore, the analysis is highly substrate specific, and the development of HPLC assays is time consuming because of the large number of parameters for optimization (i.e. column type, eluent composition, flow rate, etc.). Alternatively, enantiopurity of CPA can be calculated based on the optical rotation measurement if the reference value is available. Unfortunately, very few specific optical rotation measurements of CPA compounds have been reported in the literature. Moreover, optical rotation analysis can be unreliable if the sample of CPA contains phosphate salt impurities. The major drawbacks of these analysis inspired us to develop a simple and reliable method for evaluating the enantiopurity of CPAs.

4.2 Experimental Designs

A brief survey of the literature revealed that phosphorus (V)[2] and phosphorus (III)[3] compounds are used as chiral complexing agents to determine the enantiopurity of various alkaloids, amines, alcohols, amino acids and carboxylic acids based on ^{1}H NMR analysis. For example, CPA and chiral amine could form diastereomeric ion pairs which typically have distinct physical properties such as solubility, melting point and spectral characteristics. However, the reserve analysis was not known. In other words, there was no report on the determination of the enantiopurity of chiral phosphorus compounds in the presence of a chiral discrimination agent. Based on literature precedents, we hypothesized that a chiral amine would undergo irreversible protonation by CPA and form a mixture of diastereomeric ammonium phosphates (Scheme 4.1). The key to the analysis relied on the integration of the diastereomeric ^{31}P NMR signal produced by the ion pairs. ^{31}P NMR spectrum is simple, contains less signals, and was therefore ideal for the analysis.

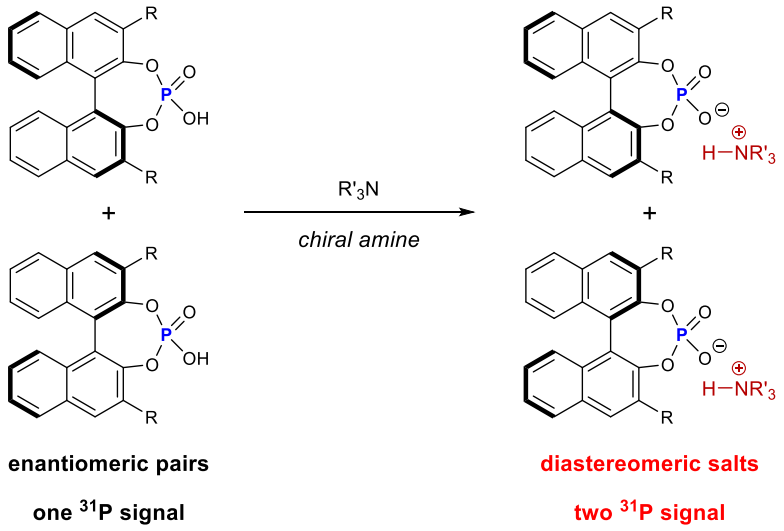

Scheme 4.1. Proposed method for analysis of enantiopurity of chiral phosphoric acids in the presence of a chiral amine as NMR discriminating agent.

4.3 Results and Discussion

After a series of screenings, commercially available amino alcohol **57** was identified as a suitable chiral discriminating agent. When a racemic mixture of CPA **17** was combined with 1.5

equivalents of **57** in deuterated chloroform, we observed two nonequivalent ^{31}P NMR signals (Figure 4.1). More importantly, the diastereomeric ^{31}P signals were observed with good resolution ($\Delta\delta$ = 2.69ppm), which allowed the accurate integration of those signals.

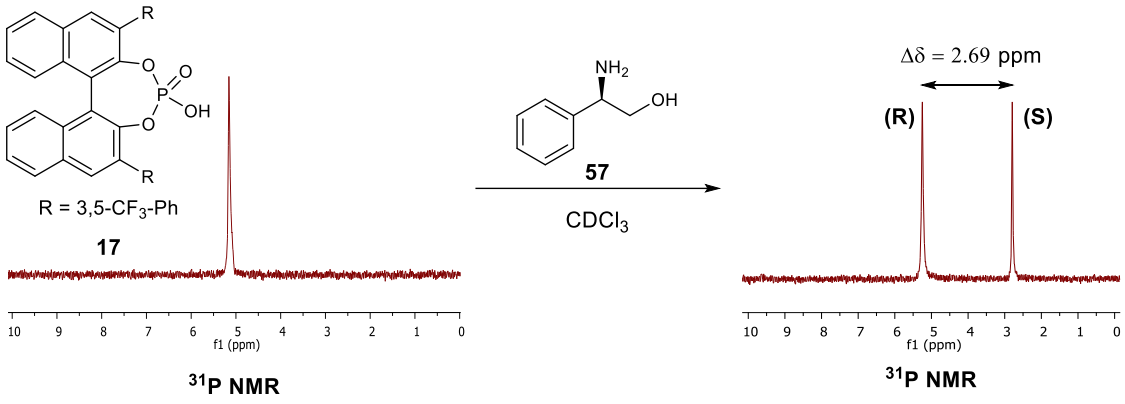

Figure 4.1. Resolution of ^{31}P signals of CPA **13** in the presence of chiral amine **57**.

The method was applicable to the analysis of most CPAs tested (Table 4.1), except for CPA **7** and **8**. In those cases, chiral amine **58** was identified as an alternative chiral discriminating agent for the same analysis (entries 6 – 8). Addtitionally, the method tolerated measurement at different concentrations without compromising the accuracy of the analysis (entries 4 – 7).

entry	CPA	Discriminating Agent	Δδ (ppm) [concentration]	Δδ (Hz) [concentration]
1	**11**	**57**	0.74	209
2	**14**	**57**	0.20	57
3	**16**	**57**	2.57	727
4	**17**	**57**	2.69 [23 mM]	761 [23 mM]
5	**17**	**57**	2.67 [4.3 mM]	754 [4.3 mM]
6	**7**	**58**	0.59 [13 mM]	167 [13 mM]
7	**7**	**58**	1.51 [4.7 mM]	244 [4.7 mM]
8	**8**	**58**	0.85	241
9	**12**	**57**	2.43	688
10	**46**	**57**	2.23	631
11	**15**	**57**	0.14	40

Table 4.1. Resolution of ^{31}P signals of various CPAs in the presence of a chiral amine as NMR discriminating agent.

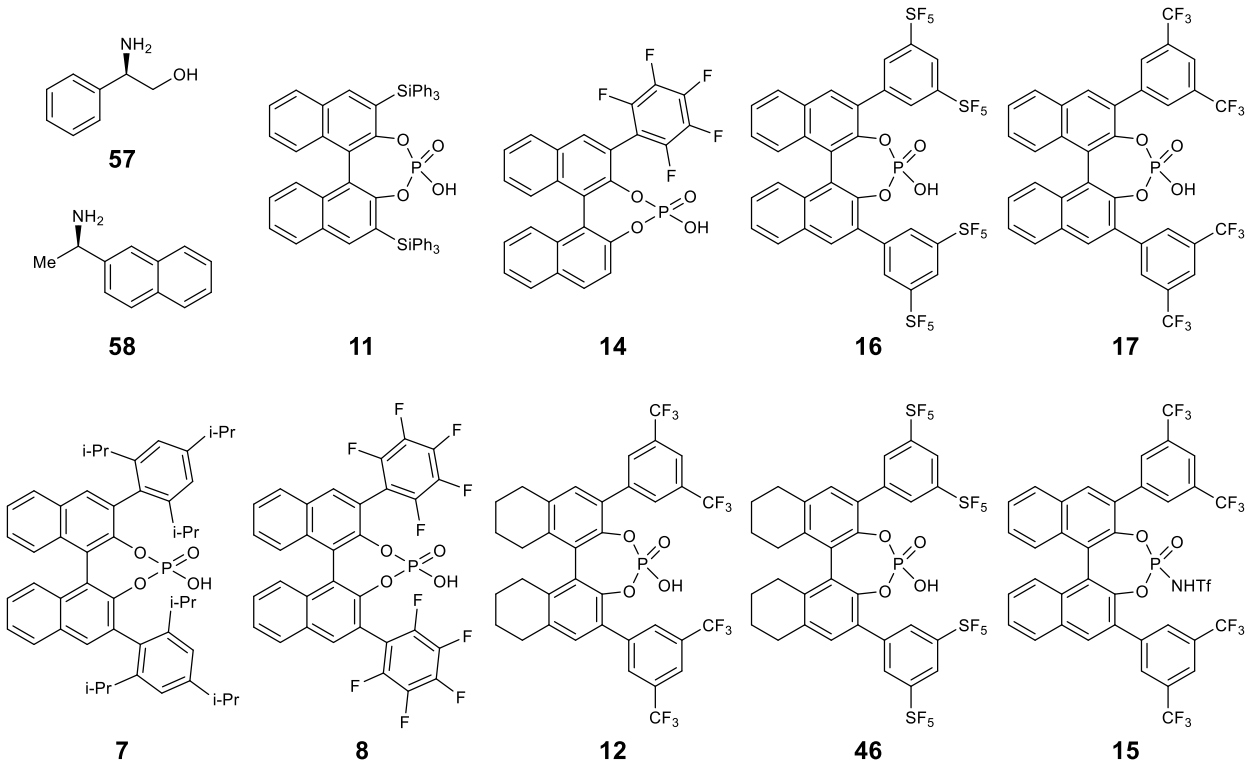

Figure 4.2. Structures of discriminating agents **57**, **58** and CPAs.

With regard to substrate scope, a mixture of **57** and H8-BINOL-derived CPAs **12** or **46** also exhibited well resolved diastereomeric ^{31}P peaks (Table 4.1, entries 9 and 10). The method was also found to be applicable to analysis of N-trifly phosphoramide **15**, even though a lower resolution was observed (entry 11). To determine the accuracy of the method, we constructed a calibration curve that compared the actual enantiopurity of CPA samples and the ee measured by integration of ^{31}P NMR signals (Figure 4.3). An excellent linear correlation was observed for the measurements (R^2 = 0.999) and the average absolute error was found to be less than 1.1%. We concluded that the method is reliable and accurate.

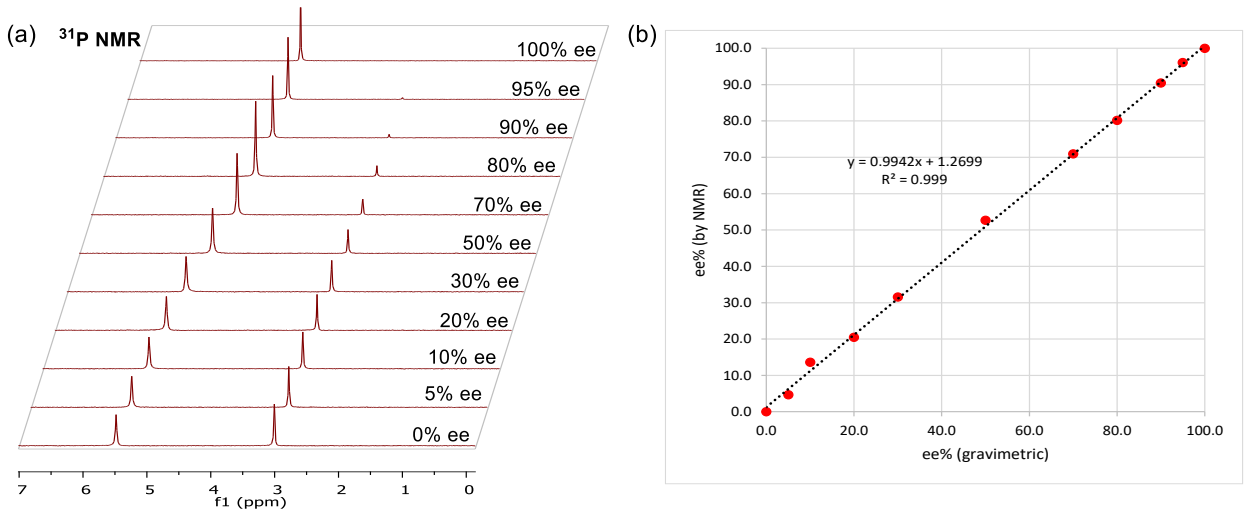

Figure 4.3. (a) ^{31}P NMR spectra of non-racemic mixture of CPA **17** in the presence of chiral discriminating agent **57**. (b) Calibration curve showing linear correlation between %ee determined by ^{31}P NMR and %ee based on gravimetric analysis.

Next, we utilized the method to evaluate the enantiopurify of CPA after the hydrogenation reaction in the presence of Pt_2O. Previously, we had to reduce the phosphate group of the H8-BINOL-based CPA product using $LiAlH_4$, and measure the ee of the resulting diol using HPLC analysis. Now, the new method based on ^{31}P NMR analysis and the use chiral amine as discriminating agent provided a significantly faster and simpler way of assessing the enantiopurity of the CPA product. Consistent with our prior result, the analysis based on ^{31}P NMR indicated that **(R)-12** synthesized from hydrogenation of **(R)-17** was enantiopure (Scheme 4.2). In other words, **(R)-17** did not epimerize under the hydrogenation conditions in the presence of Pt_2O.

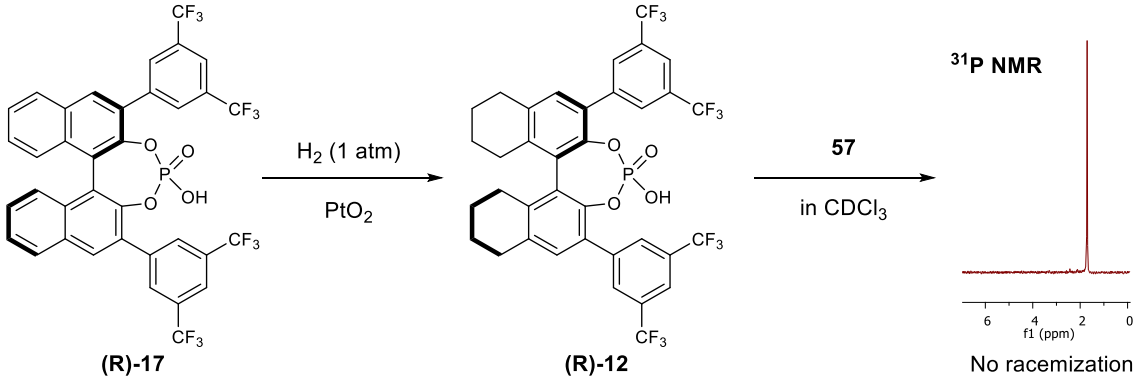

Scheme 4.2. Application of ^{31}P NMR in combination of chiral discriminating agent to determine the enantiopurity of CPA after hydrogenation catalyzed by Pt_2O.

To further demonstrate the applied use of the new method, we utilized the method to investigate the thermal racemization of CPA. BINOL and BINOL-derived phosphate methyl ester had been reported to racemize when being heated, with half-life, $t_{1/2}$ = 60 min and 100 min respectively at 220°C.[4] However, no information was known about the thermal stability of BINOL- and H8-BINOL-derived phosphoric acids. Enantiopure **(R)-17** and its H8-BINOL-derived analog **(R)-12** were subjected to heating at high temperatures, and their enantiopurities were measured afterward using the ^{31}P NMR method.

After **(R)-17** was subjected to heating at 200°C in dichlorobenzene, we measured a 4% loss in ee after the reaction ran for 24 h. **(R)-17** underwent even faster epimerization at 220°C, with enantiopurity measured at 84% ee after 18 h. Further elevation of the temperature to 250°C led to decomposition of **(R)-17**. On the other hand, enantiopure **(R)-12** was isolated after being heated at 220°C for 18 h. The results indicated therefore that H8-BINOL-derived CPA with saturated H8-BINOL backbone is configurationally more stable compared to its unsaturated analog under thermal stress.

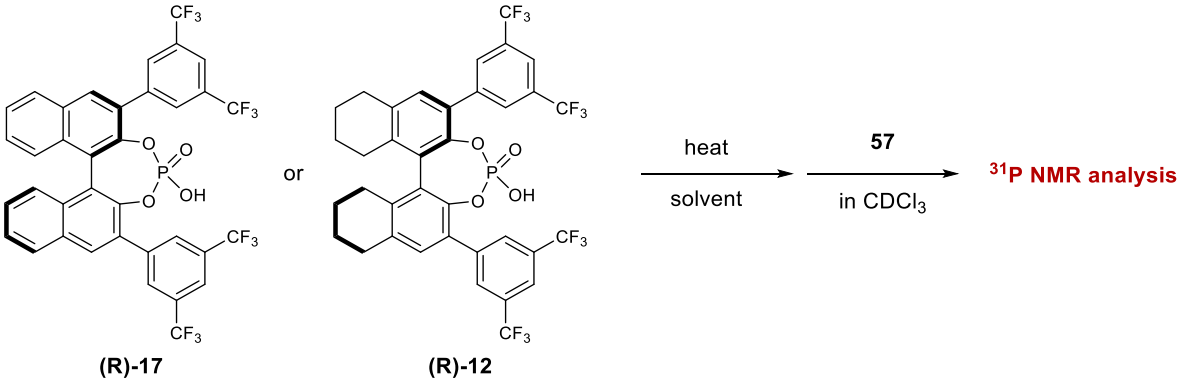

(R)-17 **(R)-12**

entry	CPA	Solvent	T (°C)	t (h)	%ee determined by ^{31}P NMR
1	**(R)-17**	1,2-dichlorobenzene	200	24	96
2	**(R)-17**	1,2-dichlorobenzene	220	18	84
3	**(R)-17**	biphenyl	250	24	-
4	**(R)-12**	1,2-dichlorobenzene	220	18	>99

Table 4.2. Application of ^{31}P NMR analysis to the study of BINOL-based and H8-BINOL-based CPA epimerization under thermal stress.

4.4 Conclusion

In summary, we developed a simple, quick and reliable method to determine the enantiopurity of chiral phosphoric acids using commercially available chiral amine as a discriminating agent and ^{31}P NMR analysis. The method is general and excellent resolution was observed for a series of CPAs tested. Using the method, we also studied the enantio-stability of CPA under hydrogenation and thermal conditions. We found that BINOL-and H8-BINOL-derived CPAs do not epimerize under hydrogenation condition in the presence of Pt_2O. However, H8-BINOL-drived CPAs are configurationally more stable than its BINOL-based analog when they are subjected to thermal stress.

4.5 Experimental Information

General Methods

All reagents and solvents were purchased from Sigma-Aldrich, Fisher Scientific, Corvinus Chemicals and were used as received without further purification unless specified. Heating was achieved by use of a sand bath with heating controlled by electronic contact thermometer. Deionized water was used in the preparation of all aqueous solutions and for all aqueous extractions. Solvents used for extraction and chromatography were ACS or HPLC grade. Purification of reactions mixtures was performed by flash chromatography using SiliCycle SiliaFlash P60 (230-400 mesh).

^{1}H NMR spectra were recorded on Varian vnmrs 700 (700 MHz), Varian vnmrs 500 (500 MHz), Varian INOVA 500 (500 MHz) or Varian MR400 (400 MHz) spectrometers and chemical shifts (δ) are reported in parts per million (ppm) with solvent resonance as the internal standard ($CDCl_3$ at δ 7.26). ^{31}P NMR spectra were recorded on Varian vnmrs 700 (283 Mhz) and referenced to residue $CHCl_3$ ^{1}H signal at δ 7.26 by absolute referencing.

General Procedures for Enantiopurity Determination based on NMR Discrimination

10 mg of nonracemic chiral phosphoric acid* was mixed with 1.5 equivalent of discriminating agent in 0.6 mL of $CDCl_3$ in NMR tubes. ^{31}P spectrum of the mixture was measure and the ee% was calculated based on the following formula:

$$ee\% = \frac{(area\ of\ major\ peak) - (area\ of\ minor\ peak)}{area\ of\ major\ peak + area\ of\ minor\ peak} * 100\%$$

*CPA was dissolved in DCM, washed with 6N HCl (aq) and dried over Na_2SO_4 prior to analysis.

General Procedures for Thermal Racemization Studies

10 mg of CPA was dissolved in either 0.5 mL of 1,2-dichlorobenene or 0.5 gr of biphenyl. The mixture was heated in a sealed 1 dr vial using sand bath. When the experiment was done, 1,2-dichlorobenzene was removed by blow-drying under a stream of N_2, while biphenyl was removed

by flash chromatograph on SiO_2 (100% hexanes then 1:1 hexanes/EtOAc). The resulting crude CPA was mixed with 1.5 equivalent of discriminating agent in $CDCl_3$ and ^{31}P NMR spectrum was taken to determine the enantiopurity of CPA.

Calibration Curve for ^{31}P NMR Analysis of 17 in the Presence of Discriminating Agent 57

Nonracemic mixtures of **17** at various %ee were accurately prepared by mixing standard solutions of **(R)-** and **(S)-17** in $CDCl_3$.

Entry	Expected %ee	%ee by ^{31}P-NMR	Error %
1	0.0	0.0	0.0
2	5.0	4.7	0.3
3	10.0	13.6	3.6
4	20.0	20.5	0.5
5	30.0	31.6	1.6
6	50.0	52.7	2.7
7	70.0	70.9	0.9
8	80.0	80.2	0.2
9	90.0	90.5	0.5
10	95.0	96.1	1.1
11	100.0	100.0	0.0
		Average	1.0

Table 4.3. Comparison between %ee based on gravimetric analysis and %ee based on ^{31}P NMR analysis.

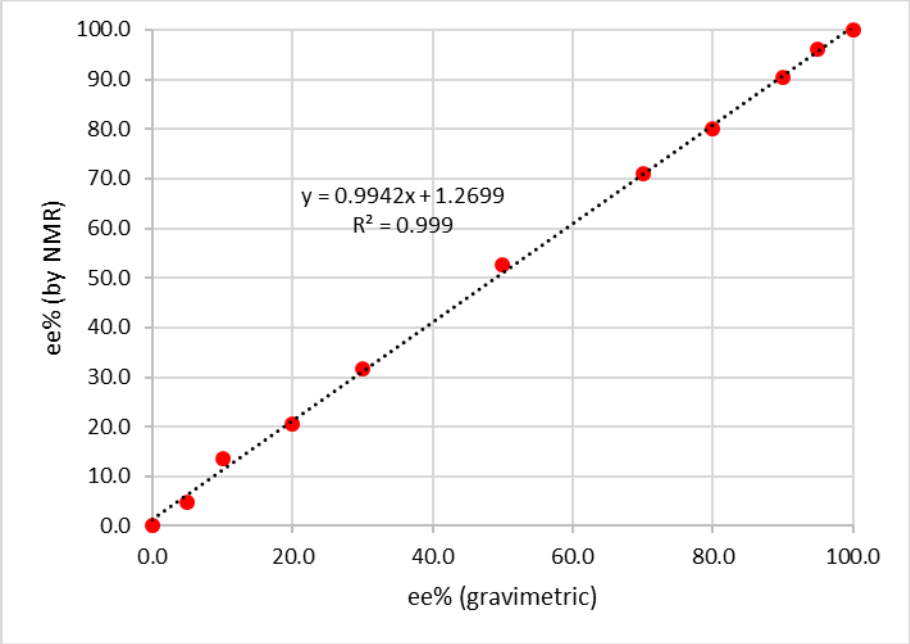

Figure 4.4. Calibration curve showing linear correlation between %ee determined by ^{31}P NMR and %ee based on gravimetric analysis.

^{31}P NMR Spectra of CPAs in the Presence of Chiral Discriminating Agent

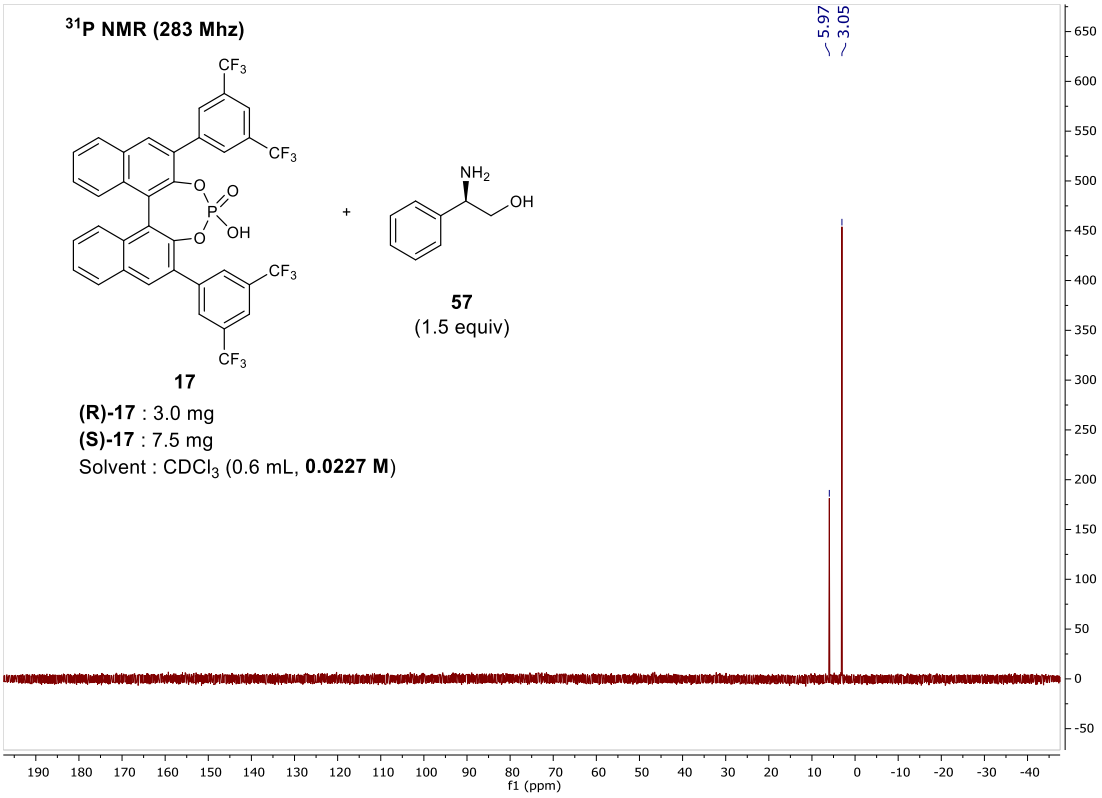

^{31}P NMR (283 Mhz)

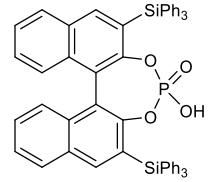

11

+

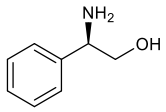

57
(1.5 equiv)

(R)-11 : 5.0 mg
(S)-11 : 5.0 mg
Solvent : $CDCl_3$ (0.6 mL)

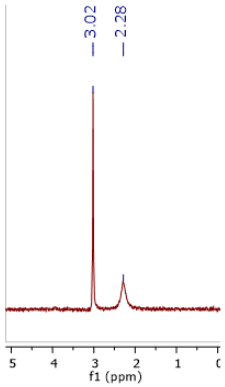

^{31}P NMR (283 Mhz)

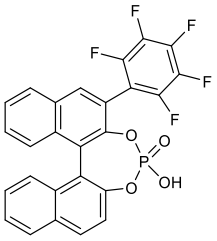

14

+

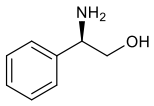

57
(1.5 equiv)

(R)-14 : 3.0 mg
(S)-14 : 7.4 mg
Solvent : $CDCl_3$ (0.6 mL)

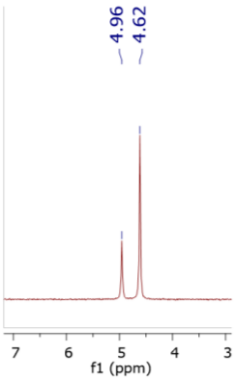

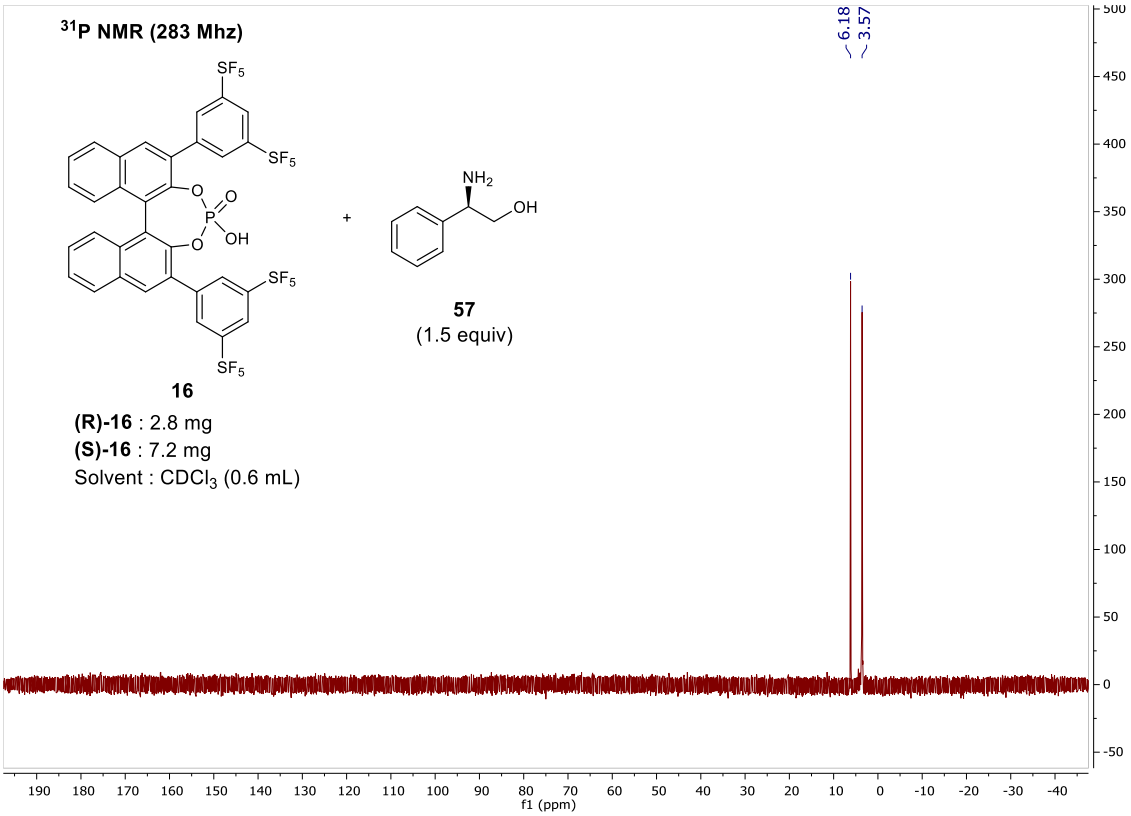
31P NMR (283 Mhz)
SF5
SF5
SF5
SF5
O
O
P
OH
O
+
NH2
OH
57
(1.5 equiv)
16
(R)-16 : 2.8 mg
(S)-16 : 7.2 mg
Solvent : CDCl3 (0.6 mL)
6.18
3.57
f1 (ppm)

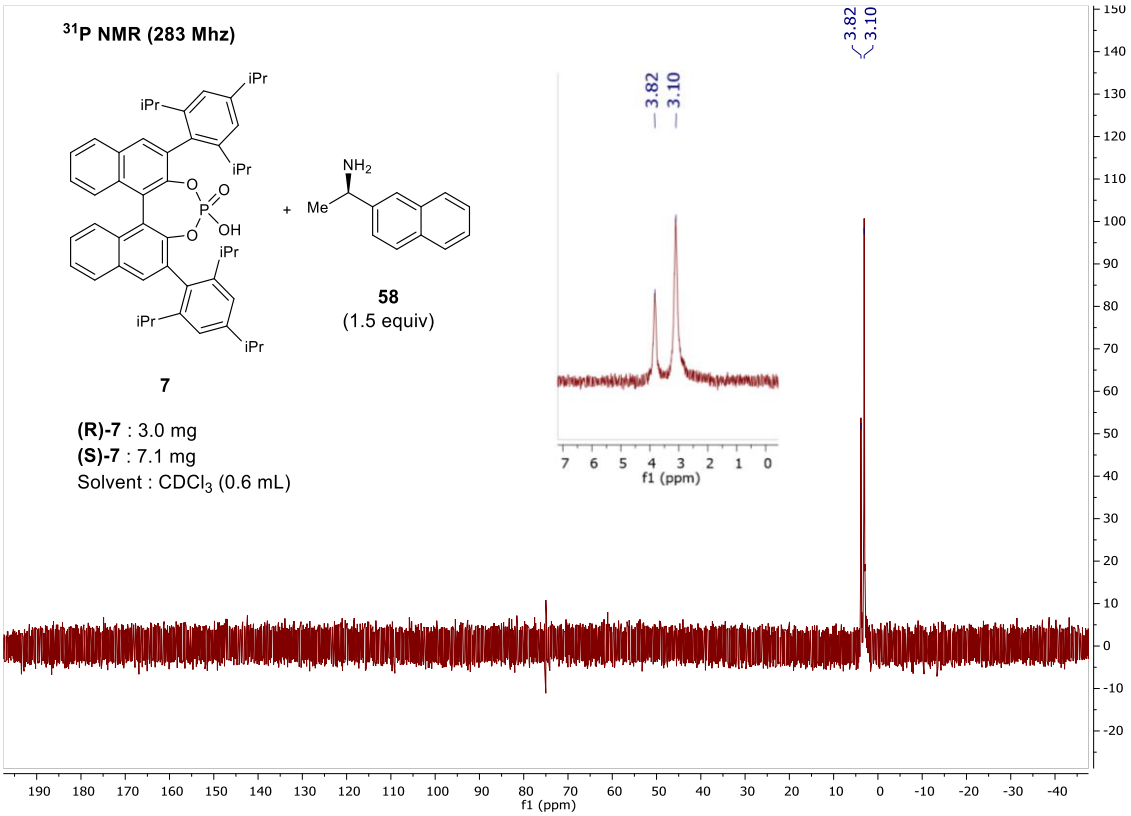
31P NMR (283 Mhz)
iPr
iPr
iPr
iPr
iPr
iPr
O
O
P
OH
O
+
NH2
Me
58
(1.5 equiv)
7
(R)-7 : 3.0 mg
(S)-7 : 7.1 mg
Solvent : CDCl3 (0.6 mL)
3.82
3.10
f1 (ppm)

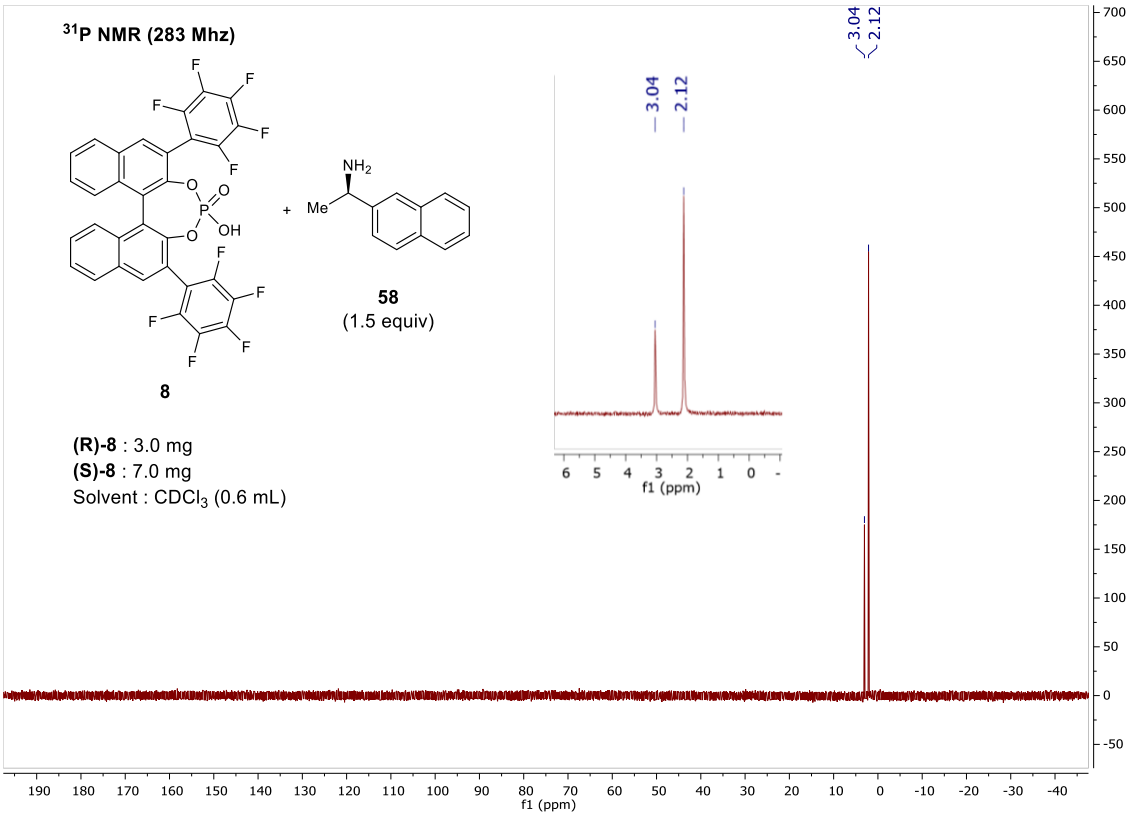
31P NMR (283 Mhz)
3.04
2.12
+
NH2
Me
58
(1.5 equiv)
8
(R)-8 : 3.0 mg
(S)-8 : 7.0 mg
Solvent : CDCl3 (0.6 mL)
f1 (ppm)

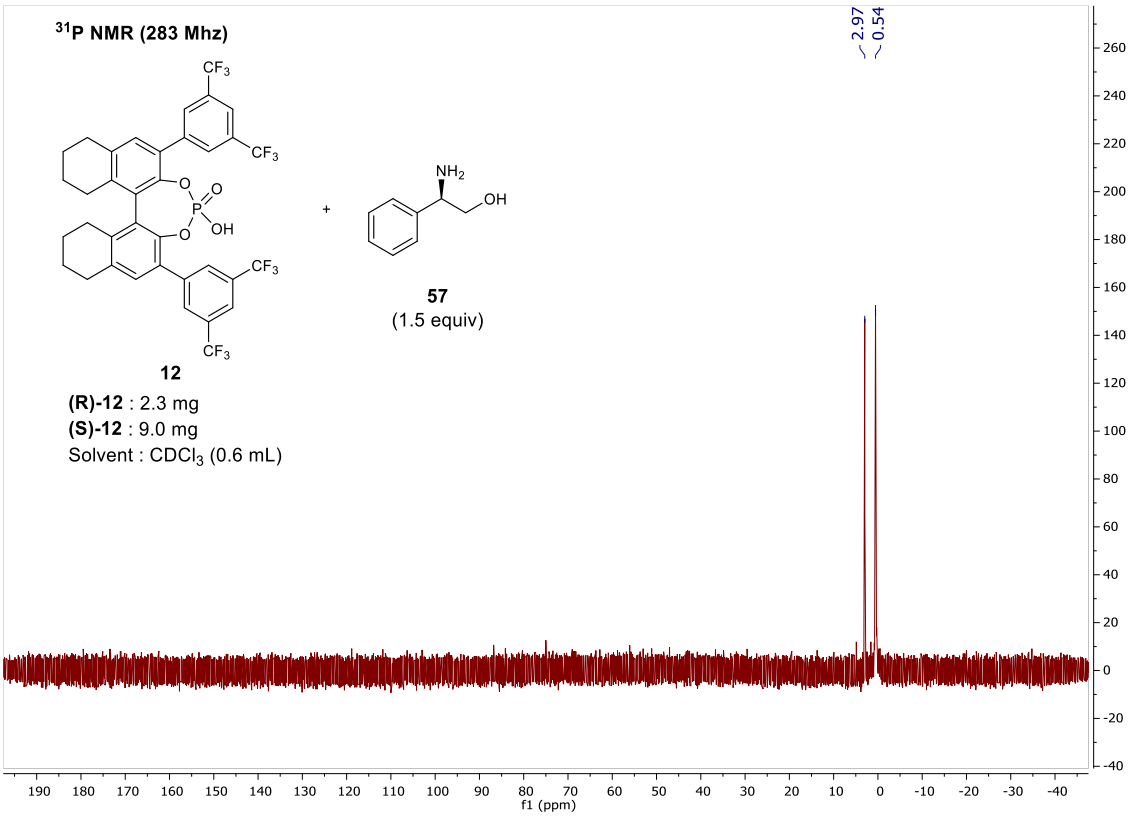
31P NMR (283 Mhz)
2.97
0.54
+
NH2
OH
57
(1.5 equiv)
12
(R)-12 : 2.3 mg
(S)-12 : 9.0 mg
Solvent : CDCl3 (0.6 mL)
f1 (ppm)

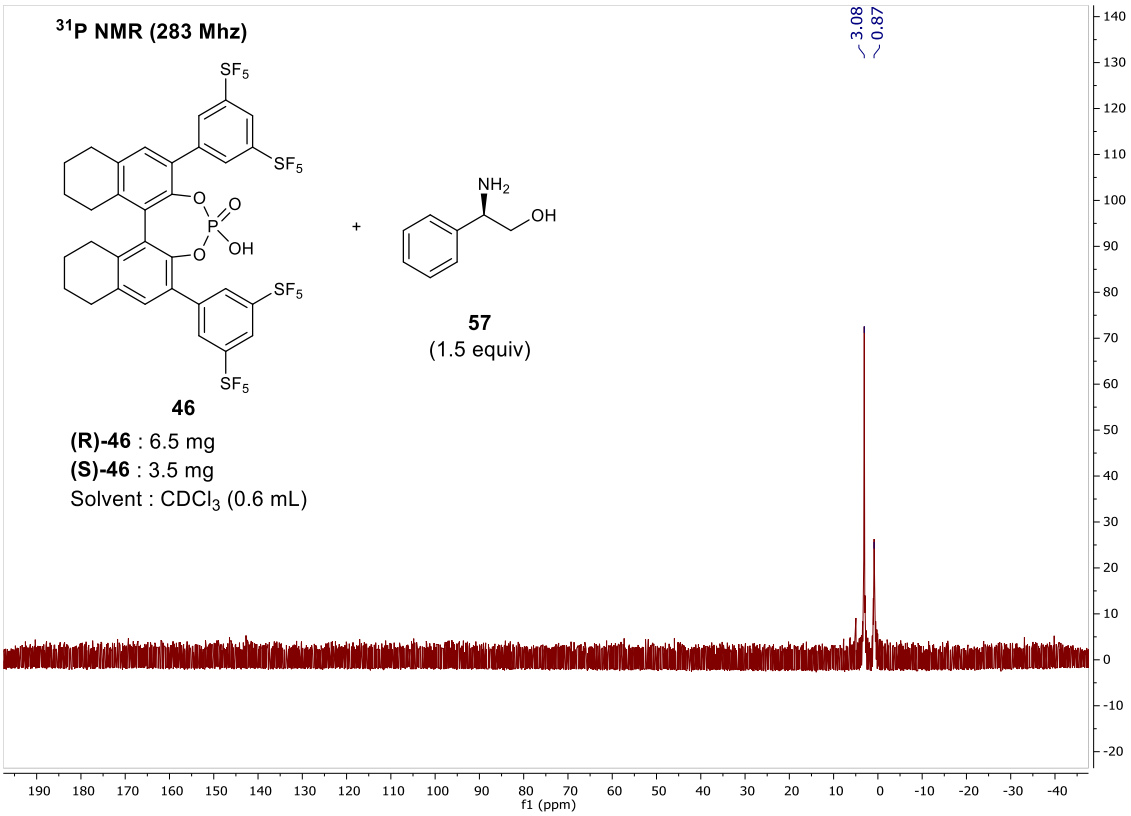
31P NMR (283 Mhz)
3.08
0.87
46
(R)-46 : 6.5 mg
(S)-46 : 3.5 mg
Solvent : CDCl3 (0.6 mL)
57
(1.5 equiv)
f1 (ppm)

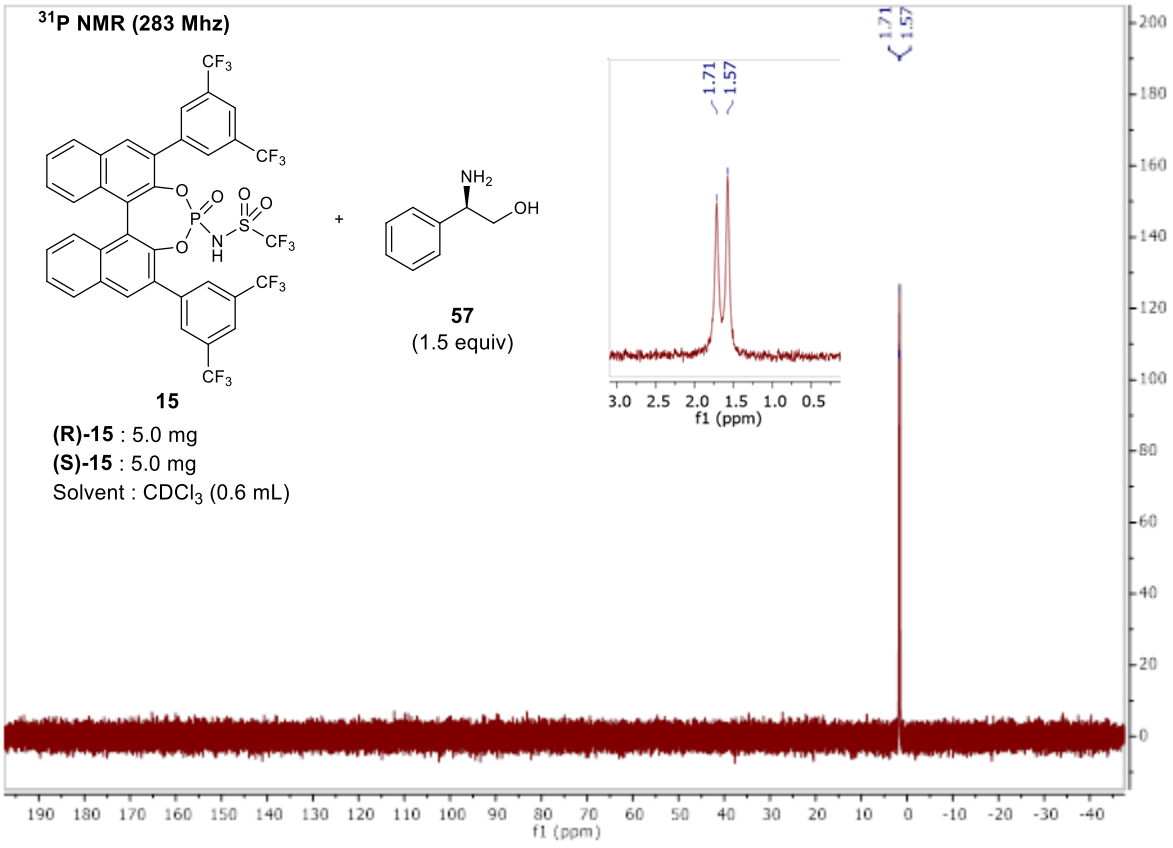
31P NMR (283 Mhz)
1.71
1.57
15
(R)-15 : 5.0 mg
(S)-15 : 5.0 mg
Solvent : CDCl3 (0.6 mL)
57
(1.5 equiv)
f1 (ppm)

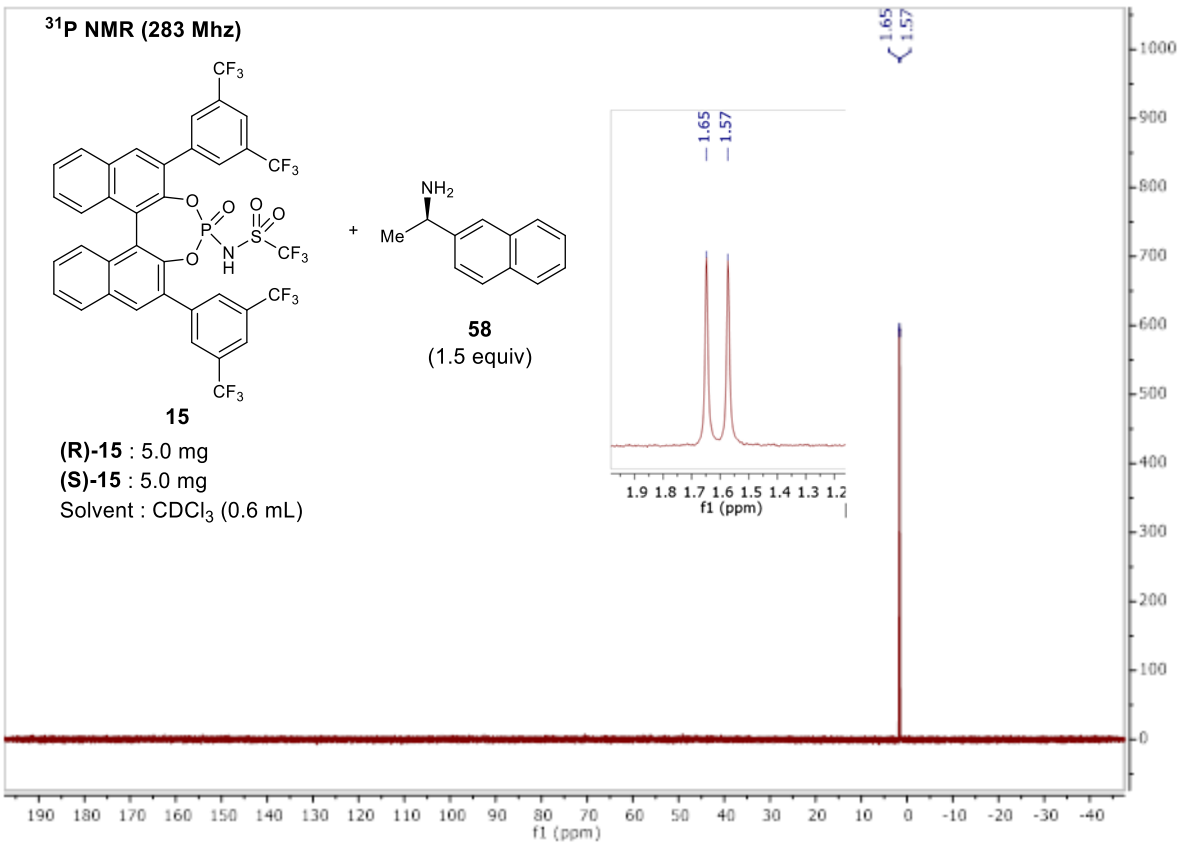

4.6 References

[1] Tay, J. H.; Nagorny, P. *Synlett* **2016**, *27*, 551.

[2] (a) Harger, M. J. P. *J. Chem. Soc., Perkin Trans. 2* **1978**, 326. (b) Shapiro, M. J.; Archinal, A. E.; Jarema, M. A. *J. Org. Chem.* **1989**, *54*, 5826.

[3] (a) Alexakis, A.; Mutti, S.; Normant, J. F.; Mangeney, P. *Tetrahedron: Asymmetry* **1990**, *1*, 437. (b) Alexakis, A.; Mutti, S.; Mangeney, P. *J. Org. Chem.* **1992**, *57*, 1224.

[4] (a) Meca, L.; Řeha, D.; Havlas, *Z. J. Org. Chem.* **2003**, *68*, 5677. (b) Hoyano, Y. Y.; Pincock, R. E. *Can. J. Chem.* **1980**, *58*, 134.

CHAPTER 5

An Efficient One-pot Protocol for the Synthesis of Natural Product Glycosides Based on the Use of Boronic Acid as Transient Protecting Group

5.1 Introduction

Organoboron compounds play a significant role in the development of carbohydrate chemistry.[1] In 1953, Soboczenski reported the preparation of various cyclic boronate compounds through condensation of phenylboronic acid with diols and monosaccharides such as sorbitol and mannitol.[2] Since then, the complexation of organoboron compounds and carbohydrates has been the subject of rigorous studies and the phenomenon has been utilized in various applications such as chromatographic science, analytical sensing, biological imaging, drug delivery and chemical synthesis.

Boronic acid is especially useful as a protecting group for diol moiety. In 1978, Fréchet demonstrated the potential of polystyrylboronic acid resin as a solid support to selectively synthesize acylated monosaccharide derivatives (Scheme 5.1 (a)).[3] The boronic acid on the resin acted as a both protecting group for cis diols on carbohydrate substrates and the linker that connected substrates to the solid support. The same strategy was later adopted by Boons to synthesize dissacharide compounds on solid support (Scheme 5.1 (b)).[4]

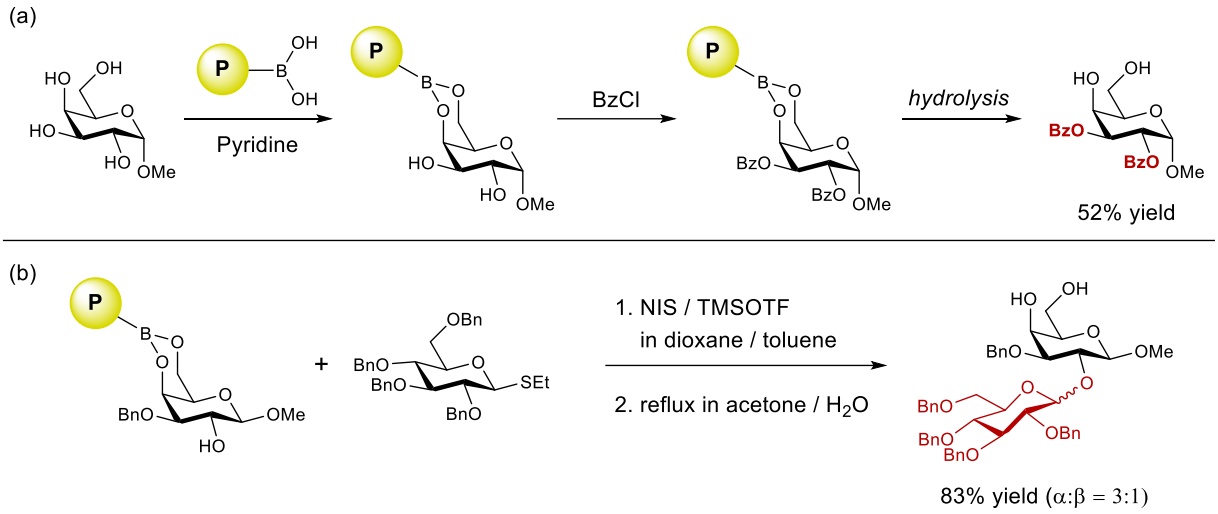

Scheme 5.1. Utilization of polystyrylboronic acid as a solid support in (a) acylation and (b) glycosylation of monosaccharides.

Beyond synthesis of simple carbohydrate derivatives, boronic acid has not been widely used in the glycosylation of natural products. One of the few examples was reported by Harmatha in 1994.[5] In his synthesis of 20-hydroxyecdysone glycoside, phenylboronic acid was used to selectively protect vicinal-diol on the D-ring side chain. After acylation of the C2-hydroxy group on the A-ring, glycosylation with glycosyl bromide and silver silicate resulted in the formation of a 1:1 mixture of C3-glycoside and C25-glycoside. To further demonstrate the utility of boronic acid in the synthesis of natural product glycoside, we aimed to develop a strategy toward the selective glycosylation of bacterial macrolactones and cardiotonic steroids that is operationally simple and efficient with regard to pot economy. We envisioned that the protection, deprotection and glycosylation of a natural product could be incorporated in a one-pot protocol through the judicious selection of reaction conditions.

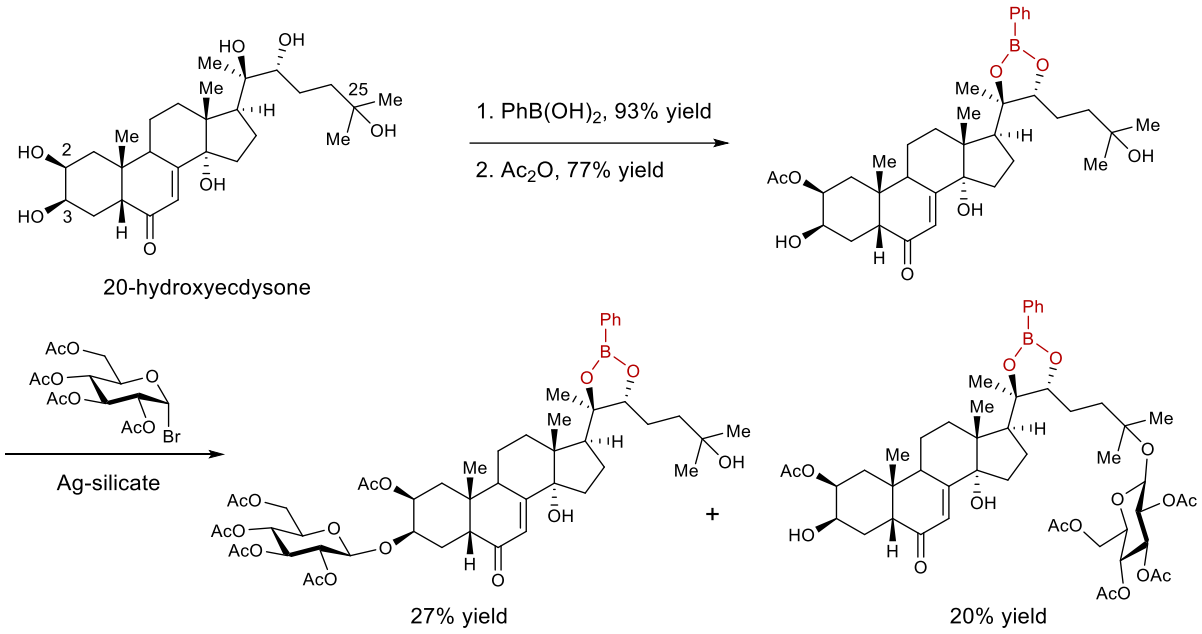

Scheme 5.2. Synthesis of 20-hydroxyecdysone glycosides involving the use of phenylboronic acid as the protecting group for vicinal diol.

5.2 One-pot Glycosylation of Antibiotic-derived Macrolactones

During our optimization for regioselective glycosylation of 6-dEB[6], we observed that the C11-hydroxyl group on the macrolactone was the least accessible for glycosylation. Since the C3- and C5-hydroxy groups were in a 1,3-syn relationship, we surmised that they could be selectively masked as boronate ester enabling glycosylation to occur at the C11-position. Indeed, the diol was successfully protected *in situ* by using phenylboronic acid in the presence of a 4Å molecular sieve as the dehydrating agent (Scheme 5.3). Subsequent glycosylation with trichloroacetimidate donor **2** and TMSOTF in the same pot, followed by a peroxide work-up, afforded the C11-glycoside **59** with good yield.

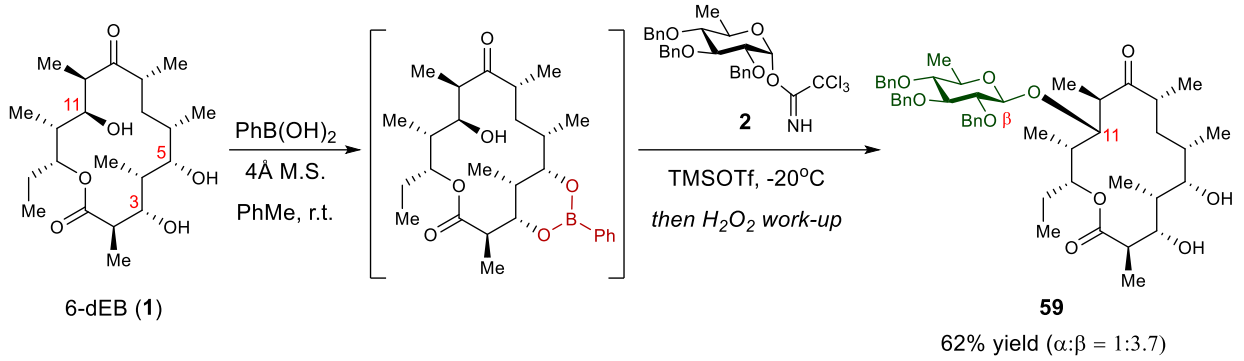

Scheme 5.3. One-pot synthesis of C11-glycoside **59** from 6-dEB (**1**).

In addition, the one-pot protocol was applied to the synthesis of C11-glycoside **60** from oleandomycin-derived macrolactone **25** (Scheme 5.4). Due to the presence of thioether, which could be oxidized during the peroxide work-up, methyl boronic acid was used instead. The methyl boronic ester was cleaved at the end of the reaction upon multiple azeotrope treatments with methanol.

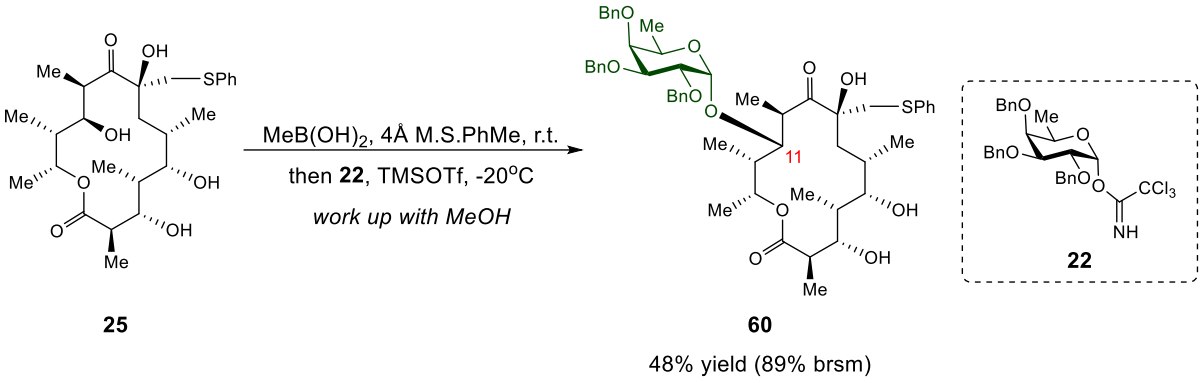

Scheme 5.4. One-pot synthesis of C11-glycoside **60** from macrolactone **25**.

5.3 Introduction to Cardiotonic Steroids

Cardiotonic steroids are an interesting class of small molecules which exhibit a diverse range of biological activities. Many members of the class have been extensively studied for their therapeutic values in treating heart related diseases, such as congestive heart failure and cardiac arrhythmia.[7] More recently, their actions on the cellular sodium-potassium ATPase pump have a been explored in the context of cancer treatment.[8] Nonetheless, the actual implementation of

cardiotonic steroids as therapeutic agents is still limited and challenging due to their toxic properties.[9] To circumvent the problem, numerous efforts have been focused on making analogues of cardiotonic steroids through total or semi-synthesis to identify compounds with improved therapeutic windows.[10]

Most cardiotonic steroids consist of a core structure of fuse rings, a lactone moiety at the C17 position and a sugar moiety connected through the C3-hydroxy group (Figure 5.1). SAR studies show that all the three major components of a cardiotonic steroid plays significant roles in determining its biological activities.[11] Given the rich structural diversity of natural and unnatural sugar, we believe that manipulation of the sugar moiety at the C3 position provides one of the most efficient routes to generate a library of cardiotonic steroid analogues.

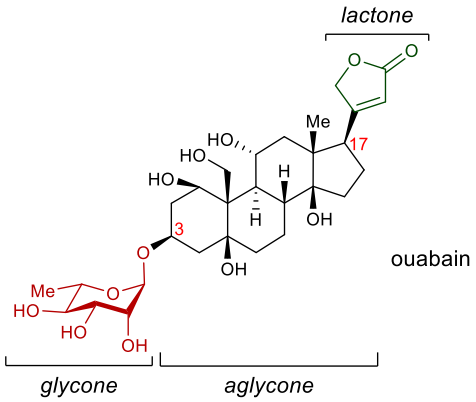

Figure 5.1. Structure of ouabain, a cardiotonic steroid.

While there is a plethora of methods developed for the formation of glycosidic linkages, the glycosylation of polyoxygenated natural products such as the steroidal core is not trivial, mainly because of regioselectivity issues. In 2017, Nagorny reported the total synthesis of cannogenol (a cardiotonic steroid) and its rhamnoside.[12] In an attempt to accomplish selective installation of rhamnose sugar at the C3-alcohol, a triol intermediate was subjected to glycosylation with rhamnose-derived trichloroacetimidate donor and TMSOTf as activator. (Scheme 5.5) Nonetheless, the reaction led to the formation of about 1:1 mixture of two regioisomeric glycosides.

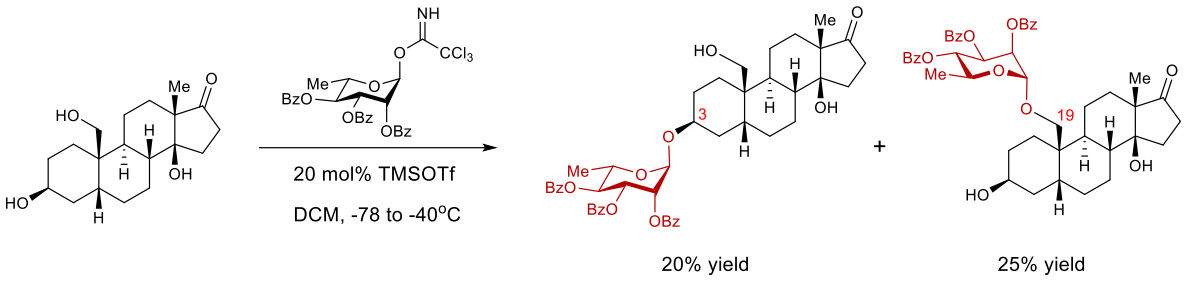

Scheme 5.5. Example of unselective glycosylation of steroidal compound.

In most synthesis of cardiac glycosides, a multistep protection/deprotection sequence is commonly used to ensure selective delivery of a sugar unit at the desired C3 hydroxy group.[10] For example, in the total synthesis of ouabain developed by Deslongchamps, the rhamnose sugar was installed onto the aglycone of ouabain (ouabagenin) through a six steps sequence.[13] (Scheme 5.6) Five steps out of the sequence involved protecting group manipulation, and the overall yield for the whole sequence ended up being 35%. Clearly, a more efficient protocol for the installation of glycone onto steroidal core is warranted.

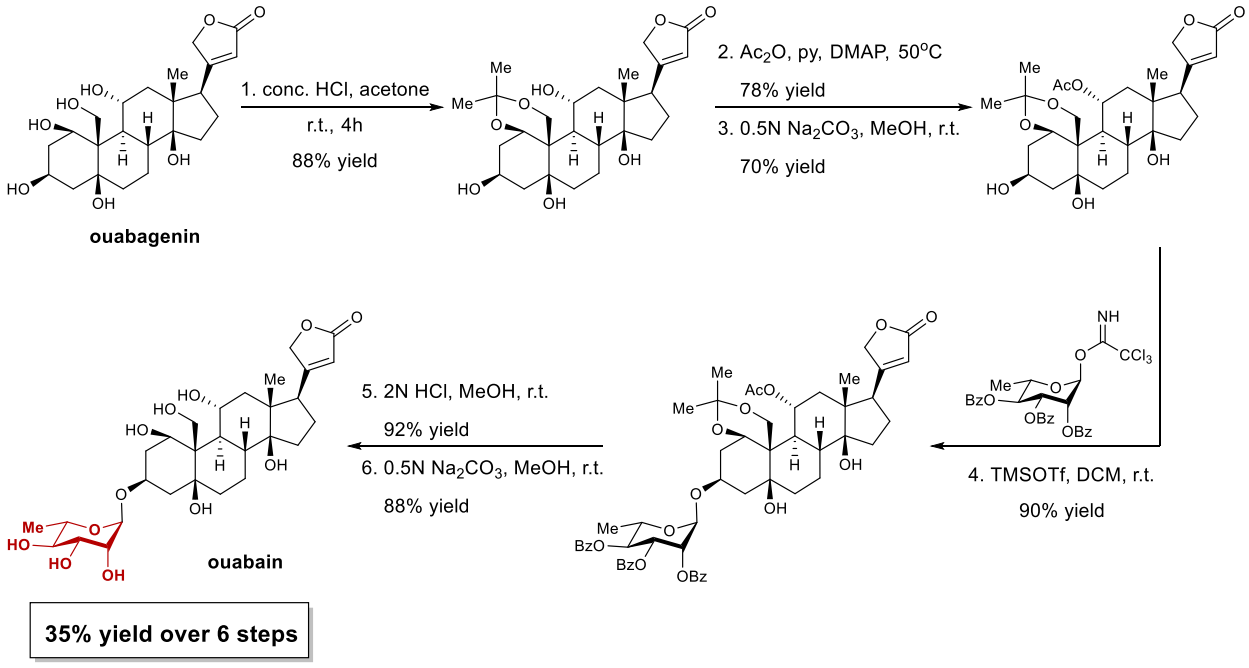

Scheme 5.6. Synthesis of ouabain from ouabagenin developed by Deslongchamps.

To streamline the synthesis of new cardiotonic steroids with different sugar moiety, we set out to develop a pot-efficient protocol for the coupling between the steroidal core and the sugar based on the use of boronic acid as the transient protecting group.

5.4 One-pot Glycosylation of Strophanthidol

We first tested our protocol using strophanthidol (**61**) as the substrate. Strophanthidol has two pairs of hydroxy groups in a 1,3-relationship: C3/C5 alcohols and C5/C19 alcohols. We hypothesized that methyl boronic acid would preferably form cyclic ester with the C5 and C19 hydroxy groups because the primary alcohol at the C19 position is sterically more accessible. Indeed, after we mixed strophanthidol (**61**) with methyl boronic acid in the presence of the 4Å molecular sieves in dichloromethane, we were able to obtain a single compound containing methyl boronic ester moiety with quantitative mass recovery (Scheme 5.7). We subsequently subjected the isolated boronic ester intermediate to a glycosylation condition with a benzyl protected fucose trichloroacetimidate donor **26** and TMS-OTf as the activator. Upon work up with MeOH to remove the methyl boronic acid masking group, we observed exclusive formation of C3-glycoside **62**, albeit with moderate yield and low diastereoselectivity. The result however supports our initial hypothesis that the formation of cyclic boronate at the C5 and C19 hydroxy groups of strophanthidol is favored exclusively.

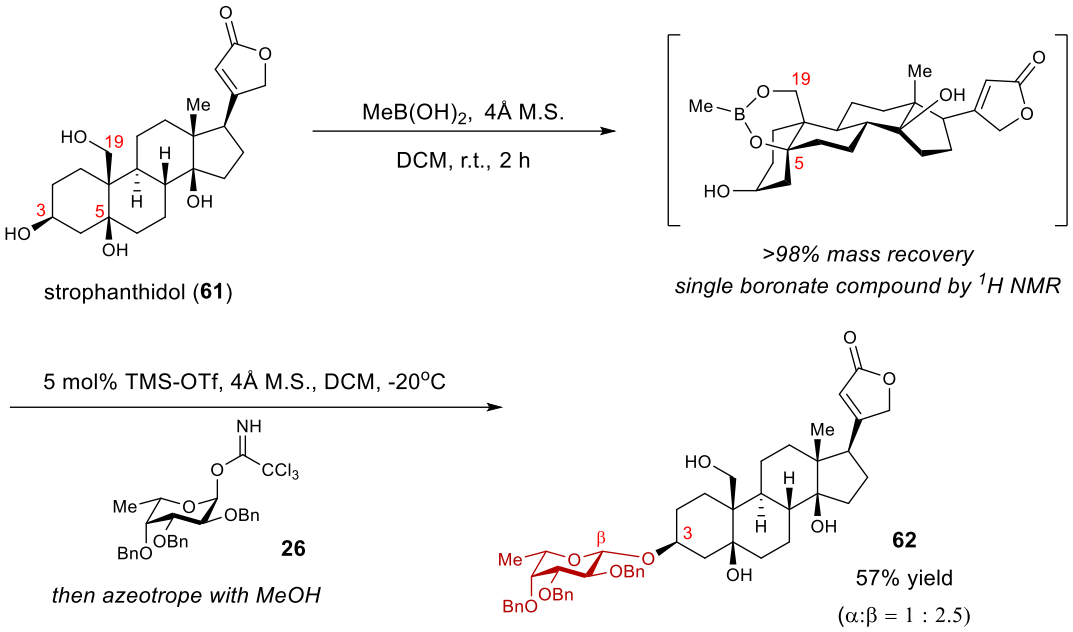

Scheme 5.7. Initial studies on boronic acid protection of strophanthidol (**61**) and subsequent glycosylation.

Next, we moved on to optimize the conditions for the glycosylation step. To address the problem of low diastereoselectivity, we switched the protecting group on the glycosyl donor from a benzyl to a benzoate group to take advantage of the anchimeric effect. After the first step for the formation of boronated protected strophanthidol, glycosyl donor **63** and the catalyst were added to the same reaction pot to initiate glycosylation (Table 5.1). We tested several general conditions for the activation of the trichloroacetimidate donor, and we found most Lewis acid activators were inefficient in promoting the glycosylation reaction (entries 1 – 3). However, when TfOH was used as the activator we were able to obtain a significantly better conversion and isolated yield (entry 4). We also noticed that the isolated yield increased by two-fold, from 37% to 76%, when portions of the glycosyl donor were added to the reaction at 30 minute intervals (entry 5). Through further optimization, we were able to obtain the C3-rhamnoside of strophanthidol **64** with good yield and exclusive formation of the α-glycosidic linkage (entry 6).

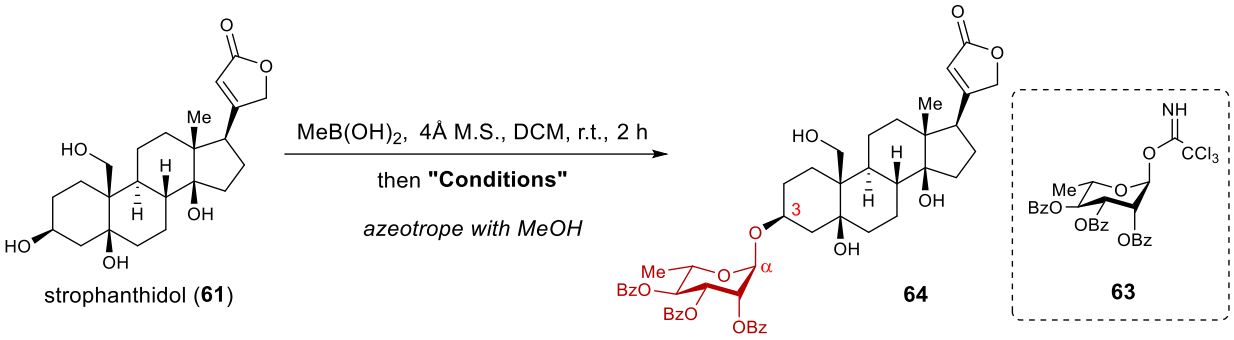

entry	"Conditions"	Conversion [a] (Yield [b])
1	TMSOTf (10 mol%), donor **63** (2 equiv.), -78°C to r.t., 2.5 h	24%
2	AgOTf(100 mol%), donor **63** (1.1 equiv.), -40°C, 1 h	4%
3	$NOBF_4$ (120 mol%), donor **63** (2 equiv.), -15°C, 1.5 h	10%
4	TfOH (20 mol%), donor **63** (3 equiv.), r.t., 3 h	57% (37%)
5 [c]	TfOH (20 mol%), donor **63** (3 equiv.), r.t., 3 h	88% (76%)
6 [c]	**TfOH (30 mol%), donor 63 (2 equiv.), 0°C to r.t., 5 h**	85% (81%)

[a] Conversion by ^{1}H NMR. [b] Isolated yield. [c] Donor was added potionwise.

Table 5.1. Optimization for one-pot glycosylation of strophanthidol (**1**) with a benzoyl-protected donor **63**.

To further enhance the efficiency of our protocol, we incorporated a deprotection condition that could remove both methyl boronic ester and the benzoate protecting group on the sugar at the end of the reaction. After the glycosylation was complete, the reaction was diluted with MeOH, bubbled with NH_3 gas and stirred at room temperature overnight (Table 5.2). After flash chromatography on silica gel, we were able to isolate the totally unprotected rhamnoside of strophanthidol **69** with good yield (entry 1). Using the one-pot protocol, we also synthesized strophanthidol glycoside with unprotected L-fucose (**70**) and D-fucose (**71**) at the C3 position with good yield. When we applied the same strategy to couple glucose and mannose to strophanthidol, we noticed a significant formation of an ortho ester by-product. Previously, Kihlberg and coworker have reported the use of a fluorine substituted benzoate group as the protecting group on the sugar donor to minimize the formation of ortho ester during glycosylation.[14] Indeed, when we used 2-fluoro-benzoate protected glucose and mannose trichloroacetimidate donor (**67** and **68**) in our reaction, the formation of ortho ester was suppressed. We were able to synthesize the corresponding D-glucoside (**72**) and D-mannoside (**73**) of strophanthidol with good yield. In all, our one-pot protocol has allowed us to efficiently synthesize five glycosides of strophanthidol,

three of which are new glycosides (**70**, **71** and **73**) that have not been reported in the literature to date.

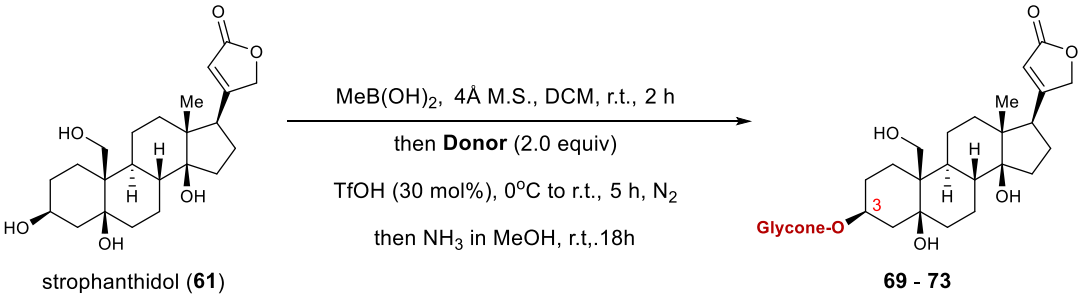

entry	Donor	Product	Isolated Yield
1	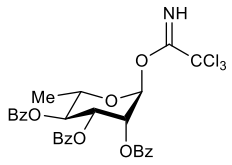 **63**	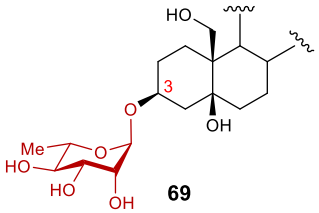 **69**	73%
2	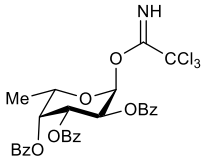 **65**	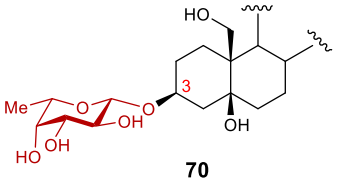 **70**	77%
3	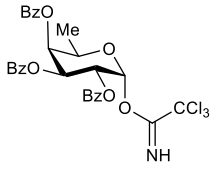 **66**	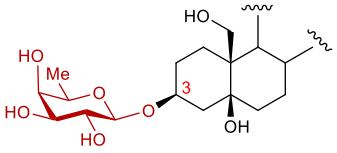 **71**	72%
4	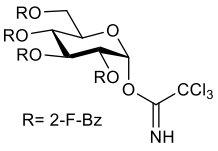 **67**	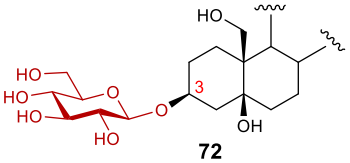 **72**	75%
5	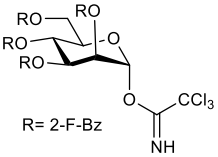 **68**	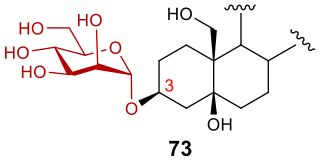 **73**	69%

Table 5.2. The substrate scope for one-pot glycosylation of strophanthidol (**61**).

5.5 One-pot Glycosylation of Anhydro-ouabagenin

Next, we applied the one-pot protocol to the glycosylation of another cardiotonic steroid, anhydro-ouabagenin (**74**). As before, we observed the formation of a single boronate compound by ^{1}H NMR when **74** was mixed with methyl boronic acid in the presence of the 4Å molecular sieve (Scheme 5.8 (a)). However, when the isolated boronate compound was subjected to glycosylation with donor **63** and TfOH as the activator, the reaction resulted in a mixture of C3-glycoside **75** and C19-glycoside **76**. We believed the boronate intermediate underwent isomerization under the acidic conditions and consequently led to unselective glycosylation at the C3 and C19 positions (Scheme 5.8 (b)). Similar intramolecular migration of a boronate group was previously reported by Taylor.[15]

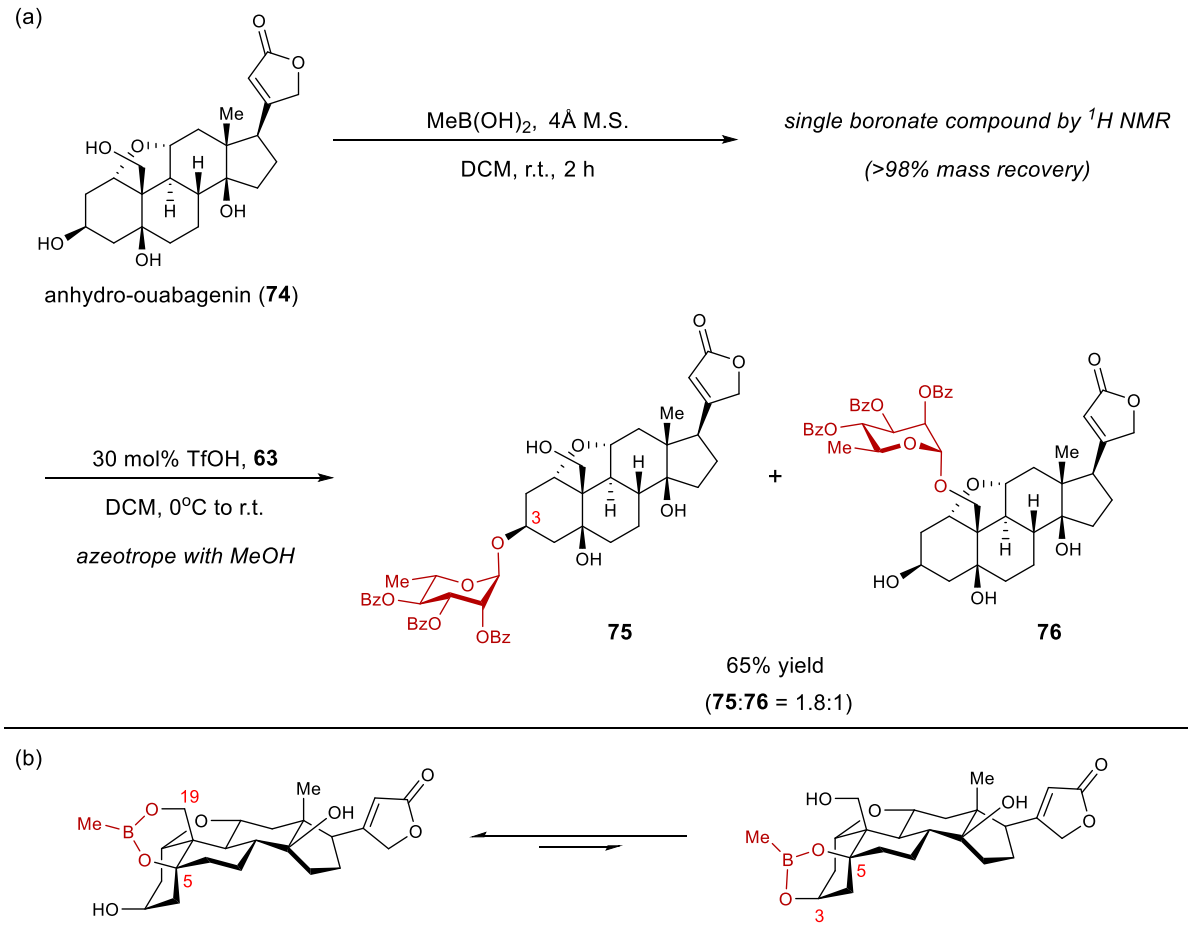

Scheme 5.8. (a) One-pot glycosylation of anhydro-ouabagenin (**74**) with trichloroacetimidate donor and TfOH as the activator. (b) Proposed isomerization of a boronate compound derived from anhydro-ouabagenin (**74**).

To circumvent the problem of unselective glycosylation, we explored other glycosylation methods that might minimize undesired isomerization of the boronate intermediate. We postulated that the isomerization could be minimized if a milder or neutral glycosylation condition with glycosyl halide were employed. Upon further screening, we identified glycosylation with glycosyl bromide **77** and Ag_2CO_3 as the optimum condition to generate C3-glycoside **75** with good yield and much improved regioselectivity (Scheme 5.9).

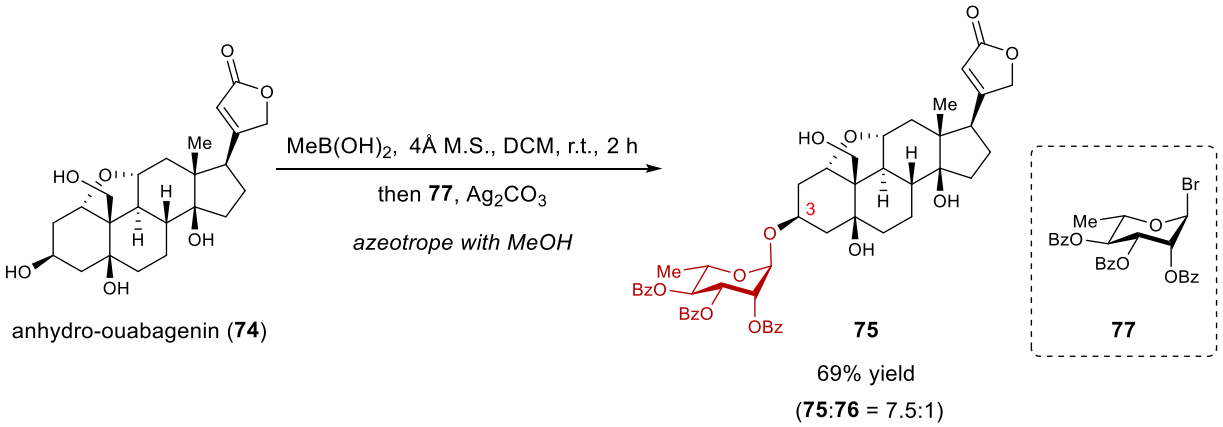

Scheme 5.9. One-pot glycosylation of anhydro-ouabagenin (**74**) with glycosyl bromide donor **77** and Ag_2CO_3 as activator.

5.6 Conclusion

In summary, the one-pot protocol provided an operationally simple and efficient route to synthesize glycosides from poly-oxygenated natural products. Simple boronic acids were proven to be highly effective transient protecting groups for complex natural products containing 1,3-diol moiety. The one-pot protocol allowed us to selectively generate glycosides from antibiotic-derived macrolactones and cardiotonic steroid cores that are otherwise difficult to access.

5.7 Experimental Information

General Methods

All reagents and solvents were purchased from Sigma-Aldrich, Fisher Scientific, and were used as received without further purification unless specified. 4Å molecular sieve was activated prior to use by heating under reduced pressure. Cooling was achieved by use of cryocool machine or ice bath. Deionized water was used in the preparation of all aqueous solutions and for all aqueous extractions. Solvents used for extraction and chromatography were ACS or HPLC grade. Purification of reactions mixtures was performed by flash chromatography using SiliCycle SiliaFlash P60 (230-400 mesh).

^{1}H NMR spectra were recorded on Varian vnmrs 700 (700 MHz), Varian vnmrs 500 (500 MHz), Varian INOVA 500 (500 MHz) or Varian MR400 (400 MHz) spectrometers and chemical shifts (δ) are reported in parts per million (ppm) with solvent resonance as the internal standard ($CDCl_3$ at δ 7.26, CD_3OD at δ 3.31, C_6D_6 at δ 7.16). Data are reported as (br = broad, s = singlet, d = doublet, t = triplet, q = quartet, m = multiplet; coupling constant(s) in Hz; integration). Proton-decoupled ^{13}C NMR spectra were recorded on Varian vnmrs 700 (700 MHz), Varian vnmrs 500 (500 MHz), Varian INOVA 500 (500 MHz) or Varian MR400 (400 MHz) spectrometers and chemical shifts (δ) are reported in ppm with solvent resonance as the internal standard ($CDCl_3$ at δ 77.16, CD_3OD at 49.0, C_6D_6 at 128.06). High resolution mass spectra (HRMS) were recorded on Micromass AutoSpec Ultima or VG (Micromass) 70-250-S Magnetic sector mass spectrometers in the University of Michigan mass spectrometry laboratory. Infrared (IR) spectra were recorded as thin film on a Thermo-Nicolet IS-50 spectrometer. Absorption peaks were reported in wavenumbers (cm^{-1}). Optical rotations were measured in a solvent of choice on a JASCO P-2000 or Autopol III digital polarimeter at 589 nm (D-line).

Synthesis of Glycoside 59

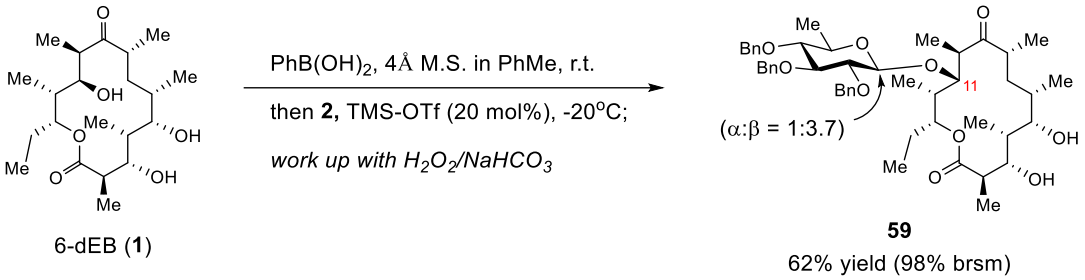

6-dEB (**1**)

59

62% yield (98% brsm)

6-dEB (5mg, 0.010mmol), $PhB(OH)_2$ (1.2mg, 1 equiv.) and 10mg of powdered 4Å molecular sieve were stirred in 100µL of dry toluene at room temperature. After 3h, sugar donor **2** (17.4mg, 3 equiv.) in 100µL of dry toluene was added to the reaction, and the mixture was cooled to -20°C. TMS-OTf (0.36µL, 0.2 equiv.) in 20µL of dry toluene was added to the reaction. After 17h, the reaction was quenched with Et_3N, warmed up to room temperature and diluted with EtOAc. 30% H_2O_2, sat. $NaHCO_3$ and water were added to the solution, and the suspension was stirred at room temperature. After 2h, the reaction was extracted with CH_2Cl_2 twice. Combined organic was dried over Na_2SO_4, filtered through glass wool and concentrated under reduced pressure. The crude mixture was purified by flash column chromatography (pipette column) on silica gel (EtOAc:Hexanes, 20:80 to 35:65 v/v) to obtain **59** (5mg, 62% yield) as colorless oil and starting material 6-dEB (1.5mg, 38% recovery). The diastereomeric glycosides were isolated by semi-prep HPLC (18mL/min, EtOAc:Hexanes, 25:75 v/v) and characterized.

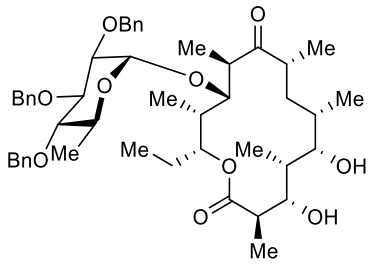

α-59

^{1}H NMR (500 MHz, C_6D_6): δ 7.41 (d, J = 7.4 Hz, 2H), 7.32 (d, J = 7.4 Hz, 2H), 7.26 (d, J = 7.2 Hz, 2H), 7.11 – 7.01 (m, 3H), 5.83 (t, J = 7.3 Hz, 1H), 5.63 (d, J = 3.4 Hz, 1H), 5.01 (d, J = 11.5 Hz, 1H), 4.98 (d, J = 10.7 Hz, 1H), 4.86 (d, J = 11.2 Hz, 1H), 4.80 (t, J = 11.5 Hz, 2H), 4.53 (d, J = 11.2 Hz, 1H), 4.15 (m, 2H), 4.05 (dq, J = 12.0, 6.0 Hz, 1H), 3.99 (d, J = 10.4 Hz, 1H), 3.67 (m, 1H), 3.52 (dd, J = 10.1, 3.4 Hz, 1H), 3.09 (m, 2H), 2.96 (s, 1H), 2.73 (dq, J = 13.4, 6.7 Hz, 1H), 2.64 (q, J = 6.5 Hz, 1H), 1.87 – 1.77 (m, 1H), 1.70 (m, 1H), 1.65 (m, 1H), 1.54 (d, J = 6.0 Hz, 3H), 1.49 (d, J = 6.7 Hz, 3H), 1.32 (d, J = 6.2 Hz, 3H), 1.26 (d, J = 6.6 Hz, 3H), 1.20 (m, 2H), 1.03 (d, J = 6.8 Hz, 3H), 1.00 – 0.93 (m, 1H), 0.81 (d, J = 7.1 Hz, 3H), 0.62 (d, J = 7.1 Hz, 3H), 0.48 (t, J = 7.3 Hz, 3H).

^{13}C NMR (126 MHz, C_6D_6): δ 211.0, 176.8, 139.9, 139.3, 139.3, 128.7, 128.5, 128.4, 128.2, 128.0, 127.8, 127.6, 127.5, 100.8, 85.0, 83.6, 82.0, 81.9, 79.0, 76.4, 75.6, 75.4, 75.4, 75.0, 69.1, 44.8, 44.2, 41.4, 39.3, 38.5, 38.0, 35.3, 26.1, 18.3, 16.7, 15.4, 13.9, 10.0, 9.9, 7.8, 7.4.

HRMS (m/z): $[M+NH_4]^+$ calcd. for $C_{48}H_{66}O_{10}$, 820.5000; found, 820.4979

TLC (EtOAc:Hexanes, 30:70 v/v): R_f = 0.3

IR (thin film, cm^{-1}): 3438, 2967, 2919, 2855, 1710, 1453, 1070

$[\alpha]_D$: -3.2 (c = 0.10 in $CHCl_3$)

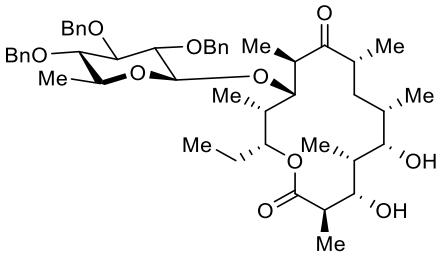

β-59

^{1}H NMR (700 MHz, C_6D_6): δ 7.46 (d, J = 7.5 Hz, 2H), 7.27 (d, J = 7.5 Hz, 2H), 7.19 (t, J = 7.6 Hz, 4H), 7.15 – 7.02 (m, 5H), 5.76 (dd, J = 8.3, 6.1 Hz, 1H), 5.07 (d, J = 11.4 Hz, 1H), 4.86 (d, J = 11.4 Hz, 1H), 4.76 (d, J = 11.4 Hz, 1H), 4.72 (d, J = 11.4 Hz, 1H), 4.67 (d, J = 11.4 Hz, 1H), 4.50 (d, J = 9.1 Hz, 1H), 4.40 (d, J = 7.3 Hz, 1H), 4.39 (d, 1H), 3.91 (d, J = 10.1 Hz, 1H), 3.78 – 3.71 (m, 1H), 3.55 (dd, J = 9.2, 7.4 Hz, 1H), 3.48 (t, J = 9.0 Hz, 1H), 3.35 (dq, J = 9.6, 6.1 Hz, 1H), 3.29 (ddt, J = 12.3, 9.3, 6.0 Hz, 1H), 3.14 (t, J = 9.1 Hz, 1H), 2.76 – 2.67 (m, 2H), 2.65 (s, 1H), 1.89 (q, J = 6.7 Hz, 1H), 1.80 – 1.76 (m, 1H), 1.74 (m, 1H), 1.64 – 1.58 (m, 1H), 1.57 – 1.52 (m, 1H), 1.40 (d, J = 6.8 Hz, 3H), 1.36 (d, J = 6.1 Hz, 3H), 1.33 (m, 1H), 1.28 (d, J = 6.7 Hz, 3H), 1.17 (d, J = 6.3 Hz, 3H), 1.11 (d, J = 6.9 Hz, 3H), 1.04 (td, J = 13.6, 3.5 Hz, 1H), 0.87 (d, J = 7.1 Hz, 3H), 0.84 (t, J = 7.4 Hz, 3H), 0.79 (d, J = 7.2 Hz, 3H).

^{13}C NMR (126 MHz, C_6D_6): δ 214.1, 174.8, 139.8, 139.4, 139.3, 128.5, 128.5, 128.4, 128.4, 128.3, 127.8, 127.7, 127.7, 127.5, 99.4, 84.8, 83.6, 83.2, 78.3, 76.1, 75.8, 75.5, 75.2, 75.1, 74.9, 71.6, 44.0, 43.9, 41.0, 39.6, 39.0, 38.7, 35.5, 26.7, 18.2, 17.2, 15.1, 14.3, 10.7, 10.2, 8.0, 7.5.

HRMS (m/z): $[M+NH_4]^+$ calcd. for $C_{48}H_{66}O_{10}$, 820.5000; found, 820.4989

TLC (EtOAc:Hexanes, 30:70 v/v): R_f = 0.4

IR (thin film, cm^{-1}): 3489, 2971, 2928, 2880, 1733, 1702, 1453, 1071

[α]$_D$: -42.3 (c = 0.23 in $CHCl_3$)

Synthesis of Glycoside 60

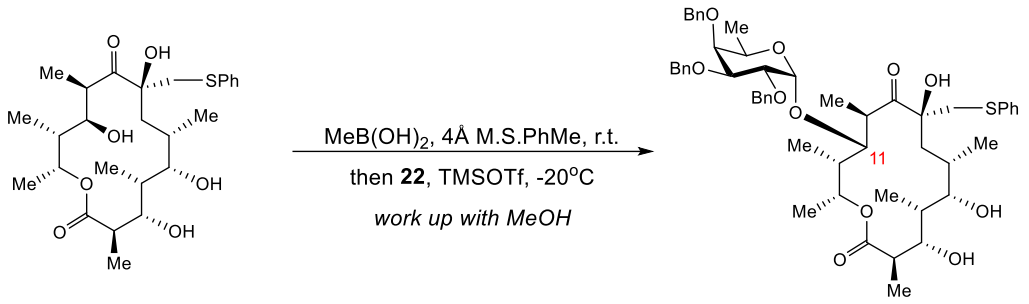

25 **60**

48% yield (89% brsm)

25 (10mg, 0.020mmol), $MeB(OH)_2$ (1.2mg, 1 equiv.) and 20mg of powdered 4Å molecular sieve were stirred in 200µL of dry toluene at room temperature. After 5h, sugar donor **22** (35mg, 3 equiv.) in 150µL of dry toluene was added to the reaction, and the mixture was cooled to -20°C. TMS-OTf (1.8µL, 0.5 equiv.) in 50µL of dry toluene was added to the reaction. After 17h, the reaction was quenched with Et_3N, warmed up to room temperature and stirred with MeOH for 30 minutes. Next, the reaction was filtered through a short pad of Celite with CH_2Cl_2 washing and concentrated under reduced pressure. The crude mixture was purified by flash column chromatography (pipette column) on silica gel (EtOAc:Hexanes, 20:80 to 60:40 v/v) to obtain **60** (8.7mg, 48% yield) as yellow oil and starting material **25** (4.6mg, 46% recovery).

^{1}H NMR (700 MHz, $CDCl_3$): δ 7.43 – 7.27 (m, 17H), 7.23 (t, J = 7.2 Hz, 2H), 7.15 (t, J = 7.3 Hz, 1H), 5.50 (d, J = 6.1 Hz, 1H), 5.06 (d, J = 3.2 Hz, 1H), 4.96 (d, J = 11.6 Hz, 1H), 4.85 (t, J = 12.0 Hz, 2H), 4.77 (d, J = 11.7 Hz, 1H), 4.69 (d, J = 11.1 Hz, 1H), 4.67 (s, 1H), 4.61 (d, J = 11.4 Hz, 1H), 4.39 (d, J = 6.8 Hz, 1H), 4.03 (dd, J = 9.8, 2.9 Hz, 1H), 3.97 – 3.90 (m, 1H), 3.89 (d, J = 10.5 Hz, 1H), 3.82 (q, J = 6.5 Hz, 1H), 3.77 – 3.71 (m, 1H), 3.65 (s, 1H), 3.36 – 3.25 (m, 3H), 2.51 – 2.44 (m, 1H), 2.38 – 2.29 (m, 1H), 1.97 – 1.91 (m, 1H), 1.81 – 1.68 (m, 3H), 1.29 (d, J = 6.7 Hz, 3H), 1.07 (d, J = 5.1 Hz, 3H), 1.02 (d, J = 7.1 Hz, 3H), 0.98 (d, J = 6.5 Hz, 3H), 0.91 (d, J = 4.4 Hz, 3H), 0.65 (d, J = 7.1 Hz, 3H).

^{13}C NMR (176 MHz, $CDCl_3$): δ 213.2, 176.0, 139.1, 138.9, 138.8, 137.6, 130.0, 129.00, 128.6, 128.5, 128.5, 128.3, 128.2, 128.2, 127.7, 127.6, 127.6, 127.5, 126.2, 99.3, 82.7, 79.8, 79.5, 79.4, 78.0, 76.8, 76.2, 75.1, 74.5, 72.9, 71.3, 67.8, 44.9, 44.7, 44.5, 42.8, 40.5, 39.3, 33.8, 18.7, 17.5, 16.9, 15.4, 9.3, 8.4, 8.0.

HRMS (m/z): $[M+Na]^+$ calcd. for $C_{53}H_{68}O_{11}S$, 935.4380; found, 935.4363

TLC (EtOAc:Hexanes, 30:70 v/v): $R_f = 0.2$

IR (thin film, cm^{-1}): 3411, 2973, 2919, 2852, 1721, 1453, 1379, 1096

$[\alpha]_D$: +8.6 (c = 0.93 in $CHCl_3$)

Synthesis of Strophanthidol

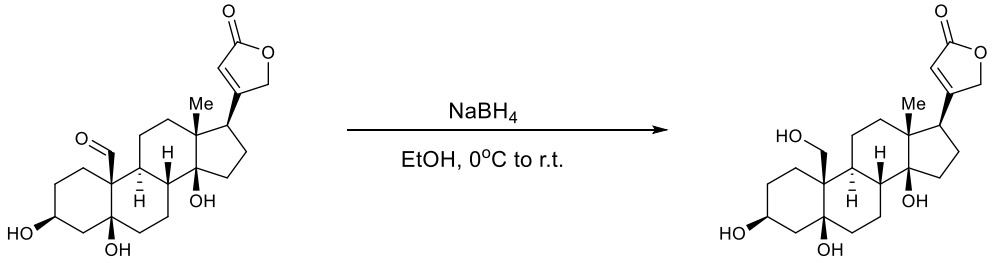

Scheme 5.10. Synthesis of strophanthidol (**61)** from strophanthidin.

Strophanthidin (500mg, 1.24mmol) was dissolved in EtOH (0.15M) and cooled in ice-bath. $NaBH_4$ (95mg, 2.0 equiv.) was added, and the reaction was warmed up to room After stirring at room temperature for 2h, the reaction was cooled in ice-bath, diluted with 50mL of EtOAc, and quenched slowly with 50mL of saturated NH_4Cl (aq). The biphasic mixture was stirred vigorously overnight. Next, the organic layer was separated and concentrated under reduced pressure. The crude mixture was purified by flash column chromatography on silica gel (MeOH:CH_2Cl_2 15:1 to 10:1 v/v) to obtain strophanthidol **61** (430mg, 85% yield) as white solid.

^{1}H NMR (700 MHz, $CDCl_3$): δ 5.87 (s, 1H), 5.75 (s, 1H), 4.97 (d, *J* = 18.2 Hz, 1H), 4.80 (d, *J* = 17.9 Hz, 1H), 4.70 (d, *J* = 7.5 Hz, 1H), 4.37 (d, *J* = 11.2 Hz, 1H), 4.20 (d, *J* = 4.1 Hz, 1H), 4.07 (d, *J* = 4.6 Hz, 1H), 3.47 (dd, *J* = 11.4, 7.5 Hz, 1H), 2.76 (dd, *J* = 9.8, 5.5 Hz, 1H), 2.55 (td, *J* = 14.7, 4.1 Hz, 1H), 2.15 (dt, *J* = 13.6, 10.0 Hz, 1H), 2.09 (dd, *J* = 15.0, 3.1 Hz, 1H), 2.05 – 1.98 (m, 1H), 1.97 – 1.91 (m, 3H), 1.86 (dtd, *J* = 14.4, 9.3, 5.4 Hz, 1H), 1.79 – 1.63 (m, 4H), 1.64 – 1.45 (m, 5H), 1.41 – 1.31 (m, 2H), 1.25 – 1.17 (m, 2H), 0.85 (s, 3H).

^{13}C NMR (176 MHz, $CDCl_3$): δ 174.8, 174.7, 117.9, 85.5, 78.2, 73.7, 67.9, 65.7, 50.7, 49.6, 42.3, 40.6, 40.2, 39.0, 36.9, 35.5, 32.7, 27.7, 26.9, 24.0, 21.4, 19.2, 15.9.

HRMS (m/z): $[M+Na]^+$ calcd. for $C_{23}H_{34}O_6$, 429.2247; found, 429.2248

IR (thin film, cm^{-1}): 3323, 2939, 1779, 1731, 1619, 1450, 1025

[α]$_D$: +30.6 (c = 1.0 in $CHCl_3$)

Synthesis of Strophanthidol Boronate and Glycoside 62

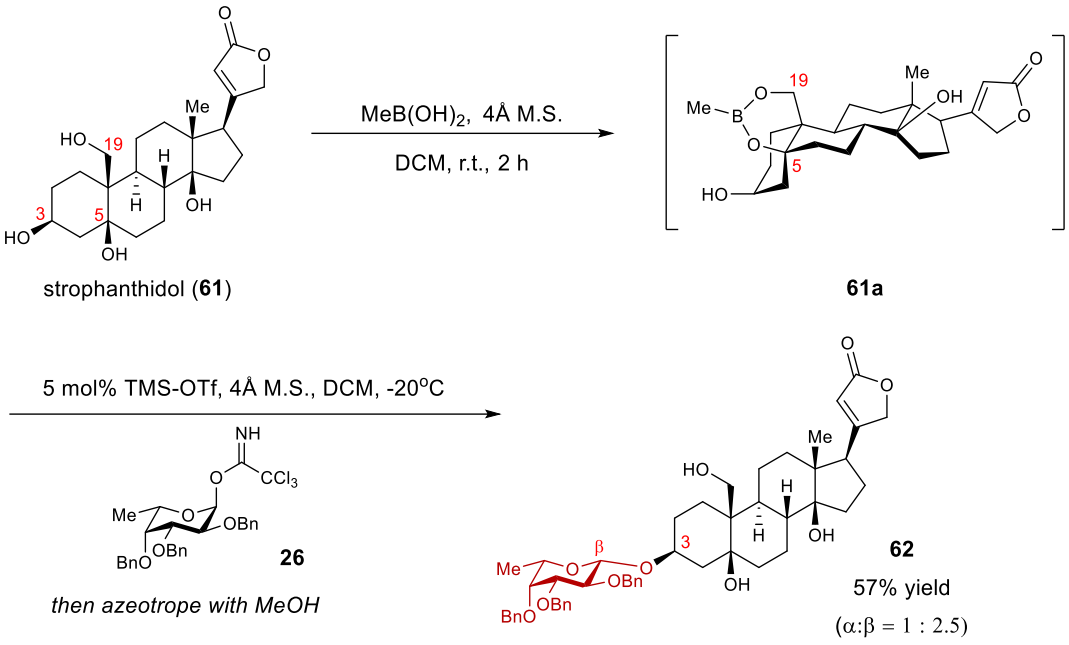

Strophanthidol **61** (8mg, 0.020mmol), $MeB(OH)_2$ (1.3mg, 1.1 equiv.) and 30mg of powered 4Å molecular sieve were stirred in 100μL of dry dichloromethane at room temperature. After 2h, the reaction was filtered through Celite and concentrated under reduced pressure to obtain boronate intermediate **61a** (>98% mass recovery).

^{1}H NMR (700 MHz, $CDCl_3$): δ 5.88 (s, 1H), 4.96 (d, *J* = 18.0 Hz, 1H), 4.79 (d, *J* = 18.1 Hz, 1H), 4.28 (d, *J* = 11.7 Hz, 1H), 4.06 – 3.98 (m, 1H), 3.59 (d, *J* = 8.3 Hz, 1H), 3.45 (d, *J* = 11.6 Hz, 1H), 2.77 (dd, *J* = 9.7, 5.5 Hz, 1H), 2.20 – 2.15 (m, 1H), 2.10 – 2.02 (m, 4H), 1.95 (dd, *J* = 13.9, 3.6 Hz, 1H), 1.88 (dtd, *J* = 14.6, 9.4, 5.4 Hz, 1H), 1.79 – 1.60 (m, 10H), 1.59 – 1.52 (m, 2H), 1.45 –

1.34 (m, 3H), 1.22 (dtd, *J* = 26.4, 13.6, 12.5, 5.8 Hz, 1H), 1.10 (qd, *J* = 13.9, 13.4, 3.8 Hz, 1H), 0.86 (s, 3H).

^{13}C NMR (176 MHz, $CDCl_3$): δ 174.6, 174.3, 118.0, 85.3, 76.2, 73.6, 66.7, 65.3, 50.6, 49.6, 41.0, 40.2, 38.6, 38.1, 36.9, 36.8, 32.9, 27.6, 27.0, 23.8, 21.4, 19.8, 15.9.

^{10}B NMR (75 MHz, $CDCl_3$): δ 32.6 (br)

IR (thin film, cm^{-1}): 3470, 2938, 1780, 1737, 1620

$[\alpha]_D$: +21.8 (c = 1.0 in $CHCl_3$)

61a and trichloroacetimidate donor **26** (23.2mg, 2.0 equiv.) was dissolved in 400μL dry dichloromethane and cooled to -20ºC. TMSOTf (0.18 μL, 0.05 equiv.) in 20μL dry dichloromethane was added to the reaction. After stirring for 16h, the reaction quenched with Et_3N at room temperature and filtered through a short pad of Celite. The crude mixture was azeotroped with MeOH multiple times and then purified by flash column chromatography on silica gel (EtOAc:Hexanes, 70:30 v/v) to obtain glycoside **62** as a mixture of two diastereomers (9.4mg, 57% yield). The diastereomeric glycosides were separated by semi-prep HPLC (18mL/min, EtOAc:Hexanes, 70:30 v/v) and characterized.

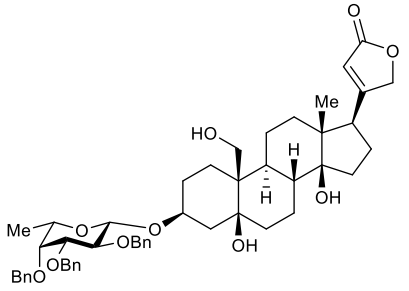

β-62

^{1}H NMR (700 MHz, $CDCl_3$): δ 7.38 – 7.27 (m, 15H), 5.87 (s, 1H), 5.01 – 4.93 (m, 2H), 4.87 – 4.81 (m, 2H), 4.79 (dd, *J* = 18.1, 1.8 Hz, 1H), 4.77 – 4.71 (m, 2H), 4.70 (d, *J* = 11.8 Hz, 1H), 4.67 (s, 1H), 4.38 (d, *J* = 7.7 Hz, 1H), 4.30 (d, *J* = 11.4 Hz, 1H), 4.24 (d, *J* = 10.2 Hz, 1H), 4.22 (s, 1H), 3.81 (dd, *J* = 9.7, 7.7 Hz, 1H), 3.57 (d, *J* = 2.9 Hz, 1H), 3.53 (dd, *J* = 9.7, 2.9 Hz, 1H), 3.50 – 3.43 (m, 1H), 3.42 (t, *J* = 10.8 Hz, 1H), 2.76 (dd, *J* = 9.7, 5.4 Hz, 1H), 2.54 (td, *J* = 14.8, 3.8 Hz, 1H), 2.19 – 2.10 (m, 2H), 2.07 – 1.96 (m, 2H), 1.95 – 1.82 (m, 3H), 1.76 – 1.71 (m, 1H), 1.70 – 1.62 (m, 2H), 1.60 – 1.44 (m, 6H), 1.39 – 1.24 (m, 6H), 1.20 (dd, *J* = 13.7, 4.5 Hz, 1H), 1.16 (d, *J* = 6.4 Hz, 3H), 0.85 (s, 3H).

^{13}C NMR (176 MHz, $CDCl_3$): δ 174.5, 174.3, 138.5, 138.4, 138.3, 128.7, 128.6, 128.5, 128.4, 128.3, 127.8, 127.7, 118.0, 101.4, 85.7, 83.1, 79.1, 76.8, 75.9, 75.7, 74.9, 74.8, 73.5, 73.2, 70.9, 64.8, 50.7, 49.5, 42.6, 40.6, 40.2, 39.1, 36.2, 35.1, 32.8, 29.9, 26.8, 24.2, 23.9, 21.3, 19.1, 17.0, 15.8.

HRMS (m/z): $[M+Na]^+$ calcd. for $C_{50}H_{62}O_{10}$, 845.4235; found, 845.4232

IR (thin film, cm^{-1}): 3441, 2935, 1780, 1742, 1620, 1453, 1063

[α]$_D$: +21.3 (c = 0.31 in $CHCl_3$)

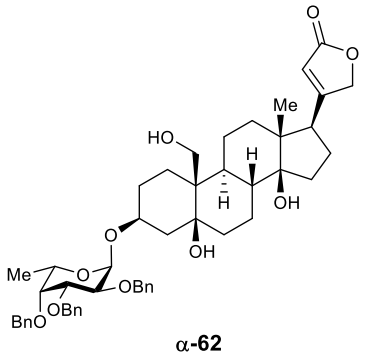

α-62

^{1}H NMR (700 MHz, $CDCl_3$): δ 7.41 – 7.27 (m, 15H), 5.88 (s, 1H), 5.21 (s, 1H), 4.99 – 4.94 (m, 2H), 4.83 – 4.77 (m, 3H), 4.77 – 4.71 (m, 2H), 4.65 (dd, *J* = 17.9, 11.8 Hz, 3H), 4.36 (d, *J* = 11.3 Hz, 1H), 4.02 (t, *J* = 2.8 Hz, 1H), 4.00 (dd, *J* = 10.0, 3.9 Hz, 1H), 3.91 – 3.83 (m, 2H), 3.65 (d, *J* = 1.4 Hz, 1H), 3.42 (d, *J* = 9.7 Hz, 1H), 2.77 (dd, *J* = 9.7, 5.5 Hz, 1H), 2.54 (td, *J* = 14.5, 4.4 Hz, 1H), 2.19 – 1.92 (m, 6H), 1.87 (dtd, *J* = 14.6, 9.4, 5.5 Hz, 1H), 1.73 – 1.44 (m, 8H), 1.34 (m, 2H), 1.31 – 1.17 (m, 4H), 1.09 (d, *J* = 6.5 Hz, 3H), 0.86 (s, 3H).

^{13}C NMR (176 MHz, $CDCl_3$): δ 174.5, 174.2, 138.6, 138.6, 138.4, 128.6, 128.4, 128.4, 127.9, 127.8, 127.7, 127.7, 118.1, 96.4, 85.7, 79.4, 77.4, 77.1, 76.7, 75.6, 75.0, 74.0, 73.5, 73.1, 72.5, 67.2, 65.0, 50.7, 49.4, 42.4, 40.6, 40.3, 39.0, 35.3, 34.2, 32.8, 29.9, 26.8, 26.2, 24.2, 21.3, 19.4, 16.8, 15.8.

HRMS (m/z): $[M+Na]^+$ calcd. for $C_{50}H_{62}O_{10}$, 845.4235; found, 845.4230

IR (thin film, cm^{-1}): 3436, 2924, 1742, 1620, 1453

[α]$_D$: -27.1 (c = 0.11 in $CHCl_3$)

Synthesis of Glycoside 64

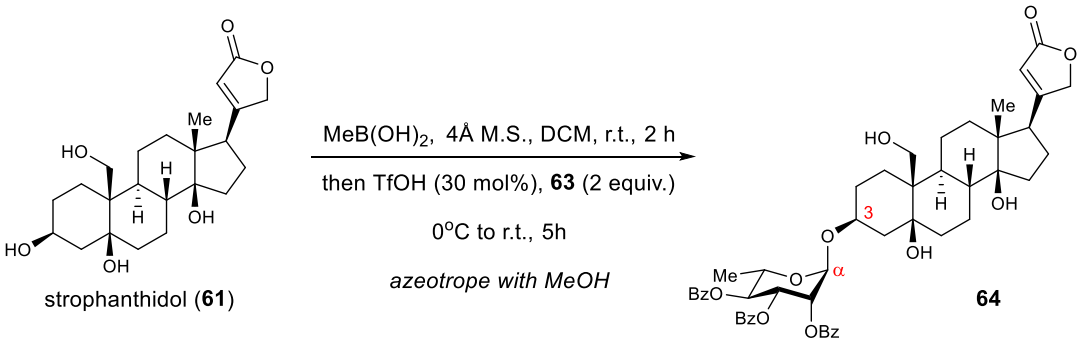

Strophanthidol **61** (16.3mg, 0.040mmol), $MeB(OH)_2$ (2.6mg, 1.1 equiv.) and 60mg of powered 4Å molecular sieve were stirred in 200µL of dry dichloromethane at room temperature. After 2h, 0.5 equiv. of sugar donor **63** in 1.8mL of dry dichloromethane was added to the reaction, and the mixture was cooled in ice-bath. TfOH (1.1µL, 0.3 equiv.) in 20µL of dry dichloromethane was added to the reaction. At 1h interval, 0.5 equiv. of sugar donor in 200µL of dry dichloromethane was added to reaction (repeated 3 times). After the last portion of sugar portion was added, the reaction was stirred in ice bath for 1 h before being warmed up to room temperature and quenched with Et_3N. Next, the reaction was filtered through a short pad of silica get/Celite and concentrated under reduced pressure. The crude mixture was azeotroped with MeOH multiple times and then purified by flash column chromatography on silica gel (EtOAc:Hexanes, 60:40 to 70:30 v/v) to obtain **64** (27.9mg, 81% yield) as white foamy solid.

^{1}H NMR (500 MHz, $CDCl_3$): δ 8.12 – 8.06 (m, 2H), 8.04 – 7.97 (m, 2H), 7.87 – 7.78 (m, 2H), 7.65 – 7.59 (m, 1H), 7.56 – 7.46 (m, 3H), 7.46 – 7.36 (m, 3H), 7.27 – 7.24 (m, 2H), 5.88 (s, 1H), 5.71 (dd, *J* = 5.5, 2.4 Hz, 2H), 5.66 – 5.60 (m, 1H), 5.16 (d, *J* = 1.9 Hz, 1H), 4.98 (dd, *J* = 18.1, 1.8 Hz, 1H), 4.81 (dd, *J* = 18.1, 1.7 Hz, 1H), 4.40 (d, *J* = 11.4 Hz, 1H), 4.30 – 4.19 (m, 4H), 3.50 (t, *J* = 10.6 Hz, 1H), 2.78 (dd, *J* = 9.6, 5.4 Hz, 1H), 2.60 (td, *J* = 14.9, 3.8 Hz, 1H), 2.20 (dd, *J* = 15.4, 3.3 Hz, 1H), 2.18 – 1.95 (m, 5H), 1.88 (dtd, *J* = 14.3, 9.2, 5.4 Hz, 1H), 1.79 (s, 1H), 1.76 – 1.68 (m, 3H), 1.64 (h, *J* = 4.3 Hz, 3H), 1.54 (tq, *J* = 11.9, 3.3 Hz, 3H), 1.36 (d, 3H), 1.35 – 1.31 (m, 1H), 1.28 – 1.15 (m, 1H), 0.87 (s, 3H).

^{13}C NMR (176 MHz, $CDCl_3$): δ 174.6, 174.4, 165.9, 165.7, 165.5, 133.8, 133.6, 133.3, 130.0, 129.9, 129.8, 129.2, 129.1, 129.1, 128.8, 128.6, 128.4, 117.9, 97.8, 85.5, 77.4, 77.3, 76.9, 73.6,

71.3, 71.1, 70.0, 68.1, 64.9, 50.7, 49.5, 42.7, 40.5, 40.2, 39.2, 35.8, 34.6, 32.7, 29.8, 26.8, 25.5, 24.1, 21.3, 19.2, 17.8, 15.9.

HRMS (m/z): $[M+Na]^+$ calcd. for $C_{50}H_{56}O_{13}$, 887.3592; found, 887.3594

IR (thin film, cm^{-1}): 3485, 2935, 1780, 1729, 1601, 1451

$[\alpha]_D$: +9.3 (c = 0.57 in $CHCl_3$)

Synthesis of Trichloroacetimidate Donor 67 and 68

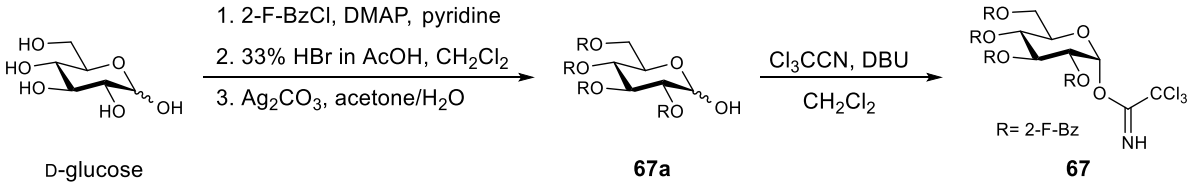

Scheme 5.11. Synthesis of 2-fluoro-benzoyl protected glucose-derived trichloroacetimidate donor **67**.

D-Glucose (300mg, 1.67mmol) and DMAP (102mg, 0.5 equiv.) were dissolved in dry pyridine and cooled in ice-bath. 2-fluorobenzoyl chloride (1.4mL, 7.0 equiv.) was added to the reaction dropwise. After stirring at room temperature overnight, the reaction was quenched with 2mL of MeOH and stirred for 1h. Next, the reaction was diluted with 50mL of DCM and washed with 2N HCl (two times), sat. $NaHCO_3$ (two times), and brine solution. The organic layer was dried over Na_2SO_3, filtered and concentrated under reduced pressure. The crude mixture was used in next step without further purification.

The crude from previous step was dissolved in 5mL of DCM and 33% HBr in AcOH was added to the reaction dropwise. After stirring at room temperature for 5h, the reaction was quenched slowly with sat $NaHCO_3$ (aq). Next, the mixture was diluted with DCM, and washed with sat $NaHCO_3$ (aq), followed by brine solution. The organic layer was dried over Na_2SO_3, filtered and concentrated under reduced pressure. The crude mixture was used in next step without further purification.

The crude from previous step was dissolved in acetone/H_2O/DCM (10mL:1mL:2mL) before Ag_2CO_3 (800mg) was added to the reaction. After stirring at room temperature for overnight, the reaction was filtered through Celite and concentrated under reduced pressure. The crude mixture was purified by flash column chromatography on silica gel (EtOAc:hexanes, 30:70 to 40:60 v/v) to obtain hemiacetal **67a**.

67a (300mg, 0.45mmol) was dissolved in 3mL of DCM (0.15M) and cooled in ice-bath. Trichloroacetonitrile (0.9mL, 20 equiv.) was added to the reaction, followed by DBU (34μL, 0.5 equiv.). After stirring at room temperature for 2h, the reaction was concentrated under reduced pressure. The crude mixture was purified by flash column chromatography on silica gel (EtOAc:hexanes, 15:85 v/v) to obtain α-trichloroacetimidate donor **67** (250mg, 68% yield) as white foamy solid.

^{1}H NMR (700 MHz, $CDCl_3$): δ 8.67 (s, 1H), 7.96 (t, *J* = 7.5 Hz, 1H), 7.89 (t, *J* = 7.5 Hz, 1H), 7.83 (t, *J* = 7.4 Hz, 1H), 7.77 (t, *J* = 7.5 Hz, 1H), 7.54 – 7.48 (m, 3H), 7.44 (q, *J* = 7.1 Hz, 1H), 7.21 (t, *J* = 7.5 Hz, 1H), 7.18 – 7.09 (m, 4H), 7.08 (t, *J* = 9.5 Hz, 2H), 7.02 (t, *J* = 9.5 Hz, 1H), 6.24 (t, *J* = 9.9 Hz, 1H), 5.80 (t, *J* = 9.9 Hz, 1H), 5.60 (dd, *J* = 10.2, 3.7 Hz, 1H), 4.67 – 4.60 (m, 2H), 4.57 (dd, *J* = 12.7, 4.9 Hz, 1H).

^{13}C NMR (176 MHz, $CDCl_3$): δ 163.9, 163.9, 163.2, 163.2, 163.2, 163.1, 163.0, 163.0, 162.9, 162.9, 162.8, 162.8, 161.7, 161.5, 161.3, 161.3, 160.7, 135.4, 135.4, 135.2, 135.2, 134.9, 134.9, 134.9, 134.8, 132.4, 132.3, 132.1, 131.9, 124.3, 124.2, 124.2, 124.2, 124.2, 124.1, 124.1, 124.1, 118.3, 118.2, 118.0, 118.0, 117.7, 117.7, 117.3, 117.2, 117.2, 117.1, 117.1, 117.1, 116.9, 93.1, 90.8, 70.8, 70.6, 70.4, 68.9, 62.7. (complex multiplet in δ 164 – 117 due to C-F couplings.)

HRMS (m/z): $[M+Na]^+$ calcd. for $C_{36}H_{24}Cl_3F_4NO_{10}$, 834.0294; found, 834.0301

IR (thin film, cm^{-1}): 1729, 1677, 1612, 1584, 1489, 1456, 1290, 1243

$[\alpha]_D$: +66.5 (c = 1.0 in $CHCl_3$)

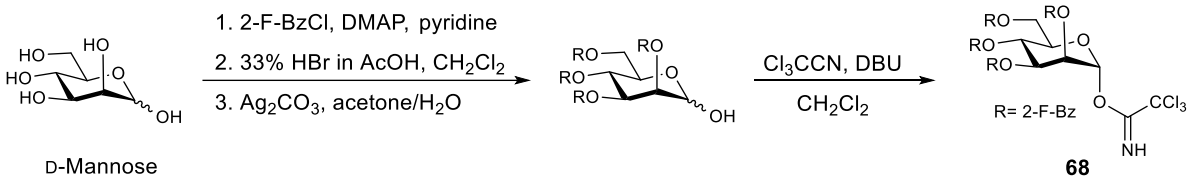

Scheme 5.12. Synthesis of 2-fluoro-benzoyl protected mannose-derived trichloroacetimidate donor **68**.

Trichloroacetimidate donor **68** was synthesized from D-Mannose following the same synthetic sequence for **67**.

^{1}H NMR (700 MHz, $CDCl_3$): δ 8.87 (s, 1H), 7.99 (q, *J* = 7.8 Hz, 2H), 7.82 (q, *J* = 7.9 Hz, 2H), 7.59 – 7.56 (m, 1H), 7.54 – 7.46 (m, 2H), 7.44 (qd, *J* = 7.0, 6.5, 2.8 Hz, 1H), 7.19 (t, *J* = 7.6 Hz, 1H), 7.16 – 7.11 (m, 3H), 7.11 – 7.05 (m, 3H), 7.01 (dd, *J* = 10.6, 8.4 Hz, 1H), 6.57 (s, 1H), 6.21 (t, *J* = 9.7 Hz, 1H), 5.97 – 5.95 (m, 2H), 4.69 – 4.65 (m, 1H), 4.62 – 4.56 (m, 2H).

^{13}C NMR (176 MHz, $CDCl_3$): δ 163.8, 163.8, 163.2, 163.2, 163.1, 163.1, 163.1, 163.0, 162.8, 161.7, 161.6, 161.6, 161.3, 159.9, 135.4, 135.3, 135.1, 135.1, 134.8, 134.7, 132.5, 132.5, 132.2, 132.1, 124.2, 124.2, 124.2, 124.1, 124.1, 124.0, 124.0, 118.4, 118.3, 117.9, 117.8, 117.7, 117.6, 117.6, 117.5, 117.3, 117.2, 117.2, 117.1, 117.1, 117.1, 117.0, 94.6, 90.7, 71.5, 70.1, 69.0, 66.4, 62.8. (complex multiplet in δ 164 – 117 due to C-F couplings.)

HRMS (m/z): $[M+Na]^+$ calcd. for $C_{36}H_{24}Cl_3F_4NO_{10}$, 834.0294; found, 834.0303

IR (thin film, cm^{-1}): 1725, 1678, 1612, 1585, 1488, 1456, 1289, 1243

[α]$_D$: -34.3 (c = 1.0 in $CHCl_3$)

General Procedure for One-pot Glycosylation of Strophanthidol

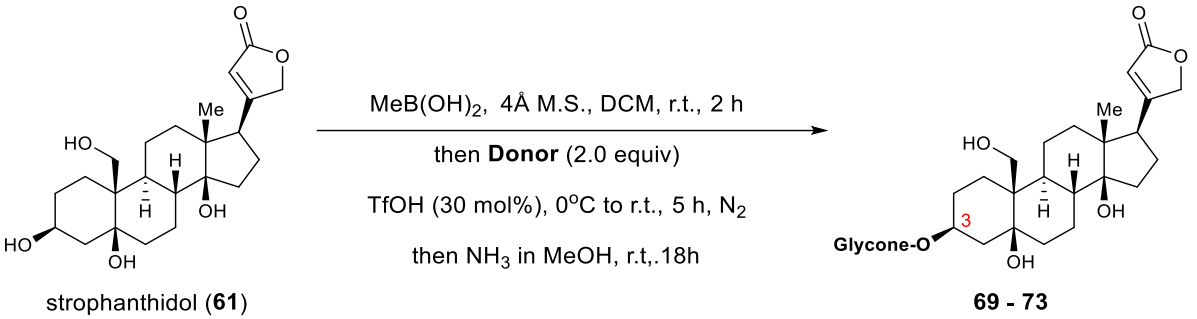

strophanthidol (**61**)

69 - 73

Strophanthidol **61** (16.3mg, 0.040mmol), $MeB(OH)_2$ (2.6mg, 1.1 equiv.) and 60mg of powered 4Å molecular sieve were stirred in 200µL of dry dichloromethane at room temperature. After 2h, 0.5 equiv. of trichloroacetimidate donor in 1.8mL of dry dichloromethane was added to the reaction, and the mixture was cooled in ice-bath. TfOH (1.1µL, 0.3 equiv.) in 20µL of dry dichloromethane was added to the reaction. At 1h interval, 0.5 equiv. of trichloroacetimidate donor in 200µL of dry dichloromethane was added to reaction (repeated 3 times). After the last portion of trichloroacetimidate donor was added, the reaction was stirred in ice bath for 1 h before being warmed up to room temperature. Next, the reaction was diluted with 3 mL of MeOH and NH_3 gas was bubbled through the reaction for 30 min. After stirring at room temperature for 18 h, the reaction mixture was filtered through a short pad of silica gel/Celite and concentrated under reduced pressure. The crude mixture was purified by flash column chromatography (on pipette column) on silica gel (starting with MeOH:CH_2Cl_2, 5:95 v/v + 0.5% of AcOH, followed by a gradient of MeOH:CH_2Cl_2, 10:90 to 20:80 v/v) to obtain glycoside **69** – **73**.

Characterization of Strophanthidol Glycoside 69 – 73

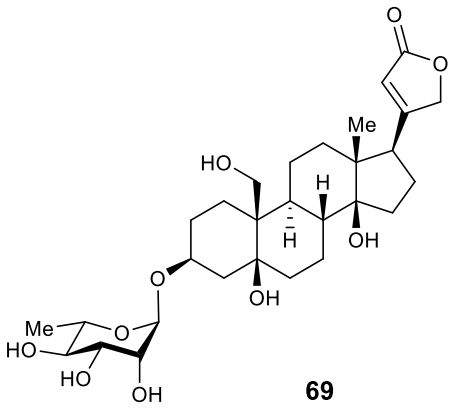

69

^{1}H NMR (500 MHz, CD_3OD): δ 5.90 (s, 1H), 5.03 (dd, *J* = 18.4, 1.8 Hz, 1H), 4.92 (dd, *J* = 18.4, 1.8 Hz, 1H), 4.85 (d, *J* = 1.8 Hz, 1H), 4.19 – 4.11 (m, 2H), 3.79 (dd, *J* = 3.4, 1.7 Hz, 1H), 3.69 – 3.59 (m, 3H), 3.40 (t, *J* = 9.5 Hz, 1H), 2.86 – 2.83 (m, 1H), 2.26 – 2.09 (m, 5H), 2.03 – 1.94 (m, 1H), 1.94 – 1.85 (m, 2H), 1.84 – 1.65 (m, 6H), 1.58 – 1.38 (m, 9H), 1.29 (s, 1H) 1.26 (d, *J* = 6.2 Hz, 3H), 1.25 – 1.19 (m, 1H), 0.89 (s, 3H).

^{13}C NMR (176 MHz, CD_3OD): δ 178.3, 177.2, 117.8, 100.9, 86.4, 77.4, 75.6, 75.3, 73.8, 72.5, 72.4, 70.7, 65.2, 51.9, 50.8, 44.1, 41.5, 41.1, 40.0, 36.2, 35.9, 33.0, 27.9, 26.4, 25.0, 22.8, 20.4, 18.0, 16.3.

HRMS (m/z): $[M+Na]^+$ calcd. for $C_{29}H_{44}O_{10}$, 575.2826; found, 575.2828

IR (thin film, cm^{-1}): 3342, 2938, 1732, 1449, 1021

$[\alpha]_D$: -3.68 (c = 1.0 in $CHCl_3$)

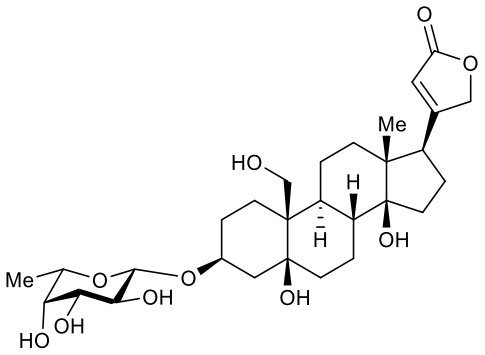

70

^{1}H NMR (500 MHz, CD_3OD): δ 5.90 (s, 1H), 5.03 (dd, *J* = 18.4, 1.8 Hz, 1H), 4.91 (dd, *J* = 18.4, 1.7 Hz, 1H), 4.36 – 4.27 (m, 1H), 4.21 (s, 1H), 4.18 (d, *J* = 11.4 Hz, 1H), 3.69 – 3.62 (m, 1H), 3.60 (d, *J* = 1.6 Hz, 1H), 3.58 (d, *J* = 11.4 Hz, 1H), 3.48 – 3.44 (m, 2H), 2.85 – 2.82 (m, 1H), 2.34 – 2.22 (m, 2H), 2.21 – 2.08 (m, 2H), 2.03 – 1.82 (m, 5H), 1.77 – 1.58 (m, 6H), 1.56 – 1.35 (m, 7H), 1.26 (d, *J* = 6.4 Hz, 3H), 1.24 – 1.18 (m, 2H), 0.88 (s, 3H).

^{13}C NMR (176 MHz, CD_3OD): δ 178.3, 177.2, 117.9, 102.4, 86.4, 77.3, 75.6, 75.3, 75.2, 73.0, 72.3, 72.1, 65.4, 51.9, 50.8, 44.1, 41.4, 41.1, 40.0, 37.4, 36.5, 33.0, 27.9, 25.1, 24.1, 22.7, 20.1, 16.7, 16.3.

HRMS (m/z): $[M+Na]^+$ calcd. for $C_{29}H_{44}O_{10}$, 575.2826; found, 575.2828

IR (thin film, cm^{-1}): 3348, 2940, 1733, 1666, 1624, 1448, 1022

$[\alpha]_D$: +14.5 (c = 1.0 in $CHCl_3$)

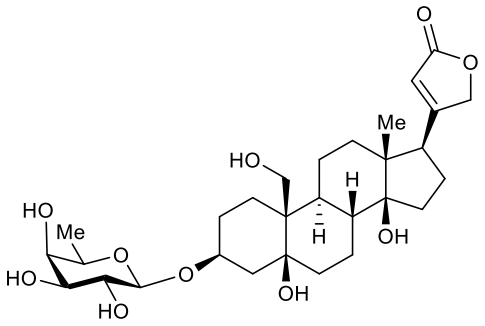

71

^{1}H NMR (500 MHz, CD_3OD): δ 5.90 (s, 1H), 5.03 (dd, *J* = 18.4, 1.8 Hz, 1H), 4.91 (dd, *J* = 18.4, 1.7 Hz, 1H), 4.36 – 4.28 (m, 1H), 4.20 (d, *J* = 11.3 Hz, 1H), 4.17 (s, 1H), 3.64 (m, 1H), 3.61 – 3.54 (m, 2H), 3.49 – 3.44 (m, 2H), 2.85 – 2.81 (m, 1H), 2.32 (td, *J* = 14.5, 3.8 Hz, 1H), 2.22 – 2.09 (m, 4H), 2.03 – 1.81 (m, 4H), 1.80 – 1.61 (m, 6H), 1.58 – 1.34 (m, 7H), 1.26 (d, *J* = 6.5 Hz, 3H), 1.24 – 1.16 (m, 2H), 0.88 (s, 3H).

^{13}C NMR (176 MHz, CD_3OD): δ 178.3, 177.2, 117.9, 102.6, 86.4, 77.3, 75.8, 75.3, 75.3, 73.1, 72.3, 72.1, 65.6, 51.9, 50.8, 43.8, 41.4, 41.1, 40.0, 36.8, 35.3, 33.1, 27.9, 26.5, 25.2, 22.6, 20.5, 16.8, 16.3.

HRMS (m/z): $[M+Na]^+$ calcd. for $C_{29}H_{44}O_{10}$, 575.2826; found, 575.2829

IR (thin film, cm^{-1}): 3354, 2940, 1733, 1666, 1624, 1449, 1024

[α]$_D$: +12.6 (c = 1.0 in $CHCl_3$)

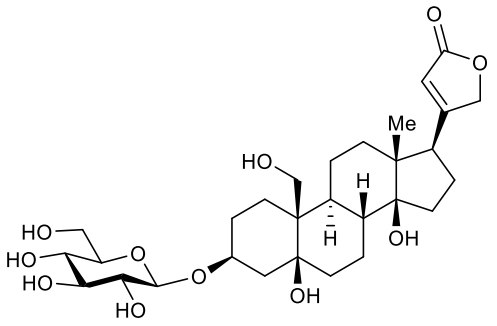

72

^{1}H NMR (500 MHz, CD_3OD): δ 5.90 (s, 1H), 5.03 (dd, *J* = 18.5, 1.8 Hz, 1H), 4.95 – 4.87 (dd, *J* = 18.5, 1.7 Hz, 1H), 4.40 (d, *J* = 7.9 Hz, 1H), 4.23 (s, 1H), 4.20 (d, *J* = 11.4 Hz, 1H), 3.86 (dd, *J* = 11.9, 1.7 Hz, 1H), 3.69 – 3.63 (m, 1H), 3.58 (d, *J* = 11.4 Hz, 1H), 3.29 – 3.26 (m, 2H), 3.18 (dd, *J* = 9.2, 7.9 Hz, 1H), 2.85 – 2.82 (m, 1H), 2.32 (td, *J* = 14.5, 4.0 Hz, 1H), 2.22 – 2.09 (m, 3H), 2.05 – 1.81 (m, 4H), 1.81 – 1.59 (m, 6H), 1.57 – 1.32 (m, 7H), 1.32 – 1.20 (m, 2H), 0.88 (s, 3H).

^{13}C NMR (176 MHz, CD_3OD): δ 178.3, 177.2, 117.9, 102.0, 86.4, 78.2, 78.2, 77.3, 75.7, 75.3, 75.1, 71.6, 65.6, 62.7, 51.9, 50.8, 43.8, 41.4, 41.0, 39.9, 36.9, 35.2, 33.1, 27.9, 26.5, 25.2, 22.6, 20.5, 16.3.

HRMS (m/z): $[M+Na]^+$ calcd. for $C_{29}H_{44}O_{11}$, 591.2776; found, 591.2791

IR (thin film, cm^{-1}): 3341, 2941, 1734, 1668, 1450, 1019

[α]$_D$: +10.1 (c = 1.0 in $CHCl_3$)

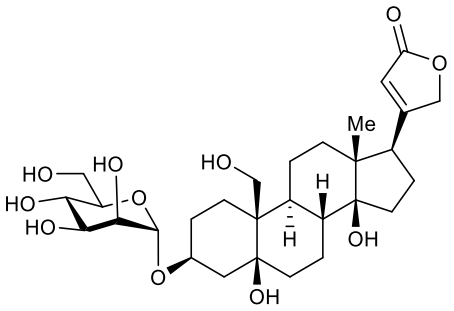

73

^{1}H NMR (500 MHz, CD_3OD): δ 5.88 (s, 1H), 5.01 (dd, *J* = 18.5, 1.8 Hz, 1H), 4.94 – 4.86 (m, 2H), 4.24 (s, 1H), 4.14 (d, *J* = 11.4 Hz, 1H), 3.86 – 3.78 (m, 2H), 3.72 – 3.55 (m, 5H), 2.82 – 2.80 (m, *J* = 9.0 Hz, 1H), 2.34 (dd, *J* = 15.3, 3.5 Hz, 1H), 2.22 – 2.02 (m, 3H), 2.00 – 1.79 (m, 5H), 1.77 – 1.59 (m, 5H), 1.57 – 1.34 (m, 8H), 1.31 – 1.15 (m, 2H), 0.87 (s, 3H).

^{13}C NMR (176 MHz, CD_3OD): δ 178.3, 177.2, 117.9, 98.5, 86.4, 77.5, 75.4, 75.3, 72.8, 72.7, 72.4, 68.6, 65.2, 63.0, 51.9, 50.8, 44.3, 41.5, 41.0, 40.0, 37.7, 36.1, 33.0, 27.9, 25.0, 23.0, 22.8, 20.0, 16.3.

HRMS (m/z): $[M+Na]^+$ calcd. for $C_{29}H_{44}O_{11}$, 591.2776; found, 591.2780

IR (thin film, cm^{-1}): 3358, 2939, 1733, 1667, 1617, 1452, 1027

$[\alpha]_D$: +46.9 (c = 0.98 in $CHCl_3$)

Synthesis of Anhydro-ouabagenin 74

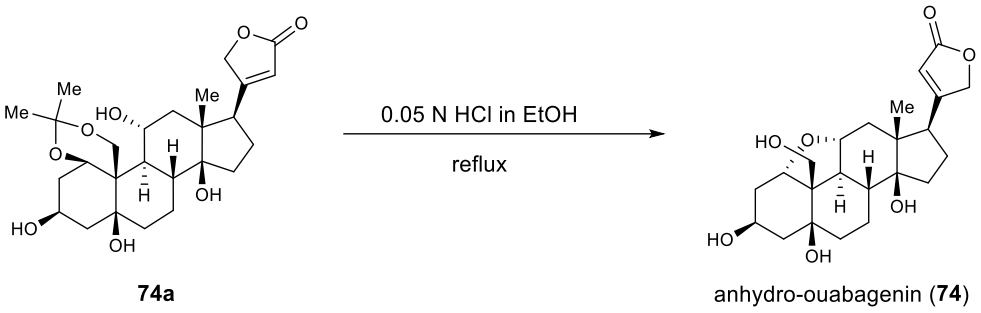

Scheme 5.13. Synthesis of anhydro-ouabagenin (**74**).

74a was prepared according to previously reported method.[16] **74a** (184mg, 0.39mmol) in 15mL of 0.05 N HCl (EtOH solution) was heated to reflux for 30 minutes. After being cooled to room temperature, the reaction was neutralized by addition of solid $NaHCO_3$. Next, the reaction was filtered through a filter paper, and the filtrate was concentrated under reduced pressure. The crude mixture was purified by flash column chromatography on silica gel (gradient of DCM:MeOH from 90:10 to 75:25 v/v) to obtain anhydro-ouabagenin **74** (50mg, 30% yield) as white solid.

^{1}H NMR (500 MHz, CD_3OD): δ 5.92 (s, 1H), 4.99 (dd, *J* = 18.4, 1.8 Hz, 1H), 4.89 (dd, *J* = 18.4, 1.8 Hz, 1H), 4.71 (t, *J* = 8.1 Hz, 1H), 4.22 – 4.12 (m, 2H), 3.92 (td, *J* = 11.5, 4.2 Hz, 1H), 3.69 (d, *J* = 11.7 Hz, 1H), 2.92 (dd, *J* = 9.6, 5.9 Hz, 1H), 2.35 (dddd, *J* = 13.3, 6.4, 3.8, 1.7 Hz, 1H), 2.27 – 2.18 (m, 1H), 2.15 – 2.04 (m, 2H), 2.04 – 1.86 (m, 4H), 1.82 (ddd, *J* = 15.1, 11.4, 4.1 Hz, 1H), 1.73 – 1.52 (m, 5H), 1.45 (t, *J* = 11.7 Hz, 1H), 1.40 – 1.22 (m, 2H), 0.92 (s, 3H).

^{13}C NMR (176 MHz, CD_3OD): δ 177.1, 176.9, 118.3, 86.4, 79.2, 79.0, 78.8, 78.5, 78.4, 75.5, 75.2, 68.5, 62.7, 54.6, 53.7, 51.5, 47.5, 39.1, 38.2, 37.3, 37.1, 33.1, 28.2, 25.8, 17.9.

HRMS (m/z): $[M+Na]^+$ calcd. for $C_{23}H_{32}O_7$, 443.2030; found, 443.2044

IR (thin film, cm^{-1}): 3323, 2943, 2832, 1449, 1024

[α]$_D$: +38.2 (c = 0.5 in DMSO)

Glycosylation of Anhydro-ouabagenin with Glycosyl Bromide

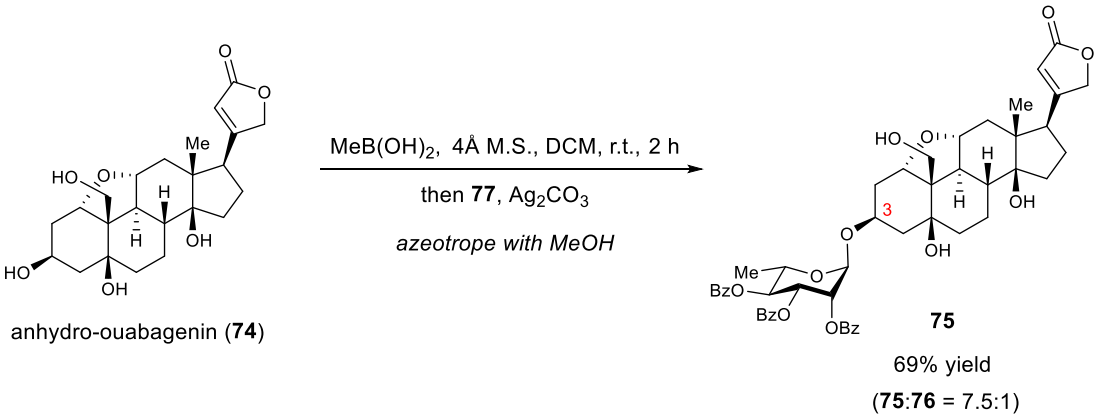

Anhydro-ouabagenin **74** (6.3mg, 0.015mmol), $MeB(OH)_2$ (1.0mg, 1.1 equiv.) and 40mg of powered 4Å molecular sieve were stirred in 400μL of dry dichloromethane at room temperature. After 3h, glycosyl bromide **77** (24.3mg, 3.0 equiv.) and Ag_2CO_3 (16.5mg, 4.0 equiv.) was added to the reaction, and the reaction vial was wrapped with aluminum foil. After stirring at room temperature for 18h, the reaction was quenched with Et_3N, filtered through a short pad of silica gel/Celite, and concentrated under reduced pressure. The crude mixture was azeotroped with MeOH multiple times and purified by flash column chromatography (pipette column) on silica gel (EtOAc:Hexanes, 80:20 to 100:0 v/v) to obtain a mixture of glycosides **75** and **76** (9.1mg, 69% yield) as white film. The regioisomeric glycosides were separated by semi-prep HPLC (18mL/min, 100% EtOAc) and characterized.

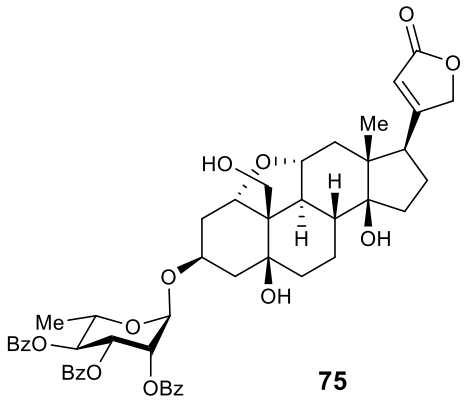

75

^{1}H NMR (500 MHz, CD_3OD): δ 8.08 (d, *J* = 7.8 Hz, 2H), 7.98 (d, *J* = 7.8 Hz, 2H), 7.83 (d, *J* = 7.8 Hz, 2H), 7.65 – 7.58 (m, 1H), 7.51 (dt, *J* = 15.7, 7.5 Hz, 3H), 7.41 (dt, *J* = 15.6, 7.5 Hz, 3H), 7.28 – 7.25 (m, 2H), 5.92 (s, 1H), 5.72 (t, *J* = 9.8 Hz, 1H), 5.65 – 5.56 (m, 2H), 5.16 (s, 1H), 5.01 (t, *J* = 8.1 Hz, 1H), 4.91 (d, *J* = 18.0 Hz, 1H), 4.79 (d, *J* = 18.0 Hz, 1H), 4.36 – 4.25 (m, 3H), 4.01 (s, 1H), 3.93 (td, *J* = 11.4, 4.2 Hz, 1H), 3.72 – 3.62 (m, 2H), 2.85 (dd, *J* = 9.7, 5.6 Hz, 1H), 2.71 – 2.68 (m, 1H), 2.26 – 2.20 (m, 1H), 2.12 (ddt, *J* = 12.4, 9.3, 5.1 Hz, 2H), 2.08 – 1.85 (m, 5H), 1.83 – 1.58 (m, 4H), 1.50 – 1.40 (m, 2H), 1.39 (d, *J* = 6.0 Hz, 3H), 1.28 (s, 1H), 0.93 (s, 3H).

^{13}C NMR (176 MHz, CD_3OD): δ 174.3, 173.2, 165.9, 165.8, 165.7, 133.9, 133.6, 133.4, 130.0, 129.9, 129.9, 129.2, 129.1, 129.1, 128.8, 128.6, 128.5, 118.5, 98.2, 86.1, 77.5, 77.3, 76.2, 73.7, 73.6, 71.1, 71.1, 70.1, 68.3, 62.0, 52.6, 50.5, 49.7, 48.3, 47.0, 38.0, 36.7, 35.9, 35.9, 33.1, 27.3, 25.2, 17.8, 17.5.

HRMS (m/z): $[M+Na]^+$ calcd. for $C_{50}H_{54}O_{14}$, 901.3406; found, 901.3403

IR (thin film, cm^{-1}): 3445, 2928, 1729, 1451, 1263

[α]$_D$: +99.9 (c = 0.14 in $CHCl_3$)

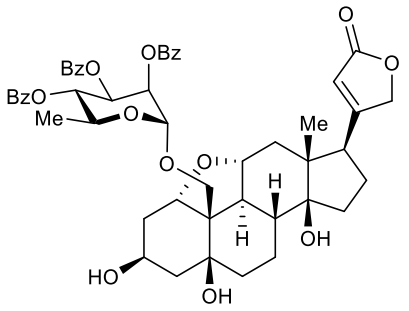

76

^{1}H NMR (500 MHz, CD_3OD): δ 8.11 (d, *J* = 7.7 Hz, 2H), 7.82 (d, *J* = 7.9 Hz, 2H), 7.79 (d, *J* = 7.9 Hz, 2H), 7.63 (t, *J* = 7.5 Hz, 1H), 7.51 (t, *J* = 7.8 Hz, 3H), 7.45 (t, *J* = 7.5 Hz, 1H), 7.31 (t, *J* = 7.7 Hz, 2H), 7.28 (t, *J* = 7.8 Hz, 2H), 5.99 (dd, *J* = 10.5, 3.0 Hz, 1H), 5.94 (s, 1H), 5.66 (t, *J* = 10.0 Hz, 1H), 5.55 (t, *J* = 2.4 Hz, 1H), 5.12 (s, 1H), 5.06 – 4.99 (m, 1H), 4.88 (d, *J* = 18.2 Hz, 1H), 4.35 (d, *J* = 10.4 Hz, 1H), 4.30 (s, 1H), 4.21 (td, *J* = 11.4, 4.2 Hz, 1H), 4.15 (dt, *J* = 12.2, 6.1 Hz, 1H), 4.08 (t, *J* = 8.3 Hz, 1H), 4.03 (d, *J* = 10.4 Hz, 1H), 3.69 (s, 1H), 3.00 – 2.93 (m, 2H), 2.79 – 2.72 (m, 1H), 2.49 (d, *J* = 4.4 Hz, 1H), 2.42 – 2.39 (s, 1H), 2.25 (q, *J* = 9.8, 7.9 Hz, 1H), 2.18 (dt, *J* = 11.9, 5.5 Hz, 2H), 2.15 – 2.07 (m, 2H), 2.07 – 1.99 (m, 2H), 1.90 – 1.78 (m, 2H), 1.75 (d, *J* = 13.6 Hz, 1H), 1.63 (t, *J* = 12.6 Hz, 1H), 1.53 – 1.46 (m, 2H), 1.41 (d, *J* = 6.2 Hz, 3H), 1.39 (m, 1H), 1.38 – 1.30 (m, 1H), 1.15 (s, 3H).

^{13}C NMR (176 MHz, CD_3OD): δ 174.2, 173.7, 166.8, 165.8, 165.6, 134.0, 133.8, 133.8, 130.1, 130.1, 129.5, 129.3, 129.0, 128.8, 128.6, 128.6, 118.4, 97.7, 86.0, 78.3, 75.9, 74.8, 74.2, 73.6, 71.5, 71.0, 70.2, 68.6, 68.6, 68.3, 53.0, 50.8, 49.2, 48.5, 47.2, 39.0, 38.8, 38.0, 36.9, 31.9, 29.9, 27.3, 25.0, 18.1.

HRMS (m/z): $[M+Na]^+$ calcd. for $C_{50}H_{54}O_{14}$, 901.3406; found, 901.3403

IR (thin film, cm^{-1}): 3405, 2924, 1726, 1451, 1261

[α]$_D$: +60.5 (c = 0.26 in $CHCl_3$)

Deprotection of Anhydro-ouabagenin Glycosides

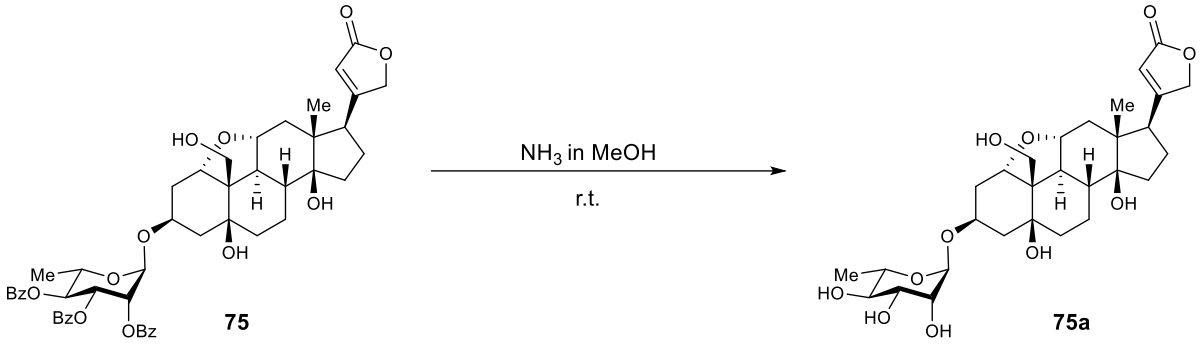

Scheme 5.14. Deprotection of C3-rhamnoside of anhydro-ouabagenin (**75**).

75 (8.5mg, 9.7μmol) was dissolved in 2mL of MeOH, and NH_3 gas was bubbled through the solution for 20 minutes. After stirring in sealed tube for 24h at room temperature, the reaction was concentrated under reduced pressure. The crude was purified by flash column chromatography (pipette column) on silica gel (CH_2Cl_2:MeOH, 80:20 v/v) to obtain **75a** (4.2mg, 76% yield) as white film.

^{1}H NMR (700 MHz, CD_3OD) δ 5.93 (d, *J* = 1.9 Hz, 1H), 4.99 (dd, *J* = 18.4, 1.8 Hz, 1H), 4.91 (dd, *J* = 18.5, 1.7 Hz, 1H), 4.83 (d, *J* = 1.7 Hz, 1H), 4.69 (t, *J* = 7.6 Hz, 1H), 4.20 – 4.12 (m, 2H), 3.93 (td, *J* = 11.6, 4.3 Hz, 1H), 3.75 (t, *J* = 2.4 Hz, 1H), 3.68 – 3.62 (m, 2H), 3.60 (dd, *J* = 9.5, 3.2 Hz, 1H), 3.38 (t, *J* = 9.5 Hz, 1H), 2.93 (dd, *J* = 9.7, 5.9 Hz, 1H), 2.36 (dt, *J* = 13.2, 5.7 Hz, 1H), 2.26 – 2.19 (m, 1H), 2.18 – 2.09 (m, 2H), 2.02 – 1.89 (m, 4H), 1.82 – 1.63 (m, 5H), 1.55 – 1.44 (m, 2H), 1.27 (d, *J* = 6.2 Hz, 3H), 0.92 (s, 3H).

^{13}C NMR (176 MHz, CD_3OD) δ 177.4, 177.0, 118.3, 100.8, 86.5, 78.6, 77.5, 75.4, 74.3, 73.9, 72.5, 72.4, 70.5, 62.5, 53.8, 51.6, 50.3, 47.3, 38.4, 37.7, 37.0, 36.0, 33.3, 28.3, 26.2, 18.0, 17.8.

HRMS (m/z): $[M+Na]^+$ calcd. for $C_{29}H_{42}O_{11}$, 589.2619; found, 589.2622

IR (thin film, cm^{-1}): 3375, 2927, 1736, 1627, 1451, 1384

[α]$_D$: -9.6 (c = 0.14 in $CHCl_3$)

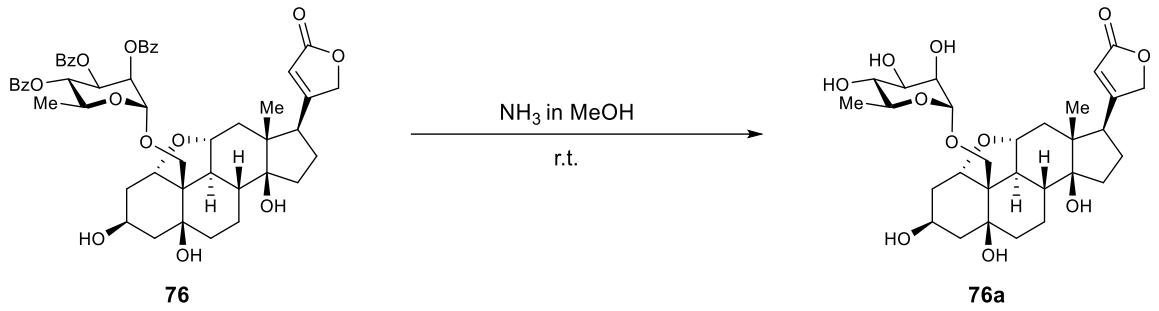

Scheme 5.15. Deprotection of C19-rhamnoside of anhydro-ouabagenin (**76**).

76 (7.0mg, 8.0μmol) was dissolved in 2mL of MeOH, and NH_3 gas was bubbled through the solution for 20 minutes. After stirring in sealed tube for 24h at room temperature, the reaction was concentrated under reduced pressure. The crude was purified by flash column chromatography (pipette column) on silica gel (CH_2Cl_2:MeOH, 80:20 v/v) to obtain **76a** (3.2mg, 71% yield) as white film.

^{1}H NMR (700 MHz, CD_3OD) δ 5.94 (s, 1H), 4.99 (dd, *J* = 18.3, 1.7 Hz, 1H), 4.95 – 4.89 (m, 1H), 4.67 (d, *J* = 1.7 Hz, 1H), 4.17 (s, 1H), 4.08 (t, *J* = 8.3 Hz, 1H), 4.02 (dd, *J* = 11.6, 4.4 Hz, 1H), 3.99 (d, *J* = 10.4 Hz, 1H), 3.86 (t, *J* = 2.4 Hz, 1H), 3.80 (d, *J* = 10.4 Hz, 1H), 3.68 – 3.59 (m, 2H), 3.40 (t, *J* = 9.5 Hz, 1H), 2.94 (dd, *J* = 9.7, 5.8 Hz, 1H), 2.30 – 2.19 (m, 1H), 2.18 – 2.08 (m, 3H), 2.06 (dd, *J* = 13.7, 4.8 Hz, 1H), 2.02 (dd, *J* = 12.1, 4.3 Hz, 1H), 1.95 (td, *J* = 13.8, 12.8, 6.7 Hz, 2H), 1.71 (dd, *J* = 13.4, 8.9 Hz, 1H), 1.66 – 1.52 (m, 4H), 1.49 (t, *J* = 11.7 Hz, 1H), 1.26 (d, *J* = 6.3 Hz, 3H), 0.95 (s, 3H).

^{13}C NMR (176 MHz, CD_3OD) δ 177.5, 177.0, 118.3, 102.7, 86.9, 80.1, 76.1, 75.9, 75.4, 73.9, 72.4, 72.2, 70.4, 69.4, 68.8, 53.8, 51.6, 49.8, 49.5, 49.5, 49.4, 49.3, 47.4, 39.4, 38.9, 38.1, 37.6, 33.0, 28.4, 25.7, 18.1, 17.9.

HRMS (m/z): $[M+Na]^+$ calcd. for $C_{29}H_{42}O_{11}$, 589.2619; found, 589.2626

IR (thin film, cm^{-1}): 3379, 2922, 2851, 1736, 1627

[α]$_D$: +6.65 (c = 0.07 in $CHCl_3$)

5.8 References

[1] (a) Duggan, P. J.; Tyndall, E. M. *J. Chem. Soc. Perkin Trans. 1* **2002**, 1325. (b) McClary, C. A.; Taylor, M. S. *Carbohydr. Res.* **2013**, *381*, 112.

[2] Kuivila, H. G.; Keough, A. H.; Soboczenski, E. J. *J. Org. Chem.* **1954**, *19*, 780.

[3] Fréchet, J. M.; Nuyens, L. J.; Seymour, E. *J. Am. Chem. Soc.* **1979**, *101*, 432.

[4] Belogi, G.; Zhu, T.; Boons, G.-J. *Tetrahedron Lett.* **2000**, *41*, 6965.

[5] Píš, J.; Hykl, J.; Buděšínský, M.; Harmatha, J. *Tetrahedron* **1994**, *50*, 9679.

[6] Tay, J. H.; Argüelles, A. J.; DeMars, M. D., II; Zimmerman, P. M.; Sherman, D. H.; Nagorny, P. *J. Am. Chem. Soc.* **2017**, *139*, 8570.

[7] Lingrel, J. B. *Annu. Rev. Physiol.* **2010**, *72*, 395.

[8] (a) Salvador, J. A. R.; Carvalho, J. F. S.; Neves, M. A. C.; Silvestre, S. M.; Leitao, A. J.; Silva, M. M. C.; Sa e Melo, M. L. *Nat. Prod. Rep.* **2013**, *30*, 324. (b) Banuls, L. M. Y.; Urban, E.; Gelbcke, M.; Dufrasne, F.; Kopp, B.; Kiss, R.; Zehl, M. *J. Nat. Prod.* **2013**, *76*, 1078.

[9] Piacente, S.; Masullo, M.; Neve, N.; Dewelle, J.; Hamed, A.; Kiss, R.; Mijatovic, T. *J. Nat. Prod.* **2009**, *72*, 1087.

[10] Heasley, B. *Chem. Eur. J.* **2012**, *18*, 3092.

[11] (a) Brown, L.; Erdmann, E.; Thomas, R. *Biochem. Pharmacol.* **1983**, *32*, 2767. (b) Laursen, M.; Gregersen, J. L.; Yatime, L.; Nissen, P.; Fedosova, N. U. *PNAS* **2015**, *112*, 1755. (c) Cornelius, F.; Kanai, R.; Toyoshima, C. *J. Bio. Chem.* **2013**, *288*, 6602.

[12] Bhattarai, B.; Nagorny, P. *Org. Lett.* **2018**, *20*, 154.

[13] Zhang, H.; Reddy, M. S.; Phoenix, S.; Deslongchamps, P. *Angew. Chem. Int. Ed.* **2008**, *47*, 1272.

[14] Sjölin, P.; Kihberg, J. *J. Org. Chem.* **2001**, *66*, 2957.

[15] Mancini, R. S.; Lee, J. B.; Taylor, M. S. *Org. Biomol. Chem.* **2017**, *15*, 132.

[16] Mukai, K.; Kasuya, S.; Nakagawa, Y.; Urabe, D.; Inoue, M. *Chem. Sci.* **2015**, *6*, 3383.